LEABHARLANN CHOLÁISTE NA TRÍONÓIDE, BAILE ÁTHA CLIATH | TRINITY COLLEGE LIBRARY DUBLIN
Ollscoil Átha Cliath | The University of Dublin

**Terms and Conditions of Use of Digitised Theses from Trinity College Library Dublin**

**Copyright statement**

All material supplied by Trinity College Library is protected by copyright (under the Copyright and Related Rights Act, 2000 as amended) and other relevant Intellectual Property Rights. By accessing and using a Digitised Thesis from Trinity College Library you acknowledge that all Intellectual Property Rights in any Works supplied are the sole and exclusive property of the copyright and/or other IPR holder. Specific copyright holders may not be explicitly identified. Use of materials from other sources within a thesis should not be construed as a claim over them.

A non-exclusive, non-transferable licence is hereby granted to those using or reproducing, in whole or in part, the material for valid purposes, providing the copyright owners are acknowledged using the normal conventions. Where specific permission to use material is required, this is identified and such permission must be sought from the copyright holder or agency cited.

**Liability statement**

By using a Digitised Thesis, I accept that Trinity College Dublin bears no legal responsibility for the accuracy, legality or comprehensiveness of materials contained within the thesis, and that Trinity College Dublin accepts no liability for indirect, consequential, or incidental, damages or losses arising from use of the thesis for whatever reason. Information located in a thesis may be subject to specific use constraints, details of which may not be explicitly described. It is the responsibility of potential and actual users to be aware of such constraints and to abide by them. By making use of material from a digitised thesis, you accept these copyright and disclaimer provisions. Where it is brought to the attention of Trinity College Library that there may be a breach of copyright or other restraint, it is the policy to withdraw or take down access to a thesis while the issue is being resolved.

**Access Agreement**

By using a Digitised Thesis from Trinity College Library you are bound by the following Terms & Conditions. Please read them carefully.

I have read and I understand the following statement: All material supplied via a Digitised Thesis from Trinity College Library is protected by copyright and other intellectual property rights, and duplication or sale of all or part of any of a thesis is not permitted, except that material may be duplicated by you for your research use or for educational purposes in electronic or print form providing the copyright owners are acknowledged using the normal conventions. You must obtain permission for any other use. Electronic or print copies may not be offered, whether for sale or otherwise to anyone. This copy has been supplied on the understanding that it is copyright material and that no quotation from the thesis may be published without proper acknowledgement.

# AN INVESTIGATION OF THE INFLUENCE OF DAILY ACTIVITIES AND LOCATION ON PERSONAL EXPOSURE TO AIR POLLUTION IN DUBLIN: MEASUREMENT, ANALYSIS, MODELLING AND APPLICATION

By

Andrew McCreddin B.A., B.A.I. (Hons), PG Dip. Stat.

A Thesis submitted to the University of Dublin for the degree of Doctor of Philosophy

Department of Civil, Structural and Environmental Engineering

University of Dublin

Trinity College

Dublin

TRINITY COLLEGE
19 JUN 2013
LIBRARY DUBLIN
Thesis 10147

# Declaration

I hereby declare that the work contained in this thesis is my own work, and has not been submitted as an exercise for a degree at this or any other university.

I also give the library permission to lend or copy this thesis, upon request, for academic purposes.

June 2013

Andrew McCreddin

# Summary

The research in this study was carried out to quantify real-time personal exposure to $PM_{10}$ in a large number of individuals residing in the Dublin area. This was carried out in order to highlight activities and locations with high personal exposure concentrations of particulate matter. In addition, the dataset was analysed using various numerical, statistical, and other techniques to develop predictive modelling tools.

The main subpopulation of individuals chosen for inclusion in the personal exposure study was office workers. The volunteers were required to monitor for 24-hour periods, which comprised one sample. The personal $PM_{10}$ exposure data for each subject was collected using a real-time nephelometer device, which recorded concentrations at two minute intervals. The subjects were also required to complete activity diaries and carry a GPS device with them at all times during sampling in order to record their movements.

Personal exposure data was collected for 255 separate 24-hour periods by 59 volunteers. The gathered dataset was comprehensively analysed using various statistical methods. The study population was found to spend over 90% of their time indoors. The mean 24-hour $PM_{10}$ personal exposure for the study population was found to below the EPA daily limit value. However, a number of indoor microenvironments were highlighted in which high concentrations could be encountered, and these included cafés, public houses, and recreation facilities such as gyms. Exposure to ETS was also found to be a large factor in raising personal exposure concentrations among subjects. The lowest personal concentrations were consistently found when the subjects were sleeping.

The $PM_{10}$ dose uptake into the respiratory system for each subject was also assessed. The largest dose uptake was found to occur when individuals were in their workplaces. While large uptake of dose was also found for other activities and locations, such as during recreation/sport and in the home. The uptake for male subjects was found to be higher than female subjects owing to their greater lung capacity.

Various modelling techniques were applied to the dataset in order to predict personal exposure to $PM_{10}$. The best performing model was found to be a time-activity weighted model based on each subject's previous data collection. Other modelling techniques such as Monte Carlo based sampling and machine learning techniques were also employed as predictive tools. The Latin hypercube population exposure simulation sensitivity analysis highlighted occupational exposure as the greatest influence on daily personal exposure concentrations.

Investigations of the influence of background $PM_{10}$ concentration and meteorological variables were also conducted. The regression analysis carried out found that background $PM_{10}$ concentration was only moderately correlated with the personal exposure data, with the Phoenix Park background station found to be the most correlated of the fixed site monitors. Regression analysis also found that the various meteorological conditions were relatively weak determinants of personal exposure. A number of baseflow separation techniques from hydrology were also utilised in order to relate background concentration data to $PM_{10}$ personal exposure.

In summary, this investigation has highlighted that personal exposure is an agglomeration of air pollution from a multitude of different sources including the background concentration.

# Acknowledgements

I would like to express my deep gratitude to my supervisor Dr. Aonghus McNabola for guiding me through this long and challenging journey. Aonghus has been there throughout my PhD research to offer valuable advice and constructive suggestions, and has always been willing to give up his time to help me with any problems I encountered along the way.

Thank you to my co-supervisor Dr. Laurence Gill for his guidance over the course of this project. I will also fondly remember his reign as head of the department with which my time as a postgraduate student happily coincided.

I wish to acknowledge the Environmental Protection Agency for providing the funding that enabled me to undertake this research project.

I would like express my sincere thanks to my fellow office colleagues and friends Aisling, Davie, Francesco, John, Mairéad, Mary, Seanie, and Ted, who have all contributed in their own unique way. My thanks also go to Paraic and Stevie for their friendship and support over the course of our postgraduate studies.

I would like to express my gratitude to all the people who volunteered to take part in this study, their efforts were greatly appreciated. Thank you to the various final year students, along with the exchange students, who helped me with various aspects of this project at different times. I would also like to extend my thanks to my fellow PhD students and staff of the Department of Civil Engineering for making it an absolute pleasure to be a part of.

Finally, I wish to thank my family for all their support along the way and it is to them that I dedicate this thesis. I would like to offer my special thanks to my parents, David and Vivienne, for all the encouragement they have given me throughout my years of education. I am also eternally grateful to my brother and sister, Robert and Suzanne, for their tremendous help and support.

# Table of Contents

**Declaration** ..... i

**Summary** ..... iii

**Acknowledgements** ..... v

**List of Figures** ..... xv

**List of Tables** ..... xxiii

**1 Introduction** ..... 3

1.1 Aims and Objectives ..... 3

1.2 Overview and Scope of Research Programme ..... 5

**2 Literarture Review** ..... 9

2.1 Introduction to Air Pollution ..... 9

2.2 Air Pollutants ..... 12

2.2.1 Carbon monoxide ..... 12

2.2.2 Nitrogen oxides ..... 14

2.2.3 Ozone ..... 17

2.2.4 Sulphur dioxide ..... 19

2.2.5 Volatile organic compounds ..... 21

2.2.6 Particulate matter ..... 22

2.2.7 Current state of Dublin air quality ..... 33

2.2.8 Summary of air pollutants ..... 35

2.3 Personal Exposure to Airborne Particles ..... 35

2.3.1 Measuring personal exposure ..... 36

2.3.2 Personal exposure studies ..... 38

2.4 Time-Activity Budget ..... 42

2.5 Determinants of Personal Exposure to PM ..... 43

2.5.1 Wind speed and direction ..... 43
2.5.2 Temperature ..... 46
2.5.3 Precipitation ..... 47
2.5.4 Traffic ..... 48
2.5.5 Indoor sources ..... 49
2.5.6 Occupational exposure ..... 53
2.5.7 Infiltration ..... 55
2.6 Comparison of Personal Exposure with Fixed Site Monitors ..... 57
2.7 Modelling Personal Exposure ..... 60
2.7.1 General concepts ..... 61
2.7.2 Exposure models ..... 62
2.7.3 Monte Carlo and Latin hypercube simulation methods ..... 69
2.8 Modelling of the Human Respiratory Tract ..... 72
2.9 Justification for Research ..... 75
2.10 Summary of Literature Review ..... 78
**3 Methodology ..... 83**
3.1 Introduction ..... 83
3.2 Experiment Design ..... 83
3.2.1 Particulate matter monitoring ..... 84
3.2.2 Location monitoring ..... 86
3.2.3 Activity monitoring ..... 88
3.2.4 Sampling protocol ..... 89
3.2.5 Ancillary microenvironmental monitoring ..... 90
3.3 Quality Control and Calibration ..... 94
3.3.1 Zero calibration ..... 94

3.3.2 Flow rate ..... 95
3.3.3 Accuracy ..... 96
3.3.4 Repeatability of the Aerocet-531 ..... 104
3.3.5 Effects of relative humidity ..... 105
3.4 Gravimetric Analysis ..... 108
3.4.1 Electrostatic effects ..... 109
3.4.2 Air buoyancy ..... 111
3.4.3 Weighing procedure ..... 113
3.4.4 Environmental conditions of weighing room ..... 117
3.4.5 Laboratory blanks ..... 119
3.5 Meteorological Data ..... 120
3.6 Data Analysis Methods ..... 121
3.7 Summary of Methodology ..... 122
**4 Results and Analysis ..... 125**
4.1 Monitoring Campaign ..... 125
4.1.1 Target population ..... 125
4.1.2 Home locations ..... 128
4.1.3 Failed samples ..... 130
4.2 Time-Activity Budget ..... 131
4.2.1 Location and activity categories ..... 137
4.3 Personal Exposure Analysis ..... 140
4.3.1 24-hour $PM_{10}$ exposure data ..... 140
4.3.2 Mean concentrations of 24-hour activity and location categories ..... 141
4.3.3 Cooking ..... 145
4.3.4 Individual 24-hour sampling periods ..... 152

4.3.5 Smoker data ..... 161
4.3.6 Other unusual activities and sources ..... 163
4.4 Descriptive Statistics of Ancillary Data ..... 166
4.4.1 Additional smoker data sampling ..... 167
4.4.2 Shopping centre monitoring ..... 172
4.4.3 Taxi monitoring ..... 177
4.5 Summary ..... 183
**5 Dosimetry ..... 189**
5.1 Introduction ..... 189
5.2 ICRP Model Background ..... 190
5.3 Respiratory Tract Morphology ..... 190
5.3.1 Deposition of particles ..... 193
5.4 Form of the Deposition Model ..... 193
5.4.1 General formulation of particle deposition from tidal airflow ..... 194
5.5 Filtration efficiencies specification ..... 197
5.5.1 Intake ..... 197
5.5.2 Regional deposition efficiency ..... 198
5.6 Parameters of the Model ..... 198
5.6.1 Inhalability ..... 198
5.6.2 Breathing habit ..... 199
5.6.3 Scaling of deposition efficiency for body size ..... 200
5.6.4 Age and sex specific effects ..... 200
5.6.5 Ventilation parameters ..... 202
5.6.6 Inhaled daily volumes of air ..... 203
5.7 Modelled 24-Hour Dose Uptake ..... 206

5.7.1 Overall study population dose ..... 206
5.7.2 Individual microenvironment and activity doses ..... 208
5.7.3 Comparison of dose uptake and mean personal $PM_{10}$ concentrations ..... 211
5.7.4 Gender differences for dose uptake ..... 214
5.7.5 Dose uptake of smokers ..... 217
5.7.6 Analysis of travel modes ..... 219
5.7.7 Comparison between two dose methods ..... 224
5.8 Summary ..... 226
**6 Exposure Modelling ..... 233**
6.1 Introduction to Exposure Modelling ..... 233
6.2 Exposure Model Development ..... 235
6.2.1 Integrated time-activity models ..... 235
6.2.2 Model evaluation ..... 236
6.3 Integrated Time-Activity Model Results ..... 238
6.4 Exposure Simulation ..... 242
6.4.1 Population exposure simulation ..... 243
6.4.2 Individual sample simulation ..... 251
6.5 Neural Network Modelling ..... 258
6.5.1 Feed Forward Neural Networks ..... 260
6.5.2 Generalised Regression Neural Networks ..... 263
6.5.3 FFNN model development and results ..... 264
6.5.4 GRNN model development and results ..... 271
6.6 Summary ..... 274
**7 Background and Regression Modelling ..... 281**
7.1 Regression Analysis ..... 281

7.1.1 Simple linear regression ..... 282
7.1.2 Multiple linear regression ..... 282
7.2 Fixed Site Monitor Comparison ..... 283
7.2.1 FSM locations in Dublin ..... 283
7.2.2 Phoenix Park FSM analysis ..... 284
7.2.3 FSM near to workplace analysis ..... 289
7.2.4 FSM near to home analysis ..... 290
7.2.5 MLR of combined FSMs ..... 291
7.2.6 Relationship between FSMs and occupational exposure ..... 292
7.2.7 Spatial variability ..... 294
7.3 Meteorological Determinants ..... 295
7.4 Analysis of Multiple Determinants ..... 299
7.5 Baseflow Separation Methods ..... 302
7.5.1 Conceptual design ..... 303
7.5.2 Boughton method ..... 304
7.5.3 Sliding-interval method ..... 304
7.5.4 Baseflow separation results: Boughton method ..... 305
7.5.5 Baseflow separation results: Sliding interval method ..... 307
7.6 Summary ..... 310
**8 Discussion ..... 317**
8.1 Overview of Topics Raised ..... 317
8.2 Time-Activity Patterns ..... 317
8.3 Personal Exposure Concentrations ..... 319
8.3.1 Occupational exposure ..... 321
8.3.2 Commuter exposure ..... 324

8.3.3 Cooking ..... 325
8.3.4 ETS exposure ..... 326
8.4 Uptake of $PM_{10}$ ..... 327
8.5 Modelling of Personal Exposure ..... 329
8.6 Determinants of Personal Exposure ..... 331
8.7 Baseflow Separation ..... 332
8.8 Limitations of the Study ..... 333
**9 Conclusions and Recommendations ..... 341**
9.1 Conclusions ..... 341
9.2 Recommendations for Future Research ..... 344
**References ..... 349**
**Appendices**

# List of Figures

Figure 2.1: London smog episode in December 1952 (Retronaut, 2012)..... 10
Figure 2.2: Trends in $SO_2$ emissions in Ireland from 1990 to 2008 (EPA, 2010)..... 20
Figure 2.3: Relative size of particles (US EPA, 2012)..... 23
Figure 2.4: An idealised size distribution showing the different modes that comprise fine and coarse particles. Also shown are the major growth and formation mechanisms of the four modes (US EPA, 2004)..... 25
Figure 2.5: Particle penetration curve of an ideal inlet for five different size-selective sampling criteria (US EPA, 2004)..... 26
Figure 2.6: Loss in statistical life expectancy that can be attributed to anthropogenic contributions to $PM_{2.5}$ for the year 2000 (left) and the projection for 2020 (right) (EEA, 2007)..... 30
Figure 2.7: Pollutant dispersion in a regular street canyon (Dabberdt et al., 1973)..... 45
Figure 2.8: An example of a wintertime temperature inversion (NOAA, 2012)..... 47
Figure 2.9: Total personal exposure contains both ambient and non-ambient exposures (Wilson and Brauer, 2006)..... 62
Figure 2.10: An example of the *EXPOLIS* @Risk population exposure distribution for Helsinki (Jantunen and Kansanterveyslaitos, 1999)..... 70
Figure 2.11: An example of the *EXPOLIS* @Risk cumulative population exposure distribution for Helsinki (Jantunen and Kansanterveyslaitos, 1999)..... 71
Figure 2.12: Example of an @Risk sensitivity analysis output (Jantunen and Kansanterveyslaitos, 1999)..... 71
Figure 3.1 An Aerocet-531 particle mass profiler..... 85
Figure 3.2: A typical un-calibrated Aerocet-531 24-hour period output for $PM_{10}$..... 86
Figure 3.3: Garmin GPSMAP 60CSx..... 87
Figure 3.4: An example of a volunteer's track recorded by the GPS..... 88
Figure 3.5: (A) - Dundrum Shopping Centre, and (B) - Jervis Street Shopping Centre. 92
Figure 3.6: Aerocet-531 with a zero filter..... 95
Figure 3.7: Flow testing an Aerocet-531..... 96
Figure 3.8: Haz-Dust EPAM-5000 with (A) filter cassette, (B) 47mm filter, (C) Size selective impactor, (D) Zero filter, (E) Impactor sleeve..... 97

Figure 3.9: $PM_{2.5}$ (left) and $PM_{10}$ (right) impactors. ..... 98
Figure 3.10: Indoor calibration graph of Aerocet-531 versus gravimetric analysis..... 99
Figure 3.11: Outdoor calibration graph of Aerocet-531 versus gravimetric analysis... 100
Figure 3.12: Indoor calibration plot of Aerocet-531 versus Haz-Dust with no intercept. ..... 101
Figure 3.13: Outdoor calibration plot of Aerocet-531 versus Haz-Dust with no intercept. ..... 101
Figure 3.14: Combined indoor and outdoor calibration plot without an intercept..... 102
Figure 3.15: Indoor $PM_{2.5}$ calibration plot of Aerocet-531 versus Haz-Dust. ..... 103
Figure 3.16: Outdoor $PM_{2.5}$ calibration plot of Aerocet-531 versus Haz-Dust..... 103
Figure 3.17: Comparison of two-hour averaged pDR to BAM $PM_{2.5}$ concentration ratio as a function of relative humidity (Chakrabarti et al., 2004). ..... 106
Figure 3.18: Cahn C-33 Microbalance. ..... 109
Figure 3.19: Staticmaster..... 111
Figure 3.20: Desiccator cabinet..... 114
Figure 3.21: Silica gel beads with no moisture (left) and with moisture absorbed (right). ..... 115
Figure 3.22: A Kestrel 4500 Pocket Weather Tracker. ..... 118
Figure 3.23: Weather station locations at Dublin Airport (A), and Phoenix Park (B).. 121
Figure 4.1: Pie chart of the percentage of male and female volunteers recruited. ..... 126
Figure 4.2: The percentage of volunteers in each age group. ..... 127
Figure 4.3: Home locations of subjects in the Greater Dublin Area and surrounding commuter towns. ..... 128
Figure 4.4: Home locations of volunteers living in Dublin City. ..... 129
Figure 4.5: Types of residence of the study population. ..... 130
Figure 4.6: Pie chart showing the mean daily percentage of time the volunteers spent in six different locations. ..... 133
Figure 4.7: A summary for the overall population 24-hour $PM_{10}$ personal exposure samples collected by the volunteers. ..... 141
Figure 4.8: Column chart of the population main activities and locations by descending mean $PM_{10}$ personal exposure concentration ($\mu g/m^3$). ..... 142

Figure 4.9: An example of frying in the home of a volunteer and the removal of the large peak. ..... 148
Figure 4.10: Individual value plot of $PM_{10}$ concentrations for six different methods of cooking. ..... 151
Figure 4.11: Boxplot of the reported ventilation conditions present while cooking. ... 152
Figure 4.12: A boxplot of six sampling days completed by Volunteer A, with the mean (circular marker) and median values (horizontal lines) marked. ..... 154
Figure 4.13: A dot-plot for each of the six sampling days completed by Volunteer A. 154
Figure 4.14: GPS tracks for Volunteer A with the first 3-day sampling period shown in green, and second sampling period track shown in pink. Also shown are the home and office locations for this volunteer. ..... 155
Figure 4.15: Cooking events from Volunteer A. ..... 160
Figure 4.16: An example of a smoking event in the home of a volunteer. ..... 162
Figure 4.17: An incense burning event that was reported in the home of a female volunteer. ..... 164
Figure 4.18: Example of deodorant being sprayed in the vicinity of the Aerocet-531. 165
Figure 4.19: A bus commute of a volunteer showing an increase in concentration as the bus passed a burning vehicle. ..... 166
Figure 4.20: In-home time series of $PM_{10}$ concentrations ($\mu g/m^3$) for Smoker A, with all reported smoking events (red stars) and cooking events (purple stars) marked. ..... 169
Figure 4.21: In-home time series of $PM_{10}$ concentrations ($\mu g/m^3$) for Smoker B, with all reported smoking events (red stars) and cooking events (purple stars) marked. ..... 171
Figure 4.22: Location of the Jervis Street (left) and Dundrum (right) shopping centres. ..... 173
Figure 4.23: Mean in-car $PM_{10}$ concentrations ($\mu g/m^3$) for each driver work shift. .... 178
Figure 4.24: GPS tracks of all four taxi drivers (D1 - Blue; D2 - Green; D3 - Turquoise; D4 - Red). ..... 180
Figure 4.25: The area defined as 'city centre' as highlighted by the red border. ..... 181
Figure 5.1: The anatomical regions of the human respiratory tract (ICRP, 1994). ..... 191
Figure 5.2: Panel (a) illustrates basic airway anatomy. Structures are epithelial cells, EP; basement membrane, BM; smooth muscle cells, SM; and fibrocartilaginous coat, FC.

Panel (b) illustrates the relative amounts of liquid, tissue, and blood with distal progression (US EPA, 2009). ..... 192
Figure 5.3: Empirical representation of inhalability of particles and their deposition in the extrathoracic, bronchial, bronchiolar, and alveolar-interstitial regions of the respiratory tract during continuous cyclic breathing by transport through a series of filters (ICRP, 1994). ..... 194
Figure 5.4: A general representation of aerosol deposition for tidal flow through a series of filters (ICRP, 1994). ..... 197
Figure 5.5: Intake efficiency of the human head at random orientation to moving air (ICRP, 1994). ..... 199
Figure 5.6: Summary statistics for the 24-hour dose uptake of the study population... 207
Figure 5.7: Boxplot of the top four microenvironments/activities with the largest dose associated ..... 210
Figure 5.8: Boxplot of population dose uptake across all other major activities and locations. ..... 211
Figure 5.9: A comparison of the mean dose uptake of the study population in various microenvironments with the corresponding personal $PM_{10}$ concentrations in each. .... 213
Figure 5.10: Summary statistics and dose distribution for male subjects. ..... 214
Figure 5.11: Summary statistics and dose distribution for female subjects. ..... 215
Figure 5.12: Comparison of lognormal distributions for the male and female dose data. ..... 216
Figure 5.13: Comparison of the mean 24-hour dose uptakes of smokers and non-smokers of the study population ..... 218
Figure 5.14: Mean dose uptake of each travel mode for the study population. ..... 220
Figure 5.15: Distributions of doses for each mode of travel (μg). ..... 221
Figure 5.16: Comparison of total dose for 25 randomly selected 24-hour samples using two different estimation methods. ..... 225
Figure 6.1: Plot of the 24-hour personal exposure concentrations of the observed data (green line), and the simulated 24-hour exposures of Model 1 (blue line) and 2 (red line) for each subject test case. ..... 239

Figure 6.2: Correlation between the simulated 24-hour personal exposure $PM_{10}$ concentrations and the corresponding observed 24-hour concentrations for Model 1. 239
Figure 6.3: Correlation between the simulated 24-hour personal exposure $PM_{10}$ concentrations and the corresponding observed 24-hour concentrations for Model 2. 240
Figure 6.4: Distributions for (a) the 25 observed personal exposure concentrations, (b) the results obtained from Model 1, and (c) the results obtained from Model 2..... 241
Figure 6.5: Comparison of the exposure distributions for the 25 observed concentrations, Model 1 results, and Model 2 results..... 242
Figure 6.6: Example of the effect of stratification in Latin hypercube sampling (Vose, 2008). ..... 243
Figure 6.7: Beta distribution for the population time fraction of time spent at work... 246
Figure 6.8: Comparison of observed and Latin Hypercube simulated exposure distributions. ..... 248
Figure 6.9: Correlation coefficients for simulated total exposure inputs of microenvironment concentrations ($C_i$) and the time fractions ($f_i$). ..... 249
Figure 6.10: Tornado graph of the regression mapped values of the simulation model inputs. Each value represents the change in total exposure with a one standard deviation change in a particular input, with all others held constant..... 250
Figure 6.11: The probability distributions for all microenvironments. ..... 253
Figure 6.12: Linear regression of observed exposures versus modelled exposure for the 100 iterations simulation..... 255
Figure 6.13: The 24-hour personal exposure concentrations of each of the 25 test subjects from the 100 iteration simulation..... 255
Figure 6.14: Probability distribution for the homes of smoking subjects..... 256
Figure 6.15: Probability distribution for the activity of sleeping for smokers. ..... 256
Figure 6.16: Monte Carlo simulated personal exposures with additional smoker test cases. ..... 258
Figure 6.17: An example of a single input neuron. ..... 259
Figure 6.18: The general structure of a FFNN (Firat and Gungor, 2009). ..... 260
Figure 6.19: The general structure of a GRNN (Cigizoglu and Alp, 2006). ..... 263

Figure 6.20: A schematic diagram of the FFNN used to predict the 24 hour exposures. ..... 265
Figure 6.21: Correlations for the training, validation, testing and overall performance of the FFNN model ($\mu g/m^3$). ..... 268
Figure 6.22: The model output (dotted line) compared with the observed 24-hour target data (grey line). ..... 268
Figure 6.23: Plot of the training, validation, and test performances of the FFNN model. ..... 269
Figure 6.24: Error histogram for the FFNN model ($\mu g/m^3$)..... 270
Figure 6.25: Residual errors of the FFNN predicted personal exposure data values.... 270
Figure 6.26: Regression of the GRNN model predicted personal exposures versus the observed data during model training. ..... 271
Figure 6.27: Histogram of the training errors between the targets and the outputs. ..... 272
Figure 6.28: Correlation for the test cases between the predicted personal exposures and observed data. ..... 273
Figure 6.29: Residual errors of the GRNN predicted personal exposure data values... 273
Figure 7.1: Locations of the FSMs showing $PM_{10}$ (red), $PM_{2.5}$ (blue), and collocated $PM_{10}$ and $PM_{2.5}$ (green) monitoring sites. ..... 284
Figure 7.2: A graph of all subject sampling days showing the background concentration measured at the Phoenix Park (red line) and the 24-hr personal exposures (blue line). ..... 286
Figure 7.3: Linear regression plot of the log-transformed 24-hr $PM_{10}$ personal exposure concentrations versus the background concentration measured at the Phoenix Park. .. 287
Figure 7.4: Linear regression plot of the log-transformed occupational $PM_{10}$ personal exposure concentrations versus the background concentration measured at the Phoenix Park..... 288
Figure 7.5: Linear regression plot of the log-transformed 24-hr $PM_{10}$ personal exposure concentrations versus the corresponding FSMs nearest to the workplace of each individual..... 289
Figure 7.6: Linear regression plot of the 24-hr $PM_{10}$ personal exposure concentrations versus the corresponding FSMs nearest to the workplace of each individual. ..... 291

Figure 7.7: Plot of the $PM_{10}$ personal exposure concentration while at work versus the corresponding FSM concentration nearest to the workplace of each individual. ..... 293
Figure 7.8: Example of a wind rose created from Dublin Airport meteorological data for a randomly selected day, illustrating the predominant wind direction on that day. ..... 296
Figure 7.9: Comparison of the Boughton method predicted background concentrations versus the observed background concentrations ($\mu g/m^3$). ..... 306
Figure 7.10: Time series plots of a 24-hour personal exposure sample and Boughton separated baseflow for the sample. ..... 306
Figure 7.11: Comparison of the second Boughton method predicted background concentrations versus the observed background concentrations ($\mu g/m^3$). ..... 307
Figure 7.12: Time series plots of a 24-hour personal exposure sample and three sliding interval separated baseflows for the sample. ..... 308
Figure 7.13: Comparison of sliding interval separated (10 mins) predicted background concentrations versus the observed background concentrations ($\mu g/m^3$). ..... 309
Figure 7.14: Comparison of sliding interval separated (30 mins) predicted background concentrations versus the observed background concentrations ($\mu g/m^3$). ..... 310
Figure 7.15: Comparison of sliding interval separated (1 hour) predicted background concentrations versus the observed background concentrations ($\mu g/m^3$). ..... 310

# List of Tables

Table 2.1 Size distributions for the modes of particulate matter. ..... 24
Table 3.1: One-way ANOVA table for Aerocet-531 comparison. ..... 104
Table 3.2: Calculated effects on the change in weighed masses caused by the buoyancy effect due to a change in weighing room environmental conditions (Koistinen et al., 1999). ..... 113
Table 3.3: Kestrel 4500 specifications for temperature, relative humidity and pressure. ..... 118
Table 3.4: Summary of environmental conditions present in the weighing room. ..... 119
Table 4.1: Time spent in different microenvironments (min $d^{-1}$). ..... 134
Table 4.2: List of activity codes of the most common activities and locations reported by volunteers. ..... 137
Table 4.3: Example of a 24-hour activity pattern as reported in the activity diary, containing beginning and ending times, activity and location summary, and time spent in each microenvironment visited. ..... 139
Table 4.4: The mean, standard deviation, maximum and median values for the primary activities and microenvironments of all the 24-hour $PM_{10}$ personal exposure samples. ..... 143
Table 4.5: Summary descriptive statistics of volunteer sampling days that reported cooking. Both before and after the removal of cooking events are shown. ..... 149
Table 4.6: Summary statistics of the primary cooking methods when reported as the sole type of cooking taking place by a subject. ..... 150
Table 4.7: Descriptive statistics based on all data for Volunteer A. Time spent and concentrations of $PM_{10}$ recorded in the respective microenvironments by Volunteer A. ..... 157
Table 4.8: Comparison of the mean personal exposure for each sampling day with two fixed site monitors in Dublin City. ..... 159
Table 4.9: Descriptive statistics for the sampling days of Smokers A and B. ..... 172
Table 4.10: Comparison of peak and off-peak $PM_{10}$ concentrations ($\mu g/m^3$) for various locations in Dundrum shopping centre. ..... 175

Table 4.11: Comparison of peak and off-peak $PM_{10}$ concentrations ($\mu g/m^3$) for various locations in the Jervis Street shopping centre. ..... 176
Table 4.12: Summary of Taxi driver shift times, $PM_{10}$ concentrations ($\mu g/m^3$) and in-vehicle environmental conditions..... 179
Table 4.13: Average $PM_{10}$ exposure and work shift durations for all drivers over their respective sampling periods. ..... 180
Table 4.14: Mean $PM_{10}$ concentrations ($\mu g/m^3$) while drivers are inside and outside the city centre area, and stationary at taxi ranks. ..... 182
Table 5.1: The fraction of total ventilator airflow ($F_n$) passing through the nose in nasal augmenters and in mouth breathers (ICRP, 1994). ..... 200
Table 5.2: Biometry and lung volumes for Caucasian adults (ICRP, 1994). ..... 201
Table 5.3: Reference respiratory values for a general Caucasian population at different levels of activity (ICRP, 1994)..... 202
Table 5.4: Recommended values of daily ventilation rates ($m^3$) for sedentary adult workers (ICRP, 1994). ..... 203
Table 5.5: Physical exertion levels used for various activities in the Human Respiratory Tract model for subject dose estimation. ..... 204
Table 5.6: Reference respiratory values for a general Caucasian population for the activity of cycling..... 206
Table 5.7: Descriptive statistics for dose of the study population for the main activities and microenvironments. ..... 209
Table 5.8: Results from a Mann-Whitney U test to assess if the difference between male and female dose uptake data was significant. ..... 217
Table 5.9: Summary of dose uptake in the homes of Smokers A and B..... 219
Table 5.10: ANOVA of the absolute difference between the mean ranks and ranks of travel groups, the non-parametric equivalent of Levene's Test. ..... 221
Table 5.11: Kruskal-Wallis Test results on the travel mode doses. ..... 222
Table 5.12: Post-hoc tests on pairs of travel modes for dose uptake. ..... 223
Table 6.1: The types of distributions assigned to each of the main microenvironments and activities..... 245
Table 6.2: Observed and simulated population exposure distribution values ($\mu g/m^3$). 247

Table 6.3: Results of the different Monte Carlo simulations on the test sample days.. 254
Table 6.4: The input parameters for the FFNN and GRNN models. ..... 266
Table 6.5: Summary of each of the personal exposure models used for the prediction of individual 24 hour personal exposure concentrations ($\mu g/m^3$). ..... 274
Table 7.1: Multiple linear regression analysis of log transformed 24-hour personal exposure concentrations versus the FSM data. ..... 292
Table 7.2: Model summary with the dependent variable as the Log-occupational exposure ($\mu g/m^3$) and the predictor of Log-FSM concentration ($\mu g/m^3$) nearest to each working location. ..... 293
Table 7.3: Model summary for Log-occupational personal exposure with predictor variables of Log-$PM_{10}$ concentration ($\mu g/m^3$) from the FSM nearest to each workplace and the distance (km) to that FSM. ..... 295
Table 7.4: Model summary for the stepwise MLR of influence of weather variables on log transformed 24-hr exposure. ..... 297
Table 7.5: ANOVA of the stepwise MLR model. ..... 297
Table 7.6: Coefficients of the predictors in the MLR model for steps 1 and 2. ..... 298
Table 7.7: Excluded variables from the MLR model after the second iteration. ..... 299
Table 7.8: Model summary for the MLR analysis. ..... 300
Table 7.9: ANOVA of the stepwise MLR model. ..... 300
Table 7.10: Coefficients of the predictors in the MLR model for steps 1 to 4. ..... 301
Table 7.11: Excluded variables from the MLR model after the last step. ..... 302

# Chapter 1

Introduction

# 1 Introduction

## 1.1 Aims and Objectives

Epidemiological studies have shown that the low levels of air pollution in most industrialised societies are still linked to adverse health outcomes. There has been much research activity to investigate the possible associations between short term fluctuations in airborne particulate matter and morbidity, and mortality from long term exposure. However, most of the epidemiological investigations rely on measurements of the pollutant at some central location in the city and then use these data as a surrogate for individual exposure.

Owing to the exposures encountered due to certain activities and microenvironments, background concentration may in many instances be an unsatisfactory basis on which to solely investigate the impacts of air pollution on human populations. A more relevant measure for individual subjects of an air pollutant health impact assessment would be personal exposure. This can be quantified by recording personal exposure data over 24-hour periods on a real-time basis incorporating different activities (e.g. commuting, shopping, working, sleeping, etc.) and different locations. However, rather than attempt to collect personal exposure data from a broad spectrum of the general population, the specific sub-population of office workers was identified for monitoring.

This research study aims to gather sufficient data of this nature to be used in the development of predictive modelling tools. Different statistical methods will be applied in order to investigate a number of novel approaches to the prediction of 24 hour personal exposure concentrations, as well as dose. The successful implementation of this approach will lead to a personal exposure model on a macroscopic scale which could be used to investigate the health impacts of personal exposure to air pollution in a more extensive and comprehensive manner than using background concentrations.

In addition as it is impractical to monitor personal exposure on a long term basis, and due to the fact the monitoring of background data is a legal requirement in many

countries, it is also the aim of this research project to develop methods of predicting personal exposure from background monitoring data. This will be achieved through the investigation of background monitoring data from monitoring stations located across the Dublin region in conjunction with GPS data on subject locations.

In combination, the development of personal exposure models from activity and location data, and from background monitoring data, will enable health assessment researchers to carry out more robust investigations.

The primary aims of this research project are:

- Quantify the daily personal exposure of office workers to particulate air pollutants for individuals living and working in different areas of Dublin and its satellite towns.

- Provide a statistical analysis of the dataset to highlight locations or activities with high personal exposure concentrations of particulate matter and disseminate this information to the public.

- Examine the personal dose encountered by the volunteers which will highlight the activities and locations which have the highest uptake into the lungs.

- Analyse the dataset using various numerical, statistical, and machine learning techniques to develop novel predictive modelling tools.

- Apply these new models to the prediction of personal exposures groups and compare these predictions with actual measurement data.

- Examine and develop relationships between the background concentrations of PM recorded near homes and workplaces, as well as other city centre outdoor environments, and the personal exposure to particulate matter measured by individual participants in the study.

## 1.2 Overview and Scope of Research Programme

The research programme involved an extensive review of the history of air quality and atmospheric science, air pollution epidemiology, personal exposure sampling, personal exposure modelling methods, as well as human respiratory tract modelling. An air quality sampling campaign was subsequently conducted to measure the daily personal exposure concentrations of individuals from Dublin and surrounding satellite towns.

The research work was funded by the EPA, and as such, much of the boundaries of the project were predefined. The stipulations of the EPA funding stated that particulate matter was the main air pollutant to be measured during the personal exposure campaign. The scope of the project also meant that the location (Dublin), type of volunteers (office workers), and number of samples were also circumscribed by the conditions of funding. Furthermore, the particulate matter personal sampling campaign was one of the three unique elements of the overall EPA funded *PALM* project.

The sampling campaign itself lasted a 28 month period between February 2009 and June 2011. During this time a total of 255 successful sampling days were obtained from the volunteers for personal exposure to particulate matter. This personal exposure sampling also collected large amounts of data on the activities and the movements of the study population as supplementary information. Running concurrently with the volunteer sampling was the calibration campaign, which involved taking 49 separate calibration samples, indoor and outdoor, in order to correctly calibrate the personal monitoring equipment. Finally, additional personal exposure sampling was collected for smokers, an additional occupation (taxi drivers), and also other common destinations (shopping centres). Extra samples were obtained from shopping centres as this location was under sampled from when compared to on street shopping.

On completion of the experimental sampling aspect of the research programme, the 24 hour personal exposure samples were statistically analysed. This phase involved identifying the microenvironments and activities which contributed most to the daily personal exposure of the study population. The effects of sources such as cooking and

smoking were also analysed and discussed. Additionally, the activity patterns of the study populous were established and summarised.

Following on from the initial analysis and summaries of the personal exposure samples, a number of different modelling techniques were applied to the dataset. Firstly, a human respiratory tract model was used in order to calculate and assess the dose uptake experienced by all of the subjects. The personal exposure samples for all days could be converted into particle deposition in the lungs with use of the respiratory tract model. This model enabled the identification of the activities and microenvironments which had the largest dose uptake associated with them during the sampling campaign.

Following the human respiratory tract model, a number of modelling methods were used to estimate personal exposure. These included time-weighted activity modelling, Monte Carlo based simulations, as well as machine learning techniques which included several different neural network approaches. A risk analysis of personal exposure for the study population was also conducted using a Latin hypercube sampling simulation.

Finally, the influence of other determinants on the daily personal exposure of the study subjects was also investigated. This was done primarily through the construction of simple and multiple linear regression models. The variables examined included various background particulate monitoring stations, along with numerous meteorological parameters. A number of hydrological baseflow techniques were also employed as a means of deriving the background concentrations from the time series of the collected personal exposure data.

# Chapter 2

## Literature Review

# 2 Literarture Review

## 2.1 Introduction to Air Pollution

Air pollution is defined by the US EPA as *"The presence of contaminants or pollutant substances in the air that interfere with human health or welfare, or produce other harmful environmental effects"*. Over the last few decades the need for better air quality has been recognised and efforts have been made internationally in establishing minimum quality standards for the ambient air. During the twentieth century, this increased awareness of air pollution coupled with advances in control and monitoring technologies has served to deepen our understanding of atmospheric processes in the field of environmental science. However, air pollution science is not an exclusively modern branch of science, but in fact can trace its roots back through the centuries.

The effects of urban air pollution were first recognised in cities as far back as classical times. Classical writers such as the poet Horace have mentioned the blackening of buildings in ancient Rome. Even Emperor Nero's tutor Seneca wrote in AD 61 that no sooner did he leave Rome's oppressive fumes and culinary odours than he felt better. These ancient cities in which Horace and Seneca resided were often small and overcrowded as a result of the need for defences and to simplify the movement of goods and people. Indeed, medieval European cities often gave rise to street canyons due to the densely packed tall buildings that lined narrow streets. These conditions coupled with small scale industries that were in operation, especially lime production, would have given rise to serious air quality problems inside the cities. In fact, the earliest attempts at control of air pollution were made in medieval London with the setting up of a commission in 1285 to investigate the pollution problem from coal burning. This action eventually led to a proclamation in 1306 issued by the commission which banned the use of sea-coal in the city (Brimblecombe, 1987).

Up until the middle of the 19$^{th}$ century increased mortality due to environmental causes, such as air pollution episodes, were accredited to miasma (Anderson, 2009). This theory prevailed from ancient times from Europe as far China, and led people to believe that

diseases such as the Black Death and cholera were caused by *"bad air"* or *"stinking fogs"*. The theory of miasma was eventually displaced by germ theory, but the reasons why mortality increased during air pollution episodes remained unclear. The introduction of the Bills of Mortality in London in the 17th century followed by the introduction of death registration in England in 1837 eventually enabled easier identification of increased mortality due to air pollution episodes (Anderson, 2009). However, up until the 1930's it was generally believed that the observed increased death rate during a pollution episode was due to extremely cold weather that accompanied winter temperature inversions, rather than the accompanying air pollution (Russell, 1926).

Figure 2.1: London smog episode in December 1952 (Retronaut, 2012).

It was not until the London smog episode that occurred between the 5th and 9th of December 1952 (Figure 2.1) that the risk to public health was finally established beyond any doubt. Prior to this, it was two episodes in a small town in the Meuse Valley, Belgium, and in Donora, Pennsylvania, which led to widespread acceptance that air pollution, at least very high concentrations, could increase mortality in the short-term independently of the cold conditions associated with winter temperature inversions

(Anderson, 2009). In both these locations there was a large increase in deaths, but because of their low populations the actual number of mortalities was small, and furthermore, there was a suggestion of specific toxic chemicals playing a role in the mortalities due to the industrial nature of both locations (Anderson, 2009). In London however, smoke concentrations were recorded at three to five times normal levels during the 1952 smog episode which resulted in an estimated 4,000 excess deaths in the following three weeks, but according to a recent retrospective study which looked at deaths through to March 1953, the figure was closer to 12,000 deaths (Bell et al., 2003). The London smog was the first major air pollution episode to be extensively investigated in a large city, and it was this event, coupled with smog events that often enveloped other cities around the world, that succeeded in making the public acutely aware of the dangers of air pollution.

From the 1960's and 70's onwards public awareness of environmental issues developed and environmental movements sprang up throughout the western world, and one of the best examples of this is the founding of Greenpeace in 1971. The increase in awareness is partly explained by the increased wealth of these nations. As countries in North America and Western Europe grew wealthier, the public had an environmental awakening whereby people recognised it was not necessary to suffer environmental contaminants, such as air pollution, in order to have a prosperous economy. Though this environmental movement has been led primarily by the upper middle classes, it is the poor who are most often exposed to the most severe air pollution as well as other environmental insults (Nevers, 2000). This is reflected in many of the developing nations of Asia today, cities in China and India, where poverty is rife, can suffer far higher air pollutant concentrations than developed cities of the west (Anderson et al., 2010).

Today, air pollution emissions derive from almost all economic and societal activities. In Europe, emissions of many air pollutants have decreased since 1990. Much progress has been made in tackling air pollutants such as sulphur dioxide ($SO_2$), carbon monoxide (CO), and benzene ($C_6H_6$), while other pollutants still present a serious threat to the health of Europeans and the environment (European Environment Agency, 2012).

In Ireland, one of the less desirable impacts of increased prosperity over the last two decades has been the traffic congestion resulting from the large increase in car ownership. The number of vehicles on Irish roads more than doubled between 1990 and 2006. Over this period the total increased by 118% (5% per annum on average) to reach 2,138,680 vehicles in 2006. Increasing traffic volumes have resulted in increased congestion in the past few years, and major roads around Dublin such as the N4, N7, and M50 have all been widened to accommodate extra traffic lanes. During the Celtic Tiger years, escalating land prices in the city resulted in many people purchasing homes in adjacent counties and now commute in and out of the city each day. Air pollution from traffic is therefore an important source of emissions in Dublin, and many of these air pollutants will be discussed in the following section.

## 2.2 Air Pollutants

There are several main types of air pollution that originate from a variety of sources, all of which have well known effects that have implications for the wellbeing of human health and the environment. Many of these harmful pollutants enter the atmosphere from sources that are beyond the control of mankind. However, in the most densely populated areas of the globe the principal sources of these pollutants are emitted through anthropogenic activities. These air pollutants are either emitted directly into the atmosphere as primary sources, or else can form indirectly within the atmosphere as a secondary source. The physical state of air pollutants in the atmosphere fall into two distinct categories of either gaseous pollutants, which are present as gases and vapours, or particulate pollutants, which comprise material in solid or liquid phase suspended in the atmosphere. This section will provide a synopsis of many of the major air pollutants that pollute our towns and cities, and will briefly describe the formation and some of the accompanying undesirable effects associated with each.

### *2.2.1 Carbon monoxide*

Carbon monoxide (CO) is a colourless, odourless, flammable gas that is a product of the incomplete combustion of carbon containing materials and is one of the most common and widely distributed air pollutants (WHO, 2000). Worldwide annual emissions of CO

have been estimated to be as high as 2.6bn tonnes, of which 40% are from natural processes and approximately 60% are a result of human activities (US EPA, 2000). The largest anthropogenic source of CO is from vehicle exhausts, especially those with petrol engines. Indeed, petroleum derived emissions have increased hugely over the last few decades (Cullis and Hirschler, 1989). Other major contributing sources include coal fired power stations, various industrial processes and waste incinerators.

In urban areas, up to 95% of CO is emitted by motor vehicles (Hill, 2010). It is closely associated with the quantitative and temporal levels of other vehicular pollutants such as nitrogen oxides and volatile organic compounds (Derwent et al., 1995; Dor et al., 1995). Concentrations of CO are often highest inside cars, where it has been reported to be two to five times higher than levels measured on the street (Rudolf, 1994; Fernandez-Bremauntz and Ashmore, 1995). Lesser sources of CO include tobacco smoke and facilities that burn coal, natural gas or biomass. In homes, high concentrations of CO have been measured where there are faulty or unvented combustion appliances and where ventilation is poor (WHO, 2000). Moreover, it is often in the kitchen of homes where there are the highest CO concentrations from the use of gas burners (Brunekreef et al., 1982; US EPA, 2000).

High concentrations of CO that are often found in city traffic can aggravate heart problems and can cause congestive heart failure in older people (Hill, 2010). It is so toxic because it affects the blood protein haemoglobin which is responsible for transporting oxygen from the lungs to the body's cells. Approximately 80–90% of the absorbed CO binds with haemoglobin because it has 250 times greater affinity for the iron atom in haemoglobin than oxygen (Raub, 1999). This displacement of the oxygen molecule reduces the oxygen carrying capacity of the haemoglobin and impairs the release of oxygen from haemoglobin to extravascular tissues and the heart. Lower levels of oxygen reaching the brain can also cause headache, dizziness, fatigue and drowsiness (Hill, 2010). Higher levels of CO can eventually cause CO poisoning, possibly resulting in coma and death.

In Ireland, carbon monoxide levels are low and primarily originate from traffic sources. Typically the highest emission rates occur in heavy traffic in urban areas where frequent stopping and starting and low average speeds all contribute to increased levels of CO (O'Mahony et al., 2000). Levels of CO have dropped significantly in recent times in North America and Western Europe through mitigating efforts by regulators. In the early 90's for example, the introduction of oxygen containing fuel additives to petroleum helped improve efficiency of engines by enhancing burning in winter, leading to a dramatic drop in CO emissions (Hill, 2010).

### *2.2.2 Nitrogen oxides*

In recent years, and as a result of legislation to curb pollutants such as particulates and lead in the urban atmosphere, a set of photochemical contaminants are being generated in the air in greater amounts. Photochemical smog was first described in the 1950's, but since then the problem has increased greatly as our ownership of private vehicles has grown in the subsequent decades. Cleaner air with less particulate pollution has meant more sunlight and hence an increase in photochemical processes occurring in the atmosphere. This means there is more photo-oxidation of contaminants in urban air which can create a photochemical smog problem, at the heart of which are nitrogen oxides ($NO_x$).

The emissions of nitrogen oxides globally from natural sources are far greater than those generated by anthropogenic activities (WHO, 2006). However, background concentrations from natural sources are very small because they are distributed over the entire surface of the earth. Nitrogen in fuels such as coal, oil and gas is converted to oxides of nitrogen during combustion, and since 1900 global $NO_x$ emissions from combustion sources have increased by a factor of ten (Bowman, 1992). The $NO_x$ formation process occurs during high temperature combustion of these fuels when atmospheric nitrogen and oxygen are combined to form oxides of nitrogen. Road traffic and electricity generation are the predominant sources of these gases due to their high temperature combustion of fuels. The oxides of nitrogen formed through this route are

mainly emitted as nitric oxide (NO), but approximately 5% of the total is emitted as primary nitrogen dioxide ($NO_2$) (WHO, 2006).

Nitric oxide formation is an endothermic process and thus requires temperatures in excess of 1000 ºC to synthesize from molecular nitrogen and oxygen in the atmosphere. In nature a major source is due to lightning, but in urban areas anthropogenic combustion processes represent a significant source of NO production. The principal reactions involved in the thermal production of NO are shown in the following endothermic reactions:

$$N + O_2 \rightarrow NO + O \qquad \text{Eqn. 2.1}$$

$$N_2 + O \rightarrow NO + N \qquad \text{Eqn. 2.2}$$

Though there are many different species of nitrogen oxides, the air pollutant species that is most important from a human health perspective is nitrogen dioxide. $NO_2$ is a reddish brown gas that has a pungent and irritating odour. The majority of $NO_2$ present in the atmosphere is a secondary product of atmospheric chemistry and is formed in a number of different ways through conversion of nitrogen oxides.

When NO is exposed to air it spontaneously produces nitrogen dioxide. This conversion to $NO_2$ is due to the reaction of the NO with ozone ($O_3$) which occurs in the atmosphere from a range of sources, including atmospheric transport from the earth's stratosphere. The following reaction illustrates how NO gas readily oxidises when in the presence of oxygen to form $NO_2$:

$$2NO + O_2 \rightarrow 2NO_2 \qquad \text{Eqn. 2.3}$$

This process of oxidation may occur even more rapidly in the presence of light and hydrocarbons from unburnt fuel:

$$CH_4 + 2O_2 + 2NO + h\upsilon \rightarrow H_2 + CH_2O + 2NO_2 \qquad \text{Eqn. 2.4}$$

In the previous illustrative reaction (Eqn. 2.4) a number of undesirable atmospheric components are produced in the reaction. In the equation, methane ($CH_4$) is used as an example of a hydrocarbon and is subsequently oxidised in the reaction to formaldehyde ($CH_2O$), a known carcinogen. The same reaction also sees the NO oxidise to $NO_2$.

$NO_2$ has been shown to have a wide range of biological effects in laboratory animal experiments. These include effects on pulmonary metabolism, structure, function, inflammation and defence against infections. In several rat studies, for example, it was found that short-term exposure to concentrations in excess of 100 ppm (approx. 200 $mg/m^3$) was lethal (Chitano et al., 1995; Smith et al., 1996). However, exactly what level of exposure would lead to these effects in humans is unknown because of the inherent difference in mammalian species (WHO, 2006). In general, human studies that have been conducted involving acute controlled exposures, concentrations of nitrogen dioxide in excess of 1.0 ppm (1880 $\mu g/m^3$) are required to induce changes in human pulmonary function of adults (Bylin et al., 1985; Roger et al., 1990; Salome et al., 1996). Since concentrations at such a high level almost never occur in ambient air, studies on the effects of nitrogen dioxide have focused on people with pre-existing lung disease such as asthma (WHO, 2006).

In epidemiological studies the extent of air pollution is characterised by measuring individual pollutants, but as air is a mixture, the selected pollutant is not the sole contributor. Nitrogen oxide concentration, for instance, tend to be closely related to particulate levels due to their origins from many of the same sources. The individual air pollutant of a study serves as an indicator substance of this mixture (Kraft et al., 2005). In the few large cohort studies that have examined the relationship between mortality and long-term ambient $NO_2$ exposure, several have found significant correlations between $NO_2$ levels and mortality rate (Hoek et al., 2002; Nafstad et al., 2003; Nafstad et al., 2004), yet others have failed to conclude any such correlation, including the Harvard *Six Cities Study* (Abbey et al., 1993; Dockery et al., 1993; Pope et al., 2002).

### *2.2.3 Ozone*

Ground-level ozone ($O_3$) is a pollutant that is not directly emitted by primary sources, but rather arises from complex chemical reactions in the atmosphere. It is one of the most serious and persistent air quality problems in many countries and is described by the US EPA as the *"most intractable air pollutant in urban air"* (Hill, 2010). Ordinarily there is a low background level, probably less than half of the concentration currently encountered in the northern hemisphere, which arises from downward transport of $O_3$ formed in the stratosphere by the photolytic breakdown of oxygen ($O_2$), where its presence is essential to filtering harmful ultraviolet light before it reaches the troposphere (WHO, 2006). However, motor vehicles are a major source of $O_3$ precursors, VOCs and $NO_x$. During summertime $O_3$ production is at its greatest because the heat and strong ultraviolet rays from the sun enable VOCs and $NO_x$ to react with atmospheric $O_2$. Often early morning levels of $O_3$ are low, but as vehicular exhaust from morning traffic increases, this leads to an increase in $NO_x$ and VOC concentrations. Thus, as the day progresses and the sun's ultraviolet rays grow stronger, $O_3$ generation increases over the course of the day (Hill, 2010).

The formation of $O_3$ is due to reactions in the atmosphere that are driven by the energy transferred to molecules of $NO_2$ when they absorb light from solar radiation. $NO_2$ dissociates as a result of the absorption of sunlight to form NO and an oxygen atom (O), which reacts with an oxygen molecule ($O_2$) to form $O_3$. The equations for the reactions are as follows:

$$NO_2 + h\upsilon\ (\lambda \leq 430nm) \rightarrow NO + O \qquad \text{Eqn. 2.5}$$

$$O + O_2 \rightarrow O_3 \qquad \text{Eqn. 2.6}$$

Where $h$ is Planck's constant and $\upsilon$ is the frequency of light. This chemical reaction can also be readily reversed, decomposition of $O_3$ occurs when it reacts with NO to form $NO_2$ and a molecule of oxygen:

$$NO + O_3 \rightarrow NO_2 + O_2 \qquad \text{Eqn. 2.7}$$

Each of these reactions is relatively fast, and this rapidly establishes a photostationary (equilibrium) state containing amounts of all three components. However, the photostationary cycle described in the three equations may be altered by events that consume NO or favour the production of $NO_2$. Such situations occur when there is chemically reactive hydrocarbons and bright sunshine present. In this situation, highly reactive species known as peroxy radicals are formed due to the oxidation of the hydrocarbons. The peroxy radicals react with NO and oxidise it to $NO_2$, as in Eqn. 2.8, thus causing a disturbance of the photochemical equilibrium.

$$NO + RO_2\ (alkyl\ peroxide) \rightarrow NO_2 + RO \qquad \text{Eqn. 2.8}$$

In this reaction the peroxy radical has converted NO into $NO_2$ without consuming a molecule of $O_3$. Thus, as long as free peroxy radicals are being formed then high concentrations of $O_3$ can build up.

The health effects of $O_3$ exposure are wide ranging. Acute health effects include irritation of the eyes, nose, throat and lungs as well as the reduction in optimal pulmonary function (Higgins et al., 1990; Horstman et al., 1990; Folinsbee et al., 1994). However, there is less published information on acute cardiovascular function and chronic effects of $O_3$. Of the acute cardiovascular effect studies conducted, Park et al. (2005) found a reduction in low frequency heart rate variability, while Rich et al. (2006) studied patients in the Boston area who had implanted defibrillators, and reported an increased risk of paroxysmal atrial fibrillation episodes associated with short-term increases in ambient $O_3$. Long term chronic exposure to $O_3$ causes a reduction in lung capacity and can worsen heart disease, bronchitis, emphysema and asthma (McDonnell et al., 1999; Tager et al., 2005), and it has been demonstrated to significantly increase the risk of death from respiratory causes (Jerrett et al., 2009).

### *2.2.4 Sulphur dioxide*

Sulphur dioxide ($SO_2$) is a colourless gas that is derived from the combustion of sulphur containing fossil fuels. Environmental background levels are due to natural sources such as volcanoes, but anthropogenic activities greatly increase these levels. Historically, both $SO_2$ and particulate matter have been the major components of air pollution all over the world due to the burning of fossil fuels. In urban areas this has led to serious pollution problems from the use of coal for domestic heating and industrial processes.

$SO_2$ is readily soluble in water and is a pre-cursor to acid rain and atmospheric particulates. The oxidation of $SO_2$ leads to the formation of sulphurous and sulphuric acids. The formation of sulphurous acid is shown below:

$$SO_2 + H_2O \rightarrow H_2SO_3 \qquad \text{Eqn. 2.9}$$

The reaction of sulphur trioxide ($SO_3$) with water forms sulphuric acid, which is a very strong and hygroscopic acid:

$$SO_3 + H_2O \rightarrow H_2SO_4 \qquad \text{Eqn. 2.10}$$

As a result of the formation of these acids, $SO_2$ is therefore a major contributor to acid deposition which is associated with the accelerated corrosion of buildings and monuments as well as the acidification of surface water and soils.

Aside from the detrimental environmental effects caused by $SO_2$ and the formation of sulphur derived acids, it causes an array of adverse human respiratory effects including bronchoconstriction and increased asthma symptoms (Holgate, 1992). These effects are particularly important for asthmatics at elevated ventilation rates (e.g., while exercising), with studies showing $SO_2$ causing decreases in forced expiratory volume (FEV) in subjects (Linn et al., 1987). $SO_2$ can also influence the autonomic nervous system at concentrations that can frequently be found during air pollution episodes (Tunnicliffe et al., 2001). A study in Hong Kong has suggested that a reduction in $SO_2$, at least in the concentration range below 40μg/m$^3$, leads to an immediate reduction in

deaths (Wong et al., 2001). The same study also suggests that the association of $PM_{10}$ with mortality was only marginal in contrast to $SO_2$, which was found to be more consistently associated with mortality.

In recent years, as a result of the EU NEC (National Emission Ceilings) directive there has been a considerable drive since 1990 to lower $SO_2$ emissions in Ireland and the rest of Europe. Figure 2.2 illustrates the fact that between 1990 and 2008 $SO_2$ emissions have been reduced in Ireland by 75.5% (EPA, 2010). In Dublin City alone, a 1990 ban on bituminous coal sales helped reduce $SO_2$ concentrations in the city by 34% (Clancy et al., 2002).

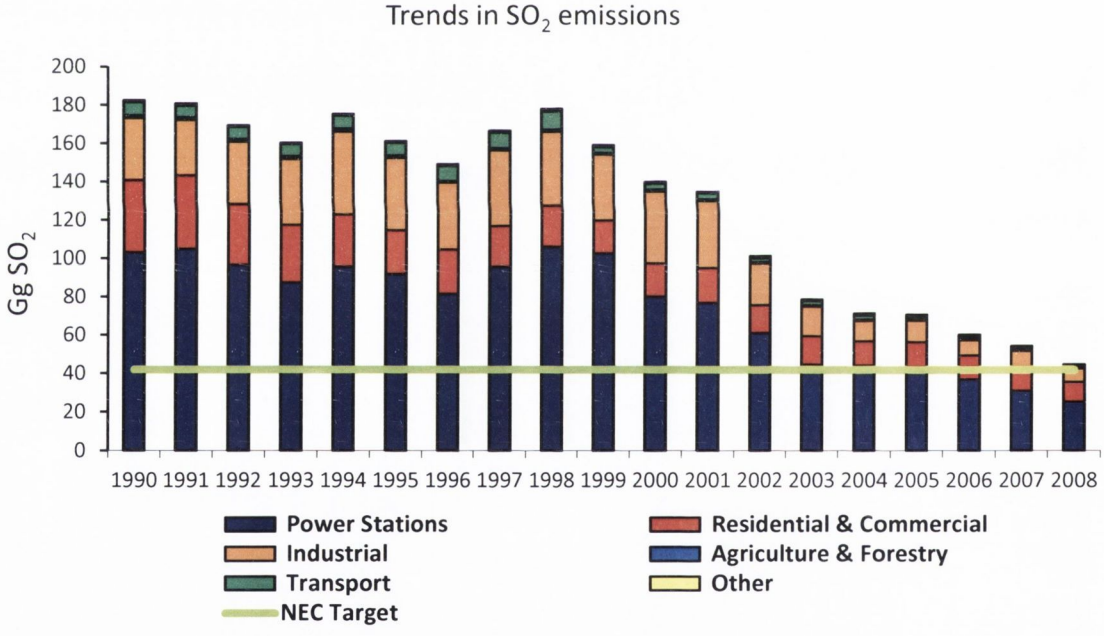


Figure 2.2: Trends in $SO_2$ emissions in Ireland from 1990 to 2008 (EPA, 2010).

It can be seen from the graph that $SO_2$ emissions are still dominated by power generation (56% contribution in 2008). The rest of the emissions are composed of mainly industrial and residential/commercial sources, with contributions of 16.2% and 23%. This reduction in $SO_2$ over the last two decades has been achieved through significant switching from the use of oil and solid fossil fuels to natural gas and reduced

sulphur content in coal and oil, and through the use of abatement technologies (McGettigan et al., 2010).

### *2.2.5 Volatile organic compounds*

Volatile Organic Compounds (VOCs) consist of hydrocarbons, halogenates, oxygenates and other carbon compounds that are prevalent in the ambient atmosphere. These organic compounds have 15 or less carbon atoms and also have a low boiling point and high vapour pressure, greater than 10 Pa at 25°C, and thus will readily evaporate at room temperature into the atmosphere (Koppmann, 2007). VOCs are released into the atmosphere by a variety of anthropogenic emission sources which include vehicle emissions, fuel combustion, industrial processes and solvent usage. It is estimated that the global emission of anthropogenic VOCs amounts to 186 Tg/year (EDGAR, 2005). However, natural sources of biogenic VOC contribute the majority to the atmosphere and are emitted from trees and vegetation, comprising of compounds such as isoprene and terpenes amongst other organic constituents (Fuentes et al., 2000; Guenther, 2002; Kesselmeier et al., 2002). Estimates of their contribution vary between 377 TgC/year (equivalent to 442 Tg/year) (IPCC, 2001) and 1150 TgC/year (Guenther et al., 1995). The distinction between anthropogenic and biogenic VOC is difficult to gauge because many VOC species are produced by both sources. In the urban environment, vehicular emissions are unambiguously detected as the main source (Derwent et al., 2000), with previous studies discovering that 60% of VOC detected were due to mobile sources (O'Mahony et al., 2000; Lee et al., 2002).

Organic compounds play a role in a wide range of environmental problems. These issues include stratospheric ozone depletion, ground level ozone production, toxic and carcinogenic health effects, the enhancement of global warming as well as the accumulation and persistence of VOCs in the environment.

The role VOCs play in both the depletion of stratospheric ozone and generation of tropospheric ozone is important. Firstly, some organic compounds are stable enough to persist in the atmosphere and reach the stratosphere, where they can cause Ozone

depletion. The organic compounds can then undergo the process of stratospheric photolysis and hydroxyl radical destruction which may lead to the release of active ozone destroying chain carriers if the compounds contain bromine and or chlorine substituents (Hester and Harrison, 1995). Secondly, organic compounds in the troposphere play a crucial role in ground level photochemical oxidant formation because they control the oxidant production in those areas where there is sufficient $NO_x$ present to maintain ozone production (Hester and Harrison, 1995). This ground level ozone generation is of great concern to human health as well as crops and other flora.

Many VOCs are classified as hazardous air pollutants (HAPs) and so pose a significant threat to human health. Effects include eye, nose and throat irritation, headaches, nausea, damage to the liver, kidney and nervous system, and some are suspected or known to cause cancer (Hill, 2010). One of the major HAPs is benzene, which is a high production chemical with many uses and is most notably found in petroleum as well as cigarette smoke. Benzene is known to cause acute myeloid leukaemia and aplastic anemia (Smith et al., 2011), but additionally it is probable that it is also associated with non-Hodgkin's lymphoma and childhood leukaemia (Khalade et al., 2010; Smith, 2010). Benzene is just one of a number of important VOCs from an urban air pollutant perspective, there are many others that originate from industrial and other sources, including formaldehyde, chloroform, toluene etc., that are also highly toxic.

### *2.2.6 Particulate matter*

Particulate Matter, or PM, is the term used to describe all the suspended aerosols and particles in the atmosphere. Unlike other pollutants, such as carbon monoxide (CO), Ozone ($O_3$), sulphur dioxide ($SO_2$), nitrogen dioxide ($NO_2$) and lead (Pb), PM is not a specific chemical entity but is a complex mixture of particles from many different sources and has diverse chemical and physical properties (Vallero, 2008). It is a common physical classification of a variety of particles found in the ambient atmosphere such as dirt, dust, smoke, soot and liquid droplets (UK Department of the Environment, 2004).

PM is measured on a dry basis in order to eliminate from the measurement water droplets and vapours, both aqueous and organic, which evaporate or are desiccated from the PM during the drying process. Particulates can be categorised into three main groups based on the size of the particles, which is determined by how the particle forms. These groups are defined as coarse grained particles for particles larger than 2.5 μm in aerodynamic diameter, fine particles smaller than 2.5 μm in aerodynamic diameter and ultrafine particles, those less than 0.1 μm. Formation of each particle type can differ significantly, for example combustion can form very fine particles, whilst mechanical processes often form larger coarse particles, the relative scale of particles can been seen in Figure 2.3. In general, the combined total of all these particles suspended in the air is known as Total Suspended Particles or TSP.

Black smoke is another type of fine particle measurement, and is measured by its blackening effect on filters. Black smoke is a measure of the elemental carbon that is emitted mainly from fuel consumption. Nowadays, due to a large reduction in domestic coal use, the major source of black smoke is from diesel engines, and as a result black smoke concentrations are appreciably elevated alongside major roads. Whilst inventories of emissions of black smoke are no longer routinely compiled, black smoke can be a better indicator of vehicle emissions than gravimetrically determined particle concentrations (Harrison, 2001).

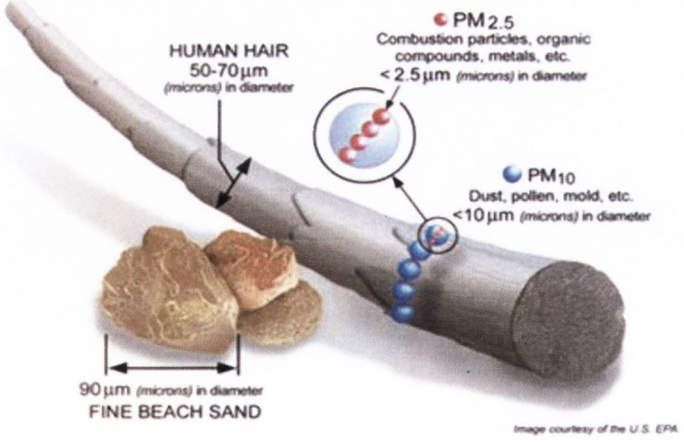


Figure 2.3: Relative size of particles (US EPA, 2012).

There are several different conventions in the classification of particles by size. Particles can be classified by modes which are based on formation mechanisms and size distributions, cut-off points that are based on the 50% cut point of a specific sampling device and are used for regulating air quality standards, and finally, occupational health sizes based on the entrance to various parts of the respiratory system (US EPA, 2004).

Generally, PM is classified by aerodynamic diameter for regulatory purposes because it is the size of the particle that is critical in determining the likelihood and location of deposition of a particle in the respiratory tract (WHO, 2006).

The modal classification is cited in the US EPA *Air Quality Criteria for Particulate Matter* as first being proposed by Whitby (1978) and consists of the following size distributions shown in Table 2.1.

Table 2.1 Size distributions for the modes of particulate matter.

| | |
|---|---|
| **Nucleation mode:** | This mode consists of newly formed particles with diameters smaller than 10 nm. They are formed through nucleation events when gas molecules come together to form stable nuclei. Currently measurement techniques cannot measure particles below 3 nm meaning the lower limit of this mode is uncertain. |
| **Aitken mode:** | This consists of particles with diameters between 10-100 nm that are formed by the growth of smaller particle or nucleation from higher concentrations of precursor gases. |
| **Accumulation mode:** | This mode is defined as particles from about 0.1 μm in size to just above the minimum in the mass or volume distributions which occur between 1 and 3 μm. Particles in the size range of 0.1-1 μm tend to accumulate, hence the name "accumulation" mode. |
| **Ultrafine particles:** | These particles are not considered a mode and are generally defined by size alone as submicron particles of less than 0.1 μm in aerodynamic. |
| **Fine particles:** | Particles with a diameter less than 2.5 μm in size. Fine particles include the nucleation, Aitken and accumulation modes. |
| **Coarse particles:** | Particles which have a diameter greater than the minimum in mass or volume distributions which occur between 1 and 3 μm. |

Modes are defined mainly in terms of their formation mechanisms but they also differ in composition, source, size and transport ability (US EPA, 2004). An idealised distribution showing all four modes is illustrated in Figure 2.4. Particles in the nucleation mode are newly formed particles that have not had a chance to grow. Subsequently these particles begin to grow by coagulation (the combining of two or more particles to form a larger particle) or by condensation of gas or vapour molecules on the surface of existing particles. Coagulation is most efficient for large numbers of particles and condensation is most efficient for large surface areas. Thus, the efficiency of both condensation and coagulation decreases with increasing particle size; this effectively results in a limit of 1 μm that cannot be exceeded by particle growth except by hygroscopic growth in humid conditions (WHO, 2006). Hygroscopic growth occurs when gas phase pollutants dissolve and react in the particle-bound water of hygroscopic particles, leading to an increase in the dry size of the particle (US EPA, 2004).

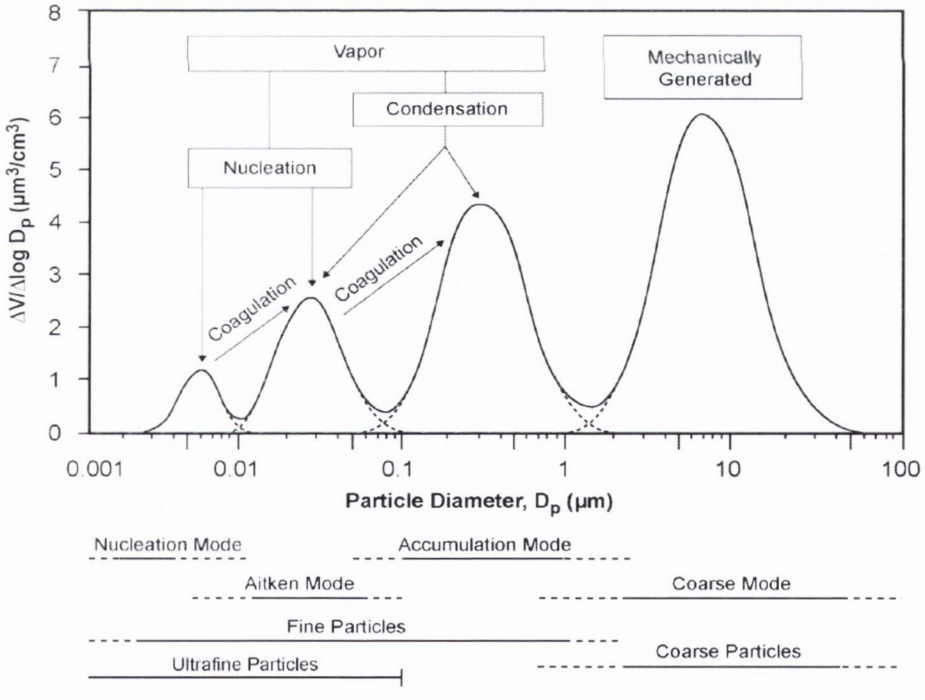


Figure 2.4: An idealised size distribution showing the different modes that comprise fine and coarse particles. Also shown are the major growth and formation mechanisms of the four modes (US EPA, 2004).

The combination of nucleation, Aitken and accumulation mode particles are called fine particles. Fine particles are composed of metals, black or elemental carbon, primary and secondary organic compounds, sulphates, nitrates, ammonium and hydrogen ions. The coarse mode differs from fine particles because it refers to particles formed by the mechanical breakdown of minerals, crustal materials and organic debris. The amount of energy required to break these larger particles down increases as the size of the particles decreases (WHO, 2006).

Particles can also be defined by size selective sampling which refers to a collection of particles below or within a specified size range. For example, $PM_{2.5}$ refers to particles collected by a sampler device that collects 50% of 2.5 μm diameter particles and rejects the other 50%. Size fractions are not solely defined by a 50% cut-off point but by various penetration curves dependent on the type of sampler. The shape of a penetration curve dictates the different size fractions of PM that a sampler would collect (US EPA, 2004). An example of penetration curves are shown in Figure 2.5, the $PM_{2.5}$ sampler shown rejects 94% of 3 μm particles, 50% of 2.5 μm particles and 16% of 2 μm particles.

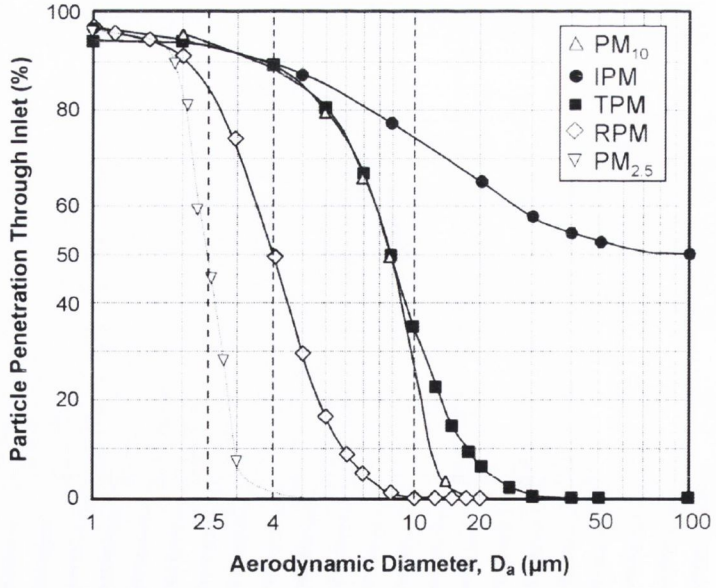


Figure 2.5: Particle penetration curve of an ideal inlet for five different size-selective sampling criteria (US EPA, 2004).

In the United States, the occupational health community have classified PM into three size fractions based in terms of their entrance into various compartments of the respiratory system. Inhalable particles can enter the respiratory tract and are inhaled through the airways in the head. Thoracic particles travel down the respiratory tract, past the larynx, into the lung airways and can reach the gas exchange region of the lung. Finally, respirable particles are a subset of thoracic particles and are more likely to reach deep into the lung to the gas exchange region. The curves that define inhalable (IPM), thoracic (TPM) and respirable (RPM) particulate matter are also shown in Figure 2.5 (US EPA, 2004).

*2.2.6.1 Sources of particulate matter*

Sources of particulates are highly variable. They may be emitted directly into the ambient air as primary particulates or may be formed in the atmosphere as secondary particles. Most particles in the coarse mode are formed by frictional processes of comminution. This includes dust and dirt that is raised by vehicles or wind from farms (fertiliser, dried manure, or dried crop residues), roads and construction sites, as well as natural sources such as pollen and sea spray from breaking waves (Hill, 2010). Coarse mode particles generally account for about 20-50% of the urban background $PM_{10}$ mass (UK Department of the Environment, 2004). Finer particles are released from combustion of fossil fuels, especially from diesel motor vehicles, electricity power stations and industrial operations. These particles are known as primary PM because they are emitted directly to the air as particles or in the form of vapours that rapidly condense to form ultrafine particles.

Particles may also form from gases that have been previously emitted. This is known as secondary particulate matter and is formed by chemical reactions of free, adsorbed or dissolved gases, for example, when gases released from fossil fuel combustion react with sunlight and water vapour (Vallero, 2008). In some parts of the world secondary PM can represent up to 50% of the total concentration of particles in the air (WHO, 2006).

Secondary particles lie predominantly in the $PM_{10}$ size range with the majority being fine particles in the $PM_{2.5}$ range. Most secondary fine PM is formed from condensable vapours generated by the chemical reactions of gas phase precursors. The processes of secondary formation can result in either new particles being formed or else enlarging of existing particles (US EPA, 2004). A common production of secondary particles occurs when gases undergo chemical reactions in the atmosphere which involve oxygen and water. Photochemical reactions are also an important step in secondary PM formation, chemical species like $O_3$ can react with radicals such as hydroxyl (OH) and nitrate ($NO_3$) radicals (Vallero, 2008).

Sulphate production in the atmosphere is one of three main reactions that contribute to the formation of secondary particles. Sulphur derived particles form through the oxidation of sulphur dioxide ($SO_2$) in the atmosphere to form sulphur trioxide ($SO_3$), which then condenses with water to form sulphuric acid (see Eqn. 2.10). It is this sulphuric acid that is then neutralised by ammonia, which is in ample supply in the atmosphere in many places, and together they form solid particles of ammonium sulphate (WHO, 2006).

Solid particles of nitrates are formed in a similar way. Nitrogen dioxide ($NO_2$) is oxidised in the atmosphere to form nitric acid ($HNO_3$), but this reaction occurs at a faster rate than $SO_2$. The $HNO_3$ that is formed is present in the air as vapour and can react with a number of different materials such as calcium carbonate, ammonia or sodium chloride to form solid particles. When the particles are in the form of ammonium nitrate they can disassociate back to nitric acid and ammonia which is favoured by conditions of high temperatures and low relative humidity. This may cause important diurnal and seasonal variations in the concentration of ammonium nitrate in the air (WHO, 2006).

The third major form of secondary PM is secondary organic aerosol. These secondary organic particles are formed in the atmosphere from the reaction of nitrous gases with VOCs under the radiation of sunlight (2007). There are both biogenic VOCs and anthropogenic VOCs that oxidise in the atmosphere to form secondary organic aerosols.

Trees emit α-pinene that is a highly reactive biogenic VOC and along with anthropogenic VOC, which forms species of lower volatility, both sources can create a significant source of secondary organic aerosol (WHO, 2006).

Airborne particulate matter along with its associated precursors and transformation products are removed from the atmosphere through wet and dry deposition processes. This cleansing of the atmosphere ensures there is not a long term lethal build-up of pollutants in the air and also limits the potential for direct human health effects caused by their inhalation. Particles are removed from the atmosphere through wet deposition by rain and snow, and by occult deposition via fog, mist and cloud-water that hide it from measurements used for quantifying wet and dry deposition. Dry deposition occurs much slower with coarse particles settling out due to gravity, but fine PM does not readily dry deposit so tends to travel large distances in the air before eventually depositing via precipitation (US EPA, 2004).

#### *2.2.6.2 Health effects of particulate matter*

Over the last few decades, the body of evidence for the adverse health effects of particulate pollution on human populations has been growing. Today there is a vast amount of literature on the adverse health outcomes for both short and long-term exposure to PM at levels usually experienced by urban populations in both developing and developed countries. The literature includes a variety of epidemiological, clinical and toxicological studies.

PM is routinely chosen as the ideal summary indicator for estimating the health impact of urban air pollution because it is the pollutant associated most consistently with a variety of adverse health outcomes, ranging from acute symptoms, morbidity and premature mortality to long-term effects (Martuzzi et al., 2006).

Exposure to PM increases the risk of mortality, both in the long term and through acute, short-term effects. Chronic exposures have been associated with reductions in life expectancies, due to cardiopulmonary mortality and lung cancer. There have been a number of large cohort studies conducted that have found strong associations between

particulate pollution and mortality (Dockery et al., 1992; Dockery et al., 1993; Pope et al., 1995; Abbey et al., 1999; Hoek et al., 2002).

Many of the studies have linked $PM_{10}$ to both cardiopulmonary and lung cancer deaths, but often it is the fine particulate ($PM_{2.5}$) fraction which is observed to have the strongest association with these deaths (Pope et al., 2002; Pope and Dockery, 2006; Pope et al., 2009; Turner et al., 2011).

According to a report by the European Environmental Agency (EEA) the average loss of life expectancy from PM exposure in the year 2000 was estimated to be approximately nine months, this was for EEA countries where there were estimates available. The worst loss in life expectancy occurred in the Benelux countries, the Po valley in Italy, and Silesia in Poland, where the estimated life expectancy loss was 12-36 months (EEA, 2007). The estimates that were made are believed to be conservative as mortality was only calculated for populations over 30 years and not for infants. The health impact from $PM_{2.5}$ mass concentrations across Europe is shown in Figure 2.6.

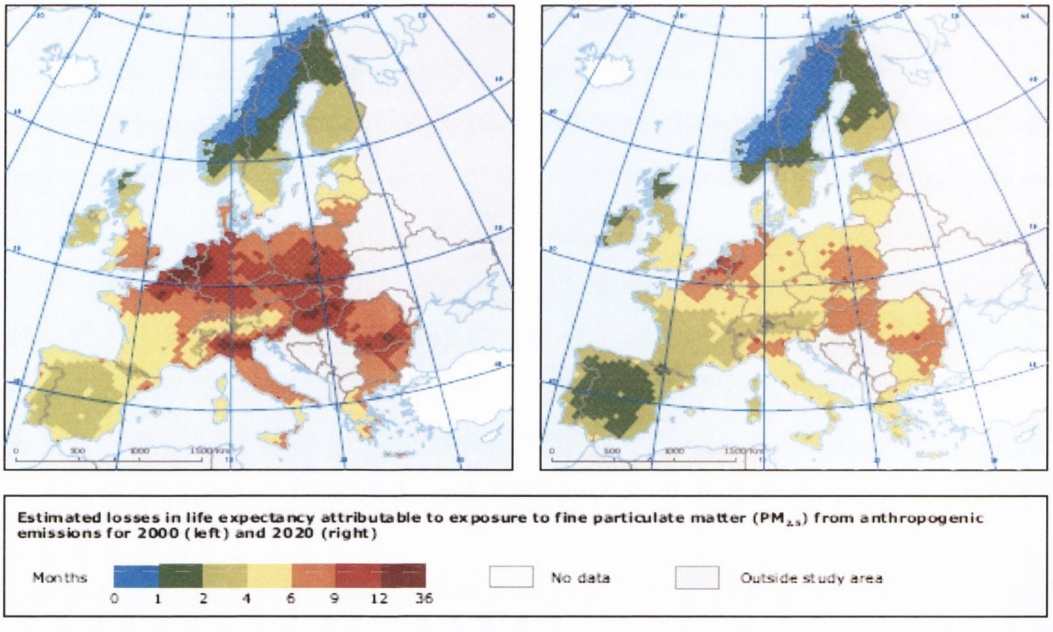


Figure 2.6: Loss in statistical life expectancy that can be attributed to anthropogenic contributions to $PM_{2.5}$ for the year 2000 (left) and the projection for 2020 (right) (EEA, 2007).

Attention is increasingly turning to the effects of ultrafine particles, with a diameter smaller than 0.1 μm. These particles contribute little to PM mass but they dominate particle number and surface area metrics. As a consequence of their minute size it has been suggested that they can more readily exit the lung, where they may directly affect cells and organs of the cardiovascular system (Cozzi et al., 2007). The mechanisms linking cardiovascular events and mortality with particulate matter are still under debate. A study conducted by Pope III et al. (1999) attempted to identify these biologic mechanisms which underlie the link between fine particulates and cardiopulmonary mortality. The study found that changes in cardiac autonomic function reflected by changes in mean heart rate and heart rate variability may be one of the pathways linking cardiovascular mortality with PM. Pope III et al. (1999) also hypothesised that PM, especially ultrafine particles, may provoke alveolar inflammation resulting in increased blood coagulation. Evidence for the alteration of haemostasis due to PM exposure is found in research by Cozzi et al. (2007), who found that clot formation is promoted and clot resolution is impeded in susceptible individuals when exposed to fine particles.

#### *2.2.6.3 Environmental effects*

Particulate matter is responsible for environmental effects such as corrosion, soiling, and damage to vegetation, as well as reduced visibility. Atmospheric PM may affect vegetation directly by deposition on foliage, or indirectly by altering the chemistry of the soil, or by reducing solar radiance through PM induced climate change processes. Coarse grained PM can cause physical and chemical effects to vegetation. Deposition of dust on plants can cause a rise in leaf temperature, blockage of the stomata of the plant, and change the amount of solar radiation received. This may lead to a decrease in photosynthesis, transpiration and respiration of the plant. Also, depending on the chemical composition of the PM, it may be the key phytotoxic factor leading to plant injury. Fine PM tends to be mainly secondary in nature and the major effects are indirect and occur through the soil. The impact in ecosystems of fine PM, particularly nitrates, sulphates, and metals, is determined by their effects on the growth of the bacteria involved in nutrient cycling and the fungi involved in plant nutrient uptake (US EPA, 2004).

Fine PM in the atmosphere is responsible for haze and a reduction in visibility. Visibility is defined as the degree to which the atmosphere is transparent to visible light, or alternatively it can be quantitatively defined as that distance at which a black object can be seen against the horizon. The degradation of visibility is due primarily to the scattering and absorption of light by fine particles suspended in the atmosphere (US EPA, 2009). Absorption of visible light is most effective at particle diameters of approximately 1.0 μm because this diameter size is close to the wavelength of light. Scattering of light occurs over a range of particle diameters but occurs mostly due to aerosol between 0.2 and 2.0 μm in diameter (QUARG, 1996). Studies cited by the Quality of Urban Air Review Group (1996) suggest that it is scattering that is the dominant process for light extinction, *"with absorption being responsible for between 10% (in rural areas) and 30% (in urban areas) of extinction"*. Scenic vistas and other areas of natural beauty can often be diminished due to the effects of haze and the degradation of visibility. In the United States, legislators have put an emphasis on improving the visibility in national parks since 1977 when the Clean Air Act was amended to make it a goal to reduce impairment from manmade pollution.

The gaseous precursors that form secondary particulate matter can have long term harmful effects on ecosystem structures and functions. Nitrogen and sulphur compounds can lead to acidification of soils, as well as lakes and rivers. Nitrogen compounds not only have acidifying effects, but are also important nutrients. Excess of nitrogen deposition from the atmosphere can lead to eutrophication in the soil of terrestrial ecosystems due to a surplus in nitrogen. Subsequently, excess nitrogen can leach from the soil into groundwater, rivers, lakes, coastal areas, and the sea causing eutrophication in these bodies of water. This in turn can lead to changes in unique aquatic or marine animal and plant life, including biodiversity loss (EEA, 2007).

Pollutants in the atmosphere are related to both aesthetic and physical damage to materials. Particles that are primarily carbonaceous compounds can cause soiling of commonly used building materials and culturally important items like statues and works of art. Soiling occurs as the result of deposition of particles less than 10 μm in size on surfaces by impingement. Soiling is considered an optical effect, it reduces the

transmission of light through transparent materials and it also changes the reflectance from opaque materials. Deposition of sulphur containing pollutants such as those of secondary particulate matter is associated with the formation of gypsum on stone structures. This gypsum is dark in colour and can be attributed to soiling by carbonaceous particles from nearby combustion processes. Gypsum formation on stone structures can be quite damaging and tends to form on limestone, sandstone, and marble, when exposed to $SO_2$ aerosol. The gypsum occupies a larger area than the original stone and as a result the surface becomes rough with cracks and pits, and this serves as a deposition place for airborne particles. Overtime as the gypsum grows it loosens and breaks off (US EPA, 2004).

Particulate matter is also responsible for the soiling of structural painted surfaces. Coarse mode particles (> 2.5 μm) initially contribute more to the soiling of vertical and horizontal painted surfaces than fine mode particles (< 2.5 μm). But the coarse particles are more easily washed off by rain and so primarily soil horizontal surfaces, whereas accumulation of fine particles promotes remedial action such as cleaning or repainting the surface. As well as discolouring painted surfaces, the overall durability of the surface can be affected by particles acting as a carrier for corrosive pollutants leading to erosion, blistering and peeling (US EPA, 2004).

### *2.2.7 Current state of Dublin air quality*

Over the past 20 years the air quality in Dublin has shown significant improvement in levels of black smoke, lead, $SO_2$, benzene, and carbon monoxide. This has been largely due to the regulatory ban on bituminous coal in the Dublin region and the elimination and reduction of other materials in vehicle fuels (Dublin City Council et al., 2009). New legislation introduced over the last 15 years has continued to drive further reductions.

The legislative framework for air quality in Ireland was set down in the Air Quality Standards Regulations 2002 (S.I. 271/2002) which transposed the European Air Quality Framework Directive (96/92/EC 1996) and the first two Daughter Directives into Irish law. These established the air quality standards for $SO_2$, $NO_2$, Pb, $PM_{10}$, CO, and

benzene. There are additional air quality regulations with regard to ozone which are dealt with in the Ozone in Ambient Air Regulations 2004 (S.I. 53/2004). Legislation for additional pollutants was established in the Arsenic, Cadmium, Mercury, Nickel, and Polycyclic Aromatic Hydrocarbons in Ambient Air Regulations 2009 (S.I. 58/2009) which was transposed from the fourth and final Daughter Directive (2004/107/EC) into Irish law.

The latest piece of air pollution legislation is entitled the Ambient Air Quality and Cleaner Air for Europe (CAFE) Directive (2008/50/EC) which was published in May 2008. It replaced the Framework Directive and the first, second and third Daughter Directives. The fourth Daughter Directive (2004/107/EC) will be included in CAFE at a later stage. The main elements of the CAFE directive are to merge most existing directives into a single all-encompassing directive, as well as introducing a limit value for $PM_{2.5}$. The CAFE Directive was transposed into Irish legislation by the Air Quality Standards Regulations 2011 (S.I. 180/2011).

The air pollution regulations specify the dates by which the limit values or target values for each of the pollutants must be achieved and also the reference methods for sampling, analysis, and measurement. There are also specific requirements in relation to providing the public with information on ambient air quality.

The two pollutants that are identified as of most concern in the Dublin Regional Area Air Quality Management Plan 2009-2012 are $NO_2$ and $PM_{10}$. The reason for this is that concentrations of these pollutants have not decreased at the same rate as observed for other pollutants. The key challenge in relation to $PM_{10}$ for the local Dublin authorities is to ensure compliance with the daily and annual limit values. Concentrations have approached the limit values in recent years and there is a risk that limit values could be exceeded in the Dublin area (Dublin City Council et al., 2009). The regional management plan also makes reference to the *"dearth of information currently available on the full range of emission sources that exist"*. Therefore, an improved knowledge base with respect to these pollutants may have major implications in terms of developing strategies for air quality management.

### *2.2.8 Summary of air pollutants*

In conclusion, this section on air pollutants has reviewed the most common pollutants in the urban ambient air and has identified the main sources and formation processes attributed to each. The review of the effects of each pollutant has also highlighted their negative impact on human health. The adverse health effects create a burden on society through a reduction in life expectancy and loss of economic productivity from mild and severe impairments, and consequently increased hospital admissions burden health care systems worldwide.

Of all the pollutants discussed, particulates were deemed the most significant for further study and monitoring in Dublin. The nature of $PM_{10}$ means that it is a good measure of the complex mixture of gaseous and particle pollutants that originate from fossil fuel combustion in vehicles and power generation, thus, it is the pollutant of choice for assessing health impacts of air pollution. PM forms the basis of many epidemiological studies of air pollution and is widely studied in urban areas where traffic related emissions can greatly influence the air quality of a city. Additionally, the significantly higher PM concentrations often observed in personal exposure studies when compared to background monitoring stations warrants further examination of $PM_{10}$. This will be discussed further in Section 2.6.

## 2.3 Personal Exposure to Airborne Particles

Studies on the health effects of airborne particles have almost exclusively relied upon the use of urban background PM concentration measurements as a surrogate for the exposure of all the individuals in the study population. Cohort studies have employed a variety of different methods for inferring the exposures of the study subjects. For instance, the frequently cited Dockery et al. (1993) U.S. *Six Cities Study* used centrally sited fine and coarse particle monitors in communities, whereas in the *Seventh Day Adventist Study*, $PM_{2.5}$ concentrations were derived using regression equations that related $PM_{2.5}$ and visibility (McDonnell et al., 2000).

Many more of the epidemiological studies have echoed the *Six Cities Study* and used centrally located monitoring points in order to represent exposure of individuals in the community (Schwartz and Morris, 1995; Burnett et al., 2000; Filleul et al., 2006). However, adverse health effects depend on the actual exposure of an individual, and therefore improved means of differentiating the exposures within the study population would prove beneficial to epidemiological studies by increasing the ability to characterise effects and detect thresholds. For instance, Michaels and Kleinman (2000) found short-term excursions into high exposure levels of PM elicited adverse effects in both animals and humans. This type of actual short-term peak exposure of an individual would not be apparent in daily data from background monitoring. Thus, the collection of personal exposure and activity data may provide useful knowledge for investigating health impacts of air pollution and in the development of predictive personal exposure models.

### *2.3.1 Measuring personal exposure*

There are several methods that can be used to measure personal exposure to airborne particles. The procedures employed by researchers for monitoring particle exposure have been adapted from those that are used in the workplace (UK Department of the Environment, 2004). The two types of techniques generally used for PM personal exposure sampling are either a gravimetric sampling based method, or alternatively a nephelometer based method.

The equipment used for the gravimetric sampling based method generally consists of a small battery operated pump connected to a size selective sampling head that contains a filter paper collection system. However, there are problems associated with this kind of system which arise because of low airborne mass concentrations, and therefore require sampling for relatively long time periods. Typically, 24-hour samples must be taken when using a low flow (2 to 4 l/min) sampling method in order to collect sufficient particle mass to be weighed accurately. The maximum airflow is limited because the pump is worn by individuals for the duration of the sampling period (except when sleeping), and consequently must be lightweight and quiet. The minimum detectable

mass concentration over a 24-hour period is generally about 10 $\mu g/m^3$ (Janssen et al., 1998b), although detection limits of 25 $\mu g/m^3$ have been reported where low sample volumes (e.g. 2 l/min flow over 24 hours) have been used in conjunction with a low sensitivity balance (Brauer et al., 2000).

The low sample volume and long sampling durations required means many of the low air flow devices are not suitable for personal sampling in the ambient environment over short sampling periods of much less than 24 hours. This issue was recognised by Adams et al. (2001a), who developed a device called the High Flow Personal Sampler (HFPS). The HFPS is a gravimetric instrument which operates with a flow rate of 16 l/min and is designed to collect fine particulates with a 50% cut-off point at 2.5 μm aerodynamic equivalent diameter, which is achieved by a size selective porous polyurethane foam plug contained in the sampling head. This device has since enabled the collection of $PM_{2.5}$ personal exposure samples in numerous commuter studies in the transport microenvironment (Adams et al., 2001c; Gómez-Perales et al., 2004; Kaur et al., 2005a; Kaur et al., 2005b; McNabola et al., 2008b).

The limitations of gravimetric instrument are exposed when monitoring personal exposure over longer periods and in multiple microenvironments. This is due to the nature of collecting a single sample on a filter; meaning exposures in different places can only be estimated by the use of time-activity diaries and estimating the penetration and indoor sources of a microenvironment, or by changing of the sampling head and filter for each place. However, continuous monitoring can be achieved through the use of personal samplers which measure particle number concentration by means of light scattering.

The basic operating principle of optical particle counters involves drawing air into the instrument by means of a small pump, which then passes the air through a light scattering sensor called a nephelometer. This nephelometer emits light via a low power laser diode, which is then scattered in the presence of airborne particles. The scattered light is then detected by a photo detector circuit and measured. The detector output signals are empirically proportional to the number and size of particles and the data is

presented as number of particles per litre, which is then subsequently converted through a proprietary algorithm for typical-density aerosols into micrograms per cubic meter ($\mu g/m^3$) (Ruprecht et al., 2011).

### *2.3.2 Personal exposure studies*

The types of PM personal exposure studies vary widely in their nature and scope, many of which will be reviewed here. In previous investigations (Adams et al., 2001b; Int Panis et al., 2010) the impact of influencing factors such as traffic and meteorological conditions on personal exposure have been examined. Other studies have been concerned with the health impacts of particular activities both in terms of acute exposure to PM (Michaels and Kleinman, 2000; Oberdörster, 2000) and in the subsequent post exposure uptake of particulates into the lungs (McNabola et al., 2006; McNabola et al., 2007).

One of the most common activities studied has been commuting which has been examined in numerous cities including Dublin (O'Mahony et al., 2000; O'Donoghue et al., 2007a; McNabola et al., 2008a). Outdoor personal exposure when in the vicinity of transport (O'Donoghue et al., 2007a; O'Donoghue et al., 2007b; McNabola et al., 2008a) or industrial sources (Querol et al., 2004a) have been shown to be exceed background concentration levels regularly. Differences between commuting modes also have an important influence on the personal exposure to PM and there have been studies conducted which have illustrated the difference between modes of transport such as cycling and commuting by bus, car etc. (McNabola et al., 2008b; Zuurbier et al., 2010).

Other studies have identified indoor activities such as smoking, cooking, and the use of open fires, which may have a significant impact on personal exposure of an individual (McNabola et al., 2006; Goodman et al., 2007). These activities and associated high personal exposures highlight the importance of indoor air pollution which may not be reflected in background air monitoring data (Dimitroulopoulou et al., 2001a; Dimitroulopoulou et al., 2001b). It is during these brief high exposure periods that significant health effects can be caused which are not reflected by background air

quality data (Michaels, 1998; Michaels and Kleinman, 2000). While some personal exposure studies have found little or no relationship between the exposure of an individual and the background concentration (Gulliver and Briggs, 2004; Kaur et al., 2005a), other studies have in fact demonstrated a relationship between personal exposure and background concentrations (Pérez Ballesta et al., 2008). Many of these factors which have been mentioned will be discussed in greater detail in Section 2.5.

There have been a number of different PM personal exposure studies conducted for 24-hour durations of exposure or longer. Scapellato et al. (2009) measured personal $PM_{10}$ exposure in asthmatic adults over a two year period in Padova, Italy. In total, 80 24-hour samples were collected over a two year period using the gravimetric sampling technique, with samples examined for seasonal variability and other factors (meteorological, occupation, smoking status, etc.). The main finding of their study was that smoking was the primary source of $PM_{10}$, while for non-smokers outdoor $PM_{10}$ was most important source of personal $PM_{10}$ exposure. The outdoor $PM_{10}$ concentrations found in the study also confirmed Northern Italy as a severely polluted region of Europe.

In another study by Brauer et al. (2000), $PM_{10}$ was measured by a gravimetric method over 24-hour periods for industrial and office workers, as well as school students with personal indoor-outdoor relationship being examined and regression analysis used to establish determinants of exposure. The highest personal $PM_{10}$ concentrations were found in the industrial worker group, followed by students and then office workers. Of the overall variability in personal $PM_{10}$ exposures for office workers and students, 17% was explained by regression models with outdoor $PM_{10}$ and nicotine as the only significant predictors.

Rojas-Bracho et al. (2000) studied 18 individuals with chronic obstructive pulmonary disease in Boston and simultaneously collected 12-hour personal, indoor and outdoor $PM_{10}$, $PM_{2.5\text{-}10}$, and $PM_{2.5}$ samples. These samples were obtained while the subjects were at home using gravimetric sampling for personal exposure, and activity diaries were kept in order to identify particle sources. Personal exposures were higher than

corresponding indoor and outdoor concentrations for all particle measures and for all seasons, except for winter indoor $PM_{2.5-10}$ levels, which were higher than personal and outdoor levels. The authors speculated that higher personal exposures may be due to the proximity of the individuals to particle sources, such as cooking and cleaning. Also, the study found that personal $PM_{2.5}$, but not $PM_{2.5-10}$, exposures were associated with outdoor levels. Additionally, air exchange rates were found to be important determinants of both indoor and personal levels.

Van Roosbroeck et al. (2007) monitored personal $PM_{2.5}$, soot and $NO_x$ concentrations of 54 school children over 48-hour periods, and again collected data through the use of gravimetric sampling. The key finding from this study was that increased personal exposure to the traffic-related air pollutants soot and $NO_x$ was seen for children attending a school within 100 metres of a motorway. However, only a minor difference in $PM_{2.5}$ was found when the school located beside a motorway was compared with the two schools which were not beside a motorway.

However, for sampling of $PM_{2.5}$ some studies have employed the use of optical particle counters, as opposed to gravimetric methods that have been used in many of the PM personal exposure studies. In a pilot study, Vallejo et al. (2004) used a nephelometer to monitor the personal exposure of 40 subjects to $PM_{2.5}$ in Mexico City over 13 hour periods beginning at 09.00 each day, and results were examined with multivariate analysis in order to describe the variability of $PM_{2.5}$ concentrations in outdoor and indoor microenvironments. The multivariate analysis corroborated that $PM_{2.5}$ concentrations were mainly determined by geographical locations and hour of the day, but not by the type of microenvironment.

Branis and Kolomazníková (2010) measured personal $PM_{2.5}$ with a DustTrak continuous nephelometer every five minutes for a total of 239 days for one individual who was a student. Descriptive statistics for each microenvironment were reported and multiple linear regression was used to determine the relationship with background concentrations. The study found the highest 5-min $PM_{2.5}$ average concentration was detected in restaurant microenvironments, with the second highest recorded in indoor

spaces heated by a stove burning solid fuels. In contrast, the lowest 5-min $PM_{2.5}$ average concentrations were observed in outdoor rural setting and indoor at home. The authors also found that there was also a high correlation between personal and fixed site aerosol concentrations.

The finest resolution of personal samples found in literature was usually at one minute intervals. Wallace et al. (2006a) took continuous (1-min resolution) weeklong measurements of personal exposures and indoor concentrations of fine particles for 37 health-impaired people in North Carolina. According to the authors, the use of continuous particle measuring instruments in this study allowed more precise identification of sources, and a better knowledge of the frequency and magnitude of short-term peak exposures. However, the pDR instrument used overestimated the gravimetric concentrations by 20-50% during calibration. No overall correction was applied to the gathered data so the authors stated that *"the concentrations reported are likely to be substantial overestimates, ranging from 6% to 63%, of the true gravimetric values"*.

Lanki et al. (2002) also took 1-min averaged samples with a nephelometer for personal $PM_{2.5}$ exposures of elderly people, investigating the concentrations observed and correlation to gravimetric analysis. Some of the findings reported by Lanki et al. included large changes in concentrations in the minutes after cooking or when changing microenvironments. The median of daily 1-hour maxima was over twice the median of 24-hour averages. Personal $PM_{2.5}$ exposure for elderly people was also examined in an earlier study by Janssen et al. (2000), but in this case gravimetric sampling was used and regression analyses conducted for each subject separately. They found that personal, indoor, and ambient concentrations were highly correlated within subjects over time. The led to the authors concluding that their findings provided further support for using fixed-site measurements as a measure of exposure to $PM_{2.5}$ in epidemiological time-series studies.

## 2.4 Time-Activity Budget

Personal exposure of an individual to airborne particulates will depend greatly on that individual's activity pattern and the time he or she spends in specific microenvironments. Human activities can explain much of the magnitude and variation of pollutant exposure because of the impact of timing and location of these activities. There have been a number of studies conducted which have attempted to quantify the activity/time patterns of the general population.

One of the earliest major studies conducted was by the California Air Resources Board (CARB). This was a state-wide survey of Californians over the age of 11 aimed at improving exposure assessments for air pollution (Jenkins et al., 1992). Participants (n = 1,762) were interviewed by telephone and completed a 24-hour diary of activities and locations, as well as responding to questions on their use and proximity to potential pollutant sources. From the information gathered, it was shown that Californians spend 87% of their time indoors, 7% in enclosed transit and 6% outdoors.

Following the CARB study, two further activity studies were conducted in North America. In the US, the National Human Activity Pattern Survey (NHAPS) was conducted over a two year period between 1992 and 1994 and involved telephone interviewing of 9,386 individuals nationally (Klepeis et al., 2001). Respondents of this survey spent on average 86.9% indoors, 5.5% of their time enclosed in a vehicle and 7.9% outdoors. These figures were very similar to the equivalent Canadian Human Activity Pattern Survey (CHAPS) as reported by Leech et al. (1996).

Activity and time budget information have also been reported in a number of 24-hour PM personal exposure studies. Quintana et al. (2001) reported participants (n = 10) spent on average 87% of their time indoors, with only 6% outdoors and a further 7% in transit – all of which are comparable to the NHAPS. In Prague, Branis and Kolomazníková (2010) reported a slightly smaller amount of time spent indoors (84%) and more time spent outdoors (10.9%), though this study involved monitoring 24-hour exposure of only one individual. Sarnat et al. (2006) observed a seasonal variation of

time spent indoors during personal exposure sampling (summer = 90.5%, autumn = 95.2%). Additionally, time spent outdoors, in transit, and near particle sources (i.e., cooking, cleaning, near a smoker) was minimal ($\leq$ 7.0%) during both seasons.

It is clear from the literature that, despite small differences, the time budget across populations in industrialised countries is by in large quite similar. Moreover, the large amount of time spent indoors by individuals is an extremely important factor for the determination of the degree of personal exposure to PM and other pollutants.

## 2.5 Determinants of Personal Exposure to PM

There are a variety of factors that determine the levels of personal exposure to PM of an individual in both indoor and outdoor environments. In the outdoor environment, factors such as meteorological conditions, traffic and urban street profile have a large influence on ambient PM concentration. While indoors, the activity of an individual can have a great effect on personal exposure, additionally, infiltration from outdoor pollution can also be an important factor. Many of these major determinants will be discussed in further detail in the succeeding subsections.

### *2.5.1 Wind speed and direction*

Perhaps the most influential meteorological determinant for outdoor PM levels is the wind. Wind speed affects the rate of transport of particles as well as the rate of dilution with cleaner air. The two main factors that dictate the dispersion of particles in the air are the mean wind speed and the characteristics of atmospheric turbulence (Pfafflin and Ziegler, 2006). Higher wind speeds have been attributed in studies to both a reduction in ambient PM concentrations (Molnár et al., 2002; Holmes et al., 2005) and personal exposure concentrations (van Wijnen et al., 1995; Kingham et al., 1998; Alm et al., 1999).

In London, Adams et al. (2001b) showed that high wind speeds were strongly associated with a decrease in road transport user personal exposure levels, and explained 18% of the variability in exposure levels. In-car taxi exposures to black

smoke (BS) were examined in Paris by Zagury et al. (2000), and it was found that high wind speeds decreased BS concentrations and explained 39% variance in exposure levels. Interestingly, however, Alm et al. (1999) observed a decrease in fine PM urban commuting exposure, yet found the coarse PM fraction increased as a result of windblown dust.

Not only does mean wind speed have a major effect on the concentration of PM, but a number of studies have identified wind direction to have a considerable influence on particles, particularly those in the fine fraction (Kaur et al., 2007). In the Netherlands, Weijers et al. (2004) examined the variability of PM concentrations along roads and motorways, and observed that people residing 100m downwind of a major traffic source were exposed to 40% more particles than those living in urban background areas. A study from Cairo found wind direction to have an influence not only on pollutant concentrations but also on the correlation between pollutants, and as expected ambient $PM_{10}$ concentrations were also reduced at higher wind speeds (Elminir, 2005).

The profile of a street too can significantly alter the concentration of pollutants from vehicles along that street. The street canyon environment of cities has been singled out as a hotspot in terms of air pollution. This is due to the sheltering effect of the buildings which inhibits wind dispersion of particles and other traffic related pollutants (Buckland and Middleton, 1999); this then facilitates a build-up of pollutants within the street canyon which can subsequently be easily introduced indoors (Park et al., 2004).

A street canyon is categorised by the aspect ratio between the width of a street and the average height of buildings (Vardoulakis et al., 2002). The aspect ratio of the street canyon combined with the direction of external wind usually determines the dispersion of pollutants (Mukherjee and Viswanathan, 2001; Chan et al., 2002b).

It is not only the height and aspect ratio of the buildings that leads to a build-up of pollutants at street level, but the orientation of the street also contributes to pollutant build up. Street canyons lined with buildings of similar mean height that are perpendicular to the direction of the wind will have poorer circulation than street

canyons that are lined with buildings of different heights and are interspersed with open areas. As the wind blows perpendicular to the top of the street canyon, it creates a secondary current or 'pollution tunnel' within the street canyon which is what facilitates the build-up of vehicular pollution (see Figure 2.7). As a result, this secondary current flow, or pollution tunnel, results in higher pollution concentrations on the leeward side of a street than on the windward side. Once on the leeward side, the pollutants are then dispersed vertically (Buckland and Middleton, 1999).

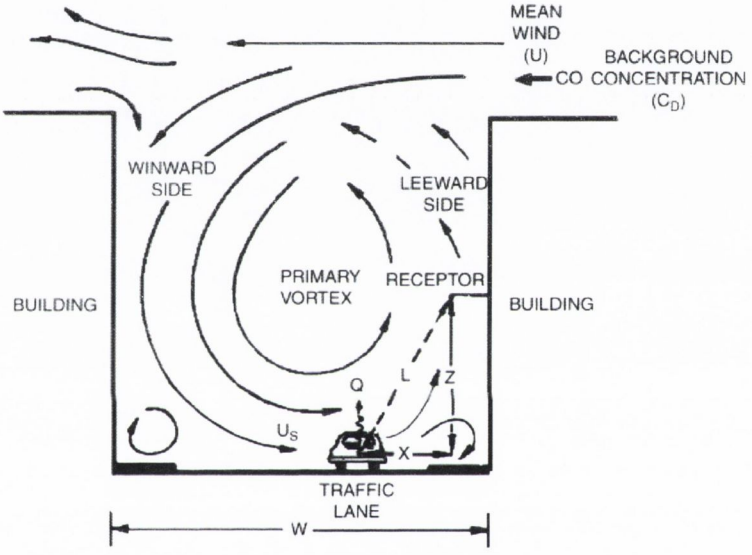


Figure 2.7: Pollutant dispersion in a regular street canyon (Dabberdt et al., 1973).

The pollution tunnels consist of high concentration levels of vehicle derived pollutants, and the highest concentrations are located at the centre of the road. The concentration of pollutants then reduces as the distance from the centre of the roadway increases. Pollution tunnels occur because the exhausts of vehicles are generally nearest to the centre of the road away from the kerb, and they subsequently get drawn into the secondary current flow caused by the wind. One result of this is that pedestrians are exposed to a lower concentration of pollution than a motorist on the road, for example, because usually they will be the furthest away from the centre of the road in the transport microenvironment. This has been demonstrated by previous research, in which pedestrians were found to have the lowest $PM_{2.5}$ exposure amongst a number of different commuter transport modes (Kaur et al., 2005a; McNabola et al., 2008b).

In Ireland, on a macro scale, the climate is strongly influenced by the Atlantic Ocean. The prevailing wind is south-westerly and the average wind speeds vary from 4m/s in the east midlands to 7m/s in the northwest of the country (Met Éireann, 2012). The nature of air mass origin in Ireland generally falls within two categories of clean westerly winds from the Atlantic or easterly winds bringing polluted air masses in from Europe and the United Kingdom (Ceburnis et al., 2006). However, due to the frequent air flow from the Atlantic, the air in Ireland is considered relatively clean. For airborne particulates the only concern are polluted urban sites, where concentrations can be increased due to primary vehicle emissions, and thus individuals in these areas will potentially have high personal exposures.

### *2.5.2 Temperature*

The effect of temperature on PM personal exposure levels appears to be very weak. A number of studies in the urban transport microenvironment have found weak correlations with meteorological factors other than wind speed, including temperature, relative humidity, and atmospheric pressure (Zagury et al., 2000; Adams et al., 2001b). However, a study by van Wijnen et al. (1995) found that temperature did in fact have a positive correlation with outdoor $PM_{10}$ personal exposure amongst cyclists, car drivers, and pedestrians.

One possible way that cold weather can affect levels of pollution in a city is through a winter time temperature inversion (Figure 2.8) like that seen in the 1952 London smog episode. A temperature inversion is a thin layer of the atmosphere where the decrease in temperature with height is much less than normal or in some extreme cases, the temperature increases with height. An inversion, also called a stable air layer, acts like a lid, keeping normal convective overturning of the atmosphere from penetrating through the inversion. An effect of this can be to trap air pollutants like PM from vehicles and industry below the inversion, which facilitates the build-up of pollution resulting in increased personal exposure across the urban area (Miller and Spoolman, 2009). As it happens, one such event like this actually occurred in Dublin City in 1982 (Kelly and

Clancy, 1984). Additionally, colder temperatures in winter also increase the amount of home and office heating that is used resulting in increased emissions of air pollutants.

Temperature also affects air pollution emissions in another way. If a vehicle has not been used for several hours, the temperatures of its engine and exhaust system will normally be similar to that of the ambient air. On starting a vehicle, rates of emissions and fuel consumption are higher during the warm-up phase than during thermally stable operation, particularly in the case of petrol engine vehicles. The emissions produced during the warm-up phase are often called 'cold-start' emissions. Some of the fundamental factors affecting cold-start emissions include the fuel and vehicle type, ambient temperature, wind speed, parking duration, and the drive cycle during the cold-start period. (Boulter and Latham, 2009).

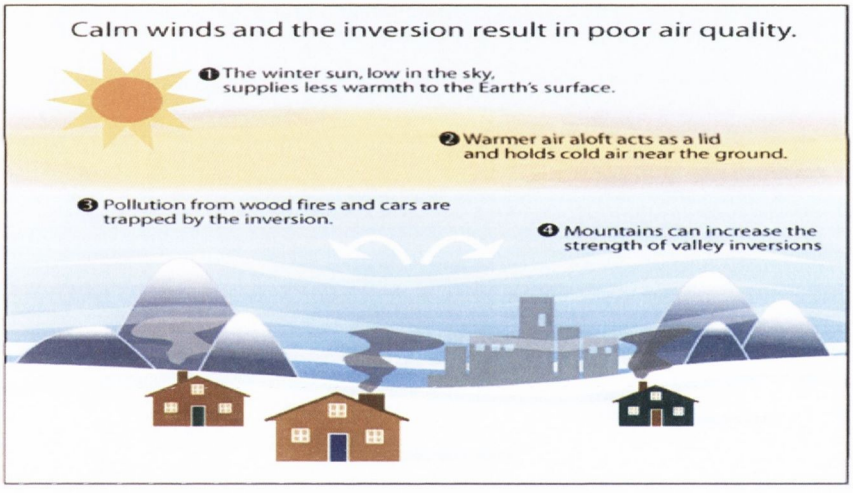


Figure 2.8: An example of a wintertime temperature inversion (NOAA, 2012).

### *2.5.3 Precipitation*

As previously alluded to, atmospheric aerosols can be removed from the atmosphere through the process of wet deposition. Wet deposition encompasses all processes in which airborne particles are removed from the air and transferred to the earth's surface in the form of rain, snow or fog. Atmospheric particles are removed in two ways, either by colliding with a droplet both within and below clouds, or else particles may serve as

nuclei for the condensation of atmospheric water to form a cloud or fog droplet and are subsequently incorporated in the droplet (Chate and Pranesha, 2004).

Not only does rainfall effectively scavenge PM from the atmosphere, but rain also further contributes by reducing the number of particles from resuspension due to road traffic. This can have important seasonal consequences for particulate matter concentrations. For example during the drier summer months there may be increased PM levels along roadways resulting from the extra resuspended particles. Many of these resuspended particles are coarse in size but some may fall into the fine particulate size fraction. Research conducted on the origin of $PM_{10}$ and $PM_{2.5}$ in different European countries have attributed higher road side concentrations in hotter southern countries to low levels of rainfall (Querol et al., 2004b; Querol et al., 2008).

In Ireland, the average number of days with more than 1 mm of rainfall in the east of the country is approximately 150, and this varies to more than 200 days in the west (Yin et al., 2005). Consequently, the frequent precipitation events are a major factor contributing to the relatively clean air in Ireland (Ceburnis et al., 2006). The overall effect of which is a reduction in background concentrations and thus a reduction in personal exposure, particularly when an individual is located in the vicinity of a road.

### *2.5.4 Traffic*

The number of vehicles on a road has a great effect on particle concentration in the ambient air. In the urban environment road transport is regarded as the largest contributor of $PM_{10}$ (QUARG, 1996). Greater traffic volumes in urban areas mean there are more vehicles to release particles into the atmosphere. High traffic volumes also means vehicles move slower which further increases the amount of particles released. Heavily congested traffic, typical in the urban environment, is constantly in a stop-start motion and is possibly the most polluting form of driving on a gram per kilometre basis (O'Mahony et al., 2000). Car journeys are also slowed down when moving through congested urban areas with average speeds of approximately 10-20 kph (Rank et al., 2001; Jensen et al., 2010). This means that the duration spent commuting by car drivers

is longer, and therefore personal exposure and dose of PM absorbed will be increased for individuals in that particular microenvironment.

The vehicles that form traffic in a city are also important in determining the type of PM present in the ambient air. Traffic dominated by diesel engine vehicles will produce much higher levels of $PM_{2.5}$ than traffic made up of mainly petrol engine vehicles. In Ireland, the vast majority of heavy duty vehicles are diesel powered, and according to the EU, diesel passenger cars also make up 18% of the private car fleet (European Commission, 2011).

Diesel PM is made up of a number of components. Firstly, the core of the PM is made up of agglomerates of primary soot particles, onto which a layer of condensed hydrocarbons is adsorbed. Sulphuric acid droplets, derived from the $SO_2$ generated from the fuel sulphur during the combustion process, can also condense, and these sulphate species can further adsorb water. Nitric acid, derived from the engine-out $NO_x$, can also condense on the primary soot particles. Finally, oil derived species such as derivatives of Ca, P and Zn can become entrained in the PM also (Walker, 2004). The fine size fraction and potentially toxic coating of these particles have implications for human exposure and well-being.

In the transport microenvironment, proximity to dense traffic and idling vehicles at traffic lights has been found to increase the personal exposure of cyclists and pedestrians, as well as raise in-car concentrations. Individuals waiting at bus stops are also more susceptible to experiencing elevated particulate exposures as traffic passes by (Kaur et al., 2006). Clearly from a personal exposure perspective, traffic volume is one of the primary determinants of outdoor PM and will greatly influence the exposure of an individual as they commute to and from their place of work.

### *2.5.5 Indoor sources*

It is well established that the indoor environment contributes significantly to human exposure to PM (Rojas-Bracho et al., 2000; Sarnat et al., 2000). A large proportion of an individual's time is spent at home, and thus, they are exposed to PM from a range of

indoor activities. Indoor PM concentrations have been measured in residential dwellings around the world by different studies. Research has shown that houses without a high level of human activity have lower indoor concentrations of $PM_{10}$ and $PM_{2.5}$ (Monn et al., 1997).

In the indoor microenvironment, particles smaller than about 5 μm are likely to remain suspended in the air for a significant period of time and so may be carried further from the source and still contribute to exposure. Many of these particles may be produced indoors by smoking, cooking, and other combustion sources. The smaller particles are predominantly lost from the air by deposition after diffusion towards surfaces and to a lesser extent by electrostatic attraction (UK Department of the Environment, 2004).

There is wide variation of PM concentrations in dwellings reported throughout the vast amount of literature. Chao and Wong (2002) found that mean indoor $PM_{2.5}$ and $PM_{10}$ concentrations in 34 homes in Hong Kong were 45.0 and 63.3 $\mu g\ m^{-3}$, respectively. Haller et al. (1999) in the United States reported that indoor $PM_{2.5}$ and $PM_{10}$ concentrations were 10.8 and 23.8 $\mu g\ m^{-3}$. In Birmingham, the UK, Jones et al. (2000) found that indoor $PM_{2.5}$ and $PM_{10}$ concentrations were 7.9 and 16.5 $\mu g\ m^{-3}$, respectively. In Helsinki, low levels of $PM_{2.5}$ (9.5 $\mu g/m^3$) were also reported in homes of volunteers (Götschi et al., 2002). Other European studies in Athens, Basel, Prague and several cities in France have observed greater fine PM concentrations for dwellings in the range of 20-36 $\mu g/m^3$ (Götschi et al., 2002; Zmirou et al., 2002).

There is a range of human activities that can contribute to indoor PM, and during some of these activities PM concentrations can be elevated as much as 10 times that of normal situations, for short or even longer periods of time (Wallace et al., 2006a). Indoor sources such as cooking, cleaning, smoking, burning of candles and incense sticks, spraying of aerosols and even walking have been found to be significant sources of indoor PM by numerous studies (Long et al., 2000; Chao and Cheng, 2002; Hussein et al., 2006; Ott and Siegmann, 2006; Glytsos et al., 2010).

Indoor/outdoor air studies have determined that smoking and cooking are the predominant activities associated with elevated concentrations of indoor particles (Wallace, 1996). Cooking has a major influence on particulate matter levels indoors. Oven cooking, toasting, and barbecuing have been reported to be the main source of fine particles when cooking, with coarse particles generated from frying and sautéing (Abt et al., 2000a). He et al. (2004) quantified the emission characteristics of indoor particle sources in 15 houses in Brisbane, Australia, and found indoor approximation of $PM_{2.5}$ concentrations showed an increase over the background concentration by 30 and 90 times during grilling and frying, respectively. Other types of cooking, for example Asian style cooking, have also been found to greatly increase particle concentrations (Lee et al., 2001; See and Balasubramanian, 2006), with some of the highest concentrations attributed to frying. Frying has been reported to be capable of increasing the total particle production due to cooking by factors of 6-10 (Wallace et al., 2004). Olson and Burke (2005) have highlighted the significance that burning food has on releasing PM into the indoor air, when examining $PM_{2.5}$ source strengths for cooking the highest mean source strengths identified were from burned food (mean = 470 mg/min), grilling (173 mg/min), and frying (60 mg/min).

Some studies have also observed that the type of cooker in a home can be important with Monn et al. (1997) reporting that indoor/outdoor ratios for $PM_{10}$ were slightly higher in homes with gas cookers. Research by Dennekamp et al. (2001) found that high concentrations of ultrafine particles were generated by gas combustion, with the highest concentrations emanating from frying, and by cooking of fatty foods. Similarly, other studies have also observed that fat generates higher particle emissions, and that emissions not only depend on the type of food cooked but also the variety of oil used and temperature of cooking (Buonanno et al., 2009).

Aside from the contribution that cooking makes to concentrations of indoor exposure to PM, smoking is also major determinant of personal exposure. In a study of particulate concentrations in inner-city homes, Wallace et al. (2003) found the major indoor fine PM source was smoking, which elevated indoor concentrations by as much as 37 $\mu g/m^3$, in the 101 homes containing smokers. The difference between smoking and non-

smoking home concentrations found in that particular study was consistent with the difference found in an early study by Spengler et al. (1981) from data collected during the Harvard *Six Cities Study*. Several *EXPOLIS* studies have reported the elevated indoor and personal concentrations of not only fine PM, but also of black smoke (BS) particles when in the presence of environmental tobacco smoke (ETS) (Koistinen et al., 2001; Götschi et al., 2002; Lai et al., 2004). Smoking areas of cafés have also been reported as having higher concentrations of fine PM than the non-smoking areas (Mohammadyan et al., 2010b). A study conducted in the Czech Republic (Branis and Kolomazníková, 2010) also found high $PM_{2.5}$ concentrations associated with being present in restaurants, and this has been attributed to ETS that is present in Czech bars and restaurants in the absence of a smoking ban.

A number of indoor other sources, such as cleaning and type of heating, can also elevate personal exposure significantly. For instance, Branis and Kolomazníková (2010) recorded some of the highest personal $PM_{2.5}$ concentrations in indoor locations which were heated by solid fuel burning stoves. Numerous studies have also been conducted in which the use of biomass burning stoves, mainly in developing nations, is responsible for large indoor particle concentrations (Zuk et al., 2007; Begum et al., 2009). However, household heating and cooking in developed nations will generally not rely upon indoor biomass combustion.

Abt et al. (2000a) identified cooking, cleaning, and movement of people as the most important indoor particle sources in homes in Boston. Thatcher and Layton (1995) also observed that household residents performing cleaning and even light activity, such as walking, could significantly increase suspended particle concentrations. Just walking into a room can increase the particle concentration by 100% for some particle sizes (Thatcher and Layton, 1995). While Ferro et al. (1999) found that pushing a vacuum cleaner, with the vacuum cleaner on or off, increased human exposure to coarse PM by approximately 20 times as compared with background concentrations.

### *2.5.6 Occupational exposure*

Occupational exposure to PM is a microenvironment that can have a major influence on daily personal exposure due to the length of time on average spent in the workplace by an individual. Previous research has indicated possible adverse health effects such as cardiovascular disease associated with occupational particulate exposures (Magari et al., 2001; Fang et al., 2010).

For some people exposure at work will provide the greatest contribution to personal exposure to airborne particles. This is particularly true of those individuals whose occupations require them to be constantly in the transport microenvironment such as bus, lorry and taxi drivers. Numerous PM personal exposure studies have been conducted in the transport microenvironment and have identified associated high personal exposure concentrations. Many of these studies have been primarily concerned with personal exposure of commuters to $PM_{10}$ and $PM_{2.5}$ (Adams et al., 2001c; Chan et al., 2002a; Kaur et al., 2007; McNabola et al., 2008b). Nevertheless, some researchers have examined the exposure of drivers in the transport microenvironment.

Bus drivers in Sari, Iran, have been reported by Mohammadyana et al. (2009) to have a an extremely high mean $PM_{10}$ personal exposure of 180.9 $\mu g/m^3$, which in contrast is far higher than their Stockholm counterparts who had a mean exposure of 44 $\mu g/m^3$ (Lewné et al., 2006). In the same study Lewné et al. (2006) also found high $PM_{10}$ exposure concentrations for lorry drivers (57 $\mu g/m^3$), but relatively low concentrations for taxi drivers (26 $\mu g/m^3$). This figure reported for taxi drivers is far lower than the BS concentrations (164 $\mu g/m^3$) encountered in a Parisian taxi study by Zagury et al. (2000), although BS and $PM_{10}$ cannot be directly compared, daily mean BS is a reasonable predictor of daily mean $PM_{10}$ (Muir and Laxen, 1995).

Other studies have been conducted on non-vehicle based occupations. In Bologna, the occupational $PM_{10}$ personal exposure of traffic police and parking wardens was found to be relatively high (means of 181±93.2 $\mu g/m^3$ and 185.3±67.9 $\mu g/m^3$, respectively) (Violante et al., 2006). Additionally, the $PM_{10}$ personal exposure concentration of traffic

wardens was also found to be high in Edinburgh, albeit lower than the exposures encountered in Bologna, with median values of 123 $\mu g/m^3$ and 41 $\mu g/m^3$ for two different weeks of sampling (Watt et al., 1995). Toren et al. (2007) examined whether occupational exposure to particulate air pollution increased the risk of heart disease among a cohort of 176,309 occupationally exposed Swedish male construction workers and 71,778 unexposed male construction workers. The findings of this study did indeed conclude that occupational exposure to particulate air pollution, especially diesel exhaust, increased the risk for ischaemic heart disease for the construction workers.

Office workers also seem to have higher personal exposure concentrations when at work compared to at home indoor concentrations. A study of office workers in Paris found mean personal $PM_{2.5}$ concentrations at work exceeded the corresponding at home indoor concentrations by nearly 10 $\mu g/m^3$ (Mosqueron et al., 2002). While Mohammadyan (2011) also observed a similarly increased personal $PM_{2.5}$ concentration amongst office workers in Bradford. The difference between at work and at home of both studies were in line with the *EXPOLIS* study which found mean personal $PM_{2.5}$ indoor work concentrations of 40.4 $\mu g/m^3$ and at home concentrations of 26.4 $\mu g/m^3$ across all six cities involved in the study.

The size of an office and location of the ventilation system can be important for personal exposure also. Studies have found that larger offices have higher particle concentrations than smaller quieter offices (Mohammadyan et al., 2010b). The same study by Mohammadyan et al. (2010b) also found that $PM_{2.5}$ concentrations increased inside the office when windows were opened. As part of the U.S. EPA *Building Assessment Survey and Evaluation (BASE) Study*, Mendell et al. (2008) identified risk factors for building-related health symptoms in office workers. The study found that poorly maintained heating, ventilating, and air-conditioning (HVAC) systems may be sources of contaminants that cause adverse health effects in occupants. Mendell et al. (2008) also suggested that outdoor air intakes lower than 18 stories in office buildings may be associated with substantial increases in many symptoms, which may be linked to ground-level vehicle emissions.

### *2.5.7 Infiltration*

Infiltration of particulates into a building can play an important role in determining the concentrations found within the indoor microenvironment. Knowledge of factors affecting infiltration, such as the air exchange rate of a building, indoor particle sources, and the exterior ambient concentration, aids in the understanding of how outdoor concentrations might affect concentrations inside a building. Many studies have examined the indoor/outdoor relationship of various air pollutants including $PM_{10}$. Several studies have reported lower indoor $PM_{10}$ concentrations in homes than those concentrations found outside, with indoor/outdoor ratios reported as 0.7 (Colome et al., 1992; Monn et al., 1997). While Jones et al. (2000) reported indoor/outdoor ratios for mass concentrations of particles that were generally greater than unity for all study sites, which demonstrated the influence of indoor sources.

The relationship between indoor and outdoor particle concentrations has been discussed in Özkaynak and Spengler (1996), who state in the absence of indoor sources, particle concentrations will be lower inside buildings than outside. This was certainly the case for Monn et al. (1997) who found that in homes without a high level of human activity and without indoor sources, the concentrations of $PM_{10}$ and $PM_{2.5}$ were lower than outdoor levels.

The differences in indoor and outdoor concentrations is greater for coarse particles ($PM_{2.5}$-$PM_{10}$) than for fine particles ($PM_{2.5}$) because the larger particles tend to settle out and deposit once inside, and not due to a failure to penetrate into buildings. Indeed, the reduction in particles through deposition rather than filtration losses through the building envelope has been suggested by previous research (Thatcher and Layton, 1995; Özkaynak and Spengler, 1996). Furthermore, coarse particles seem to penetrate into buildings more easily than $PM_{2.5}$, which is more dependent on active ventilation. Results from Koistinen et al. (2001) underpins this hypothesis that larger indoor particles predominantly originate from outdoor air pollution, whereas fine PM can have significant additional sources indoors. However such conclusions are countered by results from the multiple regression models performed by Abt et al. (2000b), based on

air exchange rates less than 1 exchange per hour, suggesting that there are more indoor sources of coarse particles than fine particles.

Air exchange rates can have a profound effect on indoor PM concentrations and subsequent personal exposure of an individual. A study by Abt et al. (2000a) attempted to characterise indoor particle sources and observed that low air exchange rates (< 1 exchange/hr) resulted in longer air residence times and more time for particle concentrations from indoor sources to increase. When the air exchange rates were higher (> 1 exchange/hr), indoor particle concentrations tracked outdoor levels more closely due to the impact of indoor sources being less pronounced.

As long as the ambient outdoor air has a lower PM concentration, higher exchange rates will help lower the indoor particle concentration. However, if a building is located in an area with high PM concentrations, for instance beside a busy road, higher exchange rates will only serve to bring these outdoor particles into the building (Vallero, 2008). This may explain why, for example, Mohammadyan et al. (2010b) observed that opening the windows in an office located in central Bradford increased $PM_{2.5}$ concentrations inside the office. Ventilation from window opening was also examined by Cyrys et al. (2004) who found $PM_{2.5}$ and BS I/O ratios were lowest when the windows of a building beside a major road were closed (0.63 and 0.44 respectively).

In previous research, it has been estimated that 60-75% of outdoor $PM_{2.5}$ and 65% of outdoor $PM_{10}$ effectively penetrate indoors (Koutrakis et al., 1992; Özkaynak et al., 1996). However, due to indoor sources the overall contributing proportion to the indoor concentration from outdoor PM is markedly less. A multivariate model developed by Wallace et al. (2003) indicated that outdoor particles penetrated indoors with an efficiency of 0.48, and were therefore responsible for only 25% of the mean indoor concentration. This finding is further supported by regression modelling conducted by Abt et al. (2000b) who found that for particles in the 2 to 10 μm range, only 20 to 43% of indoor particles originated from outside.

## 2.6 Comparison of Personal Exposure with Fixed Site Monitors

Traditionally, exposure to outdoor particles was considered the most important component of total exposure, but over the last few decades both the composition and concentration of ambient PM has changed. Air pollution control efforts have succeeded in removing much of the settleable dust from industry and power generation, however, these industrial control efforts have had only a minor impact on concentrations of particles in the fine or respirable range (Özkaynak and Spengler, 1996). Much of the control programmes implemented had been directed at the reduction of outdoor PM in anticipation of gaining major air quality improvements and health benefits with the reduction. However, total exposure assessment studies conducted in the nineties began to shed more light on the relative contribution of outdoor pollutants to total personal exposure (Wallace, 1996).

Many air pollution epidemiological studies have been conducted under the fundamental assumption that outdoor PM concentrations from a fixed site monitor (FSM) serve as a surrogate for personal exposure as well as dose (Dockery et al., 1993; Pope et al., 1995; Linn et al., 2000; Lipfert et al., 2000; Stieb et al., 2000). It is now well known, however, that there is substantial variability in the exposure of individuals to PM. Factors that contribute to this variability include indoor sources, spatial variability in ambient concentrations and the time-activity profile of the individuals.

There have been numerous studies that have compared PM personal exposure measurements with background monitored concentrations. The level of correlation between FSMs and personal exposure concentrations has varied greatly among studies conducted. Though there have been several which reported good correlation, many others have not done so.

Early attempts were made by Dockery and Spengler (1979) and Šega and Fugaš (1982) to determine to what extent personal exposure to total respirable particles could be assessed from data on TSP concentrations from FSMs. Both studies found good correlation between the personal and background data sets ($R = 0.69$ and $R = 0.71$,

respectively). However, Šega and Fugaš did caution, because of the large intercept observed on their regression graph, that there is a considerable contribution to personal exposure from other sources.

More recently, in a study of the transport microenvironment in London, Adams et al. (2001c) reported that road transport mode exposure levels encountered were elevated by approximately 100% compared to $PM_{2.5}$ concentrations at an urban centre monitor. The difference was primarily attributed to the difference in sampling techniques for personal exposure and the fixed site monitor. For personal exposure sampling, Adams et al. (2001c) used a manual gravimetric sampling device, whereas the urban centre monitoring instrument was a Tapered Element Oscillating Microbalance (TEOM), which they concluded may not produce identical results when run side by side. The TEOM device has in the past been found to underestimate PM concentrations when compared to gravimetric sampling methods (Ayers et al., 1999; King et al., 2000). Similarly, other papers on personal exposure in the transport microenvironment (Kaur et al., 2005a; Kaur et al., 2005b) found little correlation between the TEOM fixed site monitor and gravimetric sampled personal $PM_{2.5}$ concentrations.

Gulliver and Briggs (2004) also studied the PM personal exposure of commuters in Northampton, U.K. They reported that a kerbside $PM_{10}$ FSM gave consistent estimates of exposure for both walking and in-car modes, though concentrations were slightly underestimated in both cases. However, when the personal exposures on a commuting route over 1km away were compared with the FSM it was shown to give poor predictions of exposure for both in-car and walking, with the average $PM_{10}$ personal exposure of pedestrians being 30% higher than the FSM, and average in-car exposures 67% higher.

Several of the studies already discussed (Adams et al., 2001c; Gulliver and Briggs, 2004; Kaur et al., 2005b) have all been conducted in the transport microenvironment, and involved comparing PM personal exposure samples taken over a short amount of time while commuting with a FSM. However, other research conducted over longer sampling time periods has also concluded that personal exposure measurements can

have poor correlation with FSMs. Oglesby et al. (2000) found that $PM_{2.5}$ personal exposure concentrations gathered over 48-hour periods were poorly correlated to corresponding outdoor levels measured at a FSM (R = 0.07). This was similar to findings by Adgate et al. (2002), who also gathered 48-hour $PM_{2.5}$ personal exposure samples and found no statistical relationship between the outdoor monitored concentrations and personal exposure.

In an earlier study by Clayton et al. (1993), the 12-hour $PM_{10}$ personal exposure samples that were obtained from participants tended to exceed background concentrations on average by 50%. More recently, papers published by Brown et al. (2008) and Crist et al. (2008), both of which used gravimetric sampling of personal $PM_{2.5}$, found weak associations between ambient PM levels and the personal exposure samples taken over the course of the respective studies. Much of the research in the literature have focused on $PM_{2.5}$, but Violante et al. (2006) concluded in their study that $PM_{10}$ data provided by FSMs could not automatically be taken as an indicator of the real street-level exposure concentration encountered by street workers.

Evidently, much of this research indicates that there is a poor relationship between ambient PM concentrations and personal exposure. Yet, in certain instances, this consensus has been contradicted by studies that have yielded high correlation for the relationship between FSMs and personal exposure.

Janssen et al. (1998a) reported from a study of $PM_{10}$ personal exposure in Amsterdam that results showed a reasonably high correlation between personal and outdoor $PM_{10}$ within individuals. More recently, there have been personal exposure studies on $PM_{2.5}$ that have observed good correlations between background monitoring sites and the personal exposure of the monitored individuals. In a study of personal exposure to $PM_{2.5}$ among high-school students, Borgini et al. (2011) found a good agreement between the daily mean personal exposures of the students and background concentrations with an overall Pearson's correlation coefficient of 0.63. In another study, Branis and Kolomazníková (2010) compared the outdoor and indoor personal exposure data of the single study volunteer when she was at home, or in the vicinity of

her home, to the nearest FSM and found a correlation of 0.78. Both studies concluded that fixed site monitored data could be used as a proxy for personal exposure in different microenvironments.

Early analysis of preliminary data as part of this current study found little relationship between 24-hour mean background concentration and 24-hour personal exposure for typical office workers, living in the Greater Dublin Area (McNabola et al., 2011). However, when the 8-hour mean concentration for office working hours was examined a stronger association was found as the subjects' workplaces were located close to the FSM. This was in contrast to the home location, for example, which was geographically a greater distance away from the city centre FSM data used, and thus the background concentration recorded did not have as great an influence on personal exposure.

The discrepancy in findings between personal exposure studies clearly indicates that there are additional factors perhaps affecting the personal exposure concentrations reported. Some of the studies may have been adversely affected by particles sources in the locality of the personal exposure monitoring. Distance to the nearest FSM could have also play a role in poor correlations to personal exposure data. Thus, this is an area that may warrant further research.

## 2.7 Modelling Personal Exposure

Modelling is an important tool for assessing population exposures to air pollution. This following section will provide an introduction to modelling concepts and various models that have been reported in the literature.

Exposure models enable the estimation of pollutant exposure for groups of people and time periods for which personal monitoring has not been conducted. Modelling can be used to combine information from different sources to produce estimates for population exposures that would be very expensive or impossible to measure. The performance of a developed model is usually validated against observed data to determine how well it performs in the real world. The performance tests which a model is subjected to are

conducted in order to quantify how closely predictions match observed parameters and to identify model component deficiencies that might be responsible for poor predictions.

### *2.7.1 General concepts*

The time-integrated total exposure of an individual to airborne PM can be described by the compartmentalisation of an individual's activities over a certain time period (US EPA, 2009). This can be expressed in the form of Eqn. 2.11, where $E_T$ = total exposure over the time period, $C_j$ = PM concentration in microenvironment $j$, and $dt$ = proportion of time spent in microenvironment $j$.

$$E_T = \int C_j \, dt \qquad \text{Eqn. 2.11}$$

As microenvironments are subject to ambient ($E_a$) and non-ambient ($E_{na}$) PM exposures, Eqn. 2.11 can be decomposed into a micro-environmental model that accounts for these (Wallace et al., 2006b; Wilson and Brauer, 2006), as can be seen in Eqn. 2.12.

$$E_T = E_a + E_{na} \qquad \text{Eqn. 2.12}$$

Eqn. 2.12 is illustrated in Figure 2.9. These ambient PM sources include all the normal PM formations mechanisms such as mobile and industrial sources, biomass combustion, re-suspension of dust, and secondary particles. In contrast, examples of non-ambient PM sources include cleaning, cooking, smoking, home heating and indoor air chemistry.

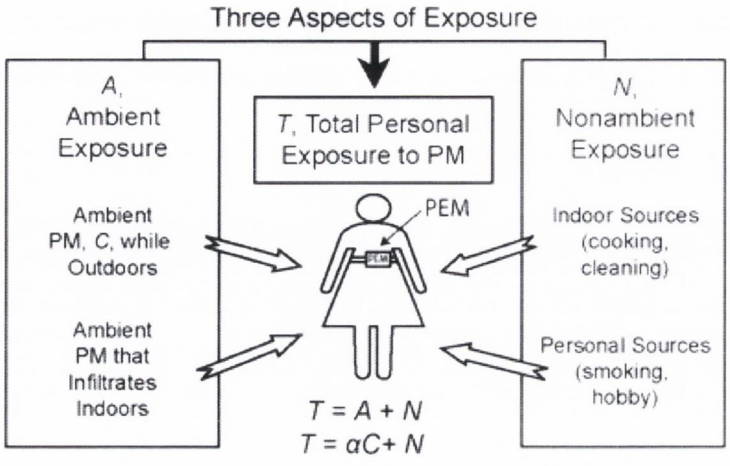


Figure 2.9: Total personal exposure contains both ambient and non-ambient exposures (Wilson and Brauer, 2006).

The ambient component, $E_a$, can be further broken down into the fraction of time spent in indoor and outdoor microenvironments.

$$E_a = [f_o + (1 - f_o)F_{inf}]C_a \qquad \text{Eqn. 2.13}$$

Giving the total exposure as:

$$E_T = [f_o + (1 - f_o)F_{inf}]C_a + E_{na} \qquad \text{Eqn. 2.14}$$

Where $f_o$ is the fraction of time spent outdoors, and $C_a$ is the ambient concentration. $F_{inf}$ is the building-specific infiltration efficiency, and represents the equilibrium fraction of the PM concentration outside the microenvironment that penetrates inside the microenvironment and remains suspended (Cohen et al., 2009; US EPA, 2009).

### *2.7.2 Exposure models*

Throughout the literature there are a number of different approaches taken in order to develop personal exposure models. The main approach initially taken in much of the literature is the general microenvironment model which was discussed in the previous

subsection. This model (Eqn. 2.15) has been described in detail by Duan (1982) and Ryan et al. (1986).

$$E = \sum_i E_i = \sum_i f_i C_i \qquad \text{Eqn. 2.15}$$

In Eqn. 2.15, $E_i$ is the exposure in the $i$th microenvironment; $f_i$ is the fraction of time spent in the $i$th microenvironment; and $C_i$ is the pollutant concentration in the $i$th microenvironment. The combination of personal exposure data with activity and time data can give reasonable estimates of total exposure for many air pollutants. The model can be further enhanced with knowledge of concentrations within the various microenvironments (Letz et al., 1984). Where there is no PM concentration data available for an indoor environment, it can be derived from Eqn. 2.16. Where $P_i$ is the effective penetration factor of the pollutant into the $i$th microenvironment, $C_a$ is the outside ambient concentration and $S_i$ is the contribution of indoor sources in the $i$th microenvironment.

$$C_i = P_i C_a + S_i \qquad \text{Eqn. 2.16}$$

This empirical modelling based on Eqn. 2.15 has also been utilised in a number of different studies more recently (Hänninen et al., 2003; Kruize et al., 2003; Delgado-Saborit et al., 2009; Harrison et al., 2009). The structure of the *EXPOLIS* stochastic exposure modelling simulation framework used the basic concept of time-weighted average exposures (Eqn. 2.15) which are the sum of the partial exposures of the visited microenvironments (Kruize et al., 2003).

The same empirical modelling technique was used in Delgado-Saborit et al. (2009), which fed into the Health Effects Institute (HEI) report by Harrison et al. (2009). For this report personal exposure to VOCs was monitored and different models were developed for exposure. Two of the models used in this study are shown in the following equations:

$$Y_{ij} = \sum \frac{t_{ijk} + X_{ik}}{T_{ij}} \quad \text{Eqn. 2.17}$$

$$Y_{ij} = \sum \frac{t_{ijk} + X_{k}}{T_{ij}} \quad \text{Eqn. 2.18}$$

In Eqn. 2.17, $Y_{ij}$ is the predicted personal exposure for a subject $i$ on a day $j$, $t_{ijk}$ is the time spent in microenvironment $k$ by subject $i$ on a day $j$, $X_{ik}$ is the concentration representative of microenvironment $k$ for subject $i$, and $T_{ij}$ is the total time spent in all microenvironments by subject $i$ on a day $j$. This model predicts the personal exposure by integrating the fraction of time spent in each microenvironment and multiplies it by the concentration in each microenvironment visited.

The model presented in Eqn. 2.18 differs from model of Eqn. 2.17 because the microenvironment concentrations used for homes and workplaces are not from the data collected directly in each volunteer's home and workplace, but are instead pooled values representative of each microenvironment. This is articulated through $X_k$, the concentration representative of a microenvironment $k$, without specific regard to a particular subject $i$.

The model shown in Eqn. 2.18 was subsequently used to implement one further model below:

$$Y'_{ij} = \alpha \times Y_{ij} + \sum B_m A_m + \sum \gamma_n F_n \quad \text{Eqn. 2.19}$$

In this model, $Y'_{ij}$ is the observed personal exposure for a subject $i$ on a day $j$, $\alpha$ is the coefficient associated with personal exposure, and $Y_{ij}$ is the personal exposure for the subject predicted in Eqn. 2.18. In this expression also, $A_m$ is an explanatory variable describing activities performed on a day $j$ by a subject $i$ or characteristics associated to a volunteer $i$, activities such as burning incense, being exposed to ETS, or living in a house with an internal garage. $\beta_m$ is the coefficient associated with the explanatory variable $A_m$. Finally, $F_n$ represents the time spent doing various activities, and $\gamma_n$ is the coefficient associated with $F_n$ (Harrison et al., 2009).

A number of studies have used time-weighted micro environmental models to estimate PM exposure. Many of these studies have used questionnaires, time-activity diaries or GPS to track exposures (Johnson et al., 2000; Elgethun et al., 2002; Olson and Burke, 2005; Cohen et al., 2009). For example, a study by Seaton et al. (1999) estimated individual exposures to $PM_{10}$ indirectly by using a mathematical model based on measurements of urban background $PM_{10}$ concentrations, diary cards and multiple measurements of microenvironments. This demonstrated that it is possible to obtain valid $PM_{10}$ exposure estimates in individuals taking part in an epidemiological study and relate them to health end-points. Furthermore, many of the studies on an individual's time-activity pattern are conducted in conjunction with personal exposure, as well as indoor and outdoor PM concentration monitoring to estimate overall PM exposure.

Wu et al. (2005) built models to predict personal PM exposures based on either microenvironmental or central-site $PM_{2.5}$ measurements, and evaluated the modelled exposures against the actual personal measurements. The $PM_{2.5}$ personal exposure data was collected for 20 asthmatic children using a personal DataRAM (pDR, Thermo Andersen, Smyrna, GA), which is a continuous personal nephelometer device. The first model Wu et al. (2005) developed was a three-microenvironmental model ("ME model") based on hourly data:

$$\hat{E}_{1hr} = F_{oh}C_o + F_{oa}C_c + (1 - F_{oh} - F_{oa})C_i \qquad \text{Eqn. 2.20}$$

Where $\hat{E}_{1hr}$ is the predicted hourly personal exposure, $F_{oh}$ is the time fraction the subject spent at home outdoors, $F_{oa}$ is the time fraction the subject spent outdoors away from home (i.e. the other outdoor, school outdoor and road/transit microenvironments). The other two models developed by Wu et al. were linear regression models, using the daily measured personal exposure as the dependent variable. The first was the central-site model shown in Eqn. 2.21, which was the simplest regression model with only $C_c$ (the PM concentration measured at the central site) as the predictor for predicting personal exposure, $\hat{E}_{CM}$.

$$\hat{E}_{CM} = \beta_o + \beta_1 C_c \qquad \text{Eqn. 2.21}$$

The second regression model produced was called the 'Time-Space' model, and used time and space information as well as $C_c$ to predict personal exposure ($\hat{E}_{TS}$):

$$\hat{E}_{TS} = \beta_o + \beta_1 C_c + \beta_2 D + \sum_{k=3}^{9} \beta_k F_k + R \qquad \text{Eqn. 2.22}$$

Here in Eqn. 2.22, $D$ is the variable that accounts for the spatial pattern of PM and is distance from the subject's home to the central site, $F_k$ is the percentage of time that a subject spent in the $k$th microenvironment, and $R$ is the run period (i.e. the two-week monitoring period used in the study). The $R$ variable, a categorical variable, represents the order of the autumn and spring runs (from 1 to 7) and it captures the average meteorological conditions. The overall results from the study reported that the regression model (Time-Space Model, $R^2 = 0.41$) performed better than the ME model ($R^2 = 0.11$).

Regression modelling has also been used elsewhere, and throughout the literature in a variety of different ways. Brauer et al. (2000) used a stepwise regression procedure in order to model the personal exposure determinants of $PM_{10}$, $PM_{2.5}$ and $SO_4^{2-}$. They attempted to predict personal exposure and tested the models for a group of industrial workers, a combination of students and office workers, and a combination for all three groups. The predictors used in the model included indoor and outdoor concentrations, type of work, time spent at home, at work and in transit, location of residence, time spent cooking and self-reported exposure to ETS. For the model that included all subjects simultaneously, type of work was a significant predictor with industrial workers significantly different from other groups. Overall, 17% of the variability for $PM_{10}$ personal exposure of office workers and students was accounted for by regression models including outdoor PM and nicotine as the significant predictors. For industrial workers, the only significant variable was travel duration, explaining 46% of the variability.

Van Roosbroeck et al. (2007) used multiple linear regression to examine the relationship between distance of traffic from schools and personal soot, $PM_{2.5}$ and $NO_x$ exposures of school children. They concluded from their model that proximity to a freeway can be used as a valid estimate of exposure in epidemiological studies in children on the effects of the traffic-related air pollutants soot and $NO_x$. In another study, Johnson et al. (2000) used regression to determine whether predictive relationships in their scripted activity study could be used to estimate exposures of their $PM_{2.5}$ personal exposure study.

Multiple linear regression was also used by Branis and Kolomazníková (2010) in order to study meteorological effects during their study. The authors developed four separate simple and multiple regression models which attempted to predict the FSM (dependent variable) data from DustTrak concentrations, as well as allowing for ambient outdoor temperature and relative humidity. From this regression modelling they found that only 68.7% of data variability could be accounted for when compared to the FSM.

In another study by Wallace et al. (2006b), regression models were developed for predicting indoor $PM_{2.5}$ with outdoor ambient $PM_{2.5}$ and other explanatory indoor activity factors. The indoor model is shown in Eqn. 2.23, where $x_I$ represents the 50 appropriate continuous/categorical variables. The list of 50 variables contained household characteristics and personal activities, which were obtained through a questionnaire. In addition, two measured quantities were also included (air exchange and outdoor temperature).

$$PM_{2.5\,in} = \alpha + \beta_{out} PM_{2.5\,out} + \beta_1 x_1 \qquad \text{Eqn. 2.23}$$

Linear regression can also be used to model personal exposure, as seen in Harrison et al. (2009):

$$Log(Y_i) = \alpha + \beta \times \log(X_{i,home}) + \varepsilon_i \qquad \text{Eqn. 2.24}$$

$$Log(Y_i) = \alpha + \beta \times \log(X_{i,home}) + \varepsilon_i \qquad \text{Eqn. 2.25}$$

The models in Eqn. 2.24 and Eqn. 2.25 assess associations between personal exposure and microenvironmental concentrations, as measured in homes and workplaces directly related to each subject. In the models, $Y_i$ is the five-day average measured personal exposure for a subject $i$, $\alpha$ is the intercept of the model, $\beta$ is the slope of the model, and $X_i$ is the home or workplace average concentration for subject $i$. Finally, the $\varepsilon_i$ term accounts for random error.

Regression based approaches can also be incorporated into time-weighted microenvironmental modelling, as already seen in Wu et al. (2005). Chang et al. (2003) took personal $PM_{2.5}$ data from two different exposure studies to compute total personal exposure based on time-weighted microenvironmental exposures for each panel subject:

$$E_T = ME_i\beta_i \sum_k f_k C_k + ME_o \sum_k f_k C_k \qquad \text{Eqn. 2.26}$$

In Eqn. 2.26, $ME$ is the microenvironment for both indoor and outdoor, $\beta$ is the regression coefficient which reflects the accuracy of the exposure estimate for a given microenvironment, $f_k$ is the fraction of time performing an activity, and $C_k$ is the personal exposure concentration associated with the activity $k$. The models were tested with hourly $PM_{2.5}$ personal exposure data, hourly ambient concentration data, and daily ambient concentration data. Chang et al. (2003) found that time-activity data improved estimates of 24-hour exposure in comparison with using 24-hour ambient $PM_{2.5}$ data, but the use of hourly ambient data was comparable to personal microenvironmental data in estimating exposure. The term $\beta$ reflected infiltration for the indoor microenvironmental estimates for a sample population when ambient concentration data was used.

There is little research work available in the literature on the use of logistic regression for the determining of personal exposure to PM. However a study by deCastro et al. (2006) determined the odds ratios of a panel of subjects' locations within a given microenvironment using multivariate logistic models for three microenvironments – indoor-home, indoor-school and outdoors. The time-location information was obtained

as part of its assessment of personal exposures to air toxins for high school students in two major urban areas. The study found that the city of residence was a significant predictor of being indoors at school, having an afterschool job was a significant predictor of being indoors at home, and age along with having an afterschool job were significant predictors of being outdoors.

### *2.7.3 Monte Carlo and Latin hypercube simulation methods*

Monte Carlo simulation is a powerful mathematical method for conducting quantitative risk analysis. Monte Carlo methods rely on random or pseudo-random sampling of values by a computer from a probability distribution which are then inputted into a mathematical model and used to calculate outcomes of interest, such as exposure for instance. The technique requires a specified number of iterations, and with enough iteration Monte Carlo sampling recreates the input distributions.

In research conducted by Ryan et al. (1986), a Monte Carlo approach was used to investigate both the total exposure distribution of children to $NO_2$ and the contribution of a variety of microenvironments to this total exposure. For this approach, a distribution type is assumed for each parameter and a value is then selected randomly from the appropriate distribution to be used for the calculation. As the model was based on Eqn. 2.16, a beta distribution was chosen for $P_i$ and $f_i$, with a gamma distribution chosen for $S_i$ and $C_{out}$. The model was iterated 500 times giving an estimation of the entire distribution of total exposure and of the exposures for each microenvironment. This work by Ryan et al. (1986) demonstrated the feasibility of employing a Monte Carlo approach to investigate the exposure of individuals to air pollutants.

As part of the *EXPOLIS* study a Monte Carlo simulation approach was used as part of the exposure modelling framework (Hänninen et al., 2003; Kruize et al., 2003). However, a more sophisticated sampling technique called Latin Hypercube sampling was utilised as an alternative to Monte Carlo sampling. In the Latin Hypercube method, the input probability distributions are stratified. This means the distribution cumulative curve is divided into equal intervals and a random sample is selected from each interval.

The advantages of this method are that fewer samples are needed to create the whole distribution when compared to the regular Monte Carlo sampling. Owing to this way of sampling, situations that occur with a lower probability are represented in the simulation output, for example, high concentrations sampled from the tail of a microenvironment concentration distribution (Kruize et al., 2003).

Kruize et al. (2003) developed the *EXPOLIS* simulation in Microsoft Excel using the add-on risk assessment software @Risk (version 3.5, Palisade Corporation). The input data required to be used in the model were again, like Ryan et al. (1986), from Eqn. 2.15 and Eqn. 2.16. The concentration distributions were assumed to be lognormal, which followed the example from literature where concentration distributions and other distributions, which have a minimum level of zero and no upper limit, are often approached as lognormal (Ryan et al., 1986). For the microenvironments that had input data available Eqn. 2.15 was implemented, whereas Eqn. 2.16 was used in the case where the concentration distribution for an indoor microenvironment was not available. Hence, it was derived from ambient outdoor concentrations, the effective penetration factors, and also the contribution from indoor sources. Examples of the @Risk outputs for the model simulations can be seen in Figure 2.11, Figure 2.11, and Figure 2.12.

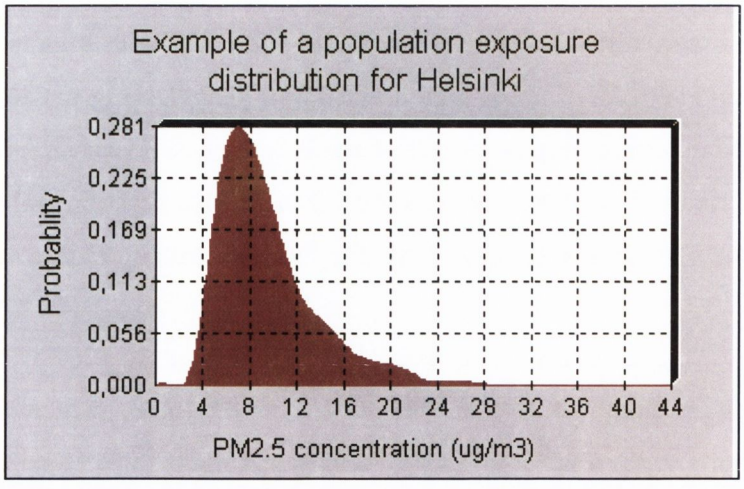


Figure 2.10: An example of the *EXPOLIS* @Risk population exposure distribution for Helsinki (Jantunen and Kansanterveyslaitos, 1999)

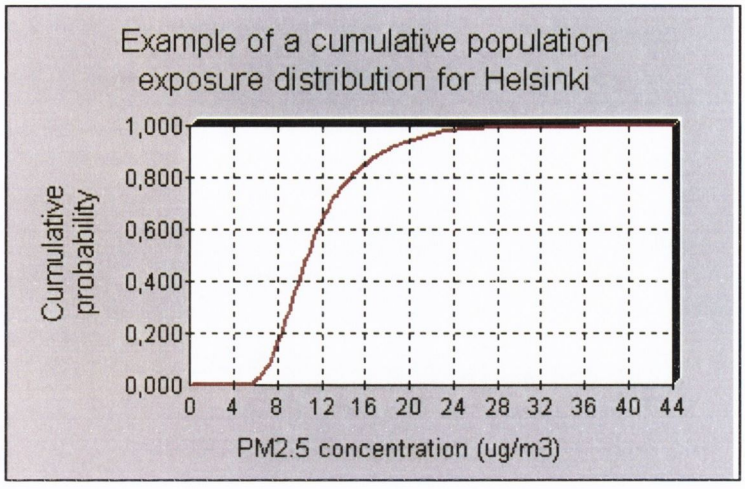


Figure 2.11: An example of the *EXPOLIS* @Risk cumulative population exposure distribution for Helsinki (Jantunen and Kansanterveyslaitos, 1999).

The results from the simulations in the *EXPOLIS* study showed that the simulated exposure concentrations for Helsinki and Basel were slightly under the observed $PM_{2.5}$ concentrations for the study populations, in contrast the Athens and Prague simulations were slightly higher than the observed values (Kruize et al., 2003). The mean population exposure concentrations for the four European cities were within 20% accuracy. From Figure 2.12 it can be seen that 'Home indoors' is the most important input distribution with a positive correlation of 0.654.

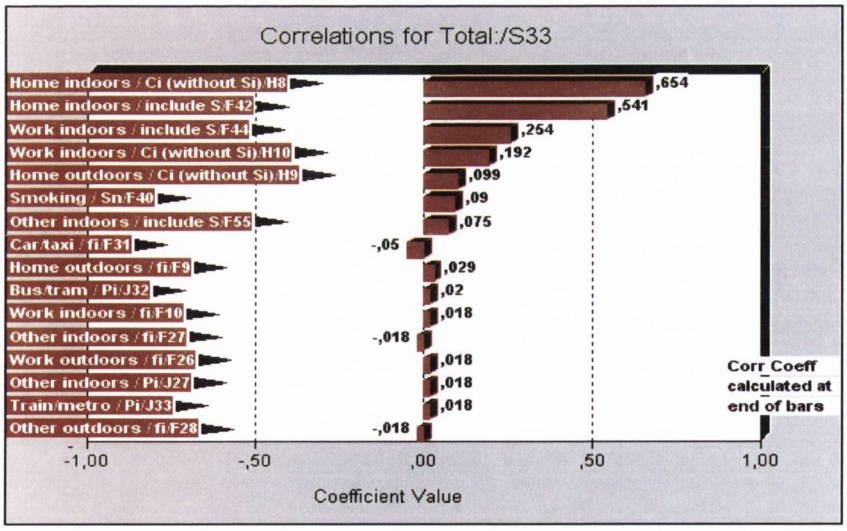


Figure 2.12: Example of an @Risk sensitivity analysis output (Jantunen and Kansanterveyslaitos, 1999)

Hänninen et al. (2003) concluded for their Helsinki study, when the required input data are available or reliably estimated for the microenvironments, that the target population $PM_{2.5}$ exposure distributions can be predicted accurately enough for most practical purposes using this kind of model. The Dutch $PM_{10}$ example presented by Kruize et al. (2003) showed a developed model, with use of the *EXPOLIS* framework, can be employed for larger more complex set ups for comparisons of subpopulations and scenarios based on different policy options. This Dutch example was derived from work by the Dutch Health Inspectorate, and Kruize et al. (2003) used directly available information from existing Dutch databases and from literature to estimate the population exposure distribution to $PM_{10}$.

For the purposes of this study, a similar approach using Latin Hypercube sampling can be implemented in order to simulate exposure concentrations on a distinct sub-population, such as office workers, rather than just general populations seen in *EXPOLIS*. The personal exposure sampling of the *EXPOLIS* study was also based on a gravimetric sampling method, which limited the number of microenvironments available for simulation. The resulting *EXPOLIS* simulations were based on defined distributions for three microenvironments of 'Work Indoor', 'Home Indoor', and 'All Other Places' (Hänninen et al., 2003). This approach may be improved upon with use of more microenvironment distributions through data collected by use of a real-time particulate monitor.

## 2.8 Modelling of the Human Respiratory Tract

Human respiratory tract models have been developed for use in a number of fields, including air pollution, pharmacology, and radiological protection. There are a number of different methods that can be utilised in order to model the human respiratory tract system, many of which will be discussed.

Early proposals to calculate particle transport onto airway surfaces used a variety of mathematical formalisms in order to do so (Heyder and Rudolf, 1984). The mathematical models developed included the temporally and spatially discrete

Findeisen formalism (Findeisen, 1935), the temporally discrete and spatially continuous Altshuler formalism (Altshuler, 1959), and the temporally and the spatially continuous Taulbee-Yu formalism (Taulbee and Yu, 1975). They are termed primary deposition models and are based on the consideration of the conservation of mass in a morphometric element of the respiratory tract of length *dx*. The number of particles deposited in the element in time *dt* must then be equal to the difference of the number of particles entering and leaving the element. Many of the primary model formalisms are adopted for use in what are termed secondary deposition models also (Heyder and Rudolf, 1984).

In more recent times the use of computational fluid dynamics (CFD) has been employed to model the human respiratory tract. The use of CFD has provided more detailed information on aerosol behaviour in the lung airspaces than early 1D (1-dimensional) modelling efforts previously discussed. There have been 2D models developed to study the aerosol transport and deposition in regions of the lung such as the larynx and alveolar region (Martonen et al., 1993; Chantal, 2001). 2D models are simplified versions of the lung with symmetrical shape, unlike real lungs which are not symmetrical. Moreover some 2D models have failed to consider the branching structure of the alveolar and they neglected the bifurcation area that connects the airways between branches. This has led to the development of more complex models in 3-dimensions.

CFD modelling has been conducted in several studies in order to model an anatomically accurate 3D adult nasal cavity (Subramaniam et al., 1998; Kimbell et al., 2001; Zhang et al., 2008). The models developed are often for the purpose of extrapolating the regional dose of an inhaled xenobiotic from laboratory animals to humans for purposes of assessing human health risk. The simulated nasal passage airflow models are useful in order to adjust for interspecies differences in the upper respiratory tract (Subramaniam et al., 1998; Kimbell et al., 2001). Other studies have also generated different areas of the respiratory system, such as the larynx, to model the flow and reactions (Gemci et al., 2003). The effect of inhaled charged particles has been numerically modelled also using CFD (Koolpiruck et al., 2004), but again this study mainly focused on the deposition in

one particular region (tracheobronchial region) represented by Weibel's tubular and double bifurcation models.

Respiratory tract modelling by CFD does however have a number of drawbacks. There is great variability in lung structure amongst individuals with each person having different lung geometry, surface area and volume. The most obvious example of this is differences in anatomical and physiological morphology observed between genders. In nasal airflow research, for example, the majority of research employed male subjects to determine nasal patency and no specific model studies have been conducted to ascertain the effect of gender on flow variables inside the nasal cavity (Zubair et al., 2011). CFD is a useful tool in giving an indication of general deposition of particles, but it may prove limited for modelling the inhalation and deposition of particles over a range of individuals. Moreover, due to the limitation of computational resources, these numerical studies are restricted to only some regions of human lung, i.e., extrathoracic, some sequences of bifurcation airways, and alveolar regions.

There have been techniques other than CFD that have also been used to model the human respiratory tract. Koblinger and Hofmann (1990) applied a Monte Carlo model to simulate the deposition of aerosol in the human lung. In this stochastic model the geometry of the airways along the path of an inhaled particle was randomly selected, with the deposition probabilities being computed by deterministic formulae. The model was derived from detailed morphometric measurements of the bronchial tree by Yeh et al. (1976) and of the acinar region by Haefelibleuer and Weibel (1988). The human lung was modelled by a sequence of tubes always branching into two daughter airways. This is known as an idealised bifurcation and the length of the parent and the angles between it and the two daughter tubes are the measured parameters which formulate the basis of the Monte Carlo model. Each bifurcation unit is therefore composed of half of the parent tube and half of the daughters, with the exception of the first unit which contains the whole of the trachea. However, though the effect of intra-subject variability of particle deposition was modelled, Koblinger and Hofmann (1990) did not have sufficient information available to derive distributions required for the consideration of inter-subject variations.

The model chosen for use as part of this thesis was the human respiratory tract (HRT) model that was developed by the International Commission on Radiological Protection (ICRP). This model was originally developed by the ICRP and used in the *ICRP Publication 30* as a means to calculate radiation doses to the respiratory tract of workers resulting from the intake of airborne radionuclides (ICRP, 1994). The model has subsequently been revised and updated as increased knowledge of the anatomy and physiology of the respiratory tract and of the deposition, clearance, and biological effects of inhaled particles has become available. Though this model has been developed for the specific use of radiological protection of workers, its design is such that it can be used for estimating dose to all hazardous particles or gases in the air. The model has been successfully implemented in previous work, with one such study by Liao et al. (2006) employing the model to calculate the personal exposure dose rates from particles due to cooking, cleaning and incense burning.

The HRT model has a number of advantages which may be beneficial to a study of this nature. Firstly, the model can provide an assessment of dose for individual members, both male and female, of populations of all ethnic groups. Secondly it can also account for various levels of physical activity, as well as varying height, weight and age. Therefore, it was deemed the most useful and conveniently implemented dose estimation model for this 24-hour personal exposure study.

## 2.9 Justification for Research

Air quality monitoring programmes have indicated that ambient PM concentrations in Ireland are lower than the limits set down in EU daughter directives (Dublin City Council et al., 2009). The introduction of legislation such as the bituminous coal ban in urban areas (Clancy et al., 2002), combined with improved vehicle engine emissions, has led to a reduction in ambient PM concentrations. It is still important, however, to establish whether or not ambient concentrations are fully reflecting the daily exposure of individuals. This may well not be the case as indoor sources could be contributing a large proportion to the personal exposure of a given subject. The use of real-time particulate matter monitoring equipment is therefore desirable, in order to quantify the

personal exposure of individuals throughout their daily routine. This approach serves to highlight activities and microenvironments with high PM concentrations and uptake.

Following the review of the published literature, it was found that there have been relatively few personal exposure studies to quantify the daily personal exposure to PM. In Ireland, personal exposure studies have almost exclusively been restricted to commuter personal exposure to fine PM and VOCs (O'Donoghue et al., 2007a; McNabola et al., 2008b). These studies have served to highlight the elevated concentrations of air pollutants that individuals may encounter in heavily trafficked areas. Furthermore, the results obtained by O'Donoghue et al. (2007a) also revealed that the overall uptake of an air pollutant in a microenvironment is dependent on the activity of an individual, for example, uptake while cycling was greater than commuting by bus. However, as seen in Section 2.4, the percentage of time a person spends commuting per day is low, usually between 5% and 7% on average.

In previous activity pattern studies, time spent in indoor microenvironments has been found to dominate the time budgets of those surveyed. Among the various indoor locations, the home and workplace are where an individual will spend the majority of his or her time. These microenvironments therefore play a key role in both the personal exposure to air pollutants and subsequent uptake.

Occupational exposure to PM can have a major influence on daily personal exposure due to the length of time on average spent in the workplace by an individual. Indeed, research has indicated possible adverse health effects, such as cardiovascular disease, associated with occupational particulate exposures (Magari et al., 2001; Fang et al., 2010). Occupational exposure has been studied previously in Dublin, Goodman et al. (2007) monitored the occupational exposure of Dublin bar workers to PM and benzene, and found high concentrations present in the various public houses examined in the study. The study assessed the effect of legislation banning smoking inside public places, and found reduced concentrations in pubs after the ban commenced. The work conducted by Goodman et al. (2007) illustrated how individuals can potentially be exposed to high air pollutant concentrations in their workplaces, which would not be

detected by background air monitoring stations. Moreover, it demonstrated the introduction of legislation to curb emissions from identifiable sources can be effective in improving indoor air quality.

Internationally there have been various approaches to assessing personal exposure to PM with light scattering monitoring devices. However, some of these studies have been conducted for relatively short periods of the day (Brauer et al., 1999), or have focused on indoor activities such as vacuuming (Ferro et al., 1999) or cooking, which is known to produce an appreciable mass of airborne particles in the vicinity of the cooker (Abdullahi et al., 2013). Other studies have focused on a particular demographic, for example, the personal exposure of students while at high school (Borgini et al., 2011). Only a study by Branis and Kolomazníková (2010) was found to monitor PM continuously over 24 hours using a light scattering based device, however, this was for just a single student. Various other personal exposures have also been conducted with the use of gravitational sampling devices which do not offer the resolution that nephelometer devices provide.

The use of real-time optical particulate monitors for a segment of the population in Dublin to monitor over 24-hour periods and longer can provide a valuable contribution to the area of air pollution personal exposure and epidemiology. The collected data can be analysed and used to highlight activities or locations with high personal exposure to inform the public and the governing bodies about environmental health risks. The public could then avoid such activities, or the local authorities could improve the air quality of certain locations to reduce the health risks to the population. The data could also be used by other investigators to carry out more direct epidemiological studies using personal exposure data rather than background concentrations.

In addition to highlighting microenvironments and activities that have high personal exposure concentrations associated with them, the gathered dataset can be utilised in order to model and predict the personal exposure of other individuals in Dublin. As previously seen in Section 2.7, studies have attempted to model personal exposure to PM with time-activity approaches. However, these models were based on the low

resolution PM data that have been sampled using gravimetrical samplers, or have focused on only a limited number of microenvironments. The use of high resolution continuous samplers over long durations can improve the modelling capabilities by encompassing a greater number of microenvironments.

Different modelling techniques can also be applied which have not previously been used as a means of investigating daily PM personal exposure. For example, the use of specific dose uptake modelling has been used before to investigate the uptake of fine PM on short commutes (McNabola et al., 2008b). However, in this current investigation the human respiratory tract will be modelled to calculate dose uptake for a wide range of activities and locations within each 24-hour period. Other modelling techniques such as artificial neural networks, which have not been used to model personal exposure to PM, will also be applied once the completed dataset is obtained. The relationship between personal PM exposure and the fixed site PM monitoring stations around Dublin, as well as meteorological effects, will also be assessed.

## 2.10 Summary of Literature Review

In this literature review, a broad introduction to air pollution science from its early historical origins right up until the present day has been provided. The main air pollutants that are found in the ambient atmosphere have been discussed, including the basic atmospheric chemistry involved in their formation, other sources and sinks, as well as the health and environmental effects of each. As a result of this review, particulate matter has been identified as the pollutant that warrants specific further study. This is due to its multi-source nature and the fact it is often used as an indicator pollutant for the general state of the ambient air quality. Moreover, $PM_{10}$ is one of the air pollutants (along with $NO_2$) that were identified in the Dublin Regional Area Air Quality Management Plan 2009-2012 as a cause for concern.

The health effects associated with PM exposure are well documented and as a result this makes it a prime candidate amongst air pollutants for assessment as part of epidemiological studies. Many of the epidemiological studies discussed have been

based on the background concentration of PM in the locality of the study cohort. However, owing to the exposures that can be encountered due to certain activities and microenvironments, background concentration may in many instances be an unsatisfactory basis on which to solely investigate the impacts of air pollution on human populations.

Human exposure to PM is dependent on a variety of activities such as cooking, cleaning, commuting mode, proximity to traffic, and many other potential exposure sources, most of which are not accounted for in data collected from background monitors. Hence, a more relevant measure for individual subjects of an air pollutant health impact assessment may be obtained by quantifying personal exposure.

Much of the personal exposure research reviewed has been dedicated to exposures during specific activities. A large amount of work has been conducted in the transport microenvironment, while other studies have begun to focus on specific individuals and groups. However, much of the personal exposure monitoring is over a limited time scale and is more often than not less than a 24-hour period. Moreover, the reliance on activity logs in personal exposure studies for monitoring the movements of individuals may impart a source of error in the analysis of gathered data. Complementing an activity diary with the additional ability of tracking the movement of a subject via GPS may be a more accurate method for recording time spent in specific microenvironments, and aid with the apportioning of the collected data to each particular activity and microenvironment.

The 24-hour personal exposure studies in the literature have primarily been conducted for specific sub-groups of the population (e.g. children, students, etc.), but not always on a real-time basis, for example the *EXPOLIS* study. By gathering personal exposure data over 24-hour periods with greater sampling resolution, a database can be built for particular microenvironments and activities in context of Ireland.

The use of various modelling techniques and different statistical methods has also been applied throughout the personal exposure literature. Further work in the areas of

regression analysis and risk analysis simulations will add to the knowledge of personal exposure prediction, as well as dose uptake. Successful implementation of this type of approach may aid in the development of a personal exposure model on a macroscopic scale for Ireland, which could be used to investigate the health impacts of personal exposure to air pollution in a more extensive and comprehensive manner than using background concentrations.

In addition, as it is impractical to monitor personal exposure on a long term basis and due to the fact the monitoring of background data is a legal requirement in many countries worldwide, it is also the aim of this research project to develop methods of predicting personal exposure from background monitoring data. This will be achieved through the investigation of background monitoring data located across the Dublin region in conjunction with GPS data on locations of subjects. This type of approach based on accurate geographical information for multiple subjects may improve upon work previously conducted.

As previously stated, the combination of the personal monitor with GPS technology will allow accurate assessment of personal exposure within different microenvironments. The ability to predict many of these exposures through the knowledge of a person's activity pattern may be a useful tool when implemented on a macroscopic scale for investigating the health impacts of personal exposure to air pollution. The development of a statistical modelling approach for prediction of personal exposure would also be more comprehensive and robust than using background concentration data for investigating the health impacts of personal exposure.

# Chapter 3

## Methodology

# 3 Methodology

## 3.1 Introduction

The air pollutant monitored for this research project was particulate matter, and more specifically $PM_{10}$. The experimental design is discussed in detail in the subsequent sections of this chapter along with the description of the particulate monitoring method used. Details on the calibration and quality control techniques incorporated in the study are also stated. Finally, the data and statistical analysis methods employed are also discussed.

## 3.2 Experiment Design

The task of experimental sampling required volunteers to be recruited in the Greater Dublin Area and several satellite towns. Initially, the experimental plan was that the study volunteers would represent as broad a spectrum as possible of the general population, but due to the need for statistically significant relationships when analysing the data, as well as time and logistical constraints, this study primarily focused on office workers employed in the city centre. Sampling was also restricted to weekdays as a robust dataset would be difficult to amass due to the variety of potential activities at weekends, many of which would be untypical of the rest of the week. Furthermore, keeping the battery of the personal monitor charged may have been difficult to achieve if a volunteer was away from a power supply for long durations on a weekend.

The real-time measurement of personal exposure of each of the subjects comprises continuous sampling, measured over a 24-hour period, which represented one complete sample. A number of samples were required from each subject to account for varying activities, locations, and weather conditions, and to make the analysis of the data robust.

In order to obtain a range of different commuting modes and to ensure volunteers were evenly spread throughout the city, the experimental sampling plan was to recruit volunteers from a large proportion of postal codes in Dublin as well as a number of satellite towns. The experimental plan was to recruit a minimum of 50 different

volunteers, a mixture of both male and female, as per WHO guidelines for the minimum number of subjects for a representative population (Jantunen and Kansanterveyslaitos, 1999). The volunteers were drawn from all over the city in order to cover a range of activity patterns, and ideally four to six sampling days per volunteer were required to account for variations caused by different days of the week. Therefore, the aim was to attempt to collect 300 subject sampling days in total. However, due to certain difficulties encountered throughout the sampling campaign not all volunteers were able to successfully complete six sampling days. These problems that were encountered will be discussed in greater detail in the subsequent results chapter.

As an additional component of the sampling campaign, data was also gathered from a number of taxi drivers in Dublin City in order to compare occupational exposures with that of office workers. In total four taxi drivers were recruited to sample exclusively during their work shifts for approximately five to six different days each. The result of this campaign will be discussed in subsequent chapters.

Details of the sampling protocol for both the 24-hour sampling campaign and the smaller taxi driver study are given in the Subsection 3.2.5.3.

### *3.2.1 Particulate matter monitoring*

Particulate Matter (PM) was chosen as the main pollutant to be monitored due to its health significance, its multisource nature (indoor and outdoor environments), and the ability to record its concentration using real-time monitors that are small and mobile whilst maintaining sufficient resolution and accuracy. The Met One Aerocet-531 (Figure 3.1) was the real-time particulate monitor used to sample the personal exposure of each subject. In total five of these particulate monitors were employed for sampling, and this allowed samples to be taken simultaneously by multiple subjects thus increasing the amount of data obtainable within the time constraints of the project. However, due to servicing schedules of the devices and logistics involved in the recruitment and timetabling of volunteers, simultaneously taking samples was often difficult to achieve.

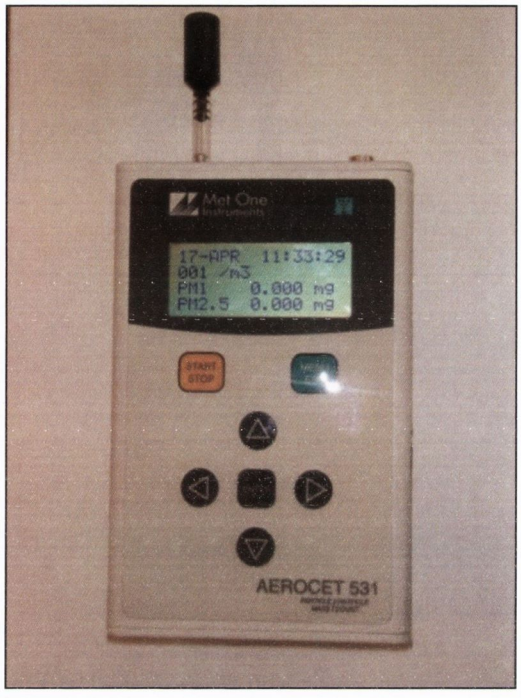


Figure 3.1 An Aerocet-531 particle mass profiler.

The Aerocet-531 was chosen because it is a portable handheld device, weighing approximately 0.88kg, which made it convenient for use in a personal exposure study of this nature. The Aerocet-531 has also been used in a number of previous studies of this nature (Nardini et al., 2004; Kumar et al., 2007; Ruprecht et al., 2011).

The Aerocet-531 measured PM concentration by counting the individual particles in the sampled air using scattered laser light and then utilised a proprietary algorithm to calculate the equivalent mass concentration (Met One Instruments, 2003). The instrument also had a particle counter operating mode but this function could not operate simultaneously with the mass profiler mode (i.e. mass concentration) so was not used during this project. The Aerocet-531 particle mass profiler mode had five mass size ranges of $PM_1$, $PM_{2.5}$, $PM_7$, $PM_{10}$ and TSP which it displayed and stored in memory as data logged values. Each sample in mass mode took two minutes to complete and had a concentration range of 0 to 1 $mg/m^3$.

Once a sampling period had been completed by a volunteer, the data stored on the Aerocet-531 was downloaded into Microsoft Excel using the AEROComm software that was provided with each of the units. A typical 24-hour time series output for $PM_{10}$ concentration from a volunteer is illustrated in Figure 3.2.

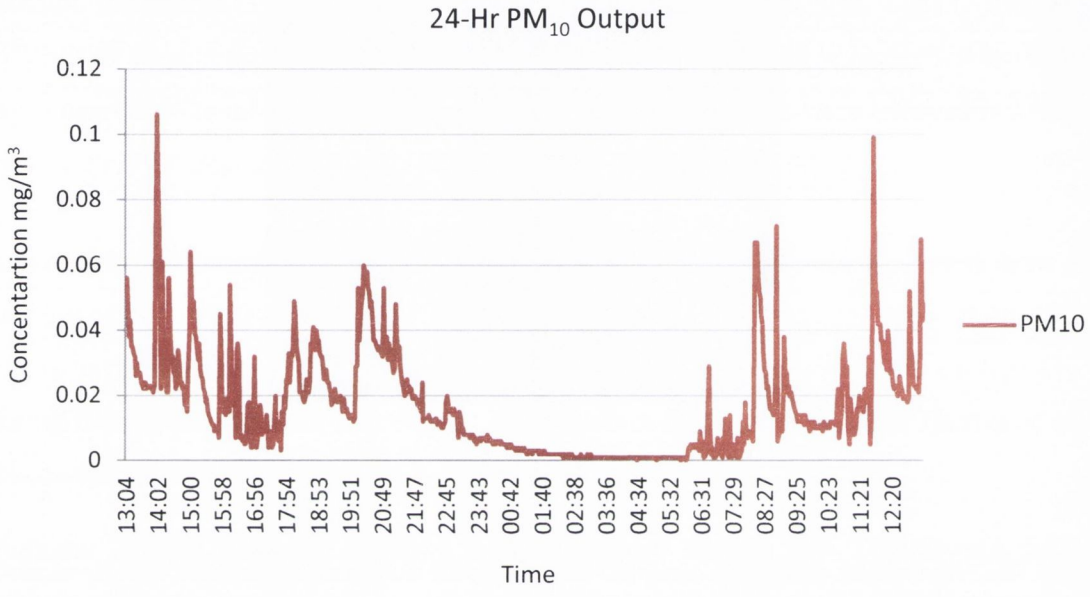


Figure 3.2: A typical un-calibrated Aerocet-531 24-hour period output for $PM_{10}$.

The volunteers were also equipped with a GPS tracking device which continuously monitored their location and all volunteers kept an accurate log of their activities during sampling (commuting; sleeping; working; shopping etc). This device, along with the activity diary, is discussed in the subsequent sub-sections.

### *3.2.2 Location monitoring*

The GPS device used as part of this research project was the Garmin GPSMAP® 60CSx, shown in Figure 3.3. This device was chosen because it had a high sensitivity GPS receiver which meant it could easily and quickly obtain a GPS satellite signal in an urban landscape. It was also a relatively small handheld device which made it convenient for volunteers to carry on their person along with the Aerocet-531 instrument, bringing the total weight of the sampling equipment to approximately 1.1kg.

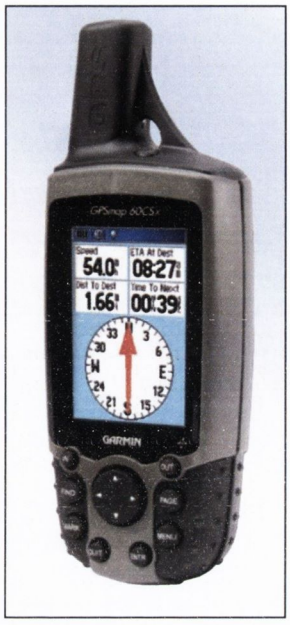


Figure 3.3: Garmin GPSMAP 60CSx.

The GPSMAP 60CSx operated by firstly acquiring satellites, and then proceeding to automatically create a track of the volunteer's movements which was then stored on the internal memory of the device. This track could then be downloaded to a PC using Garmin MapSource software which also enabled the track to be viewed using Google Earth software.

The created track contained useful information which could be used in conjunction with the activity log to break down the data obtained from the Aerocet-531. The information contained within a created track included speed, elevation, and location co-ordinates. The track showed the exact location where the volunteer lived, along with the route that the volunteer used to commute in and out of the city to work. The track also showed details such as the exact time a volunteer entered or left a building, or when they changed their mode of commute, for instance, if a person was walking in the city centre then boarded a public bus, the track would show the moment this transition occurred. An example of a recorded track from a volunteer can be seen in Figure 3.4.

Figure 3.4: An example of a volunteer's track recorded by the GPS.

### *3.2.3 Activity monitoring*

The activities of the volunteers were monitored through use of an activity log (see Appendix A). The activity log consisted of a table covering a single 24-hour period with hourly increments representing the time of day as the rows down one side and a list of the most common activities as the column headings. There was also space given for additional information to be recorded.

The main activities and locations listed were work, home, sleeping, commuting, cooking, shopping, sports/recreation, socialising, and smoking. Each volunteer was instructed to record, in as much detail as possible, the time of day they partook in a certain activity or were in a specific location. This information was then used to divide up the particle concentrations recorded by the Aerocet-531 and assign them to each individual activity. On occasion, the GPS may not have been able to acquire sufficient satellite signal before a commute commenced, but due to the volunteer noting their departure time in the activity log this potential problem could be avoided.

### *3.2.4 Sampling protocol*

As part of the sampling campaign, two different protocols were employed for the collection of office worker 24-hour samples and also for the taxi driver dataset. The taxi driver sampling is discussed in detail in Section 3.2.5.3. The first sampling procedure, for the data collection of the 24-hour samples, is shown in the following bullet points:

- Volunteers were recruited for a total of six sampling days per person, broken into two or three day blocks.

- Before sampling commenced the Aerocet-531 monitor was tested with a zero filter and flow meter to ensure proper functioning of the monitor.

- Each volunteer was given an Aerocet-531 monitor including a plug for charging, a handheld Garmin GPS device to record their movements, spare rechargeable batteries for the GPS, and finally, a log in which to record their activities while sampling.

- The Aerocet-531 was run continuously by the volunteer for the duration of the sampling period. During sampling, the monitor was set up so that it recorded a sample every two minutes. The monitor was also required to be plugged in when stationary for long periods, for example at home or at work. This was due to the battery life of the Aerocet-531 only lasting approximately six to eight hours.

- The volunteer was instructed to carry the GPS with them whenever they were moving but were advised to turn it off when stationary for long periods in order to save the battery (e.g. when sleeping, etc.).

- During the sampling period the volunteer was asked to record their various activities in the activity log, in an effort to highlight increased concentrations of PM due to sources, for example, such as cooking.

- It was also requested that the volunteers attempt to carry out their daily routines as normal over the monitoring period.

- At the end of the sampling period the equipment was returned and the data from both the Aerocet and GPS was downloaded to a PC. The GPS data, along with the activity log, was then used to break the Aerocet data down into particulate exposures due to each different activity. This data was then fed into the overall dataset for the project.

### *3.2.5 Ancillary microenvironmental monitoring*

As part of the research programme, and in order to complement the main dataset, a number of site specific studies were undertaken to increase the dataset for certain microenvironments. These activities or microenvironments were those that volunteers frequented only occasionally, and thus more data was collected in addition to the main dataset.

#### *3.2.5.1 Smoking*

During the sampling campaign it became apparent there was a dearth of smokers amongst volunteers recruited. There were a limited numbers of smokers that volunteered during the study and often it was the case that some of these recruits were casual or social smokers who smoked only intermittently. Of the volunteers that smoked more regularly during the 24-hour sampling campaign, most of these individuals chose to smoke outdoors even when at home due to the presence of cohabitating non-smokers. Meanwhile, none of the smokers recruited were permitted to smoke in their workplace under the legislation of the Tobacco Smoking (Prohibition) Regulations 2003.

To rectify this difficulty in recruiting smokers and the deficiency in smoker data, several smokers were recruited in order to monitor the $PM_{10}$ concentrations in their homes. Each smoker was requested to operate the Aerocet-531 when they were at home and were given activity logs in order to record smoking events. The smokers were instructed to locate the Aerocet-531 as near as possible to them at all times. They were also told to record any cooking events conducted in order to distinguish possible concentration

peaks originating from any cooking activities. The collected data allowed typical in-home concentrations for smokers to be established and was used to complement the main dataset.

*3.2.5.2 Shopping centres*

As well as the homes of smokers, another area that was identified as perhaps deficient in data was for the activity of shopping. Much of the data collected on shopping in the main dataset consisted of brief excursions by the volunteers into retail or convenience stores in the city for purchases such as lunch etc. As an additional source of data for the activity of shopping, data was collected from two large Dublin shopping centres. The locations of the two shopping centres are marked in Figure 3.5.

The shopping centres were located on Jervis Street in Dublin city centre and in the suburb of Dundrum in South Co. Dublin. Sampling took place in each on four separate occasions at peak times between 1.30 pm and 5 pm on a Saturday afternoon, and on off-peak times between 1.30 pm and 4.30 pm midweek. Samples were taken for 10 to 12 minutes in a number of locations in each shopping centre, as follows:

- Inside a pedestrian entrance
- Inside an entrance close to outside vehicular traffic
- The ground floor atrium
- The first floor atrium
- An entrance to a multi-storey car park
- A clothes shop
- A supermarket

The sampling time of 10 to 12 minutes in each location was chosen to allow a stabilised reading to be gathered at each sampling point. This type of short-term (10-minute) sampling in several locations has been used previously, for example, by Wallace and

Ott (2011) in order to determine indoor-outdoor ultrafine particle relationships. The total time spent sampling on each shopping centre visit would also therefore be just slightly over an hour in duration. In a previous study on air quality in shopping malls, Li et al. (2001) monitored $PM_{10}$, among other pollutants, for 1-hour periods at stationary locations inside a number of different malls. The samples were collected from representative sampling locations, which were on floors that included major entrances and exits, accesses to public transport stations, as well as the majority of shops, dining, and entertainment facilities. For this study, the portability of the Aerocet-531 afforded the opportunity to sample directly at a variety of locations. In contrast, the locations employed by Li et al. (2001) were stationary because of the prohibitive amount of equipment utilised in order to monitor a plethora of pollutants (CO, $CO_2$, HCHO, $PM_{10}$, etc.).

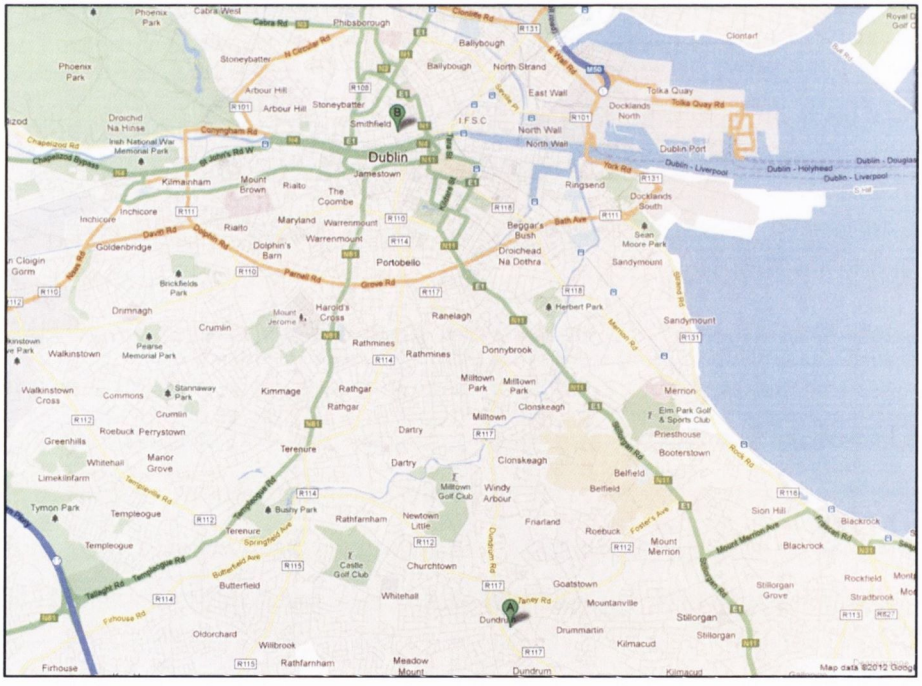


Figure 3.5: (A) - Dundrum Shopping Centre, and (B) - Jervis Street Shopping Centre.

### *3.2.5.3 Occupational comparison*

A further study was also undertaken to investigate the differences encountered in PM concentration between different occupations. As already stated, the study volunteers

were primarily office workers that worked approximately from 9 am to 5 pm in the city centre. As a comparative experiment, a number of Dublin City taxi drivers were recruited to monitor their occupational exposure.

In total four separate taxi drivers were recruited and sampled for four to seven work shifts each. The following was the sampling protocol for the Taxi study:

- Prior to sampling, the Aerocet-531 was subjected to the same checks as stated for the 24-hour sampling campaign.

- Drivers were presented with an Aerocet-531 and accompanying charger. The Aerocet-531 was powered by its internal battery when particle monitoring was undertaken, as no power socket was available in any of the vehicles.

- The drivers were instructed to place the Aerocet-531 as close to their breathing zone as possible while in the vehicle.

- Drivers were assigned a Garmin GPSMAP 60CSx device which recorded their tracks and locations for each work shift. Rechargeable batteries along with a charger were also provided.

- The drivers were provided with an activity diary to record events during their shifts that may have an effect on the in vehicle particulate concentrations.

- All drivers began monitoring at the start of their work shifts and ran the Aerocet-531 until they returned home. Once at home they were instructed to place the instrument on charge in preparation for the next day's sampling period.

- Each sampling period lasted for approximately three days so as not to exceed the data storage limit of the GPS. On completion of the sampling period, the instruments were returned and downloaded via their respective AEROComm and Garmin Mapsource software.

The activity diary that each driver was given can be viewed in Appendix A. Each driver was instructed to record a number of events in order to aid in the processing of the data. The main activities that drivers were told to record were any use of air conditioning or fan, the opening of windows, and finally if there happened to be any smoking in the vehicle. The smoking column was included as a precaution in the event any driver did in fact smoke inside the vehicle, for instance while on a break. However, current Irish taxi regulations stipulate that smoking in any taxi is illegal so it was unlikely any smoking occurred inside the vehicle.

## 3.3 Quality Control and Calibration

### *3.3.1 Zero calibration*

Quality control is important for the reliability and validity of the experimental data. Before any sampling period commenced the Aerocet-531 samplers were tested for any leaks with a zero filter, as shown in Figure 3.6. False measurements caused by air leaks or spurious noise would cause errors that are especially apparent when sampling in a relatively clean aerosol environment. The zero filter was attached to the Aerocet-531 inlet nozzle and it removed 99.99% of all particles larger than 0.3 microns. Since the air passing through the inlet of the Aerocet-531 was virtually particle free the output should read zero micrograms. During the sampling campaign a zero error was detected in none of the Aerocet units.

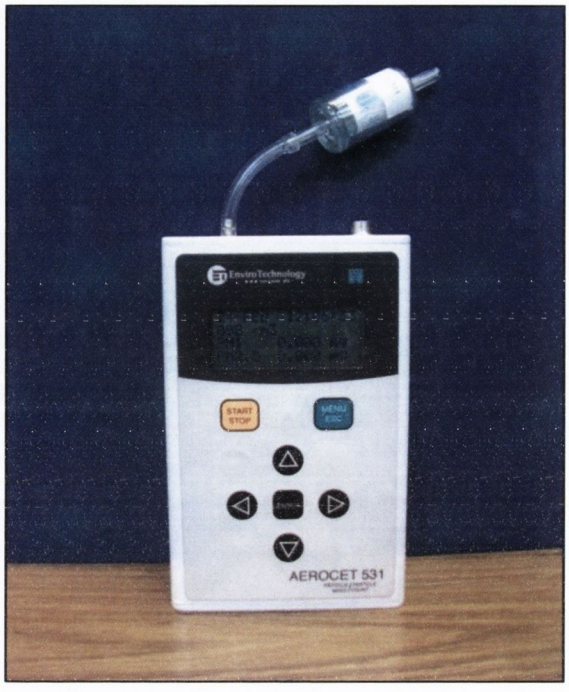


Figure 3.6: Aerocet-531 with a zero filter.

### *3.3.2 Flow rate*

The flow rate of the Aerocet-531 pump must be 2.83 litres/min +/-5% (Met One Instruments, 2003) and this was checked on a regular basis for all monitors using a Dwyer Flow Meter (Figure 3.7). The manufacturer recommends that the Aerocet-531 particulate monitors are flow rate tested on a monthly basis, but for the purposes of this study and to ensure accuracy of results obtained, the flow was tested before every sampling period.

Unlike the zero calibration of the Aerocet instruments which never returned errors, it was common to discover the pump air flow of the instruments had deviated slightly from the desired 2.83 litre/min flow rate. This problem was easily rectified by adjusting the flow control on the device returning the flow to the correct setting. Typically the Aerocet-531 samplers had to have their flow adjusted every three weeks or so depending on the level of use. It is important to state that each time the flow rate had altered it was always still within the allowed limit of +/-5% of 2.83 litre/min.

Figure 3.7: Flow testing an Aerocet-531.

### *3.3.3 Accuracy*

The Aerocet-531 units were calibrated against a Haz-Dust EPAM-5000 particulate monitor (Figure 3.8) in order to ensure the accuracy of the measurements taken by the Aerocet instruments. It was important to compare different methods of personal particulate sampling in order to establish the degree of correlation between them. In this circumstance the optical light scattering technique was compared to the established particulate sampling method of filtration and gravimetric analysis. In addition to the calibration procedure, the effects of water vapour and relative humidity on the instrument are also discussed in Section 3.3.5.

#### *3.3.3.1 Haz-Dust EPAM-5000*

The Haz-Dust EPAM-5000 particulate monitor had the dual capabilities of gravimetric analysis (Section 3.4) as well as a light scatter method, similar to that employed in the Aerocet-531 monitor. The Haz-Dust was chosen as the device for use in the calibration of the Aerocet-531 because it was also a portable device that could be easily transported to the location that required monitoring. This meant that it was convenient for comparing the method of gravimetric analysis with the Aerocet-531 in multiple locations. These locations included the indoor and outdoor microenvironments,

including in outdoor areas that were in close proximity to road traffic as well as outdoor locations where background concentrations would be expected to be low.

The filter gravimetric air sampling was conducted by inserting a specially prepared 47mm glass microfiber filter into the filter cassette of the Haz-Dust instrument. The gravimetric filter sampling and the light scattering method were conducted simultaneously.

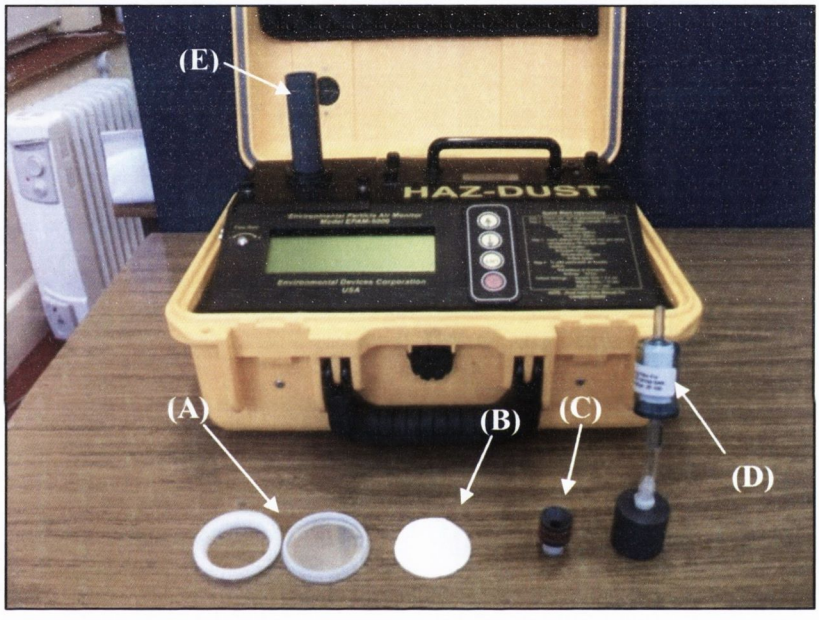


Figure 3.8: Haz-Dust EPAM-5000 with (A) filter cassette, (B) 47mm filter, (C) Size selective impactor, (D) Zero filter, (E) Impactor sleeve.

The Haz-Dust instrument operated as follows. Air flowed through the impactor sleeve of the Haz-Dust at 4 litres/min and passed through a size selective impactor, shown in Figure 3.9. The impactors had openings whose diameters determined the size of particles that passed around the impactor plate which was set just behind the inlet hole. Larger particles could not change their direction fast enough to navigate around this impactor plate so they were deposited on the plate. As the inlet hole reduced in size the velocity of air passing through it increased, and this resulted in only particles that were small enough being able to avoid the impactor plate. The impactor plate was also coated in a special lubricant which aided in the deposition and adhering of the particles onto the plate.

Once the particles of the monitored size fraction passed through the impactor sleeve they were deposited on the 47mm glass microfibre filter, which was located in the filter cassette at the base of the inlet sleeve. Unlike the Aerocet however, which was capable of sampling five different size fractions of PM concurrently, the Haz-Dust was restricted by the impactor contained in the impactor sleeve and thus could only sample one particular size fraction of PM at a time.

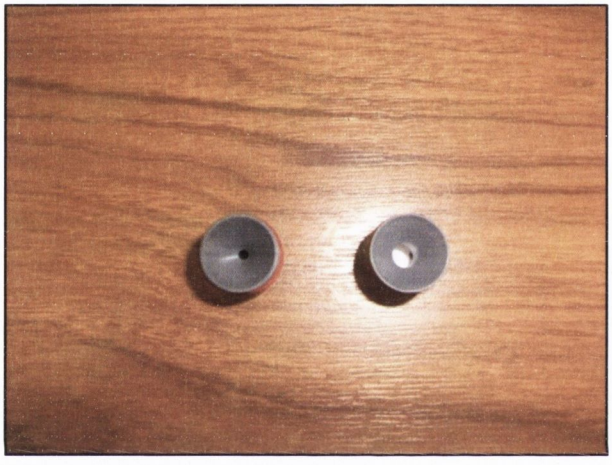

Figure 3.9: $PM_{2.5}$ (left) and $PM_{10}$ (right) impactors.

The Haz-Dust was subject to similar quality control checks as the Aerocet-531. Before sampling the Haz-Dust air flow was checked with a flow meter to ensure it was operating at the correct flow of 4 litres/min. The instrument was also checked with a zero filter to ensure there was no leak in the air flow.

### *3.3.3.2 $PM_{10}$ calibration results*

The calibration of the Aerocet-531 consisted of running the Aerocet instrument side by side an instrument that could record ambient concentrations using the traditional method of particulate monitoring, which is called gravimetric analysis. Gravimetric analysis and the procedure involved in conducting it is discussed in detail in Section 3.4, but essentially it involves passing a known volume of air through a size selective inlet which then deposits the particles of interest on a filter. This filter can then be weighed and a concentration ($\mu g/m^3$) can be deduced from the change in mass that has occurred in the period between pre and post sampling.

For the calibration of the Aerocet-531, 24 samples were taken in an indoor environment and 25 samples from an outdoor environment. These calibration samples represented approximately 20% of the samples in the main dataset. Each sample consisted of running the two monitors together, and for a long enough period to enable enough mass to accumulate on the filter in the Haz-Dust for the post sample weighing. This was usually for a period of approximately eight hours. The results of the calibration campaign are illustrated in Figure 3.10 and Figure 3.11.

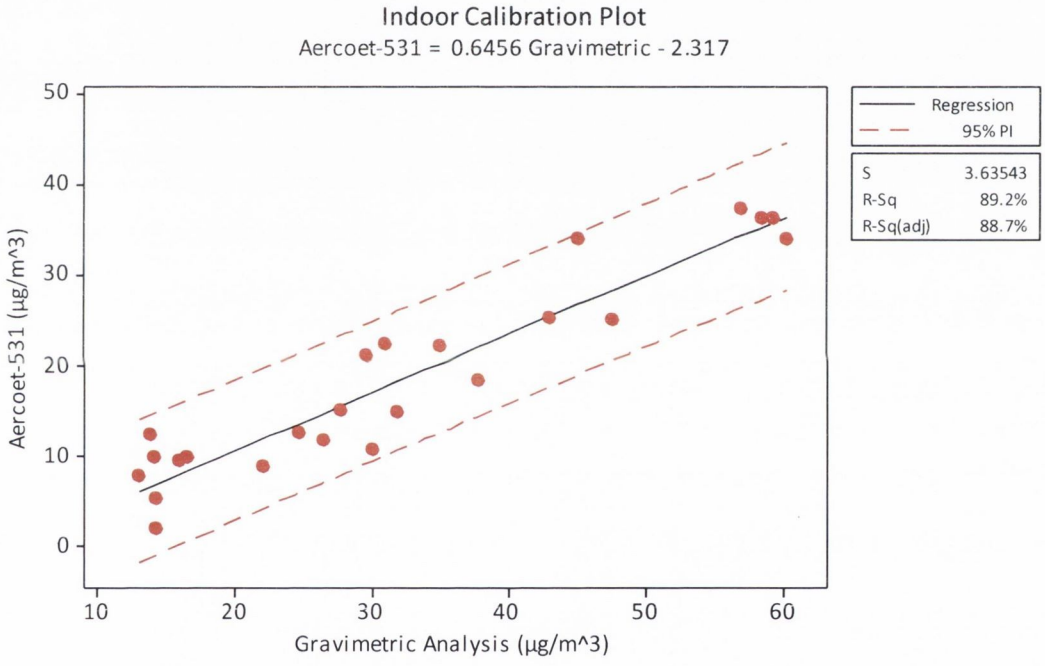


Figure 3.10: Indoor calibration graph of Aerocet-531 versus gravimetric analysis.

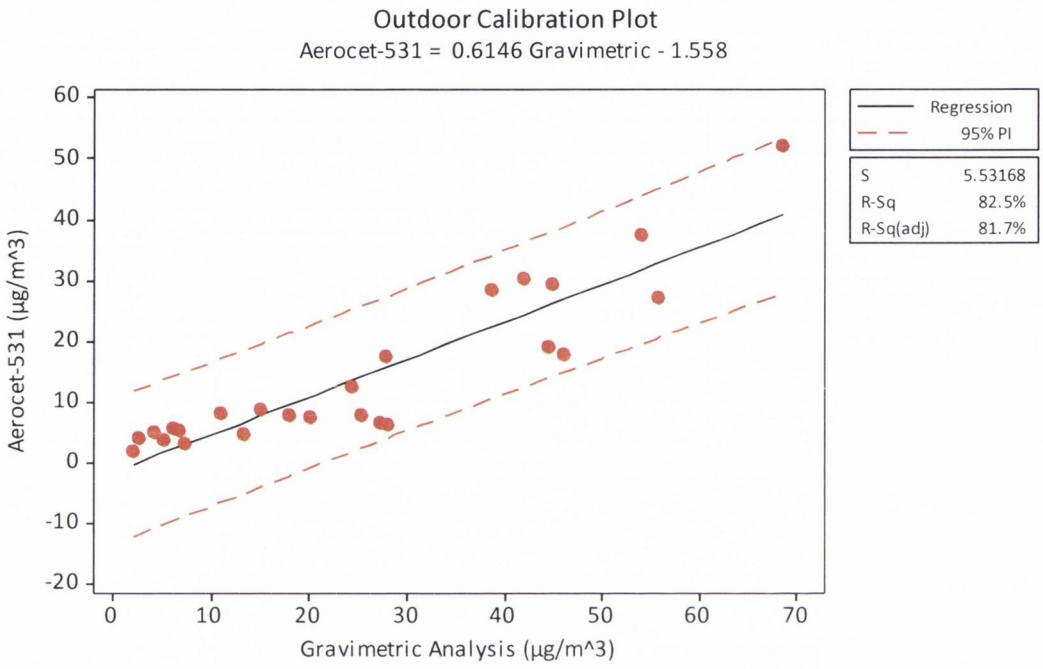


Figure 3.11: Outdoor calibration graph of Aerocet-531 versus gravimetric analysis.

From Figure 3.10 it can be seen that the indoor calibration had an $R^2$ of 0.89. The outdoor calibration proved to be more variable with an $R^2$ of 0.82. The prediction intervals are shown in red on each graph and any outliers have been removed. The linear regression equations for both the indoor and the outdoor calibration plots are shown in Eqn. 3.1 and Eqn. 3.2.

Indoor Calibration: $y = 0.6456x - 2.317$ Eqn. 3.1

Outdoor Calibration: $y = 0.6146x - 1.558$ Eqn. 3.2

Where $y$ is the Aerocet-531 concentration in units of µg/m$^3$, and $x$ is the Haz-Dust gravimetric analysis data value, also in units of µg/m$^3$. In both linear regression equations there is also a small intercept included in each equation. This intercept was eliminated by fitting the intercept of the line through the origin (0, 0), in order to simplify the calibration factors to be applied to the data (see Figure 3.12 and Figure

3.13). The updated graphs for both indoor and outdoor plots had an $R^2$ of 0.88 and 0.82 respectively. The equations for the indoor and outdoor calibration plots are shown in Eqn. 3.3 and Eqn. 3.4.

Indoor Calibration: $y = 0.5871x$ Eqn. 3.3

Outdoor Calibration: $y = 0.575x$ Eqn. 3.4

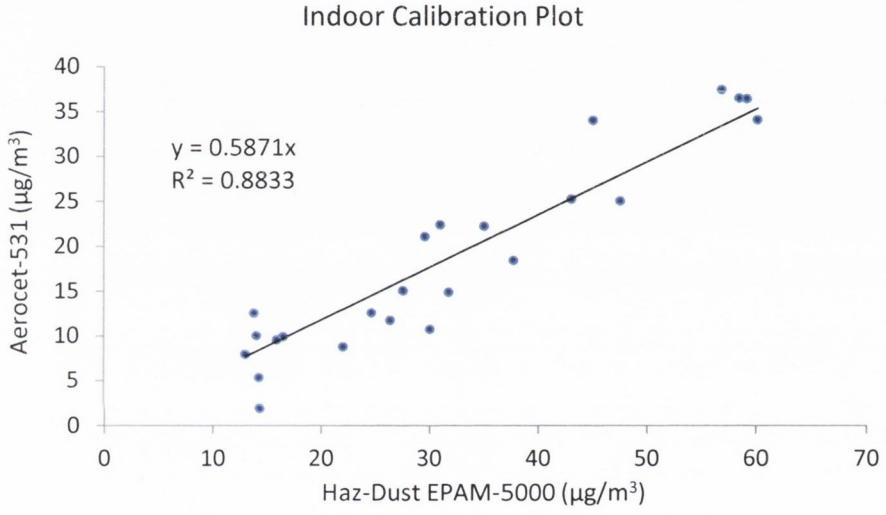


Figure 3.12: Indoor calibration plot of Aerocet-531 versus Haz-Dust with no intercept.

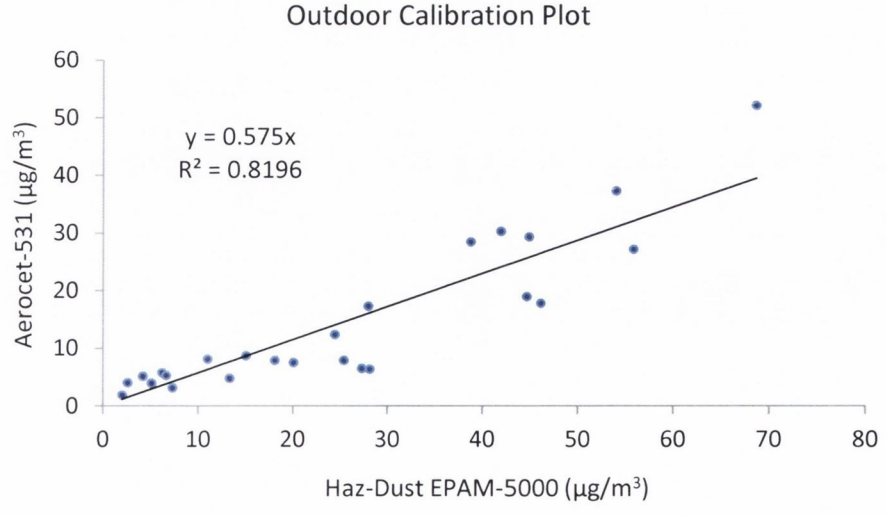


Figure 3.13: Outdoor calibration plot of Aerocet-531 versus Haz-Dust with no intercept.

On inspection of the calibration plots presented in Figure 3.12 and Figure 3.13, there was only a minor difference observed between the two linear equations (Eqn. 3.3 and Eqn. 3.4) of both graphs. Therefore, in order to simplify the calibration process further, the data was combined into a single calibration plot, as shown in Figure 3.14.

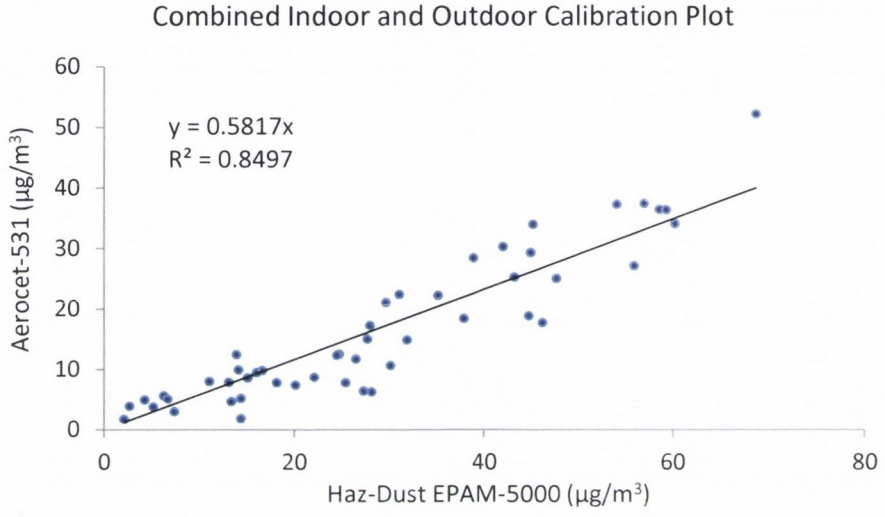


Figure 3.14: Combined indoor and outdoor calibration plot without an intercept.

This new universal calibration graph had an $R^2$ of 0.85, and thus, the calibration factor applied to both indoor and outdoor data can be seen in Eqn. 3.5.

$$y = 0.5817x \qquad \text{Eqn. 3.5}$$

Where $y$ is the unadjusted Aerocet-531 concentration ($\mu g/m^3$) data value and $x$ is the equivalent gravimetric analysis concentration value, all in units of $\mu g/m^3$.

*3.3.3.3 $PM_{2.5}$ calibration results*

The $PM_{2.5}$ Aerocet-531 data also underwent the same calibration procedure as the $PM_{10}$ data calibration. This $PM_{2.5}$ calibration followed the same procedure as with $PM_{10}$, with the Aerocet-531 being compared to the gravimetric function on the Haz-Dust EPAM-5000. Yet again this process was conducted for both indoor and outdoor environments.

In total there was 23 calibration runs conducted indoors, with a further 12 calibrations for outdoors. The results of these calibrations are shown in Figure 3.15 and Figure 3.16.

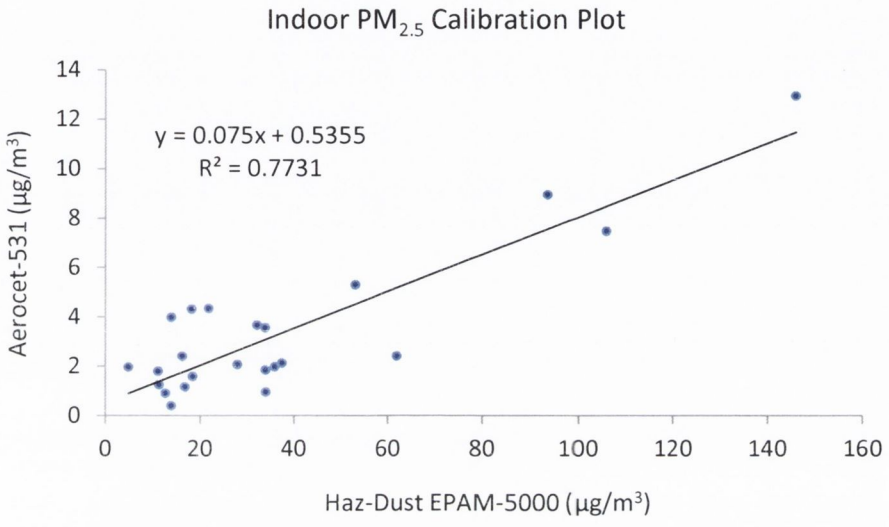


Figure 3.15: Indoor $PM_{2.5}$ calibration plot of Aerocet-531 versus Haz-Dust.

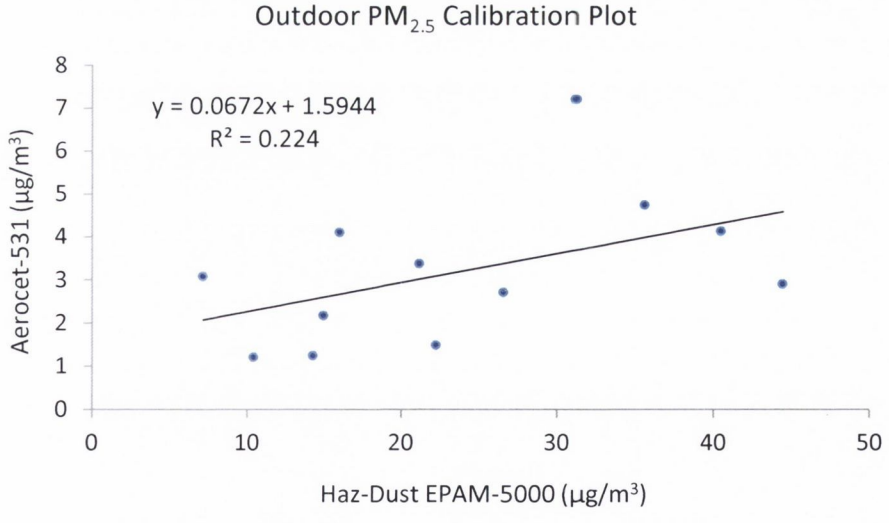


Figure 3.16: Outdoor $PM_{2.5}$ calibration plot of Aerocet-531 versus Haz-Dust.

As can be seen from the two calibration plots, this calibration campaign was rather less successful than for $PM_{10}$. The indoor calibration had an $R^2$ of 0.77, while for the outdoor calibration $R^2$ was a mere 0.22. The magnitude of the $PM_{2.5}$ values recorded by the Aerocet-531 was far lower than those recorded using the gravimetric analysis

method with the Haz-Dust. Therefore, it was deemed unacceptable to apply the calibration factor and to continue analysing the $PM_{2.5}$ samples.

### *3.3.4 Repeatability of the Aerocet-531*

The Aerocet-531 instruments were not only compared to gravimetric filter sampling for the purpose of accuracy, but they were also compared to each other to ensure the precision of the measurements recorded. As there were a number of different Aerocet-531 samplers used to collect the data it was important to compare the readings against each other. This was due to the fact monitors were manufactured and calibrated separately and hence may record slightly different concentrations. Therefore, a check of degree of variation between the instruments was deemed a requirement.

In order to determine the precision of the Aerocet-531 monitors, they were all run together in the same location for a sampling period of 30 minutes and the resulting data from each was compared. This procedure established if the monitors were out of sync and whether or not a correction factor had to be applied to the measurements. The data gathered was analysed using a one-way analysis of variance (ANOVA) test (an example of which can be seen in Table 3.1). It can be seen from Table 3.1 that the variance of the data from the seven Aerocet-531 monitors tested was not statistically significant ($p = 0.488$). Therefore, it was concluded that no inter-Aerocet calibration would be necessary.

Table 3.1: One-way ANOVA table for Aerocet-531 comparison.

| | **Sum of Squares** | **df** | **Mean Square** | **F** | **Sig.** |
|---|---|---|---|---|---|
| Between Groups | .000 | 6 | .000 | .914 | .488 |
| Within Groups | .005 | 98 | .000 | | |
| Total | .005 | 104 | | | |

The comparative procedure was repeated occasionally throughout the sampling campaign. However, due to sampling and servicing timetabling constraints, this procedure was restricted and limited in the amount of occasions it could be conducted.

Although, there was no significant differences detected amongst the monitors when they were compared.

### *3.3.5 Effects of relative humidity*

Nephelometer particle samplers are known to be effected by ambient relative humidity. The reason light scattering devices are effected is due to the increase in the average particle size as a result of the condensational growth of particles associated with water uptake by hygroscopic PM components (Sloane, 1984; McMurry et al., 1996). Another consideration is that nephelometers may also record a particle of water vapour such as fog or steam from a shower. Volunteers were requested to record events such as these to help identify artificially inflated particle concentrations owing to such events.

Particulate mass measured by filter based methods does not include most of the mass of particle associated water owing to the filter equilibration procedure (see Section 3.4.3) conducted prior to weighing, both before and after sampling. As nephelometers sample PM in situ at ambient relative humidity, they will therefore over estimate particle mass at higher relative humidity when condensational particle growth is favoured (Chakrabarti et al., 2004).

The effects of condensational growth of particles has been modelled in previous studies by Sloane (1984) and Lowenthal et al. (1995) and in both these studies results have resembled the relative humidity correction curve presented by Laulainen et al. (1993). This correction factor is shown by the empirical relationship in Eqn. 3.6.

$$CF = 1 + 0.25\frac{RH^2}{(1 - RH)} \qquad \text{Eqn. 3.6}$$

Where $RH$ is the relative humidity and $CF$ is the correction factor applied to the nephelometer data. This model has been shown to fit data presented by Day and Malm (2001) and Chakrabarti et al. (2004) quite well. In the study by Chakrabarti et al. (2004) the performance of an active-flow, personal DataRAM (MIE pDR-1200; Thermo Electron Corp., Franklin, MA) was evaluated, and the pDR continuous $PM_{2.5}$

concentrations were compared with those measured by a collocated Beta Attenuation Monitor (BAM, Model 1020, Met One instruments, Inc., OR). It was found that the modelled particle growth predicted by Eqn. 3.6 fitted the actual field data well, with a correlation coefficient of 0.88 (Figure 3.17).

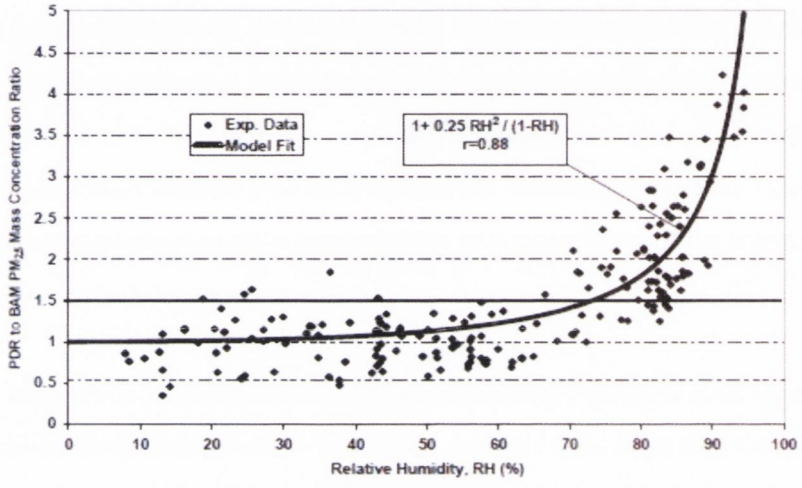


Figure 3.17: Comparison of two-hour averaged pDR to BAM $PM_{2.5}$ concentration ratio as a function of relative humidity (Chakrabarti et al., 2004).

In previous research, field measurements have found that increased humidity caused an increase in PM readings (Quintana et al., 2000; Ramachandran et al., 2003). The approaches taken in order to adjust for RH are varied in the literature. Chakrabarti et al. (2004) corrected the collected pDR data using Eqn. 3.6 when RH exceeded 60% and found reasonable agreement with the BAM measurements.

Other studies have chosen not to correct for RH at all. Branis and Kolomazníková (2010) used a DustTrak to continuously monitor personal $PM_{2.5}$ for a year but yet had no parallel RH readings, thus, there was no direct guidance for exclusion of measurements taken at high humidity levels. To judge this bias they assumed high humidity excursions seldom appear in the indoor or transit microenvironments, and because the majority of outdoor exposure takes place between 9 am and 9 pm, the frequency of such events may be similar to that of the collocated campaign (i.e. when the DustTrak was compared to a FSM). The DustTrak manufacturer stated the

instrument provides realistic data when operated below 95% RH. Thus, they estimated that during the collocation campaign 4% of the data recorded outdoors between 9am and 9 pm could be affected by excursions of relative humidity above 95% and 9% by excursions above 90%.

Guidance on correction for RH in the indoor microenvironment has been taken from researching precedence laid down in the literature. Lanki et al. (2002) stated that, since personal exposure takes place mostly indoors, the effect of relative humidity on the nephelometer readings is not significant in most indoor microenvironments. In a study of indoor environments in homes of asthmatic children, Quintana et al. (2000) observed that 99% of indoor RH readings were between 20 and 65%, a range in which the readings of the pDR instrument used were unaffected. Furthermore, in a study by Ramachandran et al. (2003) which characterised indoor and outdoor $PM_{2.5}$ concentrations, they stated that since indoor RH is typically < 60% the effects of RH on the DustTrak monitor measurements are likely to be small. Thus, indoor measurements were not corrected, but hourly RH measurements were obtained from a meteorological station at Minneapolis-St. Paul Airport, and were used to correct outdoor measurements according to Eqn. 3.6.

For this study, it was concluded that adjustment for indoor measurements due to RH would not be conducted. This was primarily due to the fact, and according to previous research, that RH indoors will be under 65% the vast majority of the time. Moreover, even though the majority of samples taken in the sampling campaign lacked concurrent RH measurements, a small number of samples were taken with a temperature and RH probe attached to the Aerocet unit. These samples demonstrated the low RH conditions that exist in the various indoor microenvironments. The mean RH in the indoor microenvironment was found to be 48.3% with a standard deviation of +/- 6%.

While the indoor samples taken were left unadjusted with regard to ambient RH, it was deemed necessary to adjust for RH for all outdoor samples. This meant that all outdoor samples were corrected once the RH exceeded 65%. The correction factor applied was calculated using Eqn. 3.5. In the absence of concurrent RH probe data for the majority

of samples, hourly RH data was obtained from the Phoenix Park meteorological station and used as a surrogate for concurrent RH readings. Once the RH exceeded the 65% threshold, all corresponding outdoor data points for that hour were than divided by the calculated correction factor. All samples in the dataset were checked and the appropriate correction measure was applied accordingly.

## 3.4 Gravimetric Analysis

Gravimetric analysis is the term given to the quantitative analysis method of accurately weighing a very small mass of a given substance. In this case the substance being weighed using this analysis was the deposition of particles on filter paper, namely $PM_{10}$ and $PM_{2.5}$. The filter papers used were Whatman™ Grade GF/A 47 mm glass microfibre filters with a pore size of 1.6 μm, which are commonly used for the determination of airborne particulate concentrations. The filters were required to be accurately weighed both before and after particulate sampling. By doing so, this obtained the change in mass of the filter due to the deposited particles, and hence by dividing by the known volume of air that has passed through the filter, a figure for the concentration of particulate matter in units of $\mu g/m^3$ could be determined.

As the change in weight between pre and post sampling of any given filter is quite small, usually less than 200 μg, the use of an accurate microbalance was a necessity. The microbalance employed for the purposes of gravimetric analysis in this project was a Cahn C-33 (see Figure 3.18). The Cahn C-33 is a six figure microbalance and this means it is ideal for measuring changes in mass as low as 1 $\mu g/m^3$. The approximate weight of a 47 mm filter prior to sampling was 92 mg, so this figure falls well within the microbalance maximum measureable tare range of 250 mg.

Figure 3.18: Cahn C-33 Microbalance.

The chamber of the microbalance contains just two items – the weighing pan and the staticmaster. The weighing pan is an extremely lightweight foil pan that hangs inside the chamber from the very delicate hang-down spring of the microbalance. The C-33 microbalance has only one hang-down position and there is no counter balance pan.

Prior to the commencement of weighing the filter, on each occasion the accuracy of the microbalance was checked using a 100 mg calibration weight. The 100 mg weight was placed on the weighing pan and the mass was recorded at 30 and 60 seconds and again 30 seconds after the weight is removed to ensure the microbalance returns to 0.000 mg. This procedure was conducted to confirm the microbalance was functioning correctly, i.e. that the value of the mass displayed is stable and not drifting excessively.

### *3.4.1 Electrostatic effects*

The second item, as mentioned previously, contained within the chamber of the microbalance was the staticmaster (Figure 3.19). The staticmaster is a three inch long device containing Polonium-210 ($^{210}$Po), an isotope of the element, which emits alpha radiation with an intensity of 500 μCi (microcuries). An alpha radiation source such as

the staticmaster was necessary because glass microfibre filters are non-conductive and will hold any static charge collected on them.

Static is the accumulation of electrical charges on the surface of non-conductive material. If the surface of a material has an excess of electrons it will have a negative charge, and conversely the surface will be positively charged if there is a deficiency of electrons. A static charge on a glass microfibre filter may cause the gravimetric analysis of the filters to be unreliable in several ways. The effects of static are such that like charges repel each other and unlike charges attract, and these forces can be quite strong if the static charges are intense. A negatively charged filter on the balance weighing pan can be strongly affected by a positively charged glass chamber window or glass hang-down tube, which can result in erroneous and unstable weight readings. Static may also degrade a sample filter by attracting contaminating particulates from the ambient weigh room air onto the surface of the filter. Thus, the most effective way of neutralising static is by using an ionising unit such as the staticmastic (CAHN, 2006).

The $^{210}$Po material in the staticmaster was subject to alpha decay resulting in the emission of alpha particles, which are a highly ionising form of particle radiation. The alpha particles are essentially the nuclei of Helium atoms that travel at high speed (15,000 km/sec) over short distances and have a low penetration depth. Inside the microbalance chamber the alpha particles travel only a few centimetres before colliding with a gas molecule. The collision ionises the gas molecule which is then available to neutralise a static charge in the chamber or on the filter paper. $^{210}$Po has a relatively short half-life of just 138 days and loses effectiveness when the activity is below about 100 μCi. The ionising staticmaster device is therefore effective for approximately one year from date of manufacture, which is stamped into the device, and is replaced thereafter (CAHN, 2006).

Figure 3.19: Staticmaster.

### *3.4.2 Air buoyancy*

As well as electrostatic effects affecting the gravimetric analysis, another potential influence on the weight of a filter in the microbalance is the environmental conditions of the weighing room. The typical change in mass of a filter is minute in comparison to the overall weight of the filter (approximately 0.1%), so the effect of the air buoyancy in the weighing room is an important issue to consider.

Archimedes' principle states any object, wholly or partially immersed in a fluid, is buoyed up by a force equal to the weight of the fluid displaced by the object. In this case we can consider air as the displaced fluid and because the change in mass of the filters is so minuscule, the weight of the displaced air cannot be treated as negligible.

The buoyancy force exerted by a fluid is dependent on its density, thus the density of air was required to be calculated. The density of air is determined by temperature, pressure and relative humidity, therefore each of these conditions in the weighing room was recorded before and after sampling for each filter. In the weighing room climate, it is the effect of air pressure that is the most significant factor influencing the change in buoyancy and density of air. The effects of temperature and relative humidity are less influential. The increase in observed mass of a filter can be up to 10-15 μg due to the environmental conditions present in the weighing room. Therefore a correction factor calculated from equation Eqn. 3.7 was applied to all weighed filters.

$$\Delta b = V_f \times (\rho_{a2} - \rho_{a1}) \times 10^9 \quad \text{Eqn. 3.7}$$

Where: $\Delta b$ = buoyancy corrected net mass

$V_f$ = filter volume ($m^3$)

$\rho_{a2}$ = air density in post-sampling weighing room conditions ($kg/m^3$)

$\rho_{a1}$ = air density in pre sampling weighing room conditions ($kg/m^3$)

Due to the fact that air buoyancy depends on air density, i.e. relative humidity, pressure and temperature, it was necessary to calculate air density using equation Eqn. 3.8.

$$\rho_a = \frac{3.484 \times P - (0.00252 \times T - 0.02058) \times RH}{273.2 + T} \quad \text{Eqn. 3.8}$$

Where: $\rho_a$ = air density ($kg/m^3$)

$P$ = atmospheric pressure (kPa)

$T$ = temperature (°C)

$RH$ = relative atmospheric humidity (%)

This correction has been applied in previous studies, most notably in the *EXPOLIS* study (Koistinen et al., 1999). In the measurement methodology of the *EXPOLIS* study, Koistinen et al. (1999) highlighted the magnitude of change of the uncorrected mass readings when the conditions change by +30 mmHg, +2 °C, or +20 % RH between pre and post weighing of a filter. The effects of which can be seen in Table 3.2, where the assumed baseline weighing room conditions are P = 740 mmHg, RH = 40%, and T = 20 °C. In this example, the PEM (personal environmental monitor) and MEM (microenvironmental monitor) filter masses are 100 mg and 120 mg, respectively, with a filter density of 800 $kg/m^3$. The large effect that the change in atmospheric air pressure (in this case measured in units of mmHg rather than kPa) has on weighed filter masses is apparent when the calculated effects shown in the table are examined.

Table 3.2: Calculated effects on the change in weighed masses caused by the buoyancy effect due to a change in weighing room environmental conditions (Koistinen et al., 1999).

| | **ΔP** (mmHg) | **ΔRH** (%) | **ΔT** (°C) |
|---|---|---|---|
| Condition Change | +30 | +20 | +2 |
| | *Corresponding Change in Balance Readings (μg)* | | |
| 37 mm PEM filter | -5.9 | +0.25 | +1.1 |
| 47 mm MEM filter | -7.1 | +0.32 | +1.3 |

When there was a change in relative humidity the correction of the previous equations (Eqn. 3.7 & Eqn. 3.8) only applies for the effect of air buoyancy. The filter mass may also need correction for relative humidity changes due to possible mass changes in hygroscopic PM collected on the filter and also for the hygroscopicity of the filter itself. However the most abundant hygroscopic compounds in the majority of fine PM samples are sulphates, and based on this the hygroscopicity of the sampled mass should not be significant below a relative humidity of 65% (Koistinen et al., 1999).

### *3.4.3 Weighing procedure*

There are a number of steps involved in the preparation of filters prior to particulate sampling that must be adhered to. Firstly, when the filters are removed from their packaging they are visually inspected for imperfections from the manufacturing process such as holes or, more commonly, loose material. Often filters may have pieces hanging loose at their edges from the manufacturing cutting process which must be removed before conditioning to prevent any potential subsequent loss of mass during sampling.

The samples must then be equilibrated for at least 24 hours prior to weighing. To do this the filters were placed in a temperature and humidity controlled desiccator cabinet, which can be seen in Figure 3.20. There was a specific range of values that these two environmental conditions were required to meet inside the desiccator cabinet. The temperature inside the cabinet was required to remain between 20 to 23 °C with a variability not exceeding +/-2 °C. While the ambient relative humidity of the interior of

the cabinet was also prescribed to remain constant between 30% and 40%, with variability not greater than +/-5%.

Figure 3.20: Desiccator cabinet

The temperature inside the desiccator was set using the temperature dial which controls the heating of the cabinet, and was set at approximately 21 or 22 $^{o}$C at all times. The relative humidity of the cabinet interior was controlled through the use of a hygroscopic material known as a desiccant. The desiccant used in this case was beads of silica gel located in a tray at the bottom of the cabinet.

The silica gel is a vitreous and porous form of silicon dioxide made synthetically from sodium silicate, and despite its name, is in fact a solid. It has a strong affinity for water molecules and is commonly used in everyday life in bead form to control humidity and avoid degradation of goods. As can be seen in Figure 3.21, the silica gel beads were usually blue in colour; however, on absorption of excess moisture in the cabinet the beads begin to lose much of this blue hue. To assess the humidity conditions present in the cabinet, a visual inspection of the bead colouration along with the reading on the humidity dial could be performed. When the humidity was observed to have started to

increase, the beads were taken out and placed in an oven at 100 °C for an hour in order to 'regenerate' them by evaporating all moisture from them.

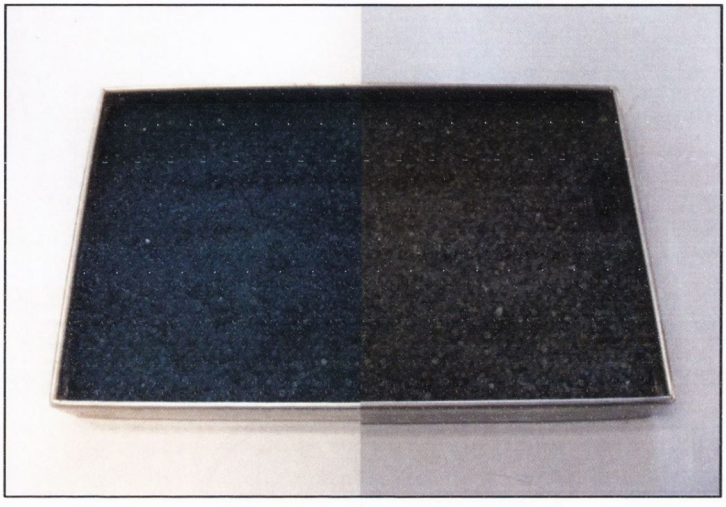

Figure 3.21: Silica gel beads with no moisture (left) and with moisture absorbed (right).

The sampling filters were equilibrated both before and after sampling to ensure the observed mass of the filters and the subsequent change in mass was not due to moisture absorbed from the atmosphere. The weighing room used for this study had a relative humidity constantly well below 65% and at all other times the filters were stored inside the desiccator. This ensured there was no change in moisture content of the filters and that a correction factor for the filter mass due to high relative humidity was not required. Once equilibrated the filters were weighed according to the following procedure:

1) The microbalance was first checked for drift and calibrated with a 100 mg calibration weight. This also warmed up the microbalance prior to the commencement of filter weighing.

2) Following calibration the microbalance was then left to stabilise for several minutes.

3) Once the microbalance was stabilised the tare button was pressed.

4) The equilibrated filters were removed from the desiccator and each side of the filter was exposed to alpha radiation by holding the filter approximately 1 cm in front of the staticmaster in order to remove any possible static charge.

5) The filter was then placed on the weighing pan inside the microbalance chamber and the mass reading was left to stabilise for approximately two minutes.

6) After the two minutes of stabilisation the mass of the filter was recorded and the procedure was repeated twice more.

7) Once the three weights were within 5 μg of each other the weighing was considered valid and the average of these three weights gave the final filter weight.

8) During the weighing procedure the relative humidity, temperature and pressure of the weighing room were recorded for the air buoyancy correction.

The microbalance used to weigh the filters is a sensitive piece of equipment and can detect mass change as small as 1.0 μg. Due to its high level of sensitivity, the microbalance was treated with the upmost care to prevent any external factors from affecting the mass read out. It was therefore necessary to take the following precautions when using the microbalance:

- The microbalance was positioned on its own dedicated stone topped table away from direct sunlight and equipment that could potentially cause vibrations.

- The weighing room was physically stable and the environmental conditions were always within the optimal operating parameters of the microbalance. The microbalance was designed to operate effectively within a range of 15 ºC to 30 ºC and a relative humidity of 5% to 95%.

- The microbalance was permanently left powered on, this included overnight and weekends, as recommended by the manufacturers. This was because a minimum of two hours warm up is recommended to ensure the precision of the

microbalance. By leaving it permanently plugged in the microbalance was constantly prepared for use, and this also reduced the need for regular calibration of the microbalance.

- The filters and the weighing pan were only ever handled by using stainless steel tweezers; this was done to avoid contamination of the sample. It was also advised that the tweezers did not have a grooved or serrated tip as the filters may incur a loss of material because of this.

- Each time the filters were weighed it was important to ensure that they were always deionised on both sides using the staticmaster. Filters were held approximately 1 cm in front of the $^{210}$Po antistatic strips for several seconds before each weighing.

- Static electricity was further controlled through the use of an aluminium foil weighing pan.

- As the filters were placed on and removed from the weighing pan, the weighing pan was disturbed as little as possible to facilitate swift stabilisation of the mass reading.

### *3.4.4 Environmental conditions of weighing room*

As previously stated, it was necessary to keep an account of the environmental conditions present in the weighing room each time filters were being weighed. This was done for the purposes of applying an air buoyancy correction factor at a later time during post sample analysis (see Section 3.4.2). Thus, the environmental conditions were recorded by using a Kestrel 4500 pocket weather tracker (Figure 3.22).

Figure 3.22: A Kestrel 4500 Pocket Weather Tracker.

The Kestrel 4500 is capable of measuring numerous meteorological conditions, but for the gravimetric analysis of the filters only three parameters were required – air pressure, relative humidity, and temperature. The specifications for each of these measurements on the Kestrel 4500 are given in the following Table 3.3.

Table 3.3: Kestrel 4500 specifications for temperature, relative humidity and pressure.

| Measurement ***Response Time*** | Units | Operational Range | Resolution | Accuracy (+/-) | Specification Range |
|---|---|---|---|---|---|
| Temperature ***1 second*** | °C | -45.0 to 125.0 °C | 0.1 | 1 °C | -29.0 to 70.0 °C |
| Relative Humidity ***1 minute*** | %RH | 0.0 to 100.0 % | 0.1 | 3.0 %RH | 5.0 to 95.0 % non-condensing |
| Pressure ***1 second*** | hPa/mb | 10.0 to 1100.0 hPa/mb | 0.1 | 1.5 hPa/mb | At 25 °C, 750 to 1000 hPa/mb |

The environmental conditions observed in the laboratory room used for gravimetric weighing are summarised in Table 3.4. It can be seen that both the temperature and the relative humidity of the room were within the acceptable range for weighing of the filters. The mean temperature was 21.2 °C with a standard deviation of 2.1 °C, while the RH was always low with a mean of 44.7% and standard deviation of 7.3%. The biggest influencing factor on buoyancy, atmospheric air pressure, had a mean of 101.3 kPa and this deviated by +/-1.4 kPa.

Table 3.4: Summary of environmental conditions present in the weighing room.

| Environmental Condition | Unit | Mean | Median | Standard Deviation |
|---|---|---|---|---|
| Temperature | °C | 21.2 | 21.3 | 2.1 |
| Relative Humidity | % | 44.7 | 45.0 | 7.3 |
| Pressure | kPa | 101.3 | 101.6 | 1.4 |

### *3.4.5 Laboratory blanks*

As part of the quality control process for the gravimetric analysis, blank filters were also weighed and equilibrated for each filter that was used for particulate sampling. This was done in order to quantify any loss or gain in mass that each filter used for sampling was subject to during the weighing and equilibrating phases. Ideally the field blank would be placed into the filter cassette of a Haz-Dust, without actually sampling particulates, and left in the unit for the duration of sampling. However, due to equipment constraints, a spare Haz-Dust was not available for this activity.

For every sample taken a blank filter was placed alongside a sampling filter in the desiccator for initial conditioning. The two filters were then weighed together under the same weighing room conditions. Once weighed one of the filters was inserted into the Haz-Dust whilst the other was placed back into the desiccator. When sampling was finished the filter in the Haz-Dust was removed and returned to the desiccator for another 24-hour equilibrating period, after which the two filters were reweighed. Any difference between the first and second weights of the blank filter was then added or subtracted from the weight of the sample filter. This difference may have been due to dust settling on the filter or the filter losing mass from handling, and was indicative of potentially similar gains or losses in the sample filter mass.

Over the course of the calibration campaign there was a mean net gain in field blank mass of 1.0 μg. However, this figure also had an accompanying standard deviation of +/- 12.4 μg. This illustrates the sensitive nature involved in handling the glass

microfibre filters, which can easily collect or suffer a loss in mass in the laboratory environment.

## 3.5 Meteorological Data

Meteorological conditions have been proven in previous studies to influence the concentration of pollutants in air. Therefore it is important to record the meteorology on any given sampling day as the prevalent conditions will have an influence on the concentrations of PM, especially in an outdoor environment. The meteorological data used was gathered from Met Éireann, the Irish National Meteorological Service.

The data was recorded at two Met Éireann weather stations. The first was located in Dublin Airport, which is in North Co. Dublin, approximately 10 km from Dublin city centre (see Figure 3.23). The second weather station was situated just 5 km from the city centre in the Phoenix Park. The daily values for a number of parameters from these stations are available online at the Met Éireann website. The weather station data available online is recorded daily data such as minimum and maximum temperature, rainfall, wind speed, relative humidity and sunshine. However, more detailed data was available from Met Éireann which allowed hourly data to be obtained for each day. This data enabled access to additional information such as wind direction and atmospheric pressure.

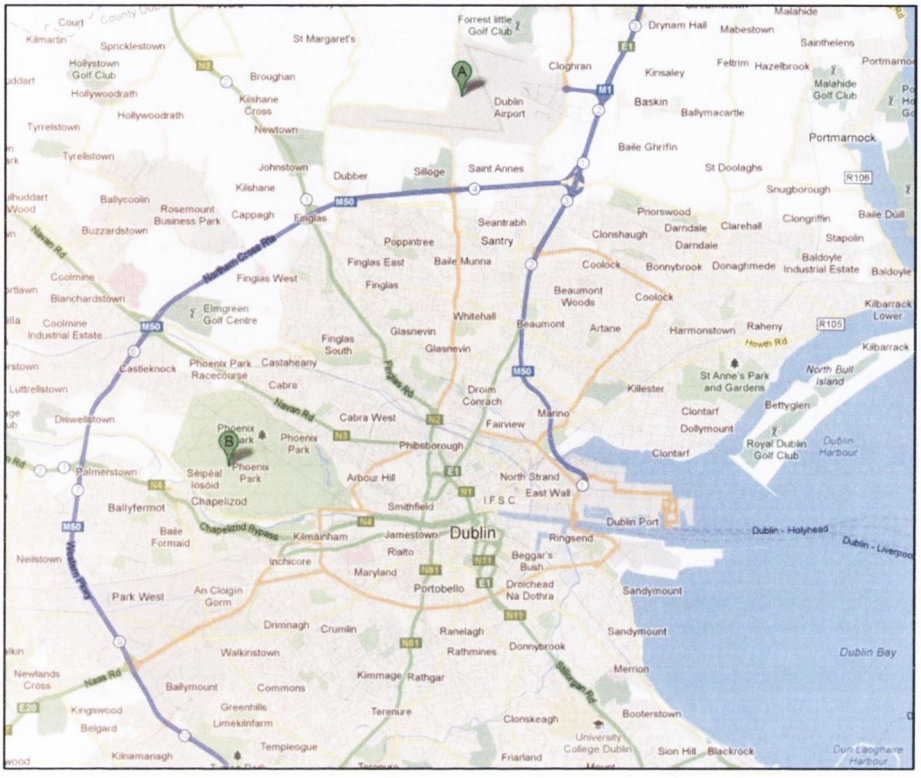


Figure 3.23: Weather station locations at Dublin Airport (A), and Phoenix Park (B).

## 3.6 Data Analysis Methods

The acquisition of such a large 24-hour data set from a multitude of different subjects allows for comparative analysis of the data. The type of analysis that could be conducted, for example, includes the comparison of personal exposures associated with living or working in location X or Y, and the highlighting of activities associated with high personal exposure concentrations. The data was investigated by using the statistics software SPSS and Minitab with non-parametric statistical tests, normality testing, simple and multiple linear regression, significance testing, and other statistical methods being employed.

An essential part of the sample analysis also included splitting each of the daily samples into components in order to quantify exposure exposures for different microenvironments. The recorded concentrations were split into indoor and outdoor exposure and then further broken down into sub-categories based on location and

activities. These categories were formed by using the GPS information and the activity log data. This work was conducted in Microsoft Excel and the data for each activity or microenvironment category was summarised into averages and standard deviations with specifically designed code using Microsoft Visual Basic (see Appendix B). Example summaries of 24-hour personal exposure samples collected by a number of volunteers can also be viewed in Appendix C.

## 3.7 Summary of Methodology

In summary, the air pollutant $PM_{10}$ was selected as the sole pollutant monitored in the personal sampling campaign. This was primarily as a result of the calibration of the Aerocet-531, which was the particulate sampler employed. The poor performance of the monitor in detecting fine particles meant that $PM_{2.5}$ was ruled out for analysis. However, the calibration for $PM_{10}$ was acceptable and subsequently all collected personal data was altered according to the calibration factor found.

The experimental design of targeting a minimum of 50 subjects in the population of interest (office workers) to sample for 5/6 sampling days each was implemented. The subjects were drawn from around Dublin City and nearby commuter towns in order to establish a dataset on a wide range of activities and travel modes.

# Chapter 4

## Results and Analysis

# 4 Results and Analysis

The following chapter examines the personal exposure data obtained through the experimental sampling campaign. An analysis of the time-activity data gathered is also provided, along with additional monitoring data sampled from other microenvironments also.

## 4.1 Monitoring Campaign

The 24-hour personal exposure monitoring campaign commenced in February 2009 and ran for a total duration of 28 months to June 2011. Volunteers were recruited though advertisement on online notice boards, solicitation of taxi and cycling groups, and through word of mouth. The recruitment of volunteers was an ongoing process over the course of the project duration, and on a completely voluntary basis by the individuals. The end result of the recruitment campaign was a total of 59 volunteers recruited for 255 24-hour sampling periods. A summary profile for each of the recruited study volunteers can be viewed in Appendix D.

### *4.1.1 Target population*

As already stated, 59 subjects were recruited for the monitoring campaign and this number of subjects was in accordance with the WHO guidance of having a minimum of 50 subjects for the sample to be representative of a target population (Jantunen and Kansanterveyslaitos, 1999). The recruitment of subjects was limited to people who reported their occupation as office worker in order to build a robust dataset on this particular group, and furthermore, sampling was restricted to weekdays only. By limiting the recruited volunteers to this occupation, a relatively uniform working pattern was established across the study population. This meant the vast majority of volunteers commuted to work between 7.30 am and 10 am during the peak morning traffic period, and also commuted home between 5 pm and 7 pm during the evening peak traffic period. Moreover, from a practical viewpoint, the office workers could keep the Aerocet-531 on constant charge when stationary at their desks during working hours.

This ensured sufficient battery life was available throughout the day and for the homeward commute which may not have been available in other occupations.

Aside from the occupation of volunteers being restricted to that of office worker, the recruitment process aimed to recruit volunteers across a broad spectrum of the age group 18 to 55 years. It was also an aim of the monitoring campaign to keep the gender ratio at 50:50 as much as possible amongst volunteers. This was achieved with varying degrees of success and will be discussed in further detail later.

As can be seen in Figure 4.1, 57% of the volunteers recruited for the study were males, while females made up 43% of the study population. These percentages equate the actual numbers in each gender as 36 males and 27 females. However, due to a number of failed samples, data from several of the other female volunteers recruited were deemed unusable in the main dataset. The failure of sampling days is discussed further in section 4.1.3.

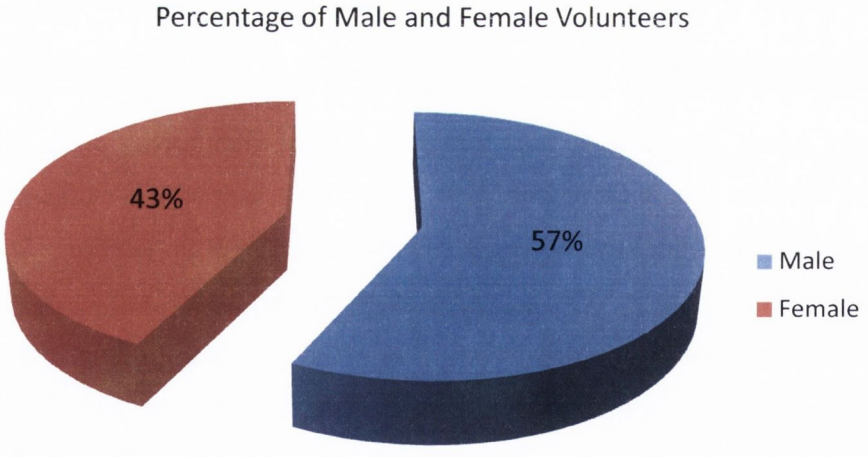


Figure 4.1: Pie chart of the percentage of male and female volunteers recruited.

The age ranges of volunteers were divided up into four main groups of 18 to 25 years of age, 26 to 35 years, 36 to 45 years, and finally, 46 to 55 years of age. The proportion of the study volunteers in each age bracket is shown in Figure 4.2. As can be seen from the

chart, the majority of volunteers (46%) fell within one of the mid-range categories between the ages of 26 and 35, while this was followed by the youngest category of 18 to 25 years which represented 27% of the sampling population. The difficulty in recruiting older candidates is reflected in the number of volunteers in the two oldest categories which make up 12 and 15 per cent respectively of the total, with these categories encompassing people in the 36 to 45, and 46 to 55 year old age bracket.

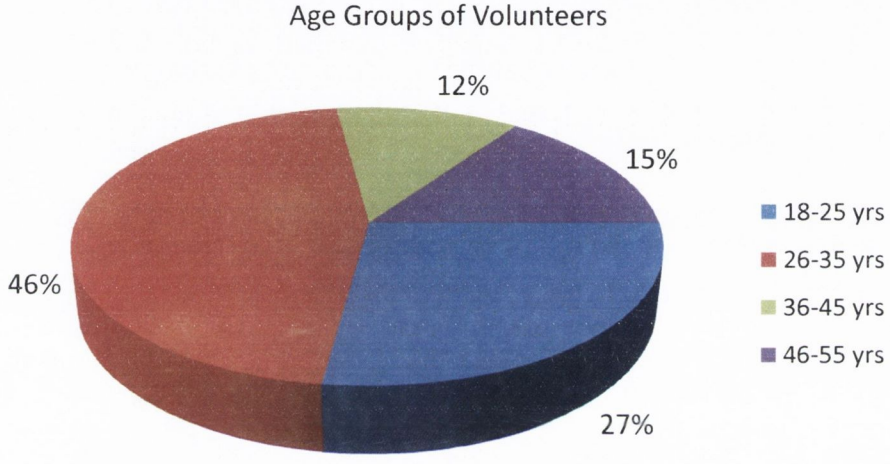


Figure 4.2: The percentage of volunteers in each age group.

One of the questions put to volunteers before sampling commenced was whether or not they were a smoker. This was important due to the potentially large influence this activity could have on the personal exposure sample taken by the individual. Thus, smoking sources had to be identified and taken into account during the data processing phase.

Of the volunteers recruited, approximately 12% declared themselves as smokers of some degree, or were in residence with a smoker. However, it transpired several of these individuals were in actual fact only casual or social smokers and thus did not report the occurrence of any smoking events while sampling. The other individuals that did smoke more regularly primarily did so at home in the evening time rather than

during the day. One of the volunteers who did not smoke himself, but reported living with a smoker, did not report being in their presence during any smoking event.

### *4.1.2 Home locations*

The volunteers that were recruited were all individuals with workplaces that were situated in Dublin city centre. However, one of the aims of the recruitment process was to obtain volunteers that had home locations that were evenly spread around the city, and also to recruit individuals that were resident outside the suburbs of the city in commuter towns. The home locations of all volunteers are shown in Figure 4.3, and represent a broad range of both Dublin postcodes and areas outside the city.

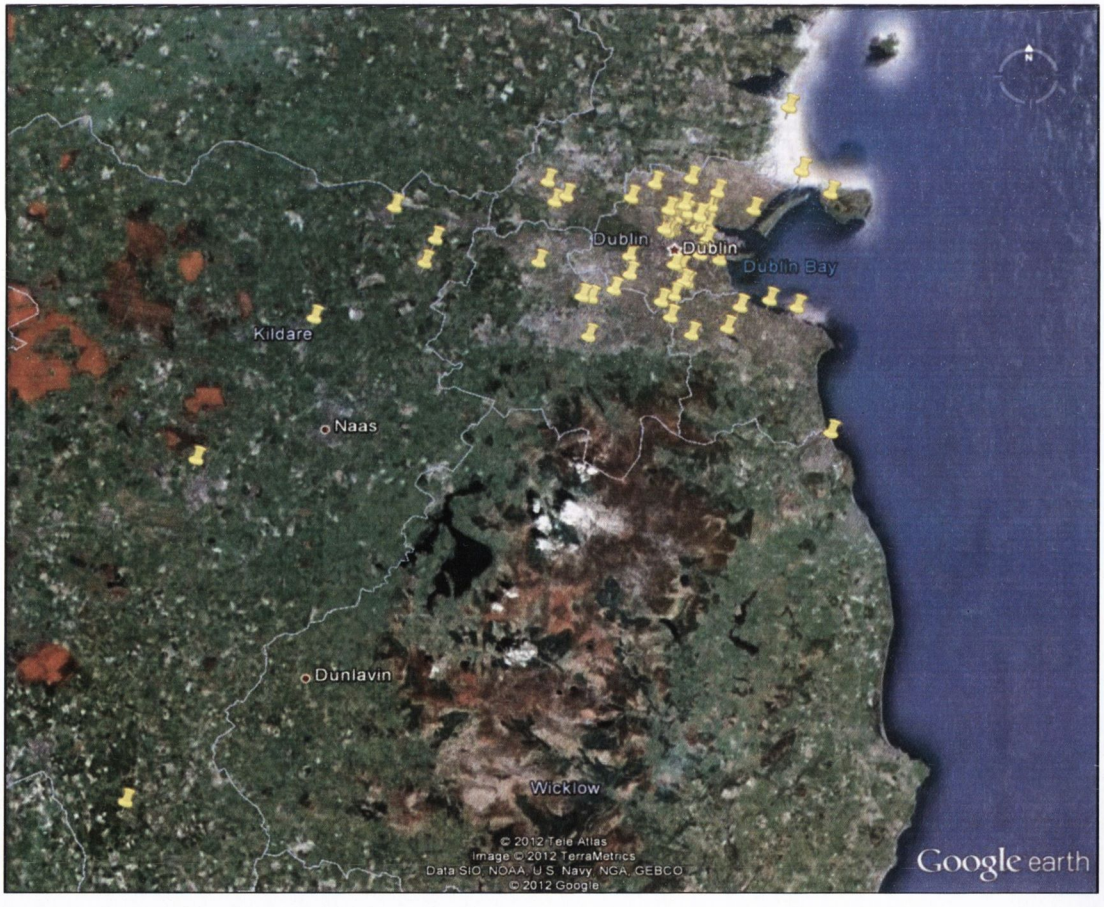


Figure 4.3: Home locations of subjects in the Greater Dublin Area and surrounding commuter towns.

In Dublin City itself, the home locations of the volunteers encompassed 16 of the 24 Dublin postal districts. The geographical spread of homes around the city is shown in Figure 4.4. In total 19 volunteers were resident on the south side of the city, 25 were located on the north side, while six more resided in west Dublin. Outside the city boundaries and the area of South Co. Dublin, there were nine more volunteers who were classified as living in commuter areas or towns. These were in counties Louth, Kildare and Wicklow, as well as in North Co. Dublin also.

Figure 4.4: Home locations of volunteers living in Dublin City.

The subjects involved in the study lived in a variety of different residences around the city. There were five main categories of homes, which are shown in Figure 4.5. These categories were classified as apartments, detached houses, semi-detached houses, terraced houses, and lastly, end of terrace homes.

As illustrated in Figure 4.5, the most commonly reported residence type was an apartment with 21 cases. This was followed by semi-detached houses and terraced

houses which was the case for 15 and 12, respectively, volunteers involved in the study. The least common occurring home types were detached with six, and finally, end of terracing homes were reported for five of the sampling population. Many of the residency types were dictated by what area of Dublin the volunteer hailed from. All those living in apartments were far more likely to live closer to the city, than for instance, those people living in semi-detached houses. Similarly, those volunteers who reported living in a detached home were more likely to live on the outskirts, or outside the Dublin area.

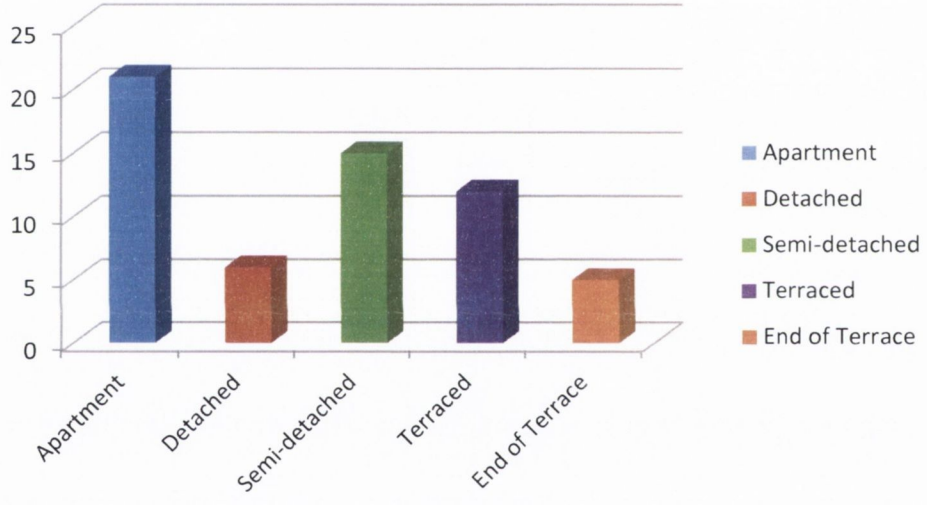


Figure 4.5: Types of residence of the study population.

### *4.1.3 Failed samples*

Over the course of the sampling campaign, a number of samples collected resulted in bad data or complete failure due to a variety of reasons. In total 23 of the 24-hour samples, or 8% of the total amount, were classified as failed sampling days. These included samples from 12 different volunteers, evenly split between males and females. The majority of failed samples from males were retaken again at a later date, except in the case of one individual. However, three of the female volunteers discontinued sampling subsequently, thus, losing the initial sampling days as well as future sampling days.

There were a number of 24-hour samples (n = 9) that failed due to the malfunction of the internal pump of the Aerocet-531. This mechanical failure of the instrument occurred on several occasions and each time the instrument would have to be sent back to the manufacturer for repair. This event, however, was quite rare and would occur suddenly without warning, as each time a sampling period commenced the flow rate of the instrument would have been checked beforehand.

Another reason responsible for the failure of some samples was due to volunteer error. These types of errors were caused by the improper operation of the Aerocet-531 instrument or the Garmin GPS device. On some occasions the volunteer would either accidently leave the Aerocet-531 at home for the day or else forget to carry the GPS device, in which case it was impossible to process the data unless the activity diary happened to be particularly accurate about activity times and commutes etc. However, these occurrences did not occur often and accounted for approximately 14 of the total failed 24-hour samples.

Other potential problems that were encountered included occasions when the handheld GPS device would fail to gain satellite reception, but ordinarily this problem would usually rectify itself after a short period of time. However, any potential missing movements during these outages could be identified with use of the activity diary of the volunteer.

Finally, during the taxi driver sampling campaign, a five day sampling period from one particular driver had to be classified as a failed sample. This failure occurred because of the returned data from the Aerocet-531 registering no concentration values for the duration of the sampling period, most likely due to some electronic fault of the device.

## 4.2 Time-Activity Budget

Human activities impact the timing, location and the extent of exposure to air pollutants, as well as playing a key role in explaining exposure variation. Human activity data has been used as major inputs for human exposure models such as the US EPA's *Hazardous*

*Air Pollutant Exposure Model* (HAPEM) and their probabilistic *National Ambient Air Quality Standards Exposure Model* (pNEM). Both of the aforementioned models rely on occurrences and time sequences of activities (Klepeis et al., 2001). Therefore, the gathering of activity data was an important task for the identification of sources and locations for this sampling campaign.

During this personal exposure study, a large amount of activity data was gathered in conjunction with the $PM_{10}$ exposure sampling. The 24-hour diary was an essential component for the personal exposure study. The diary enabled different activities, as well as locations, to be identified and matched to the dataset values obtained from the Aerocet-531 instrument. The information gained meant that $PM_{10}$ exposure concentrations could be identified for the various microenvironments frequented by the study population, as well as aiding with the identification of possible sources of particles at these locations.

The results from the sampling campaign show that for the study population, 92% of the time was spent indoors on average per day, with a further 3% spent in enclosed transit (see Figure 4.6). While the percentage of time spent outdoors by the study population in comparison was just 5%. Figure 4.6 also indicates the primary locations where the study population spent their time. It can be seen that the total indoor time percentage can be broken down into four major locations of at home in a residence, at work, in a café/public house/restaurant, or some other indoor location. The largest amount of time was spent by volunteers in a residence which represented 59% of their time, or 845 minutes each day. Of this 845 minutes that were spent at home, the average time spent sleeping was found to be 503 minutes, representing 35% of a 24-hour period, while the subjects were classified as 'active' in the home for the other 342 minutes.

The next major location outside the home that the sampling population spent their time in was at work which made up on average 30% of time (430 mins) in a person's 24-hour day. Smaller amounts of time were spent in other places such as a café, pub, restaurant or other indoor locations which made up 3% of the overall mean daily 24-hour time budget for the volunteer population. The only other significant microenvironment that

the study population spent time in, as previously stated, was enclosed transit (3%), which was also considered to be an indoor microenvironment. This microenvironment included time spent in various enclosed transport modes such as buses, cars, trains, and trams.

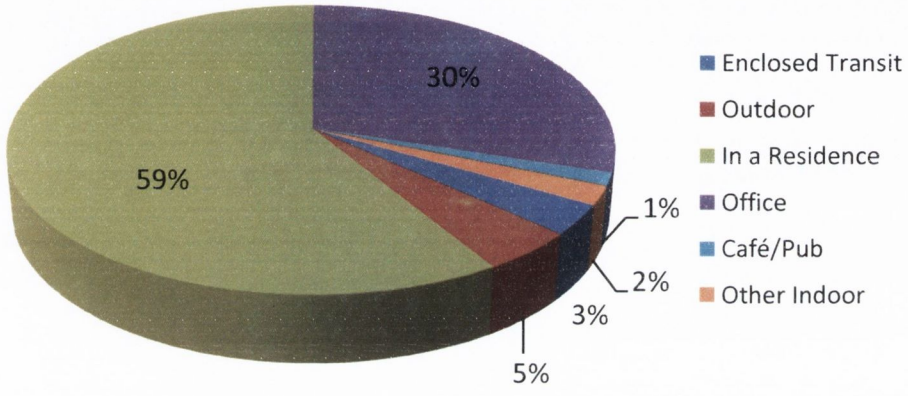


Figure 4.6: Pie chart showing the mean daily percentage of time the volunteers spent in six different locations.

The data presented in Table 4.1 highlights the average time spent by the total study population in specific microenvironments (population mean). Additionally, the data was further broken down according to the number of 24-hour samples that reported time spent in the different microenvironments. In activity pattern literature the people who report themselves as having partook in an activity on a particular day are commonly referred to as 'doers'. This convention will be applied in this study also, and furthermore each 24-hour sample is considered independently. The number of doers (*n*) and the percentage of 24-hour samples that reported spending time in a specific microenvironment (*% doers*) are both displayed in Table 4.1. Furthermore, the average time spent by those individuals on sampling days in the specific locations (*doer mean*) is also shown in the table.

Table 4.1: Time spent in different microenvironments (min $d^{-1}$).

| **Microenvironment** | **Population mean** (min $d^{-1}$) | **Doer** % | **Doer** n | **Doer mean** (min) |
|---|---|---|---|---|
| *Indoor* | | | | |
| In a residence | 845 | 100 | 255 | 845 |
| Office | 430 | 96 | 244 | 448 |
| Café/Restaurant | 12 | 24 | 60 | 51 |
| Public House | 8 | 6 | 15 | 127 |
| Shopping | 7 | 24 | 61 | 31 |
| Other indoor | 24 | 25 | 62 | 96 |
| Recreation/Sport | 6 | 9 | 22 | 73 |
| *Enclosed Transit* | | | | |
| Bus | 23 | 40 | 102 | 58 |
| Car | 17 | 36 | 91 | 48 |
| Train | 7 | 14 | 36 | 49 |
| Tram | 1 | 4 | 10 | 20 |
| *Outdoors* | | | | |
| Cycling | 10 | 26 | 67 | 38 |
| Walking | 39 | 84 | 212 | 47 |
| Recreation/Sport | 4 | 4 | 9 | 102 |
| Other outdoor | 5 | 13 | 32 | 40 |

As can be seen in Table 4.1, 100% of the study population spent time inside a residence with the average length of time spent there being 845 minutes. The next highest amount of time spent in a microenvironment was in an office, with 96% of volunteer samples reporting time spent in this location for an average of 448 minutes. 4% of the samples collected from the study population were days that the recruited volunteer chose to work from home while sampling.

Table 4.1 also shows that the population mean is an especially poor estimator of exposure duration for exposures that may occur in locations such as cafés, pubs, shops,

etc., where the doer mean is so much larger than the population mean. When PM sources are present in these microenvironments, exposures are likely to be significant and would be grossly underestimated by the use of a population mean in an exposure assessment. This disparity between the population means and the doer means indicates frequency distributions should be used in calculating population exposures for the purpose of risk assessment to air pollutants such as PM.

As mentioned there are a number of microenvironments that illustrate perfectly the disparity between population means and doer means. It can be seen that while the population mean for time spent in a café or restaurant was on average only 12 minutes per day, the actual mean length of time spent in this microenvironment by those samples that reported spending time there was 51 minutes, and this location was reported on 24% of sampling days. In contrast to cafés and restaurants, visits to a pub were reported in a far lower proportion of the samples collected, with just 6% doing so, but the average length of time spent by people (n = 15) in this microenvironment was 127 minutes.

As well as visits to the pub having a relatively low population mean (8 min $d^{-1}$), both the activities of shopping and indoor recreation/sport also had low population means of 7 minutes per day and 6 minutes per day, respectively. However, only 24% of samples reported the activity of shopping, while 9% of subject samples reported indoor recreation or sport. The activity of indoor recreation or sport primarily consisted of individuals reporting visits to a gym, a swimming pool, or some other form of indoor sport. Other less common indoor microenvironments were grouped together, and this included locations such as the library, music concert, theatre, etc. The 'other indoor' category made up 24 minutes per day of the population mean. One quarter of samples taken involved time spent in places considered as 'other indoor', and the mean time spent in these microenvironments was 96 minutes.

The mean time spent in enclosed transit for the study population are also displayed in Table 4.1. It can be seen that for the population mean, the bus was the most important mode of enclosed transport (23 min $d^{-1}$), followed by cars (17 min $d^{-1}$), and trailing both

of these were the less frequently used modes of train (7 min $d^{-1}$) and tram (1 min $d^{-1}$). However, the actual users of these modes spent a much greater amount of time on average on enclosed in these vehicles. The volunteers reported using the bus in 40% of samples taken and for an average length of time of 58 minutes per day. In car transit was the next most commonly used mode, with 36% of samples reporting time spent in a car at some point over the 24-hour sampling period and for an average of 48 minutes per day. While the population means for trains and trams were relatively low, this was due to only 14% of samples reporting transit by train and just 4% using the Luas tram system in Dublin. The actual average amount of time spent on these modes amongst samplers who did use them was far greater than the population means with people spending 49 minutes on a train and 20 minutes on a tram per 24-hour period.

As previously mentioned, time spent in the outdoor environment or undertaking outside activities was far less than the time spent indoors, making up just 5% of the 24-hour day across the population. By far the most common outside activity was that classed as 'walking' in Table 4.1. This category consisted of everything from walking to work, or walking to the bus or train, to walking to the shop etc. The population mean for this activity was calculated as 39 minutes per day, however, of the 84% of samples that contained this activity the average time spent walking outdoors was in fact 47 minutes.

Cycling was the next most common outdoor pursuit with 26% of the returned samples reporting cycling at some point. Unlike walking though, which could occur at any point during the sampling period, the majority of cycling was conducted as a means of commuting between home and work. The population mean time per day for cycling was 10 minutes, but this figure rises to on average 38 minutes per day amongst the samples ($n = 67$) that actually used this mode of transport.

There were other outdoor activities and locations that were less commonly reported during the course of sampling. The population mean for outdoor recreation and sport was a mere 4 minutes per day. This category consisted of activities like 5-a-side football and tennis, amongst others, and was only reported in 4% of samples. The average length of time that the 'doers' spent at this activity was far in excess of the population mean

with on average 102 minutes of a sampling period being dedicated to the particular activity. Finally, in 13% of samples collected the volunteer reported being present in some rather less frequent outdoor location and this was classed under the miscellaneous category of 'other outdoor'. On average the doer would spend 40 minutes at this location or activity per day, but in contrast, for the overall population mean only 6 minutes per day can be categorised as time spent in 'other outdoor'.

### *4.2.1 Location and activity categories*

In order to categorise the data obtained from the volunteer activity diaries, various activity codes were used to group the data. These activity codes were chosen to represent the most commonly reported activities and locations, and each concentration data value in the downloaded Aerocet-531 files was assigned an activity code based on information obtained from the activity diary and GPS device. Categorising the data in this manner enabled the processing to be expedited. The activity codes used are shown in Table 4.2.

Table 4.2: List of activity codes of the most common activities and locations reported by volunteers.

| Activity Code | Activity or Location | Activity Code | Activity or Location |
|---|---|---|---|
| 1 | In Office | 10 | On a Tram |
| 2 | Active at Home | 11 | Cycling |
| 3 | Sleeping | 12 | Shopping |
| 4 | Cooking | 13 | Recreation or Sport |
| 5 | In a Public House | 14 | In a Café or Restaurant |
| 6 | Walking | 15 | Other Indoor I |
| 7 | In a Car | 16 | Other Indoor II |
| 8 | On a Train | 17 | Other Outdoor |
| 9 | On a Bus | | |

The categories shown in Table 4.2 are for the most part self-explanatory, although some do need clarification as to what they actually encompassed. The activity category for recreation or sport was most commonly assigned to activities such as football, attending the gym, swimming, yoga, and other exercise activities. The categories of 'Other Indoor I & II' were generic categorical codes used to classify uncommon indoor locations that a subject visited during a sampling day. For instance, if a volunteer visited a dentist the data would be assigned the code '15' in Excel. If this same volunteer visited, for instance, a library later in the same day, this would then be assigned the code '16'. These indoor locations were rare enough that specific data distributions for them were not feasible. It was also highly unusual to have to assign both 'other indoor' codes in the same 24-hour period. Finally, the category of 'other outdoor' was assigned to outdoor activities other than travel or sport, such as eating lunch in the park for example. However, as was the case with the 'other indoor' categories, activities that fell into this category seldom occurred.

Each dataset returned after a period of monitoring had to be processed and refined into the different activities or locations for analysis, and this was done with the attribution of corresponding activity codes. An example is provided in Table 4.3 of the diary entries of a male volunteer for a single 24-hour period taken during springtime. In this example it can be seen that personal exposure monitoring began at 11am when the sampling equipment was delivered, and finished the following day at 11am. The duration of time and summary of the activities is shown, along with the corresponding activity code attributed to each microenvironment. As can be seen from the table, the largest amount of time was spent sleeping (activity code, ac = 3), followed by working in the office (ac = 1) and being active at home (ac = 2). The activity diary in this circumstance also highlighted the fact that cooking took place as well on arrival home from work, and this was given separate activity code (ac = 4) as it was quiet a significant source.

In total eight different activity or microenvironment codes occurred in the example 24-hour sample shown in Table 4.3. The activity diary in this particular example also serves to illustrate the small amount of time in general that was spent outdoors by volunteers during the working week. This volunteer spent a total of just 39 minutes

outdoors, representing 2.7% of the total 24-hour sampling period. The largest amount of time was spent at home with a total time of 820 minutes spent there. This figure was divided up between the activities of sleeping (480 mins), cooking (48 mins) and other general activities (292 mins) such as watching the television. The only other microenvironment in which a significant amount of time was spent was in the workplace, which accounted for 453 minutes (31.5%) of the 24-hour period. All other activities and locations, such as the commute, time spent in a café, and walking the dog, made up only small portions of the 24-hour period. However, combined these activities accounted for nearly 12% of the total sampling period.

Table 4.3: Example of a 24-hour activity pattern as reported in the activity diary, containing beginning and ending times, activity and location summary, and time spent in each microenvironment visited.

| **Starting time** | **Ending time** | **Summary** | **Activity code** | **Time spent** (min) |
|---|---|---|---|---|
| 11:00 | 16:00 | Working in office | 1 | 300 |
| 16:00 | 16:02 | Walked to a nearby café | 6 | 2 |
| 16:03 | 17:00 | In a café | 14 | 57 |
| 17:00 | 17:02 | Walked to office | 6 | 2 |
| 17:02 | 17:56 | Working in office | 1 | 54 |
| 17:56 | 18:36 | Got bus from outside office building | 9 | 40 |
| 18:36 | 18:38 | Walked to home | 6 | 2 |
| 18:38 | 18:42 | At home | 2 | 4 |
| 18:42 | 19:30 | Cooking, primarily frying | 4 | 48 |
| 19:30 | 20:26 | Watching TV at home | 2 | 56 |
| 20:26 | 20:47 | Walked dog | 17 | 21 |
| 20:47 | 00:00 | At home watching TV | 2 | 193 |
| 00:00 | 08:00 | Sleeping | 3 | 480 |
| 08:00 | 08:39 | Got up, at home | 2 | 39 |
| 08:39 | 08:45 | Walked to bus stop | 6 | 6 |
| 08:45 | 09:15 | On a bus | 9 | 30 |
| 09:15 | 09:21 | Walked to office | 6 | 6 |
| 09:21 | 11:00 | In office | 1 | 99 |

## 4.3 Personal Exposure Analysis

### *4.3.1 24-hour $PM_{10}$ exposure data*

The 24-hour exposure data from the sampling campaign was analysed with the statistical software package Minitab. A summary of the daily $PM_{10}$ personal exposures for the entire volunteer population (n = 255) is shown in Figure 4.7. The mean 24-hour $PM_{10}$ concentration for the study population was found to be 25.5 $\mu g/m^3$ and had a standard deviation of 15 $\mu g/m^3$. The 95% confidence interval for this mean concentration was between 23.6 $\mu g/m^3$ and 27.3 $\mu g/m^3$, while the standard deviation lay between 14 $\mu g/m^3$ and 16.7 $\mu g/m^3$ with 95% confidence. The median value for the daily personal exposure dataset was 21.6 $\mu g/m^3$, which had a confidence interval between 19.7 $\mu g/m^3$ and 24.3 $\mu g/m^3$.

The histogram shown in Figure 4.7 also illustrates the frequency distribution of the 24-hour samples collected. As can be seen, the exposure dataset was not normally distributed, with the Anderson-Darling test for normality confirming this fact with $p < 0.005$. This lack of normality is common for exposure data, as exposure data commonly have a skewed distribution with numerous low-value points and a few high value observations. Indeed as an example, the highest 24-hour $PM_{10}$ concentration in the dataset was reported as 105.7 $\mu g/m^3$, but yet 75% of the daily data concentrations were under 32.3 $\mu g/m^3$. There was thus a positive skewness of 1.8 for the frequency curve.

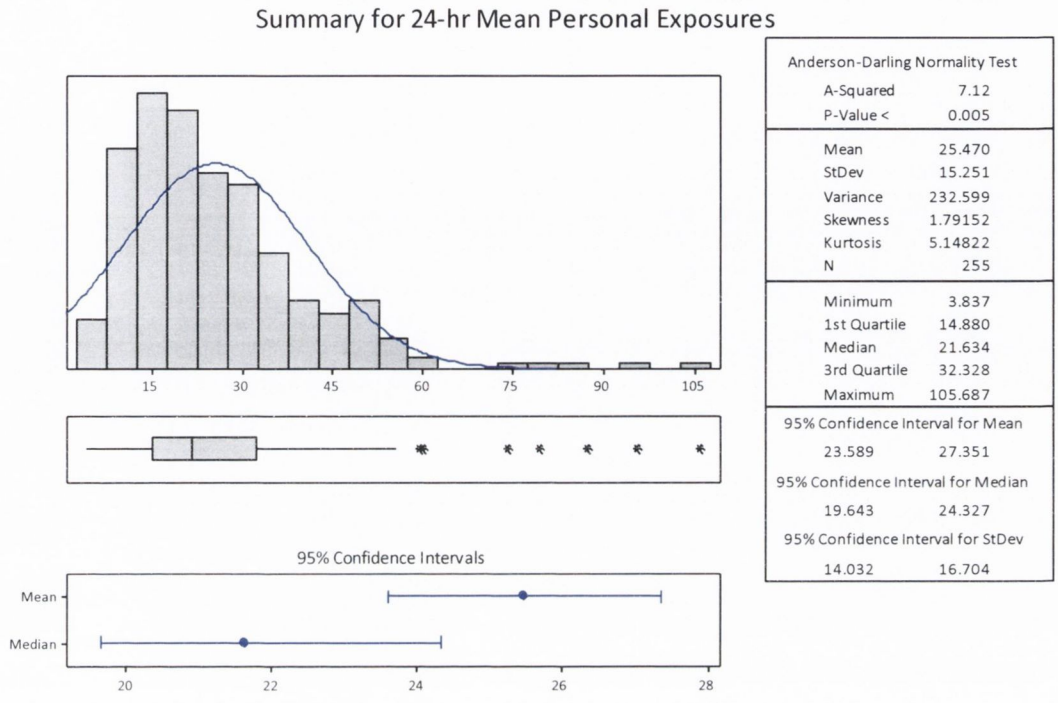


Figure 4.7: A summary for the overall population 24-hour $PM_{10}$ personal exposure samples collected by the volunteers.

### *4.3.2 Mean concentrations of 24-hour activity and location categories*

In this subsection, the results of the $PM_{10}$ personal exposure concentrations from each of the primary locations, as well as activities, will be discussed. A summary column chart for the activities and locations of the study population is shown in Figure 4.8. It should be noted at this point that many of the standard deviations for activities and microenvironments are larger than the mean. This is due to the skewed nature of exposure data, in which there often several large concentrations present within a dataset.

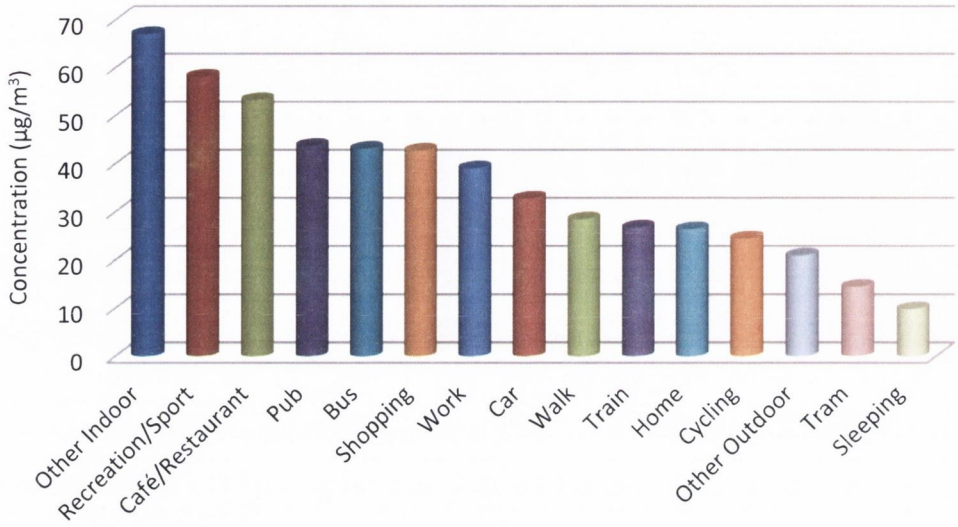


Figure 4.8: Column chart of the population main activities and locations by descending mean $PM_{10}$ personal exposure concentration ($\mu g/m^3$).

The mean 24-hour $PM_{10}$ personal exposure concentrations for each of the main microenvironments encountered during the sampling campaign study population are summarised in Table 4.4. The largest mean $PM_{10}$ concentration was found to occur under the microenvironment category of 'Other indoor' which was found to have a mean concentration of 67 $\mu g/m^3$, with a standard deviation of 67 $\mu g/m^3$. However, this category was quite general and included many one off activities undertaken in comparison to the clearly defined microenvironments such as at home or at work. Of the more specifically defined microenvironments or activities, it was the activity of recreation and sport that saw the largest $PM_{10}$ personal exposure concentrations across the entire population. The microenvironment 'Recreation/sport' had a mean personal exposure concentration of 58 $\mu g/m^3$, with an associated standard deviation of 46 $\mu g/m^3$. This activity category mainly consisted of mainly indoor pursuits, such as going to the gym or playing indoor sports, although several volunteers did participate in outdoor activities such as sailing, tennis and 5-a-side football.

Following sport and recreation, the activity or microenvironment with the next highest $PM_{10}$ concentration was found to be in cafés and restaurants. These locations had a mean $PM_{10}$ concentration of 53 $\mu g/m^3$ over the entire population, with a standard

deviation of 84 $\mu g/m^3$. The large standard deviation perhaps reflects the nature of the variability of this microenvironment; firstly, some volunteers may have been exposed to environmental tobacco smoke depending on where in the establishment they chose to sit. Secondly, it was possible the Aerocet-531 monitor may have detected particles that originated in the kitchen of the café/restaurant from cooking events.

Table 4.4: The mean, standard deviation, maximum and median values for the primary activities and microenvironments of all the 24-hour $PM_{10}$ personal exposure samples.

| **Activity or Microenvironment** | **N** | **Mean** ($\mu g/m^3$) | **Standard Deviation** ($\mu g/m^3$) | **Maximum** ($\mu g/m^3$) | **Median** ($\mu g/m^3$) |
|---|---|---|---|---|---|
| At Work | 244 | 39 | 36 | 241 | 28 |
| At Home | 255 | 26 | 21 | 249 | 22 |
| Sleeping | 255 | 10 | 8 | 48 | 7 |
| In a Pub | 15 | 44 | 34 | 155 | 31 |
| Walking | 212 | 29 | 28 | 238 | 21 |
| Car | 93 | 33 | 27 | 116 | 26 |
| Train | 35 | 27 | 15 | 69 | 26 |
| Bus | 100 | 43 | 31 | 165 | 38 |
| Tram | 10 | 14 | 8 | 28 | 14 |
| Cycling | 67 | 24 | 25 | 140 | 17 |
| Shopping | 61 | 43 | 44 | 282 | 30 |
| Recreation or Sport | 31 | 58 | 46 | 162 | 41 |
| Café or Restaurant | 60 | 53 | 84 | 657 | 33 |
| Other Indoor | 72 | 67 | 67 | 337 | 43 |
| Other Outdoor | 33 | 21 | 20 | 101 | 13 |

Below the microenvironment of café/restaurant on the column chart of Figure 4.8, lies the microenvironment of public house. This location had both a lower mean $PM_{10}$ concentration (44 $\mu g/m^3$) and standard deviation (34 $\mu g/m^3$) for the study population than that of café/restaurant. However, this was a far less common activity than visits to cafés, having only 25% of the samples (n = 15), compared with 60 of the sampling days registering a visit to a café or restaurant. The activity of shopping also had a very

similar mean concentration for the study population as that of public house. 'Shopping' had an average $PM_{10}$ concentration of 43 $\mu g/m^3$ and a standard deviation of 44 $\mu g/m^3$.

Across the different commuting modes there was also a great deal of variation. It was the microenvironment of 'bus' that saw the largest $PM_{10}$ concentration on average. Those volunteers that used the bus for their commute could be expected to encounter, on average, 43 $\mu g/m^3$ with a standard deviation of 31 $\mu g/m^3$. The use of this mode of transport was quite common also, with the use of a bus occurring on separate 100 sampling days. The mode of car followed the bus with the next highest mean concentration of 33 $\mu g/m^3$ and standard deviation of 27 $\mu g/m^3$. The only two other forms of enclosed transit reported by the study population were the use of trains and trams. These modes of transport were much less common than the use of a bus or car, with trains reported in 35 of the 24-hour samples, and trams even less common with only 10 cases reported. Both these modes also had relatively low average $PM_{10}$ concentrations when compared to the bus or car, with the train having a mean $PM_{10}$ concentration of 27 $\mu g/m^3$ ($\sigma$ = 15 $\mu g/m^3$), and the tram just 14 $\mu g/m^3$ ($\sigma$ = 8 $\mu g/m^3$).

Of the outdoor activities, it was the mode of walking that had the highest mean $PM_{10}$ concentration. The average for walking was 29 $\mu g/m^3$, and this had a standard deviation of 28 $\mu g/m^3$. This category of walking was not exclusively limited to commutes and encompassed events such as the volunteer walking to the shop or a café from their workplace. However, many of the walking events reported were indeed part of the commute of a volunteer and could usually be seen to occur in the morning and evening times as the volunteer walked to their primary mode of transport. In contrast the activity of 'cycling' was almost exclusively limited to commuting between home and work amongst the study population. This activity had a mean $PM_{10}$ concentration of 24 $\mu g/m^3$ and a standard deviation of 25 $\mu g/m^3$. Finally, the category of 'other outdoor' was used to group unusual outdoor activities, for instance, visits to the park or eating lunch outside etc. These cases were often too rare to warrant their own category, so were included under the umbrella of 'other outdoor'.

Many of the activities mentioned so far are those that primarily occur for brief periods over 24 hours. The majority of people's time, as discussed in Section 4.2, was spent in the microenvironments of work or in a residence. Thus, these locations are of primary importance in dictating the overall 24-hour $PM_{10}$ concentration that a person encounters, and also from a health impact perspective. The microenvironment of 'at work' was found to have an average $PM_{10}$ concentration of 39 $\mu g/m^3$ across all 24-hour samples taken, with a standard deviation of 36 $\mu g/m^3$. However, the largest proportion of a 24-hour period was spent by a subject in their place of residence.

The mean $PM_{10}$ concentration while the volunteers were active 'at home' was 26 $\mu g/m^3$, with standard deviation of 21 $\mu g/m^3$. The majority of time spent in a residence by a subject was also spent sleeping, which was for approximately eight hours per day according to the results garnered from the activity diaries. This long duration spent in the one microenvironment has the potential to significantly dictate the total exposure for that sampling period. In the case of this study, the overall $PM_{10}$ concentration for the sampling population while sleeping was just 10 $\mu g/m^3$, with a standard deviation of $\sigma$ = 8 $\mu g/m^3$ also. As it transpired, this activity also had the lowest mean $PM_{10}$ concentration of all activity/location categories examined.

### *4.3.3 Cooking*

Indoor aerosols in microenvironments frequented by people are often chemically and physically unstable and extremely heterogeneous. The effects of cooking on indoor particulate concentrations have been discussed in detail previously in the literature review. The different methods of cooking can have vastly different impacts on the amount of particles released into the ambient air, and as already highlighted, particularly the method of frying. Previous studies have attempted to characterise and evaluate the performance of light scattering devices in various microenvironments, especially with respect to cooking (Liu et al., 2002; Jenkins et al., 2004; Fischer and Koshland, 2007).

Jenkins et al. (2004) investigated the relationship between nephelometers and gravimetric respirable suspended particulate matter in a controlled atmosphere chamber.

They found that real time monitors may over report actual concentrations of indoor sources such as cooking. The study also recognised the difficulties of performing calibration in a field setting, because the presence of more than one aerosol can complicate interpretation of the real-time data. Liu et al. (2002) also encountered problems in their study and it was not possible for them to compare real-time light scattering devices against conventional impactor measurements over time, as the impactor measurements were integrated over time. While, Fischer and Koshland (2007) concluded, when studying single source (cooking) rural kitchens in China, that field calibration must be performed for each distinct microenvironment in which the nephelometer is employed.

Over the course of the sampling campaign, quite a large number of volunteers reported some form of cooking on sampling days. These events often resulted in large peaks in the indoor $PM_{10}$ concentration data collected by the Aerocet-531. However, many of the cooking events involved some form of boiling or release of steam, and these released water vapour particles were then detected by the Aerocet-531. The problem that arose from this is that the water vapour artificially inflated the recorded $PM_{10}$ concentrations. Ideally in order to compensate for this, calibration of the Aerocet-531 against gravimetric analysis would need to be conducted for each event which was not feasible. Moreover, the equipment available for calibration, namely the Haz-Dust EPAM-5000, was not suitable for calibrating such short term events like cooking. The Haz-Dust flow rate was 4.0 litres/min and the gravimetric sample was integrated over time, thus making it unsuitable for calibration of cooking events which were typically for short durations of under an hour. This short period of time was not conducive for gathering enough particle mass on a filter for accurate weighing. For example, it took just over four hours for the Haz-Dust to sample 1.0 $m^3$ of air, thus, during the main calibration campaign the Haz-Dust was run for a minimum of six hours each time to ensure sufficient mass was deposited on the filter.

In addition to the equipment concerns, a further complication arises due to the fact that often multiple types of cooking occur at the same time. In many cases the subjects would report events such as frying and boiling, or oven use and boiling etc., which were

taking place concurrently. This would have made it almost impossible to identify the main source of particle emission in order to calibrate the Aerocet data. Therefore, in order to negate any possible falsely increased $PM_{10}$ concentrations, cooking event peaks were simply removed from the 24-hour sampling datasets.

*4.3.3.1 Summary of cooking data*

While the difficulties in calibration of cooking events have been discussed, the following subsection will report results from the gathered cooking event data nonetheless. The impact of some cooking events was found to be significant for causing large peak $PM_{10}$ concentrations, for example where food was burned, and cooking did raise personal exposure concentrations amongst those individuals who reported this activity. Thus, it is important to highlight the impact of certain cooking events along with the removal of these events from the 24-hour average concentrations for the population.

The activity of cooking was reported on 52% of the total sampling days collected, which represented 133 out of 255 sampling days. Typically, the effects of a cooking event indoors lasted a mean duration of 85 minutes before $PM_{10}$ concentrations returned to pre-cooking levels. The removal of a cooking event was conducted by replacing the high data concentration values caused by cooking with the average in-home $PM_{10}$ concentration before the event. An example of the removal of an extreme cooking event is demonstrated in Figure 4.9. In this particular example the cooking method used was frying, and the effects of which lasted several hours. The average $PM_{10}$ concentration over this period in the home, which was an apartment, was 189 $\mu g/m^3$. However, the mean in-home concentration before the cooking event was just 18 $\mu g/m^3$, and this was the value that was substituted in for the cooking event in order to remove it from the overall 24-hour average. This example was a more unusual case both due to its duration and the large peak $PM_{10}$ concentration associated with it.

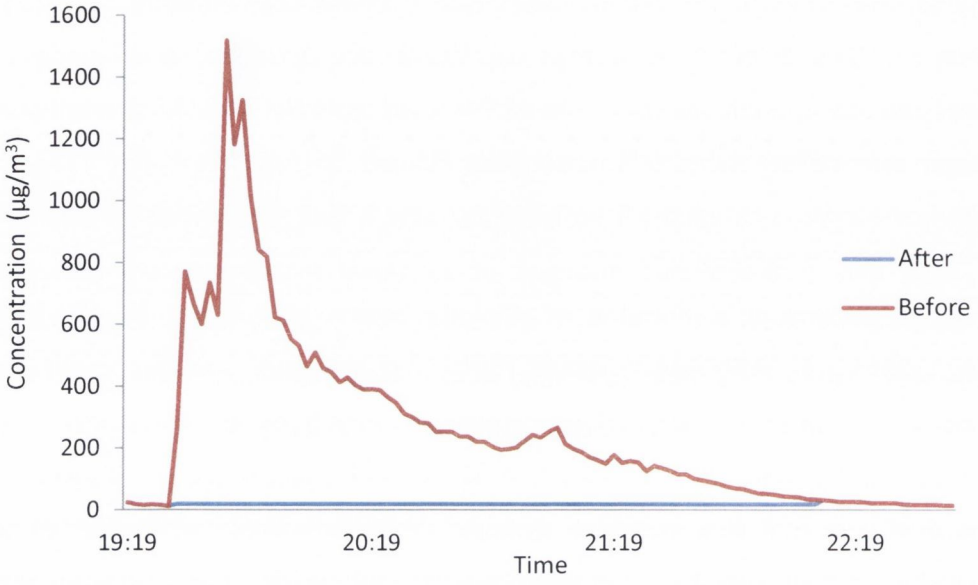


Figure 4.9: An example of frying in the home of a volunteer and the removal of the large peak.

The effect of removing the $PM_{10}$ concentrations caused by cooking events was quite dramatic. The summary statistics for the segment of the study population 24-hour samples that had cooking events reported at some point are shown in Table 4.5. The average $PM_{10}$ concentration from cooking sources across the study population who reported cooking was 149.1 $\mu g/m^3$, with a standard deviation of 195.4 $\mu g/m^3$. While the in-home $PM_{10}$ concentrations (not including sleeping) were on average 71.4 $\mu g/m^3$. The variation of the in-home concentrations was quite substantial ($\sigma$ = 125.3 $\mu g/m^3$). In contrast the median value of 36.3 $\mu g/m^3$ demonstrated that many of the cooking events did not drastically alter the at home $PM_{10}$ concentrations of the volunteers.

The 24-hour $PM_{10}$ concentration for volunteers who cooked was found to be approximately 39 $\mu g/m^3$, and had a standard deviation of 39.9 $\mu g/m^3$. However, after the cooking events were removed the 24-hour mean personal concentration for this population subgroup fell to 26.6 $\mu g/m^3$ ($\sigma$ = 15.6 $\mu g/m^3$). The mean at home $PM_{10}$ concentration for the cooking population displayed a larger decrease in comparison, dropping to 25.9 $\mu g/m^3$. The variability of the at home concentrations also declined greatly with the standard deviation falling over ten-fold to 11.1 $\mu g/m^3$.

Table 4.5: Summary descriptive statistics of volunteer sampling days that reported cooking. Both before and after the removal of cooking events are shown.

| | **Mean** ($\mu g/m^3$) | **St Dev** ($\mu g/m^3$) | **Median** ($\mu g/m^3$) |
|---|---|---|---|
| *Before removal of cooking* | | | |
| $PM_{10}$ concentration over cooking event period | 149.1 | 195.4 | 87.7 |
| 24-Hour $PM_{10}$ concentration | 39.1 | 39.9 | 28.4 |
| In-Home $PM_{10}$ concentration | 71.4 | 125.3 | 36.3 |
| *After removal of cooking* | | | |
| 24-Hour $PM_{10}$ concentration | 26.6 | 15.6 | 23.5 |
| In-Home $PM_{10}$ concentration | 25.9 | 11.1 | 24.2 |

Of the 133 subject sampling days that reported a cooking event, 83% of these reported just a single cooking event, 14% of sampling days had two separate cooking events, and just 3% of subjects who cooked recorded three cooking events in a single 24-hour period. This meant there was a total of 158 cooking events during the personal exposure sampling campaign. The types of cooking methods varied widely amongst volunteers, with the primary types being boiling, frying, grilling, microwave, oven usage, and toasting. However, in 46% of cases the volunteers failed to give specific details on the type of cooking going on despite being instructed to do so. Many of the cooking events that were reported also involved a combination of different cooking methods, which therefore hindered the identification of each method's exact contribution of particulates. Fortunately, one third of all cooking events were identified as being due to a single method, thus, the summary statistics for each method is shown in Table 4.6.

Table 4.6: Summary statistics of the primary cooking methods when reported as the sole type of cooking taking place by a subject.

| Type of Cooking | N | Mean $PM_{10}$ concentration ($\mu g/m^3$) | St Dev ($\mu g/m^3$) | Median ($\mu g/m^3$) | Average duration[a] (mins) |
|---|---|---|---|---|---|
| Boiling | 17 | 105.6 | 144.9 | 60.5 | 59 |
| Frying | 11 | 312.6 | 178.5 | 299.6 | 167 |
| Grilling | 3 | 200.1 | 23.2 | 196.9 | 89 |
| Microwave | 10 | 95.3 | 63.1 | 72.7 | 22 |
| Oven | 7 | 68.8 | 30.1 | 62.2 | 52 |
| Toasting | 6 | 51.2 | 16.0 | 44.5 | 29 |

[a] Duration of elevated $PM_{10}$ concentration due to a cooking event.

As can be seen from Table 4.6, the cooking method with the largest $PM_{10}$ concentration was frying which had a mean concentration of 312.6 $\mu g/m^3$. Additionally, the variability of the $PM_{10}$ concentrations from frying was found to be greatest ($\sigma$ = 178.5 $\mu g/m^3$) as well. The mean duration in the table is in reference to the length of time that a cooking source raised the $PM_{10}$ concentration above the original ambient in-home concentration, and not the length of time spent cooking as reported by the volunteer. It was also frying of food which was the method of cooking that took longest to dissipate in the homes of subjects, taking on average 167 minutes to return to 'normal' concentrations. After frying, the next highest concentration of $PM_{10}$ while cooking was found to originate from grilling events which had a mean of 200 $\mu g/m^3$. However, this figure is based on just three events as grilling was a far less common activity and often coincided with another form of cooking.

All other cooking methods (boiling, microwaving, oven use, toasting) had much lower mean $PM_{10}$ concentrations associated with them, ranging from 51.2 $\mu g/m^3$ to 105.6 $\mu g/m^3$. The range of mean concentrations for each of the differing cooking methods is illustrated in the individual value plot of Figure 4.10. The contribution of boiling, microwave, oven use, and toasting to raising indoor personal exposure concentrations of the subjects was also for far less time than frying and grilling, typically for less than an hour on average. In the case of microwaving, the average duration of this activity as a

source in homes as reported in Table 4.6 was 22 minutes, however, this value was misleading due to an outlier. The sample set for exclusively microwaving was rather limited in size (n = 10), and on one occasion a volunteer reported making popcorn and this was found to raise in-home personal exposure concentrations for approximately 142 minutes. Thus, once this source was excluded from the dataset, the actual mean duration that the activity of microwaving raises concentrations was for a mere 8 minutes on average.

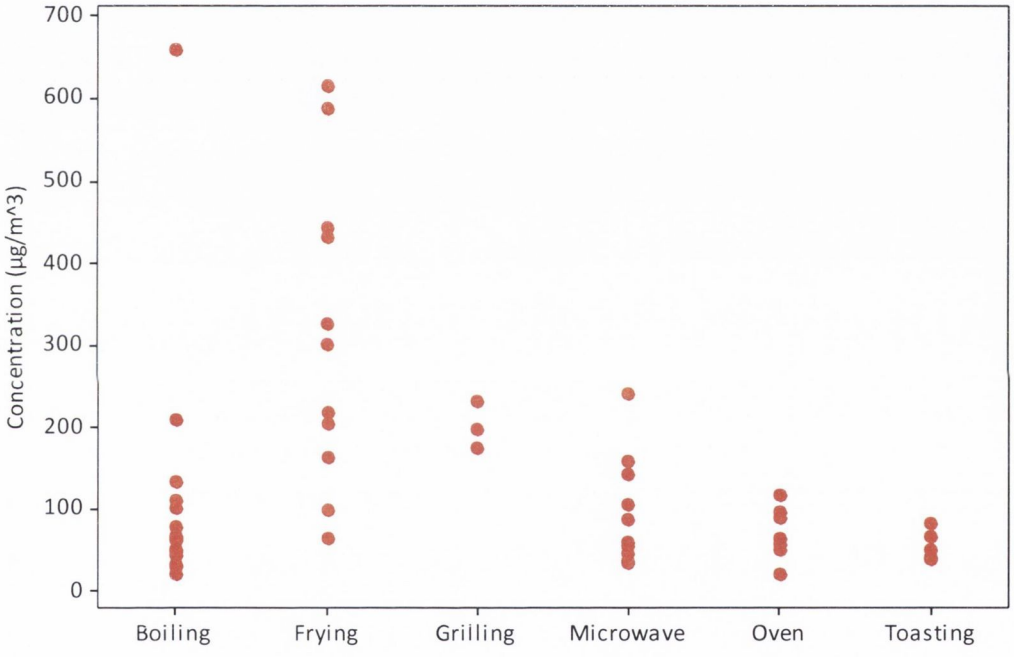


Figure 4.10: Individual value plot of $PM_{10}$ concentrations for six different methods of cooking.

The study subjects were also instructed to keep a record of the ventilation conditions that were present while cooking was on-going. However, it was found that many volunteers did not specifically note the ventilation conditions present. As a result the majority of cooking events reported in the activity diaries had no corresponding information, for example, on the whether a window had been opened or an extraction fan had been used. In total there were 16 occasions across a variety of cooking methods that did explicitly report having an extraction fan on, or alternatively a window or door

open in the kitchen. There was also a number of cooking samples (n = 13) that explicitly noted that no ventilation whatsoever was present during cooking.

The data available for both ventilation conditions is illustrated in Figure 4.11. On first look, the mean $PM_{10}$ concentration of the ventilated cooking events was 89.4 $\mu g/m^3$, while the average concentration with no ventilation used was 62.6 $\mu g/m^3$. However, without the outlier that can be seen in the figure for the 'No ventilation' data, the mean concentration drops to 65 $\mu g/m^3$. Also it was that the average length of time that the $PM_{10}$ concentrations were elevated was 56 minutes for no ventilation and 50 minutes for ventilated conditions. The reason that the ventilated and non-ventilated conditions were so similar may be explained by the relatively small sample set and the fact that five of the thirteen non-ventilated cooking events were microwaving. This type of cooking commonly has no need for ventilation as the duration is usually so short, thus this may explain why the time of elevated $PM_{10}$ concentrations were similar.

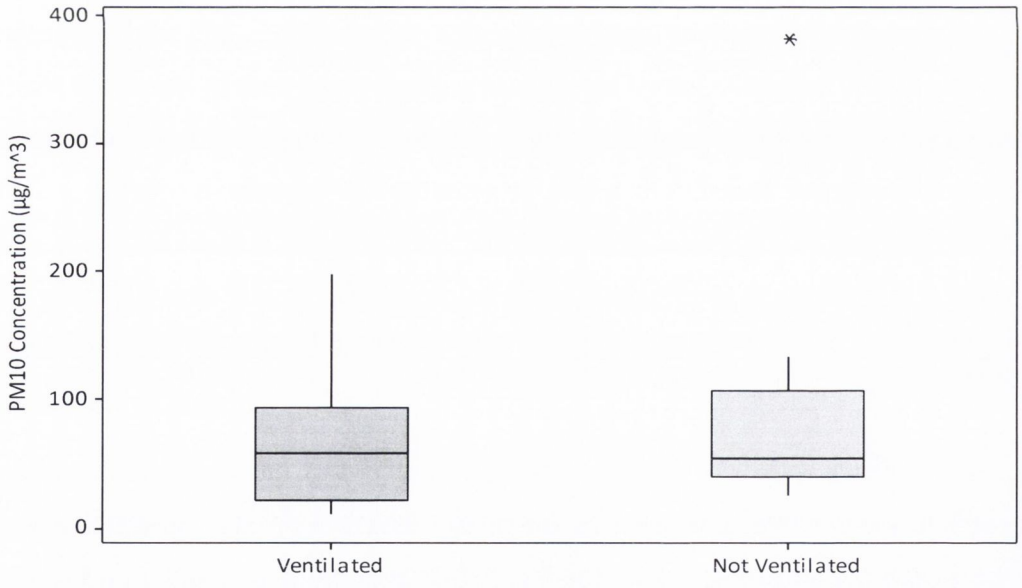


Figure 4.11: Boxplot of the reported ventilation conditions present while cooking.

### *4.3.4 Individual 24-hour sampling periods*

An important aspect of this personal exposure study was also to explore the between sample variation for the individual volunteers involved in the study. This is of

importance because not only is there a significant amount of variation of the $PM_{10}$ data across the entire study population, there can also be significant variations between sampling days of each volunteer. A sample case is provided and discussed in the following paragraphs.

*Case Study: Volunteer A*

The following case is an example of a successfully completed experimental sampling period conducted by a 28 year old male volunteer, referred to here as 'Volunteer A'. This particular volunteer completed a total of six 24-hour sampling periods, split into two sampling periods of three days each. The samples were taken in two different seasons, the first period in September while the second was collected in March. During both sampling periods, the volunteer began sampling on a Tuesday morning and completed sampling the following Friday morning at approximately the same time.

A summary of each of the six sampling days completed by Volunteer A is shown in Figure 4.12 and Figure 4.13. In the figures, Days 1, 2, and 3 represent the first sampling period completed, while Days 4, 5, and 6 are those sampling days completed during the second period of data collection. On examination of the box plot in Figure 4.12, the 24-hour mean $PM_{10}$ concentrations varied little over the first sampling period – ranging from 15 $\mu g/m^3$ to 18 $\mu g/m^3$. The second sampling period had similar 24-hour personal exposure concentrations, with mean $PM_{10}$ concentrations on two of the days being 16 $\mu g/m^3$. However, the most significant departure amongst sampling days was on Day 5, in which the mean 24-hour concentration was found to be 27 $\mu g/m^3$.

More light is shed on the higher 24-hour concentration for Day 5 when the dot plots in Figure 4.13 are examined. As can be seen from this figure, the starting points for the Day 5 dots appear more shifted towards higher concentrations. The other five sampling days have a large majority of dots clustered between 0 and 18 $\mu g/m^3$, in contrast Day 5 seems to have significant clustering of data points either side of the 36 $\mu g/m^3$ marker. Also apparent from the figures are the number of outliers that are associated with four of the six sampling days. The largest number of outliers appears to occur on Day 4, with

a large cluster appearing around the 70 μg/m$^3$ mark. This sampling day also has a large amount of very low concentration data values according to the dot plot.

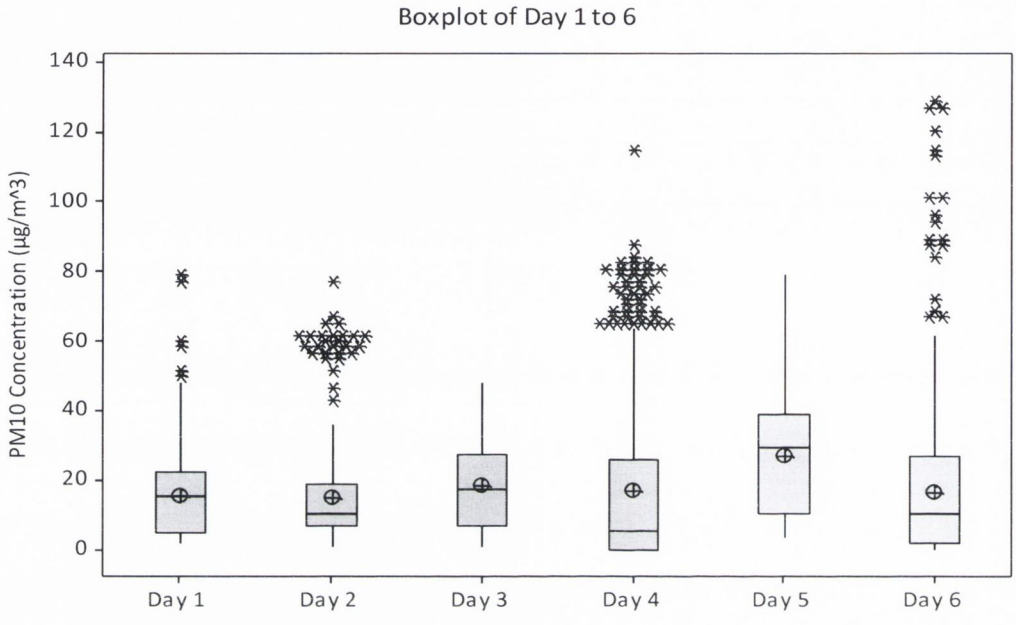


Figure 4.12: A boxplot of six sampling days completed by Volunteer A, with the mean (circular marker) and median values (horizontal lines) marked.

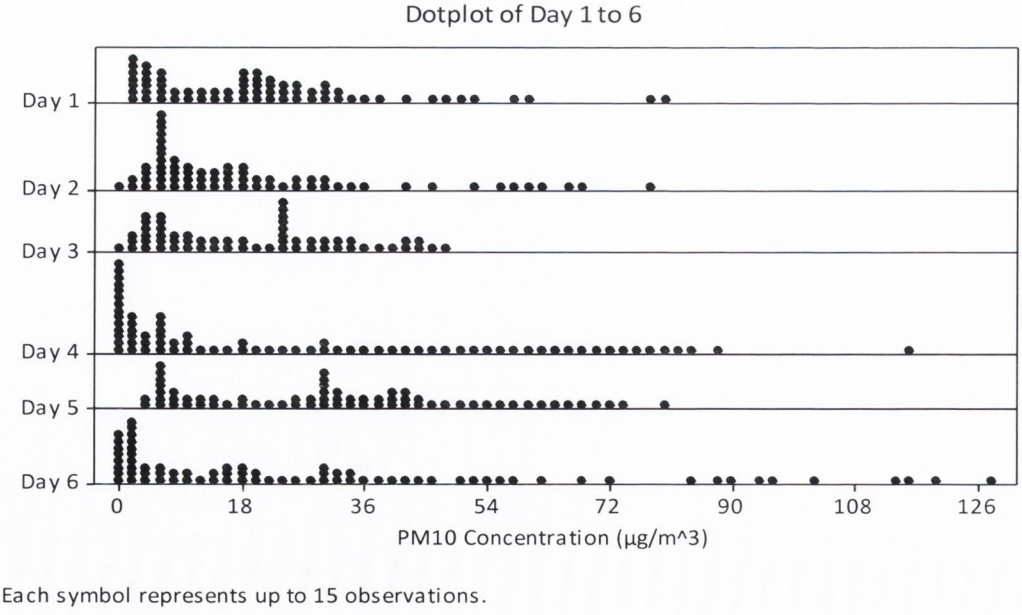


Figure 4.13: A dot-plot for each of the six sampling days completed by Volunteer A.

Volunteer A resided in Dublin City centre itself, on the north side of the city in Dublin 1. His home was a two bedroom apartment on the first floor of a block of apartments, and he lived with one other individual. Neither of the individuals living in the apartment was reported as a smoker. The workplace of Volunteer A was also in Dublin city centre, located on Pearse Street in Dublin 2. The geographic locations of the home and workplace of this volunteer are shown in Figure 4.14.

Also illustrated in the satellite image of Figure 4.14 are the GPS movement tracks for each of the separate sampling periods. The movements of this particular volunteer mainly consisted of commuting to and from work from home. The mode of commute was primarily on foot, although on two of the sampling days (Days 4 and 5) the volunteer chose to cycle at least one leg of his commute using a Dublin Bike.

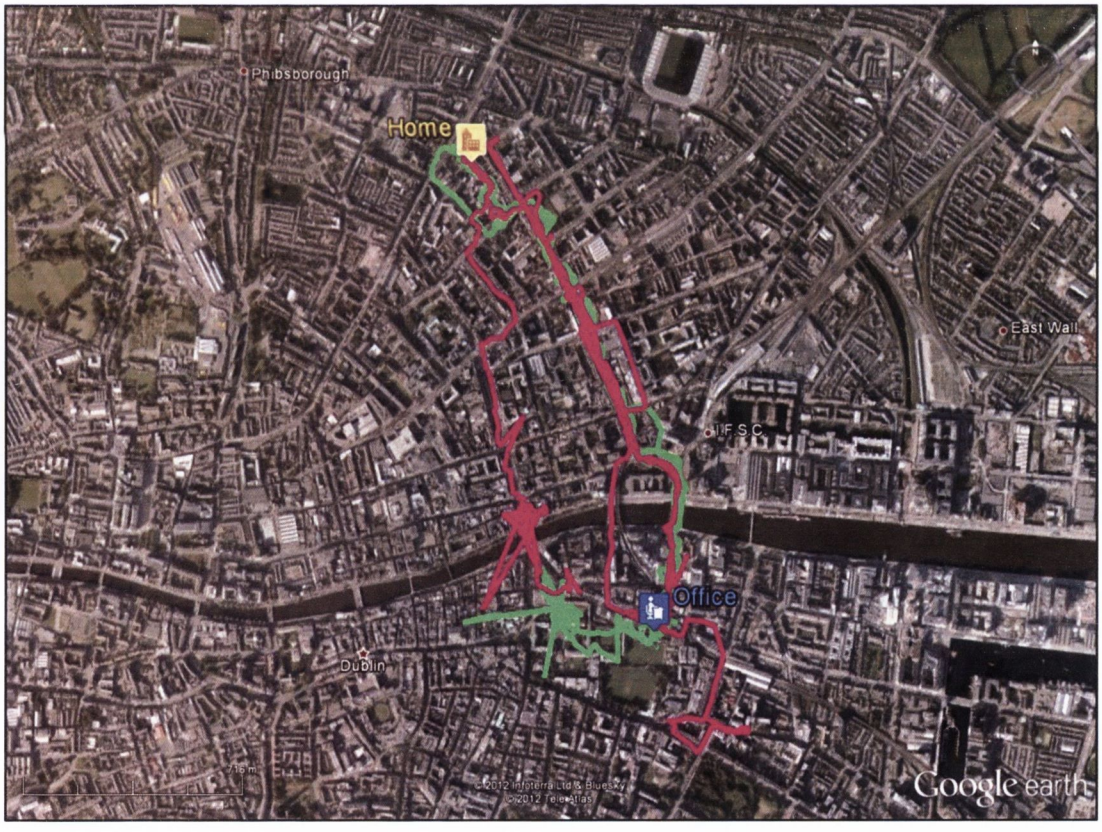


Figure 4.14: GPS tracks for Volunteer A with the first 3-day sampling period shown in green, and second sampling period track shown in pink. Also shown are the home and office locations for this volunteer.

A comprehensive break down of the activities and locations that Volunteer A sampled from over the entire sampling period is shown in Table 4.7. As can be seen from the table, the vast majority of this volunteer's time was spent in the microenvironments of his residence and workplace. On each of the sampling days, over 60% of time was spent at home, with the majority of this time being spent sleeping (nearly two thirds). The amount of time spent in the office on any given day varied too. In general, approximately 30 to 35% of time was spent in the office; however, on Day 5 the proportion of time spent in the office was as low as 20.7%

The highest personal concentration experienced by the volunteer was during a visit to a restaurant on Day 6 where there was a mean $PM_{10}$ concentration of 94.6 $\mu g/m^3$. Conversely, the lowest mean concentration was often found during the activity of sleeping, an activity that had a range of 2.3 $\mu g/m^3$ to 10 $\mu g/m^3$.

Of the microenvironments that Volunteer A spent the majority of his time in (in the office, at home, and sleeping), it was the workplace that displayed some of the highest mean $PM_{10}$ personal exposure concentrations. The highest of these office concentrations were recorded on sampling days four and five, with means of 52.2 $\mu g/m^3$ and 43.8 $\mu g/m^3$ respectively. However, as can be seen in Table 4.8, the concentration of $PM_{10}$ recorded by fixed site monitors in the city on these days was higher than all other sampling days. Therefore, this may in part help to explain why the working personal exposure on Day 4 and 5 were at these concentrations. Generally, 'at home' concentrations were always lower than the concentrations experienced at work, with the exception of Day 2. The mean concentrations in the home of the volunteer ranged between 15.4 $\mu g/m^3$ and 35.1 $\mu g/m^3$.

Table 4.7: Descriptive statistics based on all data for Volunteer A. Time spent and concentrations of $PM_{10}$ recorded in the respective microenvironments by Volunteer A.

| Microenvironment | Time (mins) | Mean ($\mu g/m^3$) | SD ($\mu g/m^3$) | Median ($\mu g/m^3$) | Time % | Mass % | Mass/Time Ratio |
|---|---|---|---|---|---|---|---|
| *Day 1* | | | | | | | |
| Office | 416 | 21.7 | 6.7 | 20.6 | 29 | 41.4 | 1.4 |
| Home | 324 | 22.8 | 8.6 | 24.1 | 22.5 | 33.8 | 1.5 |
| Sleeping | 580 | 5.5 | 4.8 | 3.4 | 40.3 | 14.6 | 0.4 |
| Walking | 74 | 15.6 | 14.4 | 11.8 | 5.1 | 5.2 | 1.0 |
| Shopping | 10 | 21.7 | 9.5 | 22.3 | 0.7 | 1.0 | 1.4 |
| Walked dog | 12 | 38.4 | 16.4 | 40 | 0.8 | 2.0 | 2.5 |
| Café | 24 | 20.8 | 7.8 | 18.1 | 1.6 | 2.2 | 1.4 |
| *Day 2* | | | | | | | |
| Office | 500 | 12.4 | 6.8 | 10.3 | 34.7 | 29.1 | 0.8 |
| Home | 362 | 27.8 | 15.6 | 27.5 | 25.1 | 47.1 | 1.9 |
| Sleeping | 514 | 9.5 | 5.3 | 8.6 | 35.7 | 22.9 | 0.6 |
| Walking | 50 | 3.6 | 3.4 | 2.6 | 3.5 | 0.9 | 0.2 |
| Walked dog | 14 | 2.8 | 0.9 | 2.5 | 1 | 0.2 | 0.2 |
| *Day 3* | | | | | | | |
| Office | 502 | 27.5 | 13.5 | 29.2 | 34.9 | 52.7 | 1.5 |
| Home | 332 | 18.1 | 7.9 | 24 | 23 | 22.9 | 1.0 |
| Sleeping | 562 | 11.2 | 10 | 6.9 | 39 | 24.0 | 0.6 |
| Walking | 24 | 13.4 | 3.1 | 12.9 | 1.7 | 1.3 | 0.7 |
| Walked dog | 20 | 2.2 | 0.8 | 2.5 | 1.4 | 0.2 | 0.1 |
| *Day 4* | | | | | | | |
| Office | 304 | 52.2 | 18.4 | 53.3 | 21 | 65.6 | 3.1 |
| Home | 348 | 15.4 | 9.8 | 12 | 24.2 | 22.3 | 0.9 |
| Sleeping | 744 | 1.6 | 2.3 | 0 | 51.7 | 5.0 | 0.1 |
| Walking | 24 | 42.7 | 22.5 | 36.1 | 1.7 | 4.3 | 2.6 |
| Passenger in a car | 8 | 37.4 | 9.2 | 32.7 | 0.6 | 1.3 | 2.2 |
| Cycling | 12 | 51.9 | 16.4 | 42.1 | 0.8 | 2.5 | 3.1 |
| *Day 5* | | | | | | | |
| Office | 298 | 43.8 | 14.2 | 39.5 | 20.7 | 33.6 | 1.6 |
| Home | 402 | 35.1 | 11.7 | 37.8 | 28 | 36.3 | 1.3 |
| Sleeping | 692 | 15 | 9.2 | 12 | 48 | 26.7 | 0.6 |
| Walking | 38 | 30.2 | 13.6 | 24.1 | 2.6 | 2.9 | 1.1 |
| Cycling | 10 | 28.5 | 12.5 | 29.2 | 0.7 | 0.7 | 1.1 |
| *Day 6* | | | | | | | |
| Office | 438 | 27.6 | 10.3 | 31 | 30.4 | 51.8 | 1.7 |
| Home | 160 | 17.5 | 7.4 | 18.1 | 11.1 | 12.0 | 1.1 |
| Sleeping | 748 | 3.2 | 4.1 | 1.7 | 52 | 10.3 | 0.2 |
| Walking | 54 | 40.8 | 13 | 36.1 | 3.7 | 9.3 | 2.5 |
| Restaurant | 40 | 94.6 | 21.7 | 92 | 2.8 | 16.4 | 5.8 |

Many of the commuting and transport modes that the volunteer used had high $PM_{10}$ concentrations associated with them. On two of the sampling days the volunteer cycled to work and experienced mean concentrations of 51.9 and 28.5 $\mu g/m^3$. On Day 4 the volunteer was also a passenger in a car around peak traffic hours just after 6pm and recorded a mean $PM_{10}$ concentration of 37.4 $\mu g/m^3$. The only other type of commuting mode reported by Volunteer A was walking. This activity varied greatly over the sampling periods, from as little as 3.6 $\mu g/m^3$ to as high as 42.7 $\mu g/m^3$. This category was not however exclusively limited to commutes to and from work, and may have involved other walking events such as going to a shop or café during the day. This may explain the variation seen in the data for this activity, as readings were taken at different periods during the day.

The relative contributions of the individual microenvironments and activities to total mass sampled are expressed in Table 4.7 as a mass/time ratio. On each of the sampling days the mass/time ratio value was calculated as the ratio of the cumulative mass of $PM_{10}$ recorded on a sampling day in a particular type of microenvironment (in per cent of the total mass of the sampling day) and the per cent of the total time spent in this microenvironment. The cumulative mass of recorded $PM_{10}$ for each microenvironment was calculated by multiplying the quantity of air sampled ($m^3$) by the mean concentration in that microenvironment. The mass sampled in each microenvironment was then expressed as a percentage of the total mass sampled that day.

The microenvironment values over unity contributed a higher amount to total mass sampled than those values that were below unity. Many of the microenvironments that the volunteer frequented over the course of the sampling periods displayed mass/time ratios close to unity. However, the lowest mass/time ratio was found to occur during sleeping, with the ratio for this activity varying between 0.1 and 0.6 over the six sampling days. The largest mass/time ratio occurred on day six when the volunteer visited a diner style restaurant. This ratio of 5.8 accounted for just over 16% of the total mass sampled that day, although less than 3% of the 24-hour sampling time was spent there. The large difference between the percentage of mass and time for the

microenvironment can be attributed to the large amount of aerosols in the ambient air of this restaurant due to the on-going combustion processes inside.

Table 4.8: Comparison of the mean personal exposure for each sampling day with two fixed site monitors in Dublin City.

| Sampling Day | Mean Personal Exposure ($\mu g/m^3$) | Mean Office Exposure ($\mu g/m^3$) | $PM_{10}$ Fixed Site Monitors | |
|---|---|---|---|---|
| | | | Phoenix Park ($\mu g/m^3$) | Winetavern Street ($\mu g/m^3$) |
| 1 | 15.2 | 21.7 | 4.9 | 8.5 |
| 2 | 14.8 | 12.4 | 3.7 | 6.7 |
| 3 | 18.4 | 27.5 | 5.6 | 7.3 |
| 4 | 16.7 | 52.2 | 20.9 | 25.2 |
| 5 | 27.0 | 43.8 | 11.5 | 15.5 |
| 6 | 16.2 | 27.6 | 10.3 | 10.9 |

During the course of the sampling periods, the activity diary of Volunteer A reported cooking events on two separate occasions. These events took place on days three and five of the collected 24-hour samples. Both of these cooking events were removed in accordance with the procedure employed for the treatment of cooking data. This was done to ensure the overall 24-hour $PM_{10}$ personal exposure concentration was not falsely inflated by these events. The graphs shown in Figure 4.15 show the corrected time series plots for the collected $PM_{10}$ data. The graphs are small segments extracted from the 24-hour profile for each sampling day. According to the activity diary, both cooking events occurred at home in the evening time.

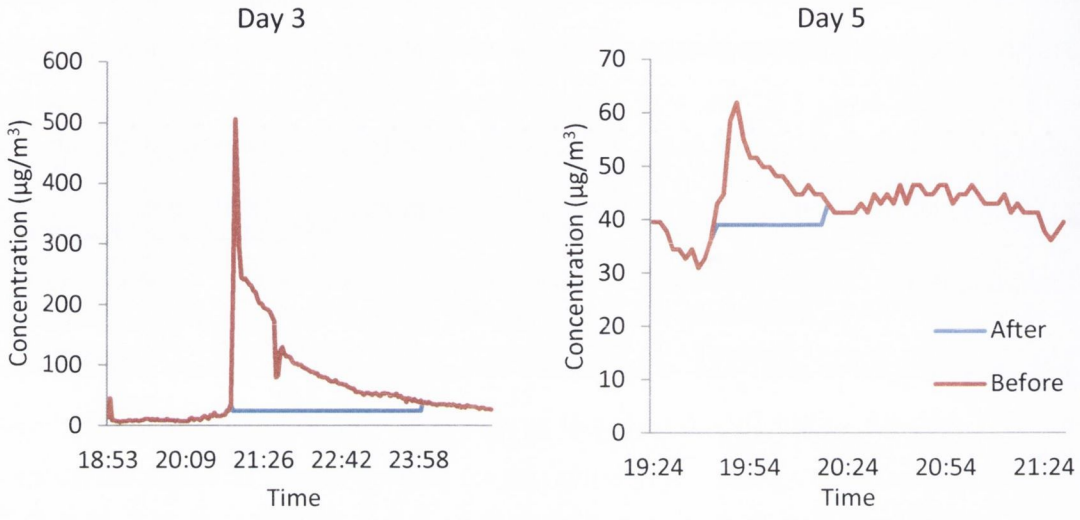


Figure 4.15: Cooking events from Volunteer A.

The first cooking event took place on Day 3 of the first sampling period and began at approximately 8.55 pm at night. As can be seen from the figure, this event resulted in quite a significant spike in the data, and was reported in the diary as 'boiled kettle'. This led to the conclusion that this peak was most certainly due to large amounts of steam being emitted from the source. The home of Volunteer A was a two bedroomed apartment, with a combined kitchen and living room area. Thus, the Aerocet-531 concentrations remained high for the next few hours due to the volunteer being situated in the same room as the source for the evening. There was also no report of ventilation, such as a window being opened, during or after this event.

The second event occurred on day five of Volunteer A's 24-hour sampling. This event was far less significant as the previous case, with the activity diary reporting it as oven usage between 7.20 pm to 7.40 pm. The resulting effect of this particular cooking event was to raise $PM_{10}$ concentrations in the home by approximately 20 $\mu g/m^3$ above the level already present in the apartment kitchen/living room area. This peak of the cooking event occurred at 7.50 pm, after the cooking period was reported to have finished, and caused lingering elevated concentrations until 8.18 pm.

The effect of these two cooking events on the 24-hour $PM_{10}$ concentrations on the respective days was significantly different. On Day 5 the oven cooking event resulted in only a 0.3 $\mu g/m^3$ increase in overall 24-hour $PM_{10}$ concentration when compared to the post-correction data. This was owing to the relatively small peak caused by the event and short duration before the concentration returned to pre-cooking levels. In contrast, the effects of the boiling event of Day 3 meant $PM_{10}$ concentrations were elevated for several hours before returning to a lower level. The $PM_{10}$ concentration recorded due to this event peaked at 505 $\mu g/m^3$. The overall effect of this cooking event prior to correction was that the 24-hour $PM_{10}$ concentration was 29 $\mu g/m^3$. However, by eliminating this event from the data the actual $PM_{10}$ concentration for the sampling day was 18 $\mu g/m^3$. This example serves to illustrate the significant effect an event such as this could potentially have on a 24-hour sample if not corrected.

### *4.3.5 Smoker data*

The activities of smoking and cooking have been identified by numerous indoor/outdoor air quality studies as the predominant sources elevating indoor concentrations of PM (Wallace, 1996). Smoking in particular can cause elevated concentrations of fine particles in a household of approximately 20 $\mu g/m^3$ per smoker (Spengler et al., 1985), along with short term peaks of 300 $\mu g/m^3$ which can persist for half an hour after smoking is finished (Chao et al., 1998). Moreover, just one cigarette can contribute 2.3 $\mu g/m^3$ to the 24-hour average indoor and personal $PM_{10}$ concentration (Janssen et al., 1998a). Indeed, as a further example of the contribution of smoking to elevated indoor PM concentrations, a study found that children whose parents smoked were exposed to, on average, personal $PM_{10}$ exposures of 40 $\mu g/m^3$ greater than children with non-smoking parents (Janssen et al., 1997). Thus, it is clear environmental tobacco smoke can be a major contributor to personal exposure and can raise personal $PM_{10}$ concentrations of non-smokers who are in the company of a smoker significantly.

The impact of a cigarette being smoked in a home of a volunteer is illustrated in Figure 4.16. In this example the volunteer arrived at his home, which was a three bedroom terraced bungalow, at 11.20 pm. The volunteer then proceeded to smoke a cigarette at

11.50 pm, before going to bed shortly after midnight. As can be seen in Figure 4.16 this event caused a large spike in the concentration in the room from an average $PM_{10}$ concentration of 20 $\mu g/m^3$ in the preceding 30 minutes, to a peak concentration of 162 $\mu g/m^3$. The high concentrations as a result of the cigarette then took the next five hours to dissipate, and only returned to pre-smoking levels at 5.00 am.

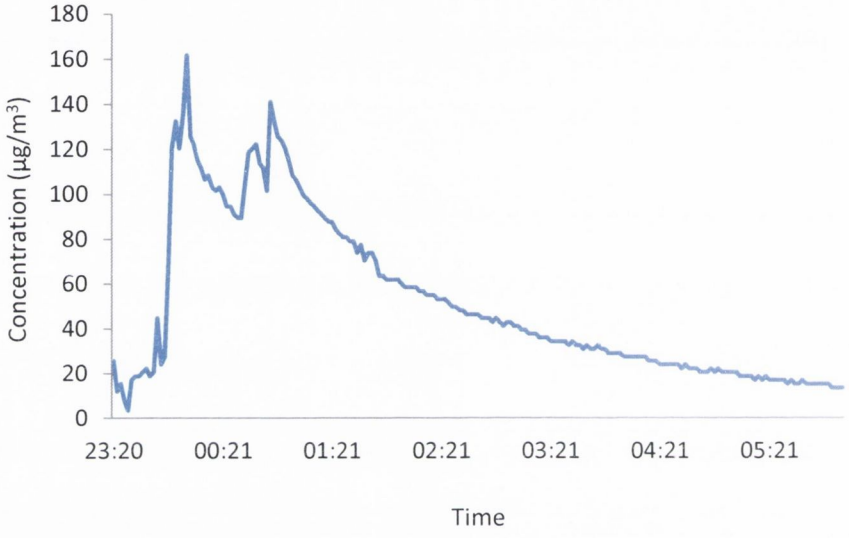


Figure 4.16: An example of a smoking event in the home of a volunteer.

In total, of the 34 sampling days conducted by the self-identified smokers involved in the study, only 12 of these days had a smoking event recorded in the activity diary. The population mean 24-hour $PM_{10}$ concentration amongst the volunteers who did report smoking events on sampling days was 35 $\mu g/m^3$. This figure was over twice the 24-hour mean $PM_{10}$ exposure of the self-identified smokers who did not report a smoking event. The non-smoking days of the volunteers had on average a 24-hour $PM_{10}$ concentration of 17 $\mu g/m^3$. The variability amongst the smokers was even greater when the 'at home' and 'sleeping' concentrations of the sampling days when the volunteer smoked were compared with days when they did not. On average, the 'at home' concentration was 64 $\mu g/m^3$ on days when they smoked compared with 23 $\mu g/m^3$ on other days. The in-home $PM_{10}$ concentration at night when the volunteers were sleeping was 19 $\mu g/m^3$ after smoking in the house, compared to just 8 $\mu g/m^3$ when there was no smoking reported.

### *4.3.6 Other unusual activities and sources*

During the sampling campaign the vast majority of volunteer 24-hour samples taken did not report any unusual events or sources that could cause a large and sudden increase in $PM_{10}$ concentration within a microenvironment. The most commonly reported events that coincided with a dramatic increase in $PM_{10}$ personal exposure concentration were the previously discussed cooking and exposure to ETS occurrences. However, over the course of the sampling campaign a number of other interesting indoor sources were reported by several volunteers.

One example of an abnormal source contributing to the 'at home' personal $PM_{10}$ concentration of a subject was in the case of one particular volunteer who on two separate occasions reported burning incense in the evening time when at home. An example of one of these incense burning events is illustrated in Figure 4.17. The volunteer in this instance had arrived home at approximately 5.30 pm and reported lighting incense for a short period at 10.07 pm. The end result of this action was to raise the mean 'at home' $PM_{10}$ concentration before the event from 26 $\mu g/m^3$ ($\sigma$ = 7.8 $\mu g/m^3$) to 74 $\mu g/m^3$ ($\sigma$ = 43.5 $\mu g/m^3$) while the incense was burning. This also included an initial peak value of 241 $\mu g/m^3$, which may have been due to the initial combustion and subsequent release of particulates from the matchstick and wick. The particle contribution from the incense burning lasted for approximately 32 minutes, and thereafter the mean 'at home' $PM_{10}$ concentration returned to similar pre-incense burning levels. The one hour period afterwards had a mean concentration of 29 $\mu g/m^3$ and standard deviation of 3 $\mu g/m^3$.

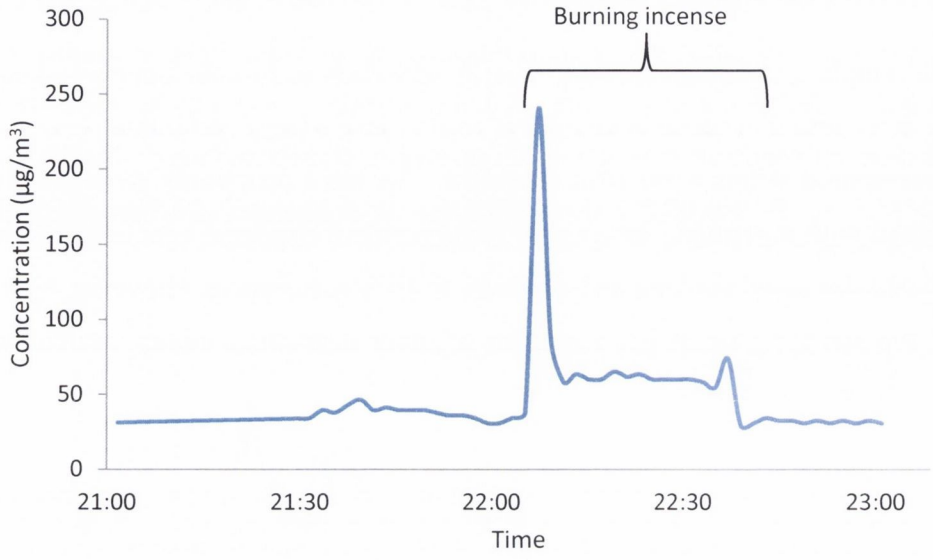


Figure 4.17: An incense burning event that was reported in the home of a female volunteer.

In another example of an unusual event observed within the dataset, the volunteer in this instance reported the use of deodorant in the morning time prior to going to work (see Figure 4.18). This was one of the very few occasions whereby a volunteer reported the use of an aerosol while in the vicinity of the Aerocet-531. This brief aerosol spraying event resulted in a peak $PM_{10}$ concentration of 504 $\mu g/m^3$. Before use of the deodorant spray, the mean in-home $PM_{10}$ concentration of the previous hour was 27 $\mu g/m^3$, and had a standard deviation of 9.1 $\mu g/m^3$. However, on release of the aerosol into the ambient atmosphere the $PM_{10}$ concentrations immediately increase to an average concentration of 213 $\mu g/m^3$ ($\sigma$ = 143 $\mu g/m^3$) for the half hour period between 9.30 am and 10 pm. As can be seen from the graph in Figure 4.18, there was also a steep decline in $PM_{10}$ concentration from the largest peak concentration and the concentrations finally level off when this volunteer commences his commute at 10 am.

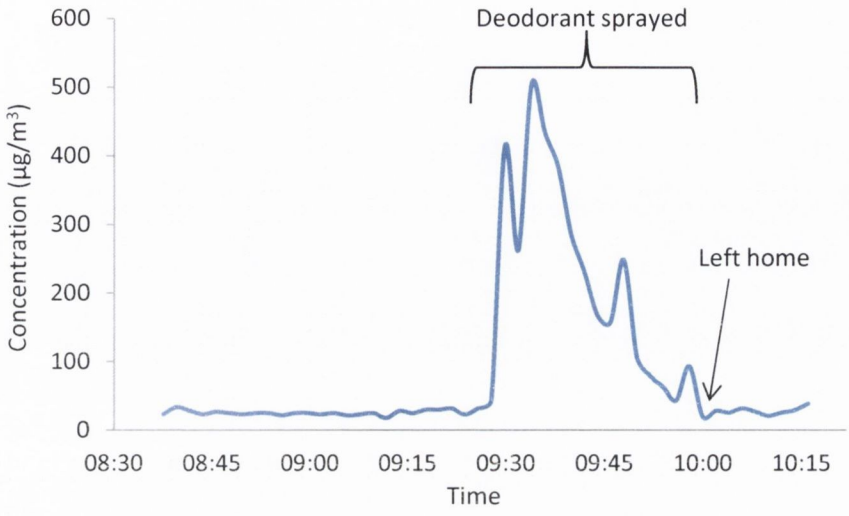


Figure 4.18: Example of deodorant being sprayed in the vicinity of the Aerocet-531.

The final example of a brief event that can cause a sudden increase in personal exposure was taken from a sample collected by a male volunteer who resided in a commuter town near Dublin, in Maynooth. On one of the sampling days while this volunteer was commuting home by bus, he reported passing near a burning car, which could be smelled inside the cabin, at 6.05 pm while the bus was on the N4 road at Lucan. When the time series graph of the $PM_{10}$ concentration for this bus journey was examined (see Figure 4.19), it could be seen that this event corresponded to a peak in the commute concentration of 29 $\mu g/m^3$ for a brief period as the bus passed through the area.

As an aside, another interesting feature of this particular time series plot of the commute was the decreasing trend of the on board particulate concentrations as the bus moves from the city centre, where the journey begins at 5.31 pm on the quays. The $PM_{10}$ concentration then steadily declines until the bus passes by the nearby fire. As the bus moves away from this the exterior source, the concentration again declines until the volunteer exits the vehicle at 6.25 pm. The overall mean personal exposure on this journey was 13.3 $\mu g/m^3$ ($\sigma = 6.5$ $\mu g/m^3$).

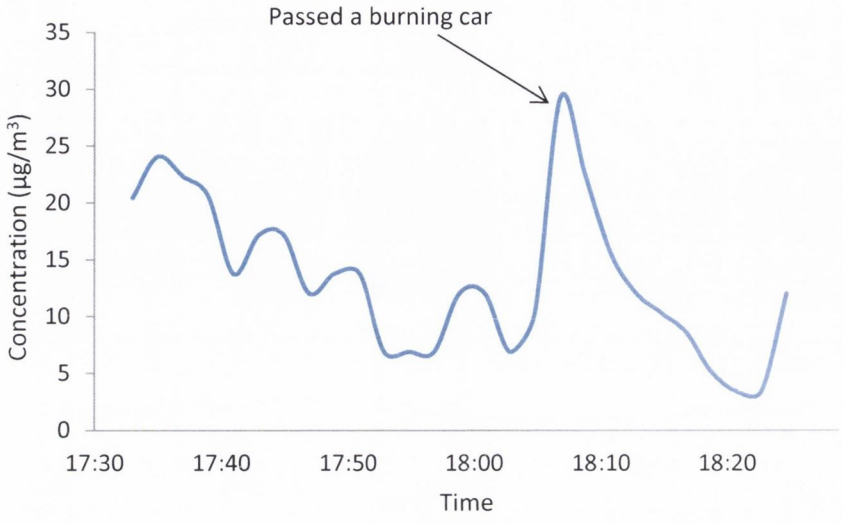


Figure 4.19: A bus commute of a volunteer showing an increase in concentration as the bus passed a burning vehicle.

The presented examples of some relatively rare or uncommon sources detected by individuals during the sampling campaign illustrate the large variability that can occur within the data. These events, and other similar ones, can cause large and sudden increases in the personal exposure concentrations of a subject within a microenvironment. Therefore, the need for proper and accurate activity diary entries is important in order to quantify the true particulate concentrations of a microenvironment. A more complete dataset for source apportionment in microenvironments, achieved through diligently completed diaries, may then aid in accurately modelling of personal exposures for the study population thereafter. However, many of the events, such as those discussed here, are responsible for only short term peaks in concentration and may have little impact on the overall 24-hour exposure concentration.

## 4.4 Descriptive Statistics of Ancillary Data

As part of the research programme it was decided to monitor in a number of locations that may have been under represented in the main dataset. The areas that were identified as perhaps requiring additional personal sampling were in shopping centres and within the homes of smokers. The additional sampling for shopping centres included both an urban and suburban shopping centre. This sampling was undertaken due to the fact that

much of the activity of 'shopping' reported in the time activity diaries was for short periods and conducted at on-street retail outlets, rather than at large retail shopping centres.

The second area requiring greater depth in the dataset was personal exposure of smokers, in particular the in-home personal exposure. The reasoning behind this was due to the relatively shallow pool of smokers that volunteered as part of the main study, and especially those who could be classed as heavy smokers. Additionally, smoking at home is often the only indoor location individuals can smoke, and by inference where ETS derived airborne particles will accumulate, due to occupational smoking laws and bans on smoking in all enclosed public areas. Therefore, information on the concentrations of PM and its residency time in the ambient air of a home can be gathered through this monitoring.

### *4.4.1 Additional smoker data sampling*

As highlighted already in Section 4.1.1, only 12% of volunteers identified themselves as a smoker, occasional smoker, or living with a smoker. However, some of these individuals did not even report any smoking events on several of their sampling days. Thus, in order to further comprehend the nature of in-home concentrations of smokers further, additional data was specifically collected from the homes of smokers over a number of days.

The additional smoker data was gathered from two separate individuals, neither of which took part in the 24-hour sampling campaign. The monitoring for these two volunteers was restricted to when they were at home on midweek days, which was most commonly in the evening time after returning for work. The volunteers were given an Aerocet-531 monitor and instructed to keep it in as close vicinity to themselves as possible at all times when monitoring. They were also presented with an activity diary where they were told to record when there was cigarette smoking and also cooking events in their homes. It was requested that the subjects monitored in-home $PM_{10}$ concentrations for three consecutive days each.

The results for the monitored days of Smoker A are shown in Figure 4.20. Smoker A was a female office worker who lived in a terraced house on the north side of the city with her husband (also a smoker) and adult son (a non-smoker). Smoker A monitored for three days, on Day 1 and 2 she began the monitoring in the evening time on returning from work. Smoking for this volunteer primarily occurred at the dining table in the kitchen, rather than in the adjacent living room.

It can be seen from Figure 4.20, that one each of these days smoking was reported on several occasions. On Day 1 cigarette smoking was reported between the hours of 9 pm and 11 pm, and the peaks from these events are evident on the graph. However, there was also an unspecified cooking event that occurred between 9 pm and 10 pm which could potentially have amplified the first peak on the graph.

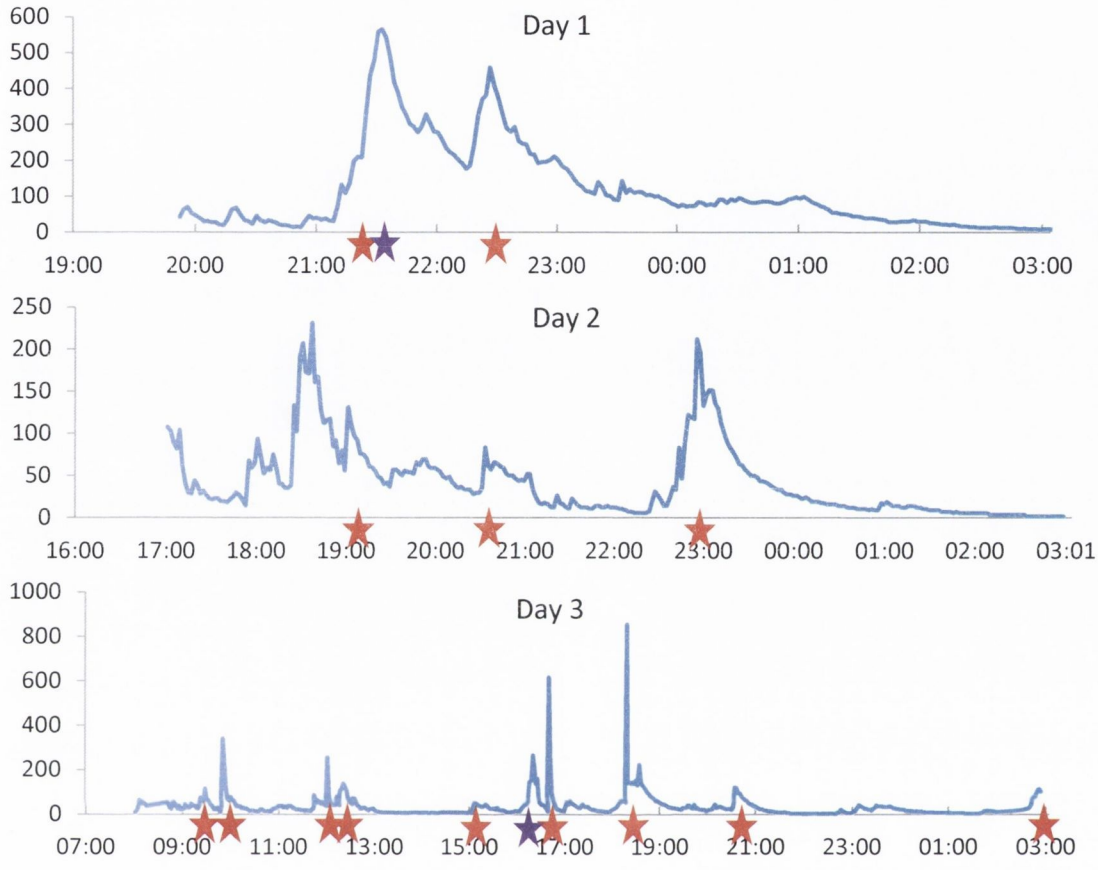


Figure 4.20: In-home time series of $PM_{10}$ concentrations ($\mu g/m^3$) for Smoker A, with all reported smoking events (red stars) and cooking events (purple stars) marked.

On Day 2, the volunteer arrived home from work earlier at approximately 5 pm. The first of several smoking events was reported between 7 pm and 8 pm that evening. However, prior to this event there was quite a large peak in the data which was unaccounted for in the diary sheet and may have been due to an omission of a cooking event, or smoking by the other smoker resident in the house. The peak concentrations were also not as high as those seen on Day 1, however, this may have been due to increased ventilation rates as the back door was left open from 5 pm to approximately 8 pm.

Finally, on Day 3 Smoker A was situated at home all day and was not at work. This resulted in far more smoking events being logged in the diary. Nearly all cigarette smoking occurring this day was carried in conjunction with the back door being opened

in the kitchen also. The majority of peak $PM_{10}$ concentrations were between 70 to 300 $\mu g/m^3$. However, the two largest peak concentrations of 614 $\mu g/m^3$ and 853 $\mu g/m^3$ happened between 5 pm and 7 pm when Smoker A relocated away from the ventilated kitchen and into the nearby living room. Also, on Day 3 there was an unspecified cooking event reported, but again the $PM_{10}$ contribution from this was hard to distinguish from the tobacco smoke.

The second smoker (Smoker B) recruited to monitor was also a female volunteer who worked in the city centre. The home of this volunteer was a detached house located in North Co. Dublin and had a total of three smokers residing there. Smoker B followed the same instructions as those given to Smoker A and commenced monitoring each day on return from work. Of the three smokers in the house it was reported in the questionnaire that Smoker B always smoked in the vicinity of the Aerocet-531, whilst of the other two smokers in the house, one occasionally smoked while in the same room but the third smoker smoked elsewhere in the house and not around the monitor during sampling.

The smoking events that the volunteer logged in the diary are shown in Figure 4.21. In contrast to Smoker A, Smoker B reported far more cigarettes being smoked, with on average 2.4 cigarettes being smoked per hour when the volunteer was active at home. On Day 1 it can be seen that there were many different smoking events and their corresponding $PM_{10}$ peaks across the day after the volunteer arrived home, with the highest peak concentration occurring just before 11 pm and reaching 603 $\mu g/m^3$. At two separate points on day one the volunteer reported leaving the house with the monitor left running - between 4 pm and just before 6 pm, and between 9 pm and 10 pm. The effect of this can be seen in the time series for Day 1, where the concentration after 4 pm reduced to approximately 10 $\mu g/m^3$, from a peak concentration of 132 $\mu g/m^3$ after the smoking event at 3.30 pm. Also, between 9 pm and 10 pm the in house $PM_{10}$ concentrations due to smoke began to dissipate rapidly.

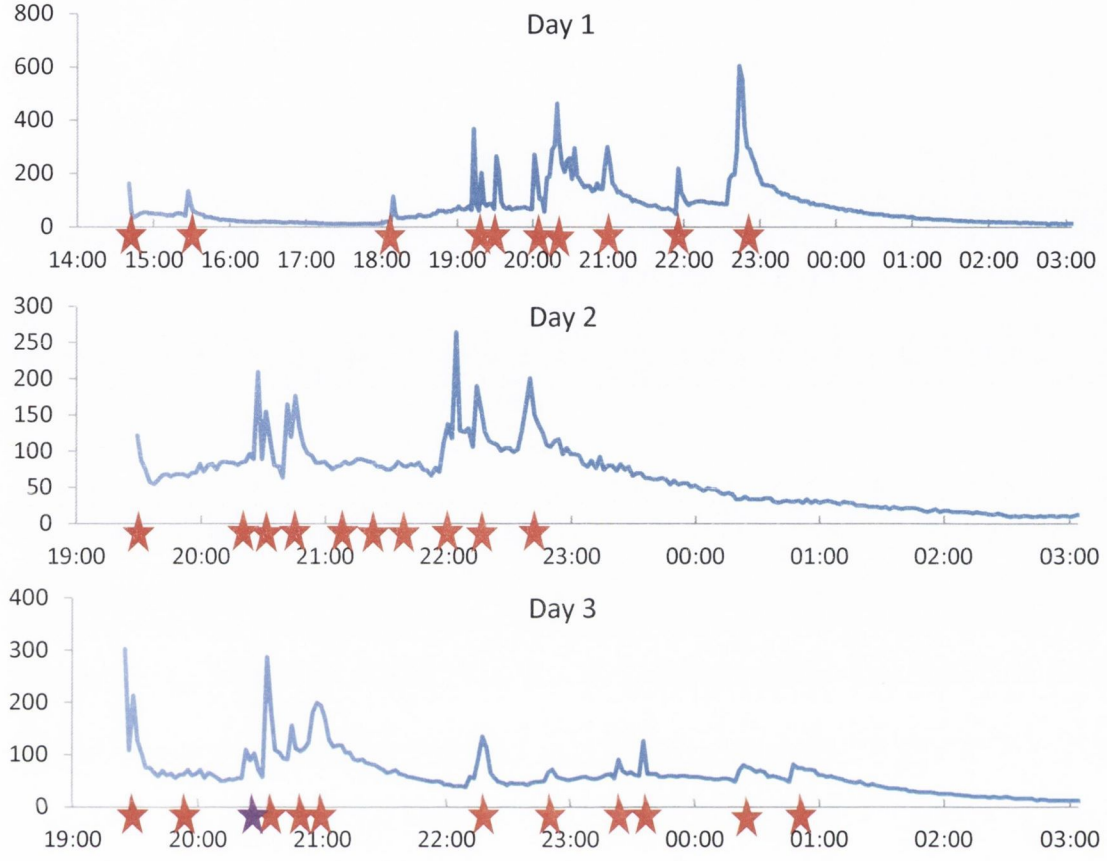


Figure 4.21: In-home time series of $PM_{10}$ concentrations ($\mu g/m^3$) for Smoker B, with all reported smoking events (red stars) and cooking events (purple stars) marked.

In the diary entry for Day 2, a dozen cigarettes were reported over a four hour period between 7 pm and 11 pm. This resulted in an almost constant personal $PM_{10}$ concentration in the vicinity of Smoker B in excess of 70 $\mu g/m^3$. The only interruption to this relatively constant high concentration was from numerous spikes in the $PM_{10}$ concentration due to additional cigarettes being lit or from puffing on a cigarette. The largest of these $PM_{10}$ concentrations recorded was 263 $\mu g/m^3$.

Day 3 of sampling by Smoker B was quite similar to Day 2, with the volunteer beginning monitoring just after 7 pm. Similarly, a dozen cigarettes were reported to have been smoked on this evening too. The peak concentration (300 $\mu g/m^3$) for this day was also at a quite similar level as Day 2. However, on Day 3 a cooking event also occurred between 8 pm and 9 pm and this was reported as pizza being cooked in the

oven. This event may have added a small amount of particulates to the ambient air but was unlikely to have contributed significantly when compared to the large amounts of tobacco smoking going on.

The descriptive statistics for each of the smokers is shown in Table 4.9. Although the graphs in Figure 4.20 and Figure 4.21 are truncated at 3 am for each sampling day, the monitoring only ceased the following morning when the volunteers were leaving for work. Thus, this simulated the equivalent 'at home' portions of a 24-hour weekday sample. The mean $PM_{10}$ concentrations shown in the table are the averages over the total sampling period, and even though they encompass both 'active at home' and 'sleeping' activities, the concentrations were still far higher than the 27 $\mu g/m^3$ population mean for 'at home'. The total in-home concentration for the study population would be even lower than this if 'at home' and 'sleeping' (10 $\mu g/m^3$) were combined. This smoker data demonstrates the large effect smoking has on indoor PM concentrations, and the potential hazard for non-smokers who are in the company of smokers for extended periods of time.

Table 4.9: Descriptive statistics for the sampling days of Smokers A and B.

| | **Day** | **Mean** ($\mu g/m^3$) | **St Dev** ($\mu g/m^3$) | **Max** ($\mu g/m^3$) | **Median** ($\mu g/m^3$) |
|---|---|---|---|---|---|
| | 1 | 81 | 107 | 566 | 40 |
| *Smoker A* | 2 | 32 | 41 | 230 | 14 |
| | 3 | 34 | 58 | 853 | 21 |
| | 1 | 61 | 77 | 603 | 34 |
| *Smoker B* | 2 | 48 | 44 | 263 | 29 |
| | 3 | 40 | 41 | 301 | 33 |

### *4.4.2 Shopping centre monitoring*

The two shopping centres selected for monitoring were the Jervis Street and Dundrum shopping centres, both of these shopping centres are shown in Figure 4.22. The Jervis Street shopping centre is located in a heavily urbanised area within Dublin city centre,

and is situated less than 400 m from heavily trafficked routes such as O'Connell Street, Parnell Street and the North Quays. In contrast, Dundrum is situated in the South Co. Dublin suburbs and has the major roadway of the M50 passing approximately 1.8 km away. However, the roads around the shopping centre can become quite congested locally at weekends.

Figure 4.22: Location of the Jervis Street (left) and Dundrum (right) shopping centres.

*4.4.2.1 Sampling procedure*

The sampling procedure involved four visits to each centre, with two visits at off peak times and two at peak times. These times were defined as between 1.30 pm and 5 pm on a Saturday for peak times, when shopping centres will most likely be busiest, and between 1.30 pm to 4.30 pm on a weekday (Mon-Thurs) for off peak time. The off peak time was chosen as the most likely time shopping centres would be quiet and avoided possible increased footfall from lunchtime and after work shoppers.

The experimental sampling for the shopping centre consisted of samples being taken at seven different locations inside the centres. These included the ground floor and first floor atriums, the pedestrian, traffic and car park entrances, and finally inside a clothing shop and supermarket. Each sample at a location lasted for approximately 10 to 12 minutes, in order to establish a stable average concentration for each place.

The locations were chosen as they were deemed the most likely areas an individual might pass through whilst on a shopping excursion. Sampling was conducted first just inside the entrance from a pedestrianised area; this was Mary Street in the case of Jervis and the outdoor pedestrianised plaza for Dundrum. Each shopping centre had a large underground car park associated with it, and thus sampling was also conducted at these entrances from the car parks. Samples were also taken by an entrance close to outdoor traffic or public road for both. This included the entrance beside Jervis Street which ran by the city centre shopping centre, however, no street ran directly past Dundrum so sampling was conducted at the entrance nearest to a large outdoor car park. Finally, the two retail units chosen for monitoring were a supermarket and a clothing shop, while both levels of the atrium were monitored in each centre too.

#### *4.4.2.2 Monitoring results*

The results from the samples taken at the Dundrum shopping centre are shown in Table 4.10. As can be seen from the table, the overall average $PM_{10}$ concentrations taken over the four visits to the shopping centre ranged from 15 $\mu g/m^3$ to 25 $\mu g/m^3$. From inspection of the data in Table 4.10, it is clear that the highest $PM_{10}$ concentrations were consistently found to be in the vicinity of the car park entrance (range of 24 to 42 $\mu g/m^3$) and the traffic entrance (range of 22 to 28 $\mu g/m^3$) of the shopping centre. The $PM_{10}$ concentration data gathered from other locations, such as around the atriums, pedestrian entrance and shops were generally lower. This was to be expected as the entrances in close proximity to trafficked areas would tend to have higher particulate pollution as a result.

Table 4.10: Comparison of peak and off-peak $PM_{10}$ concentrations ($\mu g/m^3$) for various locations in Dundrum shopping centre.

| | **Off-peak time** | | **Peak time** | |
|---|---|---|---|---|
| | Visit 1 *Mean (SD)* | Visit 2 *Mean (SD)* | Visit 1 *Mean (SD)* | Visit 2 *Mean (SD)* |
| Car park entrance | 24 (10) | 42 (9) | 35 (4) | 34 (6) |
| Clothes shop | 5 (3) | 14 (11) | 19 (3) | 15 (5) |
| 1st Floor Atrium | 11 (1) | 17 (1) | 25 (7) | 25 (4) |
| Ground Floor Atrium | 16 (4) | 11 (2) | 21 (1) | 19 (1) |
| Pedestrian entrance | 16 (5) | 30 (4) | 16 (3) | 30 (8) |
| Supermarket | 11 (9) | 15 (4) | 22 (4) | 28 (10) |
| Traffic entrance | 26 (13) | 22 (3) | 27 (5) | 28 (3) |
| Overall | 15 (10) | 22 (12) | 24 (7) | 25 (9) |

The results from $PM_{10}$ monitoring in the Jervis Street shopping centre are shown in Table 4.11. The overall $PM_{10}$ concentrations over the four visits displayed greater variability than in Dundrum, with a range for the averages of 16 to 50 $\mu g/m^3$. The highest mean concentrations for the monitoring periods were on off-peak time Visit 1 and peak time Visit 2. On the occasion of off-peak time Visit 1, the highest concentration was found to be at the pedestrian entrance at Mary Street (119 $\mu g/m^3$), while ground floor atrium also had a high $PM_{10}$ concentration (66 $\mu g/m^3$). Less surprisingly, the traffic and car park entrances had relatively high $PM_{10}$ concentrations also (51 and 41 $\mu g/m^3$, respectively).

Table 4.11: Comparison of peak and off-peak $PM_{10}$ concentrations ($\mu g/m^3$) for various locations in the Jervis Street shopping centre.

| | **Off-peak time** | | **Peak time** | |
|---|---|---|---|---|
| | Visit 1 *Mean (SD)* | Visit 2 *Mean (SD)* | Visit 1 *Mean (SD)* | Visit 2 *Mean (SD)* |
| Car park entrance | 41 (23) | 17 (6) | 23 (4) | 37 (2) |
| Clothes shop | 10 (4) | 14 (4) | 15 (4) | 35 (11) |
| 1st Floor Atrium | 37 (3) | 18 (2) | 32 (13) | 35 (1) |
| Ground Floor Atrium | 66 (15) | 12 (5) | 17 (4) | 27 (4) |
| Pedestrian entrance | 119 (93) | 23 (6) | 37 (4) | 61 (15) |
| Supermarket | 21 (13) | 10 (5) | 12 (7) | 10 (5) |
| Traffic entrance | 51 (29) | 15 (4) | 7 (1) | 68 (14) |
| Overall | 50 (48) | 16 (6) | 20 (12) | 41 (22) |

On the peak time Visit 2 the highest concentration was observed at the entrance adjacent to traffic (68 $\mu g/m^3$), but yet again the pedestrian entrance also had high $PM_{10}$ concentration levels associated with it (61 $\mu g/m^3$). The large personal exposure concentrations found at the pedestrian entrance can be explained by the loitering of smokers in this location. A number of smokers were observed just outside the entrance and evidently some of the secondary smoke was migrating inside the entrance. On the other two monitoring days (off-peak time Visit 2 and peak time Visit 1) the traffic entrance concentrations were quite low and this may have been due to local low local traffic levels or climatic conditions. Over the four monitoring periods the lowest concentrations in the shopping centre were generally to be found in the clothing store (range of 10 to 35 $\mu g/m^3$) and supermarket (range of 10 to 21 $\mu g/m^3$). This was similar to the situation found in the Dundrum town centre also.

Although the data was collected from the shopping centres on just eight separate occasions, it does give an indication of the concentrations of $PM_{10}$ that are found in large shopping complexes. The data display a large amount of variability, and personal exposures would seem to vary according to where in the complex a subject was located. However, as most individuals spend the majority of time inside atriums and shops rather

than loitering at entrances (apart from some smokers), the concentrations in these areas would be more pertinent to personal exposure. Thus, using PM data based on these interior concentrations may prove useful for exposure modelling of this microenvironment.

### *4.4.3 Taxi monitoring*

In addition to the overall sampling campaign, data was also gathered for an alternative occupation for use as a comparison to the occupational exposure of the office workers. This consisted of the recruitment of a number of Dublin City taxi drivers to gather data whilst working. Each of these drivers was presented with an Aerocet-531 and Garmin GPS device and sampled according to the protocol laid down in Section 3.2.5. A temperature and relative humidity probe was also attached to the Aerocet-531 monitors, except in the case of one driver when the probe was unavailable for use.

In total four different taxi drivers were recruited to gather data and were asked to sample for five different work shifts each. The drivers were recruited through the contacting of several different taxi firms, and were all middle-aged males. Sampling was conducted over a number of weeks from the end of August to the beginning of November 2011.

Drivers 1, 2 and 4 all successfully completed the sampling target of five different work shifts, with both Drivers 2 and 4 completing additional sampling days also. However, Driver 3 could only complete three samples unfortunately, due to sampling and driver time constraints. In total, the drivers monitored their in-vehicle personal exposure for 21 different work shifts. The mean personal exposure for each driver work shift is illustrated in Figure 4.23, while detailed descriptive summary statistics of each of the work shifts from the driver sampling campaign can be seen in Table 4.12.

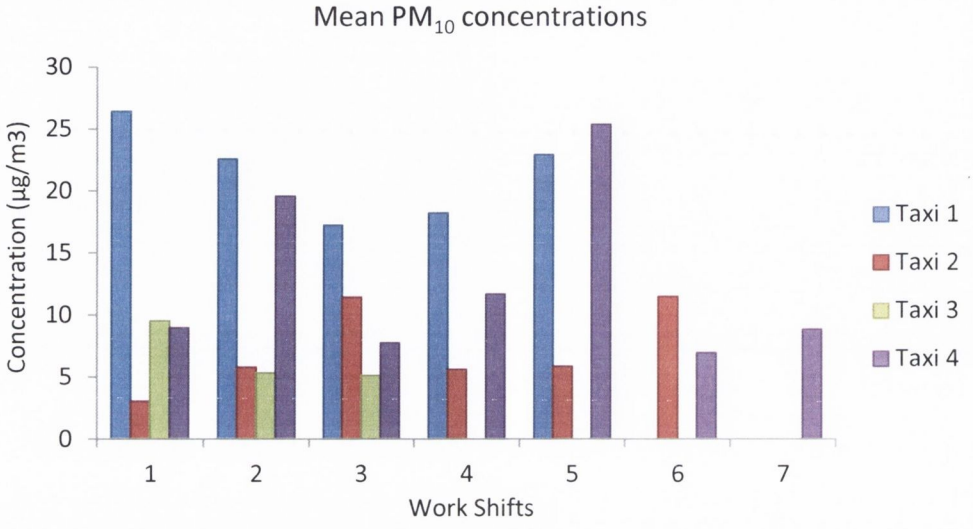


Figure 4.23: Mean in-car $PM_{10}$ concentrations ($\mu g/m^3$) for each driver work shift.

The overall average $PM_{10}$ personal exposure concentrations for each driver, along with their mean sampling durations are shown in Table 4.13. Driver 1 had an overall mean $PM_{10}$ concentration over the entire sampling period of 21 $\mu g/m^3$ with a standard deviation of 36 $\mu g/m^3$, while the mean duration spent sampling while working was 6 hrs 40 mins. In contrast, the mean $PM_{10}$ concentration experienced by Driver 2 was far lower, with an average personal exposure to $PM_{10}$ of just 7 $\mu g/m^3$ with a standard deviation of 9 $\mu g/m^3$. Driver 2 also had the shortest mean sampling duration amongst the four drivers, sampling for an average duration 6 hrs 04 mins.

Table 4.12: Summary of Taxi driver shift times, $PM_{10}$ concentrations ($\mu g/m^3$) and in-vehicle environmental conditions.

| Driver | Shift # & Day | Start | Finish | Time mins | Mean $\mu g/m^3$ | Std Dev $\mu g/m^3$ | R.H. % |
|---|---|---|---|---|---|---|---|
| 1 | 1 - Mon | 09:31 | 12:51 | 200 | 26 | 26 | 54 |
| | 2 - Tues | 08:22 | 13:41 | 320 | 23 | 49 | 46 |
| | 3 - Weds | 08:07 | 16:38 | 512 | 17 | 33 | 51 |
| | 4 - Thurs | 08:22 | 16:29 | 488 | 18 | 32 | 45 |
| | 5 - Fri | 08:24 | 16:25 | 482 | 23 | 34 | 46 |
| 2 | 1 - Tues | 02:37 | 12:30 | 594 | 3 | 5 | n/a |
| | 2 - Weds | 02:54 | 07:58 | 306 | 6 | 8 | n/a |
| | 3 - Thurs | 03:33 | 07:45 | 254 | 11 | 13 | n/a |
| | 4 - Thurs | 22:03 | 02:46 | 284 | 6 | 7 | n/a |
| | 5 - Fri | 22:31 | 01:44 | 194 | 6 | 7 | n/a |
| | 6 - Sat | 11:39 | 20:50 | 552 | 12 | 10 | n/a |
| 3 | 1 - Weds | 09:16 | 15:03 | 348 | 10 | 6 | 29 |
| | 2 - Thurs | 05:12 | 13:47 | 516 | 5 | 6 | 49 |
| | 3 - Thurs | 14:46 | 23:18 | 512 | 5 | 7 | 43 |
| 4 | 1 - Thurs | 04:48 | 14:38 | 458 | 9 | 10 | 48 |
| | 2 - Fri | 12:40 | 23:02 | 552 | 20 | 22 | 37 |
| | 3 - Sat | 13:17 | 02:15 | 356 | 8 | 15 | 59 |
| | 4 - Mon | 02:30 | 08:50 | 382 | 12 | 12 | 35 |
| | 5 - Fri | 03:24 | 12:35 | 552 | 25 | 16 | 57 |
| | 6 - Sat | 04:14 | 13:06 | 532 | 7 | 8 | 46 |
| | 7 - Thurs | 03:03 | 11:12 | 490 | 9 | 8 | 45 |

Over the three different sampling days Driver 3 recorded the lowest mean $PM_{10}$ personal exposure concentration of 6 $\mu g/m^3$, with a standard deviation of 7 $\mu g/m^3$. This driver also spent on average 7 hrs and 39 mins sampling on working days. Finally, Driver 4 had an average concentration of 13 $\mu g/m^3$ with a standard deviation of 16 $\mu g/m^3$ over the seven work shifts in which he sampled. Driver 4 also recorded the longest average length of work shift of 7 hrs and 55 mins.

Table 4.13: Average $PM_{10}$ exposure and work shift durations for all drivers over their respective sampling periods.

| Driver | Overall Mean Concentration ($\mu g/m^3$) | Standard Deviation ($\mu g/m^3$) | Mean Sampling Duration (mins) |
|---|---|---|---|
| 1 | 21 | 36 | 400 |
| 2 | 7 | 9 | 364 |
| 3 | 6 | 7 | 459 |
| 4 | 13 | 16 | 475 |

Figure 4.24: GPS tracks of all four taxi drivers (D1 - Blue; D2 - Green; D3 - Turquoise; D4 - Red).

The taxi data was also broken down into categories based on the locations obtained from the GPS receiver, and the tracks for each driver are displayed in Figure 4.24. The Aerocet-531 data was broken up according to when each driver was actively working in

the city centre or outside the city centre. This city centre area can be seen in Figure 4.25 and was defined on the north-side as the area enclosed by the Conyngham and North Circular Roads as far as the Samuel Beckett Bridge over the Liffey, and the area enclosed on the south-side by the South Circular and Suir Roads, as well as the Grand Canal as far east as Grand Canal Dock. This was the area identified as the most urbanised in the city, and thus potentially the most susceptible to higher concentrations of PM from traffic emissions. Once this area was defined the GPS track data could be visually inspected and the corresponding data values assigned to each group depending on whether the GPS track location was inside or outside this cordon.

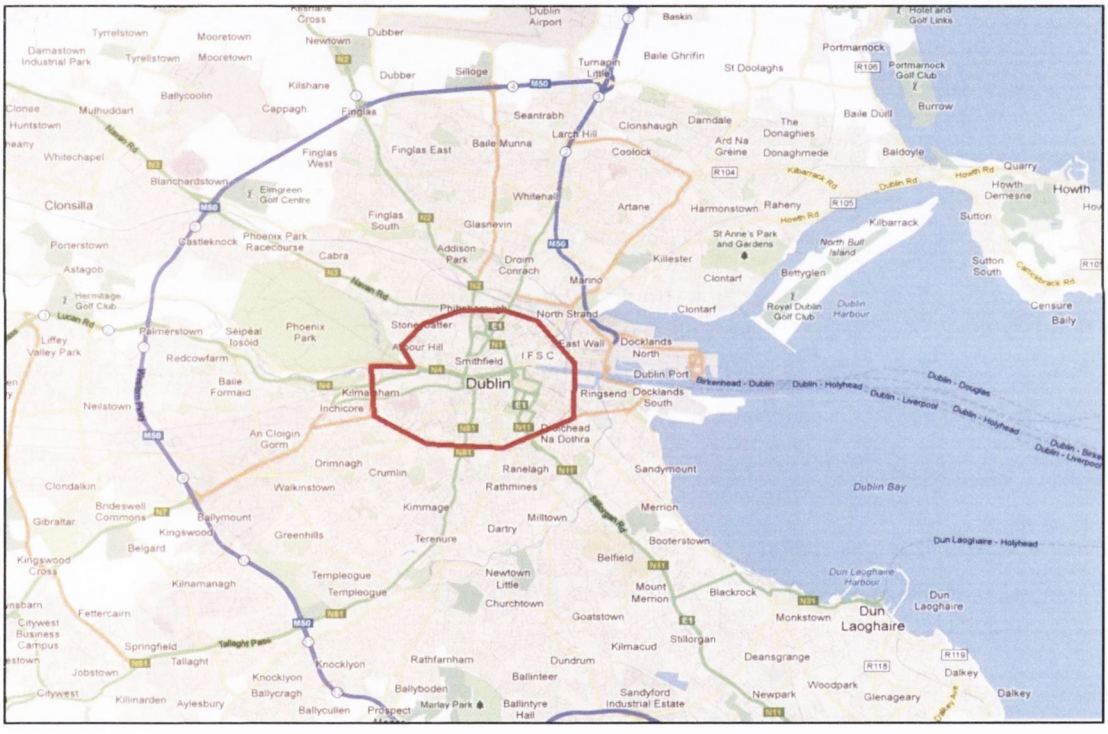
Dublin
Dublin Bay
Dun Laoghaire
Howth
Clonsilla
Blanchardstown
Finglas
Ballymun
Glasnevin
Drumcondra
Phibsborough
North Strand
Docklands
Ringsend
Irishtown
Sandymount
Merrion
Booterstown
Blackrock
Monkstown
Dalkey
Killiney
Ballsbridge
Rathmines
Ranelagh
Crumlin
Drimnagh
Walkinstown
Kimmage
Terenure
Templeogue
Kilnamanagh
Tallaght
Clondalkin
Lucan
Palmerstown
Chapelizod
Phoenix Park
Cabra
Glasnevin
Finglas East
Finglas West
Whitehall
Santry
Coolock
Darndale
Clontarf
Raheny
Howth
Sutton
Baldoyle
Portmarnock
Malahide
Swords
Lusk
Rush
Skerries
Balbriggan
Donabate
Portrane
Kinsaley
Seatrabh
Baile Munna
Larch Hill
Artane
Harmonstown
Killester
Marino
Drumcondra
Addison Park
Castleknock
Porterstown
Astagob
Liffey Valley Park
Redcowfarm
Baile Formaid
Neilstown
Inchicore
Kilmainham
Smithfield
IFSC
East Wall
Docklands North
Docklands South
Dublin Port
Ringsend
Irishtown
Sandymount
Merrion
Booterstown
Blackrock
Monkstown
Dun Laoghaire

with the driver's mean $PM_{10}$ concentrations while at the rank, which ranged from33 to 80 $\mu g/m^3$, over the four shifts.

Drivers 2 and 3 tended to spent very little of their shift times idling at taxi ranks. Driver 2 spent between 15 and 28% of the shift time at a rank, while Driver 3 often spent no time at all at a rank bar one shift were 14% of the time was spent at a rank. As can be seen from the table, Driver 2 had very low $PM_{10}$ concentrations both inside and outside the city centre area, with his time fairly evenly split between the two. These concentrations were far lower than Driver 1 most likely because Driver 2 tended to work in the early hours of the morning (see Table 4.12) when traffic levels would be very low. The hours worked by Driver 3 were a mixture of peak and off-peak traffic hours, but the concentrations experienced were relatively low. However, this may have been due to the percentage of time spent working outside the city centre area which was 74%, 85%, and 68% for all three work shifts shown in Table 4.14.

Table 4.14: Mean $PM_{10}$ concentrations ($\mu g/m^3$) while drivers are inside and outside the city centre area, and stationary at taxi ranks.

| | | Inside | | | Outside | | | At Taxi Rank | | |
|---|---|---|---|---|---|---|---|---|---|---|
| **Driver** | **Shift** | **Mean** | **St Dev** | **Time %** | **Mean** | **St Dev** | **Time %** | **Mean** | **St Dev** | **Time %** |
| 1 | 2 | 14 | 25 | 33 | 22 | 17 | 34 | 32 | 80 | 33 |
| | 3 | 16 | 21 | 39 | 11 | 12 | 16 | 21 | 45 | 45 |
| | 4 | 13 | 24 | 33 | 19 | 39 | 23 | 21 | 33 | 44 |
| | 5 | 23 | 31 | 38 | 28 | 40 | 15 | 21 | 34 | 47 |
| 2 | 3 | 14 | 18 | 22 | 11 | 12 | 63 | 8 | 5 | 15 |
| | 4 | 5 | 5 | 50 | 7 | 7 | 33 | 7 | 10 | 17 |
| | 5 | 5 | 5 | 38 | 10 | 8 | 34 | 2 | 5 | 28 |
| 3 | 1 | 9 | 4 | 12 | 9 | 6 | 74 | 11 | 5 | 14 |
| | 2 | 2 | 1 | 15 | 6 | 6 | 85 | 0 | 0 | 0 |
| | 3 | 5 | 4 | 32 | 5 | 8 | 68 | 0 | 0 | 0 |
| 4 | 1 | 7 | 2 | 4 | 14 | 10 | 61 | 1 | 2 | 35 |
| | 4 | 16 | 14 | 31 | 13 | 11 | 39 | 6 | 6 | 30 |
| | 5 | 33 | 15 | 14 | 30 | 18 | 32 | 21 | 14 | 54 |
| | 7 | 8 | 9 | 9 | 8 | 7 | 46 | 10 | 9 | 44 |

An important influencing factor on Drivers 2 and 3 work time personal concentrations was the effect of the diurnal profile of $PM_{10}$. Ambient $PM_{10}$ concentrations tend to be higher during daytime hours when there are a large numbers of vehicles on the road, as people go about their daily routine. The high concentrations then decrease overnight as the amount of transport and other emissions decrease. In the case of Driver 2, nearly all samples were obtained during late night and early mornings, while some of Driver 3's samples were also obtained at these times. Thus, the relatively low concentrations experienced by both drivers maybe somewhat explained by the diurnal $PM_{10}$ pattern.

Driver 4 was another driver that tended to spend much of the shift times outside the city centre. Of the four separate taxi shifts shown in the table, only once for shift number four did the driver spend a relatively large proportion of time (31%) within the city centre area. Much of this driver's time was spent doing airport runs and also waiting for long periods for a fare in Dublin airport. This is reflected in the percentage of time spent 'at Taxi rank', whereby 35%, 30%, 54% and 44% of the total work shifts shown were spent waiting for a fare. There was no real discernible difference between the outside city and inside city concentrations for this driver. However, at times the at rank concentration fell to low levels and this may have been due to the driver parking and exiting the vehicle at the Dublin airport taxi waiting facility.

## 4.5 Summary

The following paragraphs provide a summary of the results discussed in this chapter. Firstly, with regard to the time-activity patterns of the subjects recruited, it was found that the study population spent 92% of their time indoors. The other 8% of time was spent either in enclosed transit or else outside. The majority of the time spent indoors was spent in the microenvironment of the subject's residence, and time spent there was split almost two thirds in favour of the activity of sleeping with one third of the time whereby the subject was active in the home. In addition to the at home microenvironment, a large proportion of the study population's day was also spent at work. Other microenvironments such as commuting, shopping, recreation, etc., were responsible for only small portions of the daily routine of the study population.

The highest $PM_{10}$ personal exposure concentration amongst the various microenvironments was found to occur while volunteers were participating in the activity category of recreation or sport. This was followed by locations such as cafés and restaurants along with public houses, where there was a high possibility of sources such as smoking and cooking contributing to the PM concentrations within these microenvironments. Of the two microenvironments that comprise the overwhelming majority of time during a 24-hour period, it was at work that was discovered to have the higher concentrations of $PM_{10}$ than found in the homes of the subjects.

Among the transport modes it was found that the bus had the highest average personal exposure and this was followed by personal exposure while travelling by car. The outdoor travel mode walking followed and this personal exposure was slightly greater than travel by train. The two lowest personal concentrations were found while cycling and using the tram.

The problems associated with indoor cooking events were highlighted also in the chapter. The difficulties associated with trying to calibrate the instrumentation were discussed, and these included the short duration of the cooking events, the limitations of the equipment, as well as the mix of cooking methods. The problems were compounded by the often poorly reported details on the types of cooking used as well as the in-situ ventilation conditions. Thus, the cooking peaks from the primary dataset were removed due to these issues.

The variability of personal exposure over the course of a day for subjects was illustrated with the examples of events given such as incense burning and deodorant spraying. Events such as these can cause short term peaks in personal exposure concentrations, while some of these events can cause elevated $PM_{10}$ concentrations to linger in the home sometime after the event itself. This emphasises the need for accurate diary reporting by personal exposure study volunteers in order to correctly identify and apportion emissions from these sources.

Extra sampling was also undertaken to compliment the data collection of the main study. This was done to gather information on underrepresented microenvironments, as well as other occupations to compare with the personal exposure concentrations of office workers. The additional data collection at shopping centres found that highest concentrations occurred near the entrances, where particulates from traffic and smokers were able to ingress. However, the $PM_{10}$ concentrations were lower in the atriums and shops once inside, the places individuals would spend the most time.

The extra monitoring undertaken also highlighted the variability in $PM_{10}$ concentrations of a different type of occupation from office worker. The taxi data gave an insight into the variable concentrations that may be encountered amongst drivers, with those who work daytime hours mainly in the city centre being exposed to greater concentration than those who worked in the early hours of the morning and outside the city. However, as the sample set was relatively small, further investigation of this occupational group would be required to confirm this.

Finally, the additional in-home sampling of the smokers demonstrated the large concentrations due to ETS that people may be exposed to while in the company of smokers. This may have a large effect on an individual's overall 24-hour personal exposure depending on the duration they are exposed to this source in a microenvironment. The collection of this data can may be useful when modelling the exposure for subjects, and compliment the smoker data gathered in the primary study.

# Chapter 5

Dosimetry

# 5 Dosimetry

## 5.1 Introduction

The respiratory tract is an important route for hazardous airborne pollutants to enter the human body. The term particle dosimetry refers to the characterisation of deposition, translocation, clearance, and retention of particles and their constituents within the respiratory tract and extra-pulmonary tissues (US EPA, 2009). Traditionally, dosimetry referred to the process or method of measuring the dosage of ionising radiation. This was particularly important for workers who may be exposed to radionuclides and other hazardous airborne materials. However, dosimetry can also be applied to the general population to quantify dose from airborne pollutants such as particulates and gases.

Whether airborne particles are inhaled and subsequently deposited and retained in the respiratory tract of a person depends on a number of physical, chemical, and biological factors. The factors that determine how inhalable a particle is will include its size, density, and hygroscopicity. Physical and chemical properties will also determine the penetration of inhaled particles. These will have a bearing on the sites of deposition, along with the retention times or rates of clearance, and also the rates of absorption into the blood and translocation to other tissues. Physiological factors are also an important determinant; this includes breathing rate at time of intake and whether breathing is through the mouth or nose. The combination of all these factors will determine the dose received by an individual (ICRP, 1994).

In order to quantify dose in the context of this study, a unique approach in the realm of 24-hour multiple microenvironmental personal exposure studies was taken. The 24-hour dose for each subject who sampled over the course of this study was calculated using a specially developed human respiratory tract model. The model itself was coded and implemented for use using the software package Matlab (see Appendix E), and is discussed in detail in the proceeding subsections. The end product of this endeavour enabled the dose of each subject to be obtained over multiple activities and microenvironments. The dose uptakes could then be compared to the personal exposure

concentrations, and activities or microenvironments with potentially the greatest significance from a health perspective could be identified.

## 5.2 ICRP Model Background

The human respiratory tract model was developed by the International Commission on Radiological Protection (ICRP). The model was first used in *ICRP Publication 30* to calculate the radiation doses to the respiratory tract of workers resulting from the inhalation of airborne radionuclides. The initial model developed has subsequently been updated and revised, with the latest incarnation reported in *ICRP Publication 66*. This particular revision was motivated by the availability of increased knowledge of the anatomy and physiology of the respiratory tract and of deposition, clearance, and biological effects of inhaled radioactive particles, and finally, by greater dosimetry requirements.

According to the ICRP, there are two primary applications for which the model is intended. Firstly, its widest application was intended to be for the calculation of effective dose per unit of exposure and per unit of inhaled radioactivity to populations with similar characteristics, and the dose of individuals. The results of which can then be used in the calculation of standards for environmental and occupational exposures. The second application is for the evaluation of doses to persons who have been exposed, and for whom monitoring data are available.

## 5.3 Respiratory Tract Morphology

The characteristics of inhaled and exhaled air are greatly influenced by the morphology of the respiratory tract, which causes various alterations in pressure, flow rate, direction, and humidity as air moves in and out of the lungs. The overall result of which, together with the varying tissue surfaces encountered by inhaled air, greatly influences the rates and sites of deposition and penetration of entrained particles. This means that for the formulation of any particle dosimetry model, both the morphology and the dimensions of the respiratory tract (the morphometry) are essential elements.

The basic structure of the human respiratory tract is shown in Figure 5.1. The ICRP dosimetric model considers the respiratory tract as four anatomical regions, the first of which consists of the extrathoracic region (ET), comprising the anterior nose ($ET_1$) and the posterior nasal passages, larynx, pharynx, and mouth ($ET_2$). The second region is the bronchial region (BB), which consists of the trachea and bronchi from which deposited material is cleared by ciliary action. This action works by mucus lining the trachea to trap inhaled foreign particles that the cilia then move upward toward the larynx and then the pharynx, where it can be either swallowed into the stomach or expelled as phlegm. The third region is the bronchiolar region (bb), consisting of the bronchioles and terminal bronchioles. The final region is called the alveolar-interstitial region (AI), and this is made up of bronchioles with some alveoli apposed, the alveolar ducts and sacs with their alveoli, and the interstitial connective tissue. All three BB, bb and AI regions are components of the larger area known as the tracheobronchial region (TB).

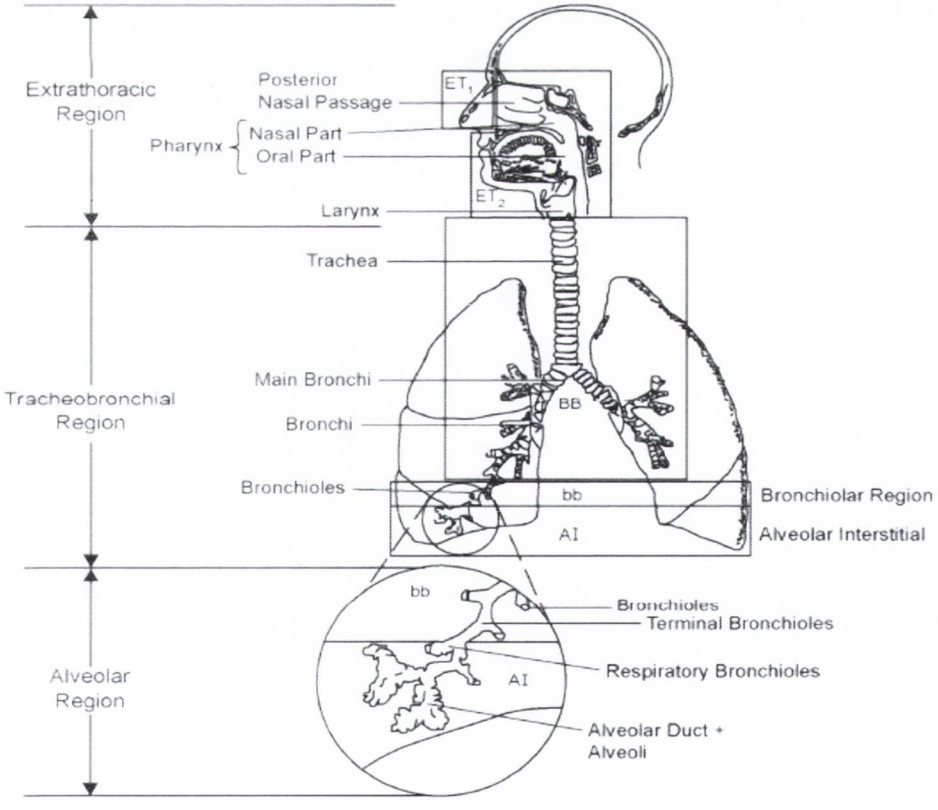


Figure 5.1: The anatomical regions of the human respiratory tract (ICRP, 1994).

The structure of the airway anatomy changes significantly with distal progression into the lower respiratory tract. As already alluded to, in the bronchi there is a thick liquid lining and mucociliary clearance rapidly moves deposited particles toward the mouth. In this region only highly soluble materials moving from the air into the liquid layer will have systemic access via the blood. However, with distal progression down into the lower respiratory tract the protective liquid lining diminishes and clearance rates slow. It is in these lower regions that soluble compounds and some poorly soluble ultra-fine particles (UFPs) may cross the air-liquid interface to enter the tissues and the blood, especially in the alveolar (AI) region. The structure of lower airways with progression from the large airways to the alveolus is shown in Figure 5.2.

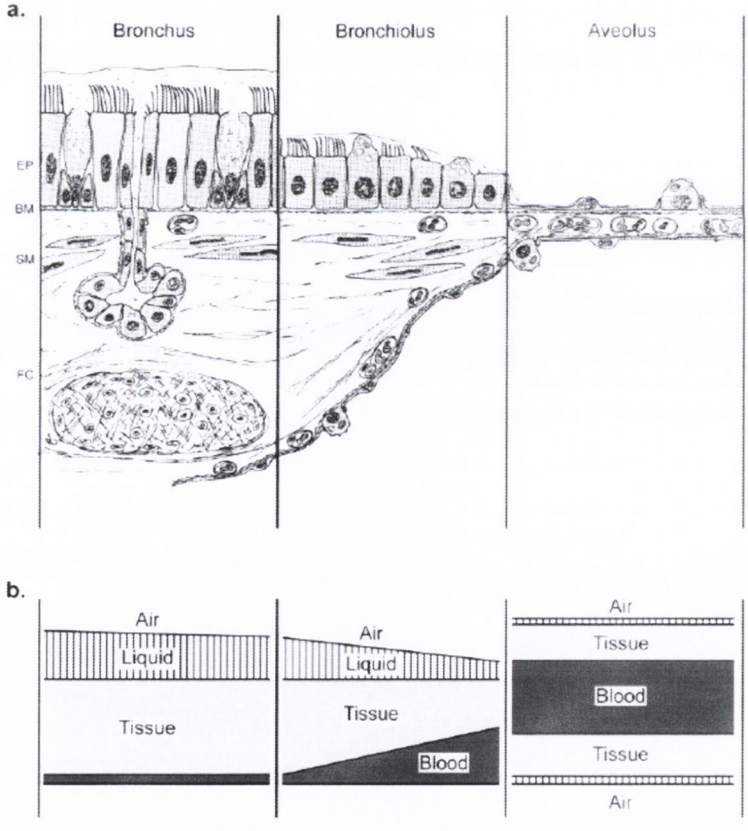


Figure 5.2: Panel (a) illustrates basic airway anatomy. Structures are epithelial cells, EP; basement membrane, BM; smooth muscle cells, SM; and fibrocartilaginous coat, FC. Panel (b) illustrates the relative amounts of liquid, tissue, and blood with distal progression (US EPA, 2009).

### *5.3.1 Deposition of particles*

The fate of an inhaled particle may be that it is either exhaled or else it gets deposited in the ET, TB, or alveolar region. A particle is deposited when it moves away from the airway lumen to the wall of the airway. The deposition of particles in the lung is mainly governed by three mechanisms which are diffusion, impaction, and sedimentation. Some of the factors that these depend on are the particle size, the route of breathing (nasal or oronasal), tidal volume (VT), breathing frequency (f) and respiratory tract morphology.

The model used an empirical method to model particle deposition in the extrathoracic airways. The deposition efficiencies were determined experimentally for adult males and were sealed on the basis of anatomical and physiological differences to predict deposition in women and children. In the thoracic airways a theoretical model for particle deposition was used to calculate deposition in each of the BB, bb, and AI regions, as well as to quantify the effects of a subject's lung size and breathing rate. The regional distributions were calculated for aerosols having log-normal particle size distributions.

## 5.4 Form of the Deposition Model

The ICRP model was designed to be straightforward whilst also accurate to apply. To achieve this, a semi-empirical approach was taken to describe values of regional deposition derived from experiments and theory by relatively simple algebraic approximations. For the model, each region of the respiratory tract is represented by an equivalent particle filter that acts in series and can be seen in Figure 5.3. The empirical filtration approach and the underlying mathematical equations are summarised in the following subsections.

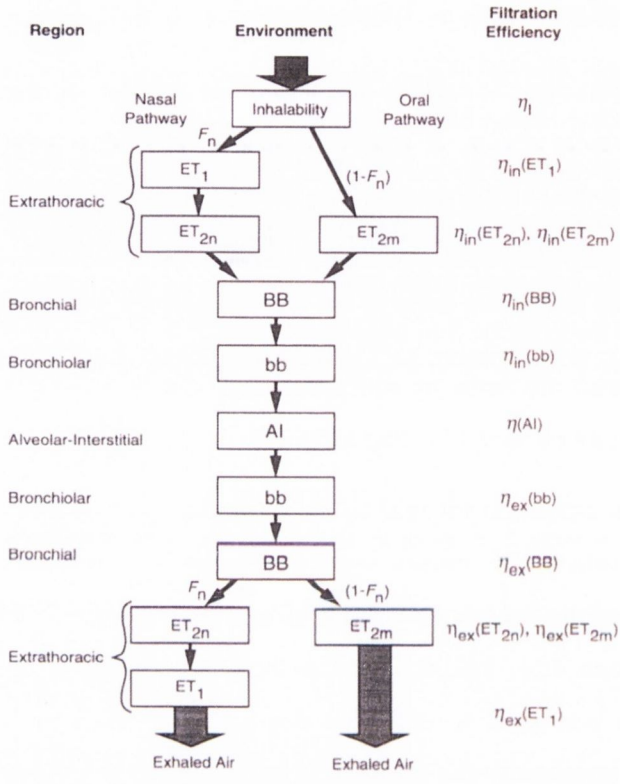


Figure 5.3: Empirical representation of inhalability of particles and their deposition in the extrathoracic, bronchial, bronchiolar, and alveolar-interstitial regions of the respiratory tract during continuous cyclic breathing by transport through a series of filters (ICRP, 1994).

### *5.4.1 General formulation of particle deposition from tidal airflow*

Within the empirical model each breath is represented by a tidal flow of air that carries particles through each anatomical region. The anatomical region in turn is represented by one or more filters in series, each of which has two characteristic parameters consisting of its overall efficiency for removing airborne particles and its volume. The fraction, $\phi_j$, of the tidal air that reaches the $j$th filter on inhalation is shown in Eqn. 5.1.

$$\phi_j = 1, \quad if\ j = 0$$

$$\phi_j = 1 - \frac{1}{V_T}\sum_{jj=0}^{j-1} v_{jj}, \quad if\ j \leq j \leq (N+1)/2 \qquad \text{Eqn. 5.1}$$

Where $V_T$ is the volume of tidal flow and $v_{jj}$ is the volume of a preceding filter, $jj$, and $N$ is the number of deposition sites in the respiratory tract for the breathing cycle (i.e. the number of filters).

On inhalation a successively smaller fraction of the inspired air (denoted $\phi$) passes through each filter. It is the cumulative volume of the preceding filters that determines $\phi$. The volume of the air that passes through a filter on inhalation is equal to the volume returning through each filter on exhalation, and this exhalation volumetric fraction $\phi$ is given by Eqn. 5.2.

$$\phi_j = \phi_{N-j+1}, \quad \text{for } j = (N+3)/2, N. \qquad \text{Eqn. 5.2}$$

This system of sequential filters means the output of the $j$th filter provides the input to the $(j + 1)$th filter. The fraction of particles entering the filter and deposits in it is known as the filtration efficiency $\eta_j$. The filtration efficiency can also be described as the complement of the filter output divided by its input (Eqn. 5.3).

$$\eta_j = 1 - I_{j+1}/I_j \qquad \text{Eqn. 5.3}$$

When the volumetric factor ($\phi$), and the efficiencies of the preceding filters in the series, the fraction $DE_j$ of the number of particles, $I_0$, sampled from the environment by the initial filter that is deposited in the $j$th filter, is given by Eqn. 5.4

$$DE_j = \eta_j \phi_j \prod_{jj=0}^{j-1} (1 - \eta_{jj}) \qquad \text{Eqn. 5.4}$$

$\phi_{jj}$ can be replaced by $\xi_{jj}$, which is defined as the quotient $\phi_{jj}/\phi_{jj-1}$, thus $\phi_{jj}$ becomes

$$\prod_{jj=1}^{j} \xi_{jj} \qquad \text{Eqn. 5.5}$$

And the expression for $DE_j$ becomes:

$$DE_j = \eta_j \left( \prod_{jj=1}^{j} \xi_{jj} \right) \prod_{jj=0}^{j-1} (1 - \eta_{jj}) \qquad \text{Eqn. 5.6}$$

The fractional deposition can be expressed recursively with both the volumetric factor $\phi$, and the efficiencies of the preceding filters in series taken into account, giving the following expression (Eqn. 5.7).

$$DE_j = DE_{j-1} \eta_j \xi_j \left( \frac{1}{\eta_{j-1}} - 1 \right), \text{ for } j = 1, \text{N} \qquad \text{Eqn. 5.7}$$

Where $N$ is the number of filters in series, excluding the initial (zero) filter. The recursive relationship is then used to evaluate the fractional deposition in each region of the respiratory tract for inhalation and exhalation in terms of that in an equivalent filter.

The general representation of the tidal flow through the filters is shown in Figure 5.4, with the initial filter denoted by the subscript zero and represents the potential loss of particles before entering the nose or mouth. The deposition efficiency, $\eta_0$, of this imaginary prefilter is the complement of the intake efficiency with which particles are inspired into the respiratory tract. The prefilter also has no volume ($v_0 = 0$), therefore from Eqn. 5.1, the volumetric fraction $\phi_0 = 1$. The fraction of the number of particles, $I_0$, sampled from the environment deposited in the first filter of the respiratory tract is found by substituting these parameters into Eqn. 5.7. For this case, the volumetric fraction of the tidal flow ($\phi_1$) that enters the respiratory tract is unity. Thus, the parameter $\xi_1$ is also unity, and the fractional deposition in the first filter of the respiratory tract is shown in Eqn. 5.8.

$$DE_1 = \eta_1 (1 - \eta_0) \qquad \text{Eqn. 5.8}$$

The value of $DE_1$ is substituted in the recursive relationship defined by Eqn. 5.7 in order to evaluate factional deposition of the ($N$ - 1) subsequent filters that represent deposition in specific regions of the respiratory tract (ICRP, 1994).

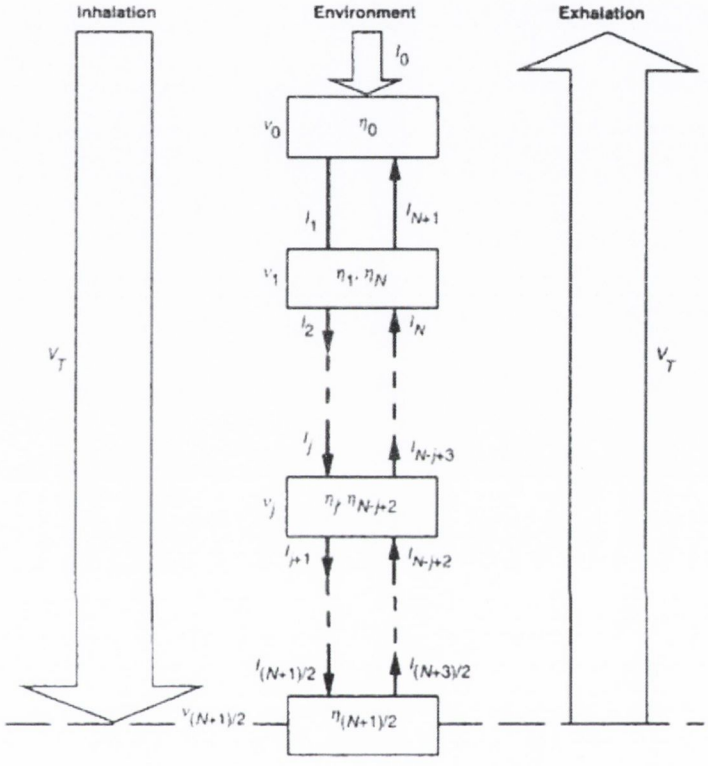


Figure 5.4: A general representation of aerosol deposition for tidal flow through a series of filters (ICRP, 1994).

## 5.5 Filtration efficiencies specification

### *5.5.1 Intake*

In the general representation for the sequential filters shown in Figure 5.4, $I_0$ represents the intake of particulates from the ambient environment by the initial filter. The nominal intake of activity, $I_0$, is given by Eqn. 5.9

$$I_0 = C_A t B \qquad \text{Eqn. 5.9}$$

Whereby $C_A$ is the particle concentration in the air ($\mu g/m^3$), $t$ is the exposure duration (in hours), and $B$ is the individual breathing rate ($m^3\ h^{-1}$).

### *5.5.2 Regional deposition efficiency*

The deposition efficiency of each respiratory tract filter is represented by two components, the first of which is $\eta_{ae}$, which represents the aerodynamic deposition process of impaction and gravitational settling. The second component is due to the thermodynamic process of particle diffusion by Brownian motion and is denoted $\eta_{th}$. It can be shown that the combined deposition efficiency of a region $i$ is given in Eqn. 5.10.

$$\eta_i = (\eta_{ae}^2 + \eta_{th}^2)^{1/2} \qquad \text{Eqn. 5.10}$$

The component of deposition due to gravitational setting and particle inertia is represented in terms of the particle aerodynamic diameter, $d_{ae}$ (in μm). Due to thermodynamic motion it is represented in terms of the particle diffusion coefficient, $D$ (in $cm^2\ s^{-1}$) (ICRP, 1994).

## 5.6 Parameters of the Model

### *5.6.1 Inhalability*

Inhalability is defined as the ratio of the concentration in the inhaled air to that in the ambient air and is determined by particle size and velocity. Particle inhalability is assumed to be the same through the nose or mouth, and also to be independent of a subject's age, gender, and ethnic group. The pre-filtration efficiency, $\eta_0$, of the respiratory tract is the complement of the intake efficiency, $\eta_I$, otherwise known as the "inhalability", thus:

$$\eta_0 = (1 - \eta_I) \qquad \text{Eqn. 5.11}$$

The particle inhalability is assumed to depend on $d_{ae}$, the aerodynamic diameter of the airborne particles. The inhalability generally decreases with $d_{ae}$, for instance, at low wind speeds the intake efficiency reaches a value of approximately 0.5 for particles less than 20 μm in aerodynamic diameter. However, at high wind speeds it has been observed that the inhalability of very large particles will in fact increase. The intake

efficiency of the human head, $I_I$, for particles less than 10 μm in aerodynamic diameter is given by Eqn. 5.12.

$$\eta_I = 1 - 0.5(1 - [7.6 \times 10^{-4} d_{ae}^{2.8} + 1]^{-1} + 1.0 \times 10^{-5} U^{2.75} \exp(0.055 d_{ae}) \qquad \text{Eqn. 5.12}$$

Where $d_{ae}$ is in units of μm and $U$ is the wind speed in $ms^{-1}$ (for $D \leq U \leq 10$ $ms^{-1}$). The graph shown in Figure 5.5 illustrates the intake efficiency as a function of wind speed. It can be seen that for particles of 10 μm or less, the intake efficiency is close to unity.

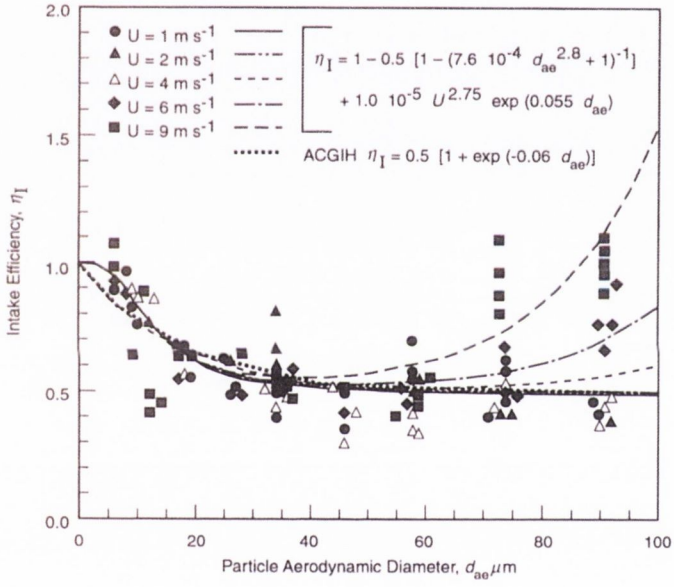


Figure 5.5: Intake efficiency of the human head at random orientation to moving air (ICRP, 1994).

### *5.6.2 Breathing habit*

A subject's breathing habit may affect the quantity of inhaled material that deposits in the lungs since the filtration efficiencies of the nose and mouth differ. The head warms and humidifies inspired air and acts as a particle filter for the thoracic airways. The nose is more efficient than the mouth at conditioning the inspired air, thus breathing at rest usually occurs through the nose. This is similar at low levels to moderate levels of exertion where most individuals breathe through their nose. However, in response to

heavy physical exercise, normal healthy subjects typically supplement airflow through the nose with oral breathing.

Although the majority of people's breathing habits follow this regular pattern, there are those who are habitual "mouth breathers" who are found to breathe oro-nasally at all levels of exertion. The values shown in Table 5.1 are the percentage of tidal air at various levels of exertion that inhaled through the nose and mouth for a normal nose breathing adult (normal nasal augmenter) and for a mouth breather. In the absence of specific information, it is assumed that the breathing habits apply to healthy young subjects and normal healthy adults alike.

Table 5.1: The fraction of total ventilator airflow ($F_n$) passing through the nose in nasal augmenters and in mouth breathers (ICRP, 1994).

| | $F_n$ | |
|---|---|---|
| **Level of exertion** | **Nasal augmenter** | **Mouth breather** |
| Sleep | 1.0 | 0.7 |
| Rest | 1.0 | 0.7 |
| Light exercise | 1.0 | 0.4 |
| Heavy exercise | 0.5 | 0.3 |

### *5.6.3 Scaling of deposition efficiency for body size*

The ICRP model makes allowances for the different body sizes of subjects. The algebraic expressions that represent the deposition efficiencies in each region of the respiratory tract in a reference subject (adult Caucasian male) are applied to the different body sizes of subjects using simple scaling factors. The factors are denoted in the model by $SF_t$, $SF_b$, or $SF_A$ and are defined by the ratio of a reference airway size in the adult Caucasian male to that in the subject.

### *5.6.4 Age and sex specific effects*

In adults, lung volumes and airflows of a healthy subject, correlated to height and weight, are relatively constant but are affected by a number of factors. The vital capacity (VC) of the lungs can be increased by training the respiratory muscles. When a

subject lies down, the VC of the lungs reduces by about 7%. A reduction for other lung factors, namely residual volume (RV), functional residual capacity (FRC) and total lung capacity (TLC), also occurs. The reduction for each of these factors is approximately 15%.

The difference between male and female lung capacity and function begins at 12 years of age. This divergence results in adult female lung function values being usually 20% to 30% lower than those of their male counterparts. After 25 years of age, lung function in humans begins to decrease linearly with age. As humans age, respiratory values for VC, TLC and the forced expiratory volume ($FEV_1$) begin to decrease, while the values of RV, FRC and the anatomical dead space ($V_D$) all start to increase.

The ICRP report gives reference values from the literature for heights, weights and lung volume for healthy Caucasians. The biometry and lung volumes for 30 year old adult Caucasians can be seen in Table 5.2.

Table 5.2: Biometry and lung volumes for Caucasian adults (ICRP, 1994).

| | **Height (cm)** | **Weight (kg)** | **TLC (mL)** | **FRC (mL)** | **VC (mL)** | **$V_D$ (mL)** |
|---|---|---|---|---|---|---|
| **Male** | | | | | | |
| *Mean* | 176 | 73 | 6982 | 3301 | 5018 | 146 |
| *SD* | 168-178 | 65-80 | 700 | 600 | 560 | 25.5 |
| **Female** | | | | | | |
| *Mean* | 163 | 60 | 4968 | 2681 | 3551 | 124 |
| *SD* | 158-166 | 54-61 | 600 | 500 | 420 | 21 |

For the purposes of modelling the dose of participants of this study, it was decided to use the reference lung volumes across the population due to a number of factors. The ICRP publication does refer to summary regressions that have been derived from various authors with respect to age (25 to 70 years) and to height. These regressions are from cross sectional studies of Caucasians and give equations for reference values for a number of different lung functions. For example, a report by Quanjer (1983) is highlighted in which VC, TLC and FRC are all estimated from equations that are

functions of height and age. While similar equations from others studies provide rough estimates of $V_D$ and $V_T$, with weight as an additional determining factor. However, the physical characteristics of precise height and weight were not available of each volunteer in this study. The alternative to using the reference lung volumes from the report would have meant relying on estimates for both height and weight, making it very difficult to calculate the exact lung biometry for numerous volunteers. Additionally, 75% of subjects recruited fell into the 25 to 40 years of age category, which is close to the age of the reference adult (30 years of age) provided in the ICRP publication. Thus, due to the lack of relevant physiological information on hand the reference values were used in estimating dose for the volunteers.

### *5.6.5 Ventilation parameters*

The ventilation parameters employed in the ICRP model are reference values for both male and female workers at different activity levels, and are shown in Table 5.3. These recommended values are not intended to be average values for the worldwide population but a coherent set of values for Caucasians. The respiratory frequencies ($f_R$), $V_T$, and ventilation rate ($B$) were estimated according to age and level of exercise. Four main activities were selected and the corresponding values of work load and ventilation rate were taken from the literature.

Table 5.3: Reference respiratory values for a general Caucasian population at different levels of activity (ICRP, 1994).

| | | **Resting** | | **Sitting awake** | | **Light exercise** | | **Heavy exercise** | |
|---|---|---|---|---|---|---|---|---|---|
| **Maximal workload (%):** | | 8 | | 12 | | 32 | | 64 | |
| **Gender (Male/Female):** | | **M** | **F** | **M** | **F** | **M** | **F** | **M** | **F** |
| **Breathing Parameters:** | $V_T$ (L) | 0.625 | 0.444 | 0.75 | 0.464 | 1.25 | 0.992 | 1.923 | 1.364 |
| | $B$ ($m^3h^{-1}$) | 0.45 | 0.32 | 0.54 | 0.39 | 1.5 | 1.25 | 3.0 | 2.7 |
| | $f_R$ ($min^{-1}$) | 12 | 12 | 12 | 14 | 20 | 21 | 26 | 33 |

The main reference values given for the ICRP model relate primarily to Caucasians, although reference values from some other ethnic groups were given when available by the ICRP. Amongst the various ethnic groups, $V_T$ is likely to show some differences in oxygen needs (indicated by body heights and weights) and in lung volumes. However, the ICRP conclude ventilation rates at rest and at various levels of exercise did not seem to be very different between studied ethnic groups, thus the same set of ventilation rate values is suitable for all subjects.

### *5.6.6 Inhaled daily volumes of air*

The ICRP also make estimates of the volume of air breathed in over a 24-hour period for unspecified sedentary workers. These ventilation rates are shown in Table 5.4. Not shown, however, are the ventilation rates required by some workers, for example, firemen, construction workers, and farm workers, although the model does provide a heavy worker class had dose estimation been required for occupations other than office workers.

Table 5.4: Recommended values of daily ventilation rates ($m^3$) for sedentary adult workers (ICRP, 1994).

| **Activity** | **Male** | **Female** |
|---|---|---|
| Sleeping (8 hours) | 3.6 | 2.6 |
| Occupational (8 hours) | | |
| 1/3 sitting<br>2/3 light exercise | 9.6 | 7.9 |
| Non-occupational (8 hours) | | |
| 1/2 sitting<br>3/8 light exercise<br>1/8 heavy exercise | 9.7 | 8.0 |
| Total air breathed ($m^3$) | 22.9 | 18.5 |

For the purposes of this study, advice on the attribution of activity levels for office workers has been taken both from literature and the values presented in Table 5.4. In a

study of various occupations in the Netherlands (Jans et al., 2007), it was found that office based workers sat for a significantly greater amount of time than other worker groups. In total, the various office workers spent on average nearly three hours of their working day sitting, which equates to approximately 38% of an eight hour day. While the evenings were also spent mainly sitting, with almost three hours spent sitting also. In total, approximately seven hours of the day was spent sitting amongst the workers surveyed as part of the study by Jans et al. (2007), with much of the rest of the time made up while commuting on buses and trams etc. Thus, in this study the exertion levels for the various activities and microenvironments were defined as follows in Table 5.5.

Table 5.5: Physical exertion levels used for various activities in the Human Respiratory Tract model for subject dose estimation.

| **Activities/Microenvironments** | **Physical Exertion Levels** |
|---|---|
| At Home | Sitting – 60% |
| | Light exercise – 40% |
| Sleeping | Resting |
| Work | Sitting – 40% |
| | Light exercise – 60% |
| Walking | Light exercise |
| Bus/Car/Tram/Train | Sitting |
| Cycling | Moderate exercise |
| Café/Restaurant | Sitting |
| Playing sport | Heavy exercise |
| Shopping | Light exercise |

As can been seen from the table, the exertion levels of the primary activities of office workers, which are working and at home in their residences, were split into sitting and light exercise, and this reflected suggested values in both the ICRP publication and literature. Of the commuting modes, walking was classified as light exercise and enclosed transit methods were all classed as sitting. Various other less common

activities were also given a classification, for instance, shopping was rated as light exercise due to the amount of walking involved, while playing sport or going to the gym were classified as predominantly heavy exercise activities. These exercise levels were implemented into the Matlab model as inputs along with their associated microenvironmental concentrations for each volunteer.

The parameters for four of the five exertion levels were extracted directly from the *ICRP Publication 66* (ICRP, 1994), and were shown previously in Table 5.3. However, the activity of cycling generally involves a light to moderate level of exercise, slightly greater than that of walking but not enough to warrant categorising as heavy exercise. Thus, a fifth moderate exercise category was derived specifically for this activity. Guidance on the minute ventilation rates for cyclists was based on previous research in literature.

O'Donoghue et al. (2007a) measured the minute ventilation rates of two male cyclist in a physiological laboratory and found the average breathing rate to be 28 l/min. Similar minute ventilation rates for cyclists were also observed by Bernmark et al. (2006) (31 l/min), and Vrijkotte (1990), who reported 29.1 l/min. In research conducted by Zuurbier et al. (2009), minute ventilation rates were estimated indirectly using heart rate measurements for a mixture of 34 male and female volunteers, and the mean ventilation rate was found to be 23.5 l/min. However, although this value was lower than the other studies mentioned, the researchers did note that the average speed of cyclists of 12 km/hr was lower than what was normally expected due to the heavy equipment carried by the volunteers. The minute ventilation used for this study was therefore assumed to be 30 l/min for males and 25 l/min for females. This was based on the studies highlighted, while the other parameters such as respiratory frequency ($f_R$) and tidal volume ($V_T$) were interpolated between the ICRP light and heavy exercise values. These respiratory values are shown below in Table 5.6.

Table 5.6: Reference respiratory values for a general Caucasian population for the activity of cycling.

| Gender | B ($m^3 h^{-1}$) | $f_R$ ($min^{-1}$) | $V_T$ (L) | $\dot{V}$ ($L s^{-1}$) |
|---|---|---|---|---|
| Male | 0.03 | 21 | 1.43 | 1.0 |
| Female | 0.025 | 25 | 1.0 | 0.83 |

## 5.7 Modelled 24-Hour Dose Uptake

### *5.7.1 Overall study population dose*

The 24-hour $PM_{10}$ personal exposure concentrations from the study population dataset were each individually inputted into the respiratory tract model in Matlab, and the dose uptake for each sampling day was obtained. The summary statistics for the modelled 24-hour doses are shown in Figure 5.6. The mean 24-hour dose uptake amongst volunteers was found to be 376.9 μg with a standard deviation of 260.7 μg. The distribution of the dose uptake of the study was similar to that of the 24-hour exposure concentrations seen in Chapter 4. It can be seen that the distribution is not normally distributed, with $p < 0.005$ for the Anderson-Darling test for normality.

The minimum dose uptake amongst subjects for a single 24-hour period was found to be for a 56 year old female volunteer who had a recorded dose of 48.6 μg. This particular sample from this subject had very low $PM_{10}$ concentrations recorded both at home and at work, with respective personal exposure concentrations in these locations of just 6.5 $\mu g/m^3$ and 4 $\mu g/m^3$. The vast majority of time was also spent in these two microenvironments, with the approximately seven and a half hours that was spent in work making up 60% (29.1 μg) of the dose uptake that day.

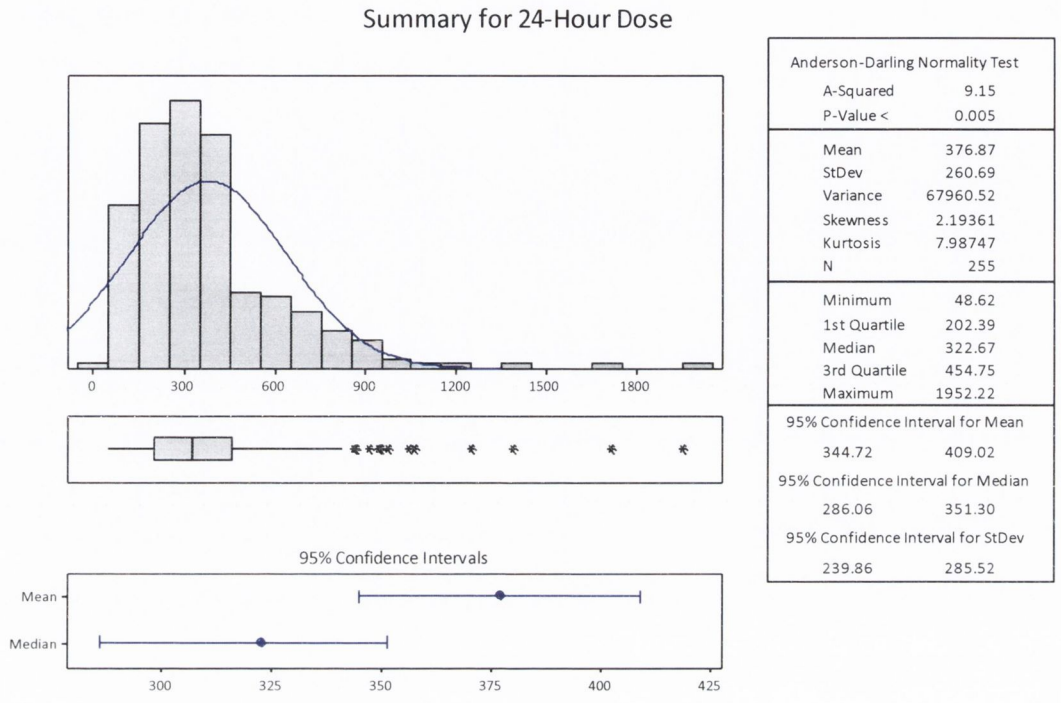


Figure 5.6: Summary statistics for the 24-hour dose uptake of the study population.

The subject also used the train as the primary mode of commuting into her workplace, which was situated on the north side of the city centre, from her home in Portmarnock, Co. Dublin. The train was found to be a microenvironment with one of the lowest personal $PM_{10}$ concentrations associated with it across the study populous, and for this subject it was no different with a concentration of 7 $\mu g/m^3$ for that sampling day. However, due to this low concentration, the 26 minutes spent on a train accounted for less than a microgram (0.62 $\mu g$) of dose. This is in contrast to time spent walking outdoors which was the activity with the highest concentration recorded on that sampling day (20.4 $\mu g/m^3$). Even though the same amount of time was spent on the train as walking, the elevated personal exposure concentration and exercise level meant that walking had eight times the dose uptake (5.4 $\mu g$) as commuting by train.

On the opposite end of the population dose distribution, the maximum single 24-hour dose that was found was 1952.2 $\mu g$. This value for dose was for a 30 year old male subject who worked in an office above the geotechnical laboratory in Trinity College. The dose uptake experienced by this volunteer was far greater than the mean dose for

the population, and this excessive amount was due to the large dose encountered while the volunteer was in his office. The $PM_{10}$ dose uptake at work was responsible for 94% of the 24-hour total, or 1833.4 μg. The average personal $PM_{10}$ concentration in this subject's workplace was 241 $\mu g/m^3$, and on top of this the volunteer was present in the workplace for just over nine and a half hours. Thus, this combination resulted in the excessively large dose uptake. However, the subject did shed some light on why the large concentrations in his office may have occurred in the activity diary that was returned with the 24-hour sample. It was stated by the subject that there was a large amount of oven usage taking place in the geotechnical laboratory situated directly below the office, and at different points throughout the day a burning smell could be detected in the air. Therefore, it is reasonable to deduce that excessive $PM_{10}$ concentrations present in the office were due to infiltration of particles generated in the laboratory through the wooden floor of the office.

The rest of the 24-hour sampling period for this individual was divided between time spent at home and commuting between work and home. Even though time spent at home was for just over 12 hours of the day, divided between being active at home and sleeping, it accounted for a mere 61.6 μg dose uptake. Of the commuting modes, walking had by far the largest dose contribution (48.9 μg) when compared to driving (7.0 μg) and the train (1.3 μg). Again, this was due to the elevated breathing rate and $PM_{10}$ concentration (127 $\mu g/m^3$) while walking outdoors. Time spent walking was just 22 minutes compared with the 84 minutes of the day that was spent inside a car.

### *5.7.2 Individual microenvironment and activity doses*

The dose uptake for the study population was found to vary considerably across the different microenvironments and activities. The dose calculated through the respiratory tract model was highly dependent on the length of time spent in a microenvironment as well as the associated breathing rate of the activity. Large concentrations also played a factor, however short durations spent in locations with high $PM_{10}$ concentrations did not necessarily have large dose uptake if contact was for a short period of time.

The dose uptake for the study population for each of the major activities and microenvironments are illustrated in Figure 5.7 and Figure 5.8, while the descriptive statistics are shown in Table 5.7.

Table 5.7: Descriptive statistics for dose of the study population for the main activities and microenvironments.

| **Activity/Microenvironment** | **Mean** (μg) | **St Dev** (μg) | **Min** (μg) | **Max** (μg) | **Median** (μg) |
|---|---|---|---|---|---|
| *Primary activities/locations* | | | | | |
| Working | 216.0 | 231.6 | 2.44 | 1833.4 | 150.9 |
| Active in Home | 84.8 | 70.1 | 1.76 | 648.5 | 68.3 |
| Sleeping | 22.9 | 19.9 | 0.67 | 105.9 | 16.6 |
| *Other activities/locations* | | | | | |
| Café/Restaurant | 11.9 | 17.5 | 0.43 | 113.6 | 6.1 |
| Other Indoor | 28.2 | 32.9 | 0.59 | 209.8 | 17.6 |
| Other Outdoor | 8.2 | 9.6 | 0.23 | 41.3 | 5.2 |
| Pub | 28.9 | 23.2 | 9.68 | 101.5 | 20.6 |
| Recreation/Sport | 127.6 | 131.6 | 15.85 | 568.2 | 81.9 |
| Shopping | 15.9 | 24.2 | 0.30 | 132.7 | 9.9 |
| *Transport modes* | | | | | |
| Bus | 15.4 | 18.9 | 0.37 | 111.8 | 8.6 |
| Car | 8.3 | 11.0 | 0.10 | 54.8 | 4.1 |
| Cycling | 18.8 | 20.9 | 0.94 | 94.4 | 12.3 |
| Train | 8.2 | 7.3 | 0.58 | 29.4 | 6.3 |
| Tram | 1.7 | 1.2 | 0.04 | 3.6 | 1.7 |
| Walking | 18.8 | 16.3 | 0.45 | 105.2 | 14.9 |

The top three activities where the highest doses were experienced can be seen in Figure 5.7. The largest dose uptake for the subjects was found to be in the working environment, which had a mean dose of 216.0 μg with a standard deviation of 231.6 μg. This was followed by recreation or sport with a mean dose of 127.6 μg for subjects who participated ($\sigma$ = 131.6 μg) and being active in the home, which had a mean of 84.8 μg along with a standard deviation of 70.1 μg. In contrast to the dosage experienced when the subjects were active at home, the mean dose that they absorbed while sleeping fell to

22.9 μg. Lagging behind the three main microenvironments was the category 'Other indoor' which had a mean dose of 28.2 μg. Even though the mean dose for this category was similar to some others in Table 5.7, the category 'Pub' for example, it had a number of outliers with the maximum value for dose in this range reaching 209.8 μg, therefore it was not included in Figure 5.7 in order to improve the resolution.

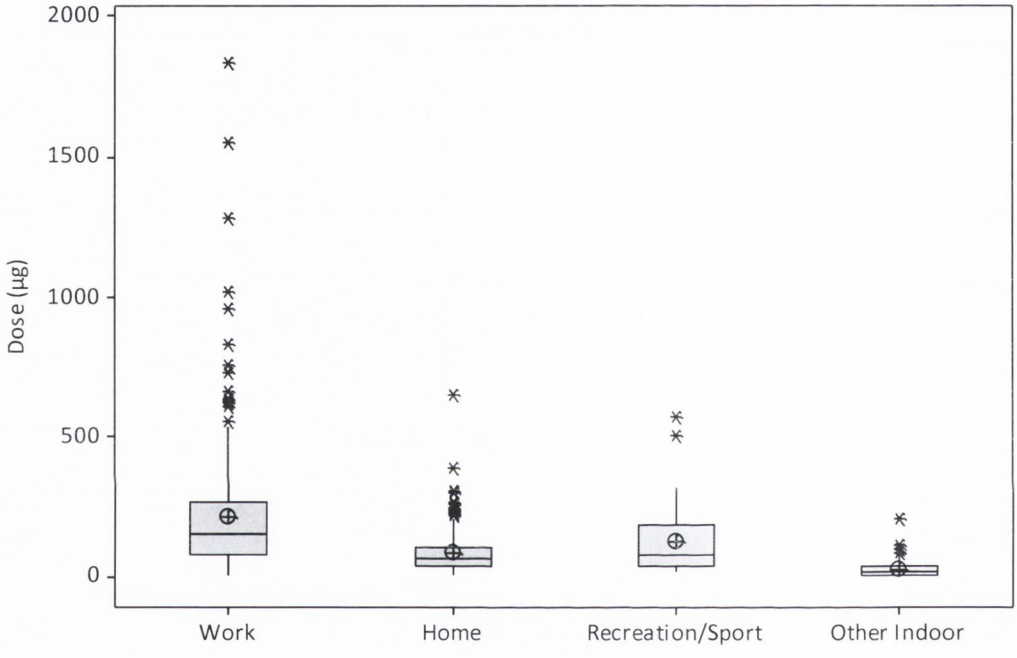


Figure 5.7: Boxplot of the top four microenvironments/activities with the largest dose associated

Of the other major microenvironments, in particular public places, the dose uptake in public houses was greatest with a mean uptake of 28.9 μg and standard deviation of 23.2 μg. This value was considerably higher than the mean dose experienced by volunteers that visited other similar public establishments such cafés and restaurants which were found to have a mean dose uptake of 11.9 μg ($\sigma$ = 17.5 μg). The mean dose uptake as the subjects went about shopping was also higher than that of cafés and restaurants, and had a mean dose of 15.9 μg with standard deviation of 24.2 μg.

The commuting modes of volunteers were observed to have some of the lowest mean doses of all microenvironments for the study population. Enclosed transit modes such as

use of cars or trains had very similar mean doses ($\mu$ = 8.3 µg, $\sigma$ = 11.0 µg & $\mu$ = 8.2 µg, $\sigma$ = 7.3 µg, respectively), while use of the Luas tram system saw the lowest mean dose of all amongst users at just 1.2 µg ($\sigma$ = 1.2), however this was also the smallest sample set amongst transport modes. Greater mean subject dose uptakes were observed when commuting by bus ($\mu$ = 15.4 µg) and by cycling ($\mu$ = 18.8 µg). Walking also had a mean dose uptake of 18.8 µg, however travelling on foot was not necessarily limited exclusively to morning and evening commutes.

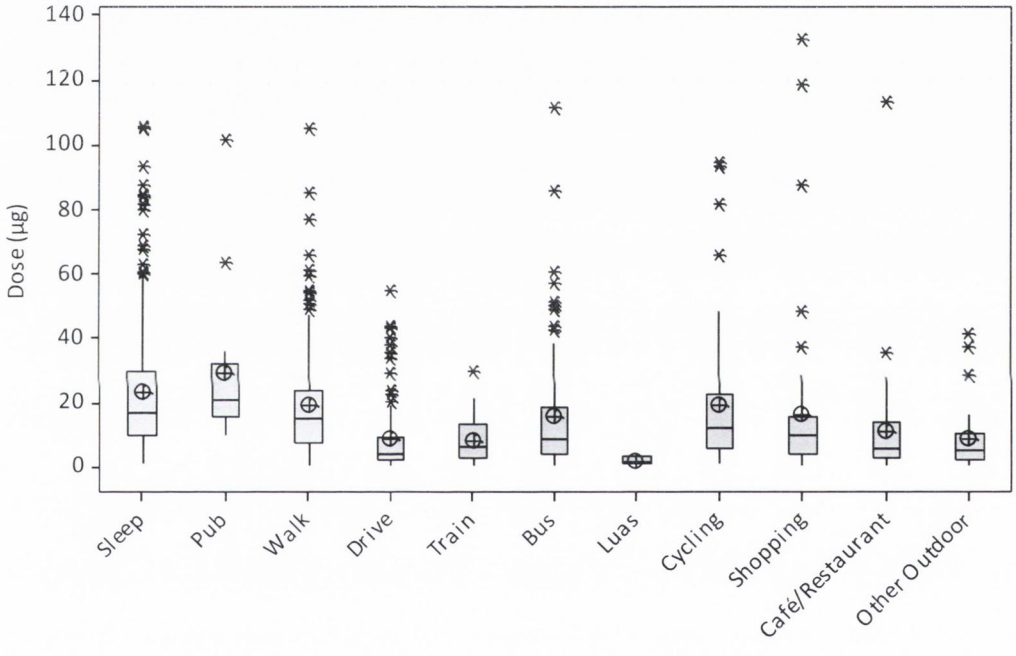


Figure 5.8: Boxplot of population dose uptake across all other major activities and locations.

### *5.7.3 Comparison of dose uptake and mean personal $PM_{10}$ concentrations*

In the previous section much of the average dose uptake in the primary microenvironments of study population were discussed. However, it is important to highlight the reasons behind why in certain microenvironments subjects were found to have far higher dose uptake than in others. As already alluded to, although high personal $PM_{10}$ concentrations in a microenvironment can be an important factor influencing the magnitude of dose absorption for a subject, it is not the overriding

determinant. The dosage absorbed by a volunteer primarily hinged on the amount to time spent in the microenvironment as well as what activity was being carried out, which ultimately determined the respiratory rate of the subject.

The comparison of the average personal $PM_{10}$ exposure concentration and the mean dose uptake for various microenvironments frequented by the study population is shown in Figure 5.9. As illustrated in the figure, some of the microenvironments that were reported in Chapter 4 as having the largest mean personal $PM_{10}$ concentrations associated with them, in fact contributed relatively little to the 24-hour dose uptake of subjects. This was particularly apparent in the case of the category 'Other indoor' along with cafés and restaurants.

During the analysis of the mean population personal exposure concentrations in Chapter 4, the category of 'Other indoor' was found to have the highest mean $PM_{10}$ concentration (66 $\mu g/m^3$). However, due to the relatively infrequent and short amount of time spent in some of these microenvironments that were classed as 'Other indoor', the actual population dose uptake over 24 hours was low (28.2 $\mu g$). A similar situation was seen with cafés and restaurants, whereby the mean dose uptake was low relative to the average concentration found in this microenvironment. On average the study participants spent less than an hour (51 minutes) in cafés or restaurants upon visiting them, and coupled with the low breathing rate due to sitting once there, the resulting dose uptake was minimal.

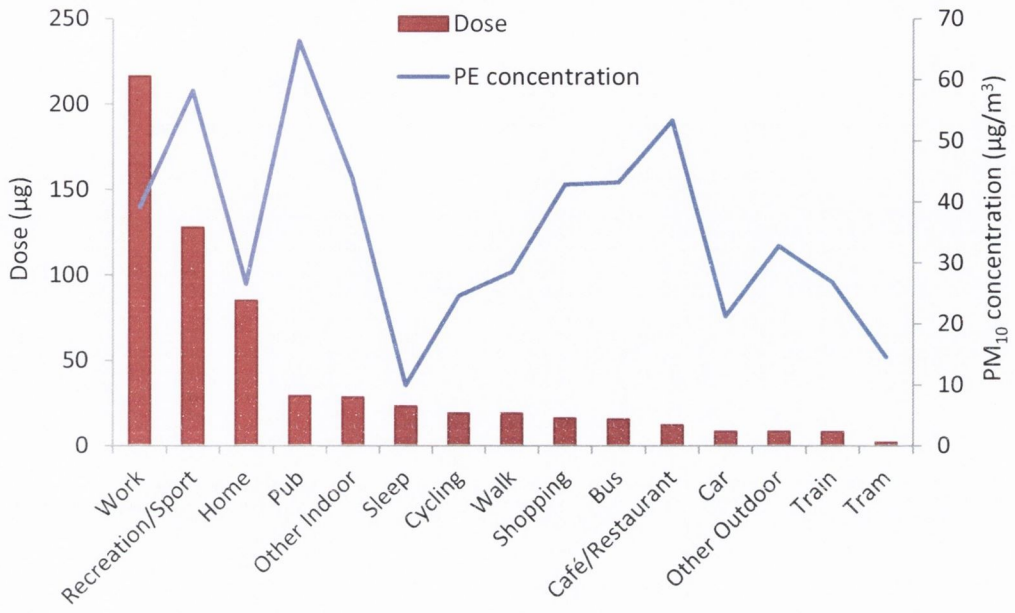


Figure 5.9: A comparison of the mean dose uptake of the study population in various microenvironments with the corresponding personal $PM_{10}$ concentrations in each.

Other microenvironments also displayed low dose uptake amongst the study subjects, in spite of having relatively high average personal $PM_{10}$ concentrations recorded. Several of the transport modes such as travel by bus or car, which had respective mean personal exposure concentrations of 43 $\mu g/m^3$ and 33 $\mu g/m^3$, were observed to have low dose contributions to the overall 24-hour total. This was again due to the limited amount of time spent in each microenvironment along with the 'sitting' exertion level also applied to each commute mode in the model. In public locations too, such as going to the pub and shopping, the dosages absorbed were low compared with personal exposure measurements due to the low ventilation rate of subjects in the case of sitting in a pub, and the relatively short time span spent shopping by most individuals.

The doses for the subjects while at work and active at home were as expected both large contributors to the 24-hour total dose of volunteers. This was due to the majority of each 24-hour sampling day being spent in either location. However, the greater activity levels while at work (40% sitting and 60% light exercise) amplified the difference in dose even though the personal concentration population average was just 13 $\mu g/m^3$ greater than 'active at home'. For example, the dose of work (216 µg) was over 150%

greater than that absorbed in the home (84.8 μg) on average, compared with the 50% difference between the two exposure concentrations. In contrast to 'at work', the activity of sleeping had a far lesser dose uptake on average. The reason for this lay in the fact that even though sleeping had a similar proportion of the day dedicated to it by volunteers, the already low concentrations found for this activity (10 $\mu g/m^3$), along with the lowest exercise level assigned to it in the respiratory tract model, ensured the comparative dose uptake was very minor.

### *5.7.4 Gender differences for dose uptake*

The dose uptake results were analysed separately for the male and female subjects of the study population. The summary statistics for the 24-hour dose uptake of male volunteers, along with the distribution theses values, are shown in Figure 5.10. The mean 24-hour dose uptake among the male volunteers was slightly greater than the overall population average, with a mean of 451 μg ($\sigma$ = 290.5 μg) and a 95% confidence interval between 404.9 μg and 497.1 μg. As can be seen also from Figure 5.10, the dose uptake data set follows a log normal distribution, and is skewed to the right in similar fashion to the overall 24 hour population dose distribution in Figure 5.6.

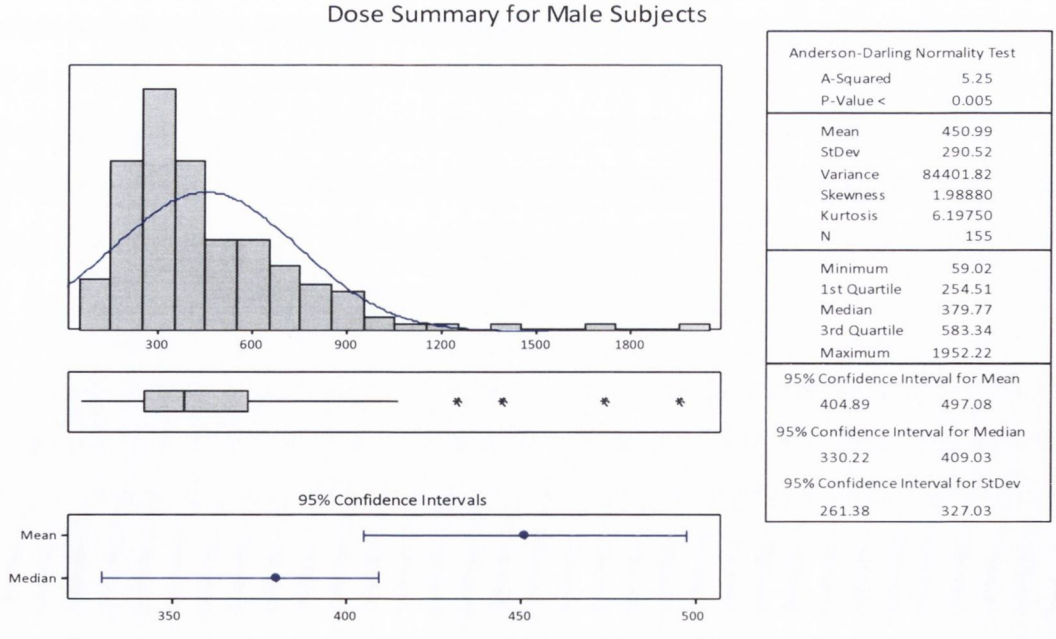


Figure 5.10: Summary statistics and dose distribution for male subjects.

The female subjects' dose uptake data set was also summarised and the statistics are illustrated in Figure 5.11. The distribution for female dose data was again, similarly to the males, not normally distributed with $p < 0.005$ for the Anderson-Darling test. The best distribution for this dataset in actual fact was a gamma distribution, which was ranked just ahead of a log-normal distribution, and this was established using the distribution fitting tool in the software package @Risk (Palisade Corporation). The mean 24-hour dose uptake for female subjects was 262 μg, which was far lower than the equivalent for males, and had a standard deviation of 145.4 μg.

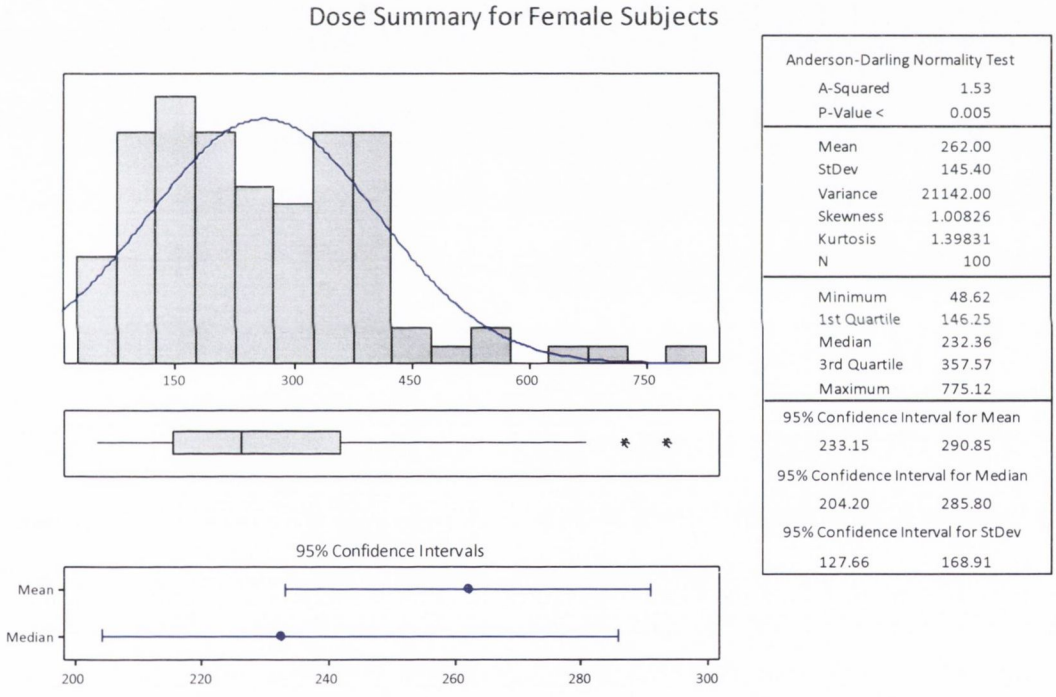


Figure 5.11: Summary statistics and dose distribution for female subjects.

The male and female 24-hour dose data sets were assessed using a non-parametric test to determine whether one group had statistically significantly larger dose than the other. The two sets of data were tested using a Mann-Whitney U test, otherwise known as the Wilcoxon Rank-Sum test. However, before applying the Mann-Whitney U test to the data, the assumptions of the test meant that the two data sets had to be examined for homogeneity of variance and that the distributions were similar. As already mentioned, the distributions for both male and female data sets generally conformed to log normal

shaped of distributions. This fact is illustrated by overlaying both data sets, as shown in Figure 5.12.

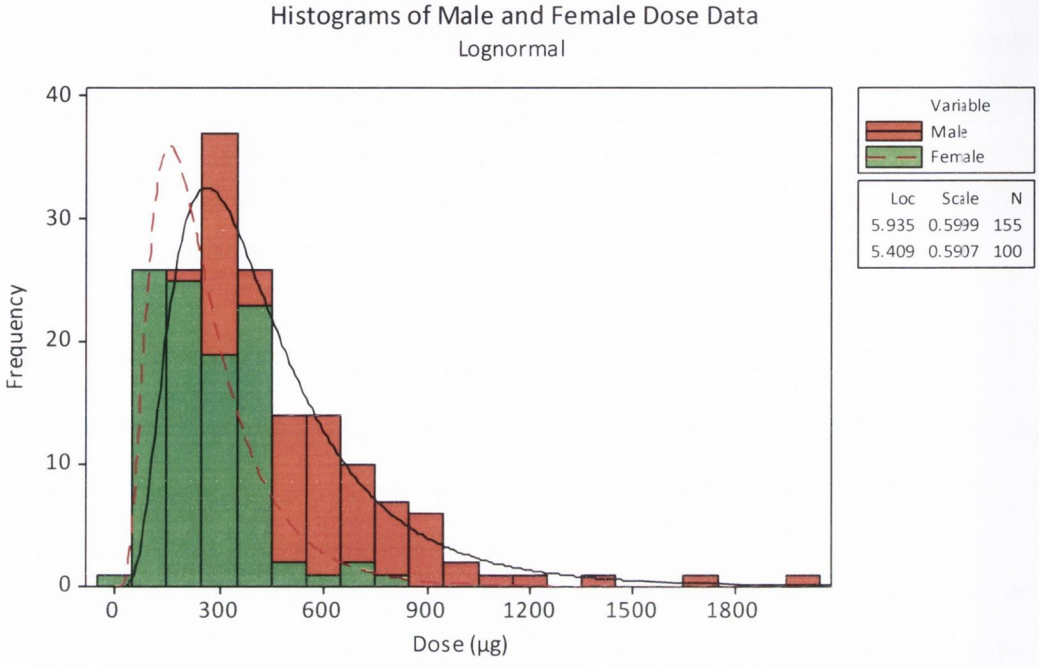


Figure 5.12: Comparison of lognormal distributions for the male and female dose data.

In order to determine that the assumption of homogeneity of variance was upheld, the data was also subjected to a non-parametric equivalent of the Levene's test. This was carried out in SPSS and involved calculating the absolute difference between the mean ranks and ranked values of dose and performing an ANOVA test. The conclusion of this analysis was that the assumption of homogeneity was indeed upheld with a p value of 0.331, meaning that there was no statistical significance between the variances of male and female dose data.

Once the Mann-Whitney U test assumptions had been proven valid for the male and female groups, the test itself was carried out in SPSS also. The results from this test can be seen in Table 5.8. As can be seen from the test statistics the mean rank for female dose uptake is statistically significantly lower than for males ($p < 0.000$). This meant that the median for the male subjects' 24-hour dose uptake (median = 379.8 µg) was

statistically significantly greater than females (median = 232.4 μg). This result was expected as the male respiratory rates used in the respiratory tract model were greater than the female equivalent. However, it was important to check in case of any difference in female activity patterns compared to males resulted in the inflation of dose uptakes amongst the female population.

Table 5.8: Results from a Mann-Whitney U test to assess if the difference between male and female dose uptake data was significant.

| **Ranks** | | | **Test Statistics** | |
|---|---|---|---|---|
| | Male | Female | | |
| N | 155 | 100 | Mann-Whitney U | 4252 |
| Mean Rank | 150.57 | 93.02 | Wilcoxon W | 9302 |
| Sum of Ranks | 23338 | 9302 | Z | -6.083 |
| | | | Asymp. Sig. (2-tailed) | 0.000 |

### *5.7.5 Dose uptake of smokers*

As part of the analysis, the dose uptake of smokers was compared to the dose uptake of the rest of the study population (see Figure 5.13). The 24-hour mean dose uptake of smokers was found to be approximately 27% higher than the non-smoking population (472.6 μg versus 373 μg for non-smokers). However, the smokers who took part in the study reported that smoking was primarily at home, so when this microenvironment was analysed the differences between the two population groups was far more pronounced. The smokers had an average 'at home' dose uptake 196.7 μg compared with 80.2 μg for non-smokers. Similarly, the dose uptake of smokers while sleeping at night was about 100% greater than the non-smokers, with a mean dose of 44.1 μg as opposed to 22.3 μg.

It is also important to note that the dose calculations were for the personal exposure to environmental tobacco smoke (ETS) and not what was directly inhaled into the lungs when smoking a cigarette. The ETS is of importance because even after a cigarette has been smoked this event will continue to impact on dose uptake for a long duration

afterwards. Additionally, the dose uptake for non-smoking individuals exposed to a microenvironment containing ETS will be amplified also.

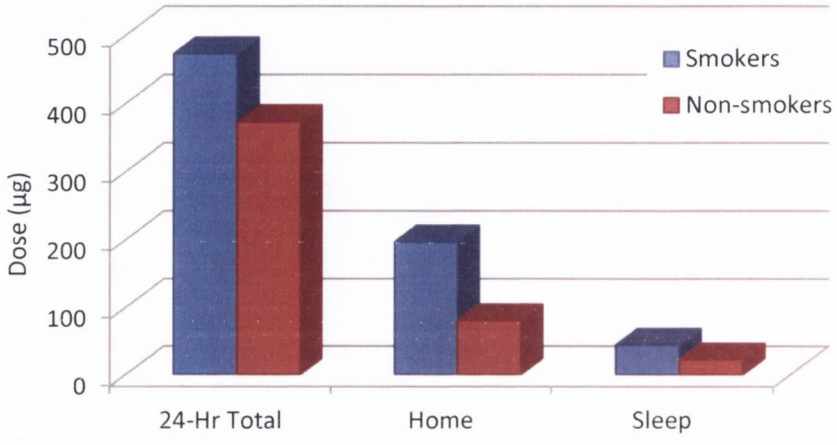


Figure 5.13: Comparison of the mean 24-hour dose uptakes of smokers and non-smokers of the study population.

The data that was collected as an additional resource from the two other smokers (Smokers A and B) and discussed in Section 4.4.1, were also inputted into the respiratory tract model in order to calculate dose. The results of this process are summarised in Table 5.9.

The profiles of the two smokers were detailed also in Section 4.4.1, but as a recap both were middle aged female office workers who sampled personal exposure in their home over a number of days. The dose for each smoker was calculated using the respiratory tract model set for female subjects. The mean dose for Smoker A at home was found to range between 242 µg and 355 µg, and for Smoker B the average dose was from 211 µg to as high as 425 µg. These dose values were calculated for various lengths of time that are also presented in the table, and represent the duration of time that the subjects reported themselves active at home on each particular day. The average doses for 'at home' for both subjects were far in excess of the corresponding mean dose for the non-smoker population (80.2 µg). They were also greater than mean 'at home' smoker population doses, albeit with only a small sample set available for Smokers A and B.

The mean doses in each of the homes of Smokers A and B while sleeping were more in line with the non-smoking population, although dose uptake at night for Smoker A was as high as 41.1 μg on one occasion, while one other evening was cut short by the Aerocet-531 running out of power due to not being plugged in correctly. As the dose uptake data was calculated for various durations for both Smokers A and B, it is perhaps more appropriate to compare the dosage per hour for each compared to the general population dose per hour. The average dose uptake per hour for non-smokers while at home was calculated as 14 μg/hr while active at home and 2.7 μg/hr while sleeping. The dosages per hour for the smokers in comparison were far higher than these values in most cases. On examination of Table 5.9, the doses per hour ranged from 18.6 μg/hr to as much as 85.3 μg/hr while active in the home. Moreover, the dosages per hour while sleeping were nearly all several times greater than that of the general populous, bar one exception.

Table 5.9: Summary of dose uptake in the homes of Smokers A and B.

| | Day | Home (μg) | Duration (min) | Dose/hr | Sleep (μg) | Duration (min) | Dose/hr |
|---|---|---|---|---|---|---|---|
| **Smoker A** | 1 | 355.4 | 250 | 85.3 | 41.1 | 400 | 6.2 |
| | 2 | 242.4 | 482 | 30.2 | 8.5 | 478 | 1.1 |
| | 3 | 289.7 | 934 | 18.6 | 8.9 | 144 | 3.7 |
| **Smoker B** | 1 | 425.1 | 560 | 45.5 | 25.0 | 372 | 4.0 |
| | 2 | 213.4 | 272 | 47.1 | 22.2 | 376 | 3.5 |
| | 3 | 211.3 | 336 | 37.7 | 19.3 | 418 | 2.8 |

### *5.7.6 Analysis of travel modes*

An analysis was carried out on the travel mode data set of the study subjects in order to determine if there was any statistical difference between each individual mode of travel. Often in previous studies the assessment of dose uptake of an air pollutant amongst different modes of travel was limited to rush hour times during the morning and evening (O'Donoghue et al., 2007a; McNabola et al., 2008b; de Nazelle et al., 2012). However,

because this study involved monitoring over 24-hour periods, the use of the various modes of travel could occur at any point during the day. Therefore, the dose of a particular transport mode may not be as high as when limited exclusively to peak traffic periods.

The mean dose uptakes of each mode of travel are shown below in Figure 5.14. As previously stated, the average dose was highest for cycling and walking, while enclosed transit modes, and in particular travel by car, train or tram, tended to be lower. This was due to the elevated breathing rates associated with these activities compared with enclosed transit modes.

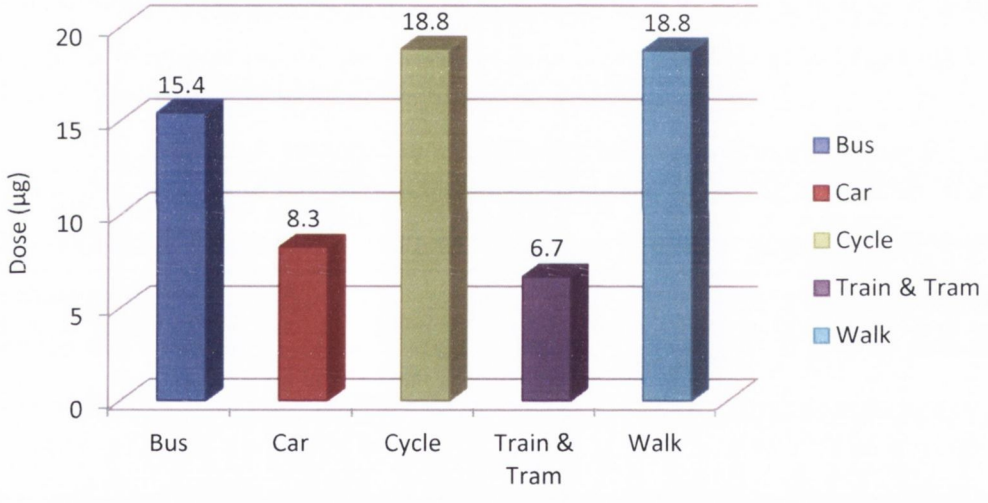


Figure 5.14: Mean dose uptake of each travel mode for the study population.

The travel mode doses were tested for statistical significance using a Kruskal-Wallis test, which is a non-parametric test and an extension of the Mann-Whitney U test for three or more groups. The same assumptions apply to the Kruskal-Wallis test also, thus, the data had to have similar distributions and be tested to ensure homogeneity of variance. The distributions for each mode of travel are illustrated in Figure 5.15. As can be seen from the figure, the doses of each travel mode have similar shapes and generally follow a log normal shaped distribution. The data sets for train and tram travel have also been merged due to the relatively small sample set for tram travel.

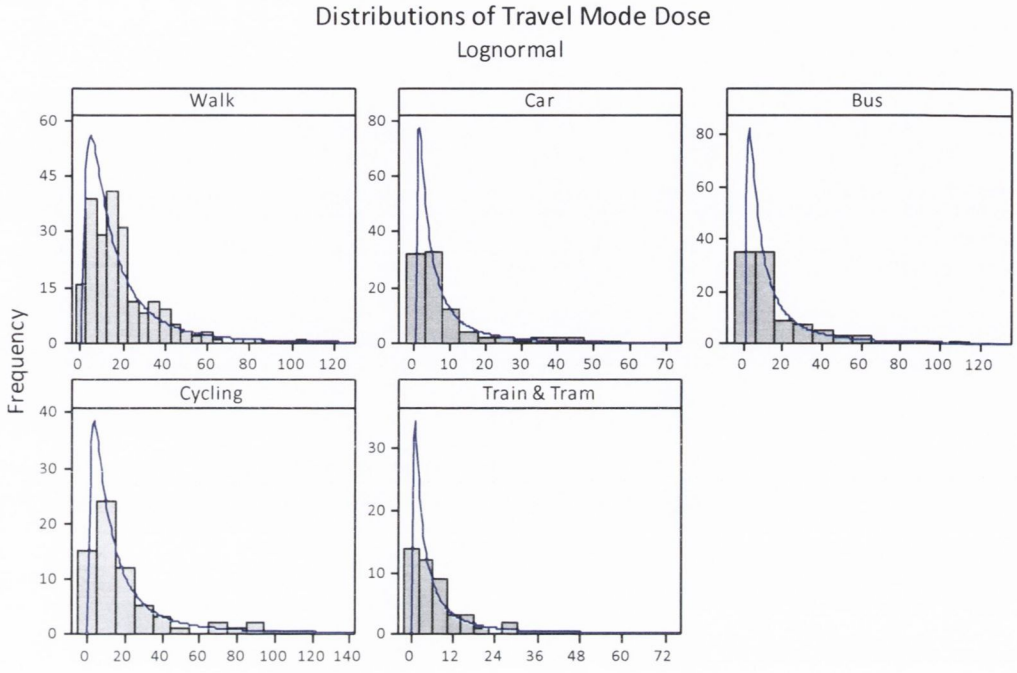


Figure 5.15: Distributions of doses for each mode of travel (μg).

The dose uptake data of the travel mode groups were also checked for homogeneity of variance. This was done using the non-parametric equivalent of Levene's Test, the results of which are shown in Table 5.10. The result of the analysis of variance of the different travel groups confirmed that there was no statistical significance between the variances of dose in each mode of travel ($p = 0.512$).

Table 5.10: ANOVA of the absolute difference between the mean ranks and ranks of travel groups, the non-parametric equivalent of Levene's Test.

**ANOVA**

| | Sum of Squares | df | Mean Square | F | Sig. |
|---|---|---|---|---|---|
| Between Groups | 18659.134 | 4 | 4664.783 | .822 | .512 |
| Within Groups | 2883869.413 | 508 | 5676.908 | | |
| Total | 2902528.547 | 512 | | | |

The test results from the Kruskal-Wallis analysis are shown in Table 5.11. The largest mean rank was found to be for the travel mode of walking, with a mean rank of 308.2, which was followed by cycling (288.4) and travel by bus (249.9). On inspection of the test statistics, there was a statistical significant difference between the modes of travel (chi-square = 78.042, p <0.001). However, although this analysis determines that there does exist a statistical difference between some of the travel mode doses, it does not identify which of the modes are different from each other. For example, the mean rank for travel by car (171.05) is quite similar to the train or tram group (161.35), but it is not apparent if the dose uptakes from using these modes of transport are in fact statistically lower than the using the bus. Therefore, further investigation of the mean ranks was carried out.

Table 5.11: Kruskal-Wallis Test results on the travel mode doses.

| **Ranks** | | | **Test Statistics** | |
|---|---|---|---|---|
| | N | Mean Rank | | |
| Bus | 99 | 249.92 | Chi-square | 78.042 |
| Car | 99 | 171.05 | df | 4 |
| Cycle | 65 | 288.45 | Asymp. Sig. | 0.000 |
| Train & Tram | 44 | 161.35 | | |
| Walk | 212 | 308.22 | | |
| Total | 513 | | | |

A number of post-hoc analysis tests were carried out in order to assess exactly which of the travel mode dosages were statistically significant from one another. The two highest ranked modes in the original Kruskal-Wallis test were cycling and walking, thus the first post-hoc test done was to test if these were statistically significantly different. The test results (Chi-square = 0.986, p = 0.321) confirmed that the difference between the two groups was not in fact significant. However, the walking dose data was statistically different from bus travel dose (Chi-square = 10.883, p = 0.001), and by inference all other travel modes too. Both bus and cycling dose were found to not be statistically different from each other (p = 0.093), however the p-value was low enough to warrant further investigation between both modes.

Table 5.12: Post-hoc tests on pairs of travel modes for dose uptake.

| **Ranks** | | | | **Test Statistics** | |
|---|---|---|---|---|---|
| | Travel mode | N | Mean Rank | | |
| Test 1 | Walk | 212 | 141.65 | Chi-square | .986 |
| | Cycling | 65 | 130.37 | df | 1 |
| | Total | 277 | | Asymp. Sig. | .321 |
| Test 2 | Walk | 212 | 167.50 | Chi-square | 10.883 |
| | Bus | 99 | 131.38 | df | 1 |
| | Total | 311 | | Asymp. Sig. | .001 |
| Test 3 | Bus | 99 | 77.45 | Chi-square | 2.820 |
| | Cycling | 65 | 90.18 | df | 1 |
| | Total | 164 | | Asymp. Sig. | .093 |
| Test 4 | Car | 93 | 80.66 | Chi-square | 14.662 |
| | Bus | 99 | 111.38 | df | 1 |
| | Total | 192 | | Asymp. Sig. | .000 |
| Test 5 | Car | 93 | 69.61 | Chi-square | .069 |
| | Train & Tram | 44 | 67.70 | df | 1 |
| | Total | 137 | | Asymp. Sig. | .793 |

Of the other travel modes, the bus doses (and thus, the cycling dose also) were found to be statistically significantly larger than the car (Chi-square = 14.662, $p < 0.001$). While the doses experienced by the volunteers while travelling by car and either train or tram were found not to be statistically significant from each other (Chi-square = 0.069, $p = 0.793$).

The largest individual contribution of transport uptake to total 24-hour dose was found to be that of a male volunteer whose overall dose uptake while in transport modes (cycling, driving and walking) was 42.6% on one sampling day. Overall though, the dose uptake as a result of travel was found to account for 9.2%, on average, of the total dose uptake of each 24 hour period, with a standard deviation of ±7.2%. The amount of time spent travelling in comparison was on average only 6.8% ($\sigma = 3.8\%$) of a 24-hour

period. Evidently, the dose uptake in the various transport modes was over contributing to the 24-hour dose relative to the amount of time spent partaking in this activity.

### *5.7.7 Comparison between two dose methods*

In previous personal exposure studies, the dose uptake of pollutants has been calculated in a number of different ways. The ICRP model, for example, has been employed by McNabola et al. (2008b) to calculate dose uptake of commuters in Dublin. However, the most common method in the literature is based on the following equation:

$$Dose = C \times IR \times ED \qquad \text{Eqn. 5.13}$$

Where $C$ is the concentration of the air pollutant ($\mu g/m^3$), $IR$ is the inhalation rate ($m^3/hr$), and $ED$ is the exposure duration (hours). This equation forms the basis for calculation of dose in numerous studies.

O'Donoghue et al. (2007a) calculated the dose of hydrocarbons by using the average concentrations collected while commuting and breathing rates for light and heavy exercise of both males and females. Zuurbier et al. (2010) also calculated dose in their comparison of commuting modes study by multiplying ventilation rates by the mean measured concentrations, however in this instance the focus was on particulate pollutants ($PM_{2.5}$, $PM_{10}$, soot). While de Nazelle et al. (2012) and Int Panis et al. (2010) also used the same method for dose uptake of commuters for gaseous and particulate pollutants. Finally, in a pilot study of cyclists at high altitudes, Fajardo and Rojas (2012) sampled $PM_{10}$ along a set route using stationary monitors and calculated dose based on the US EPA's exposure factor handbook. The difference on this occasion was that the average daily dose (ADD) was expressed per kilo of body weight ($\mu g\ kg^{-1}\ d^{-1}$), with the average reference body weights for males and females obtained from the ICRP (1994).

The common theme amongst all the studies mentioned that have calculated dose is that they are all commuter based personal exposure studies, which involve personal exposure sampling along a fixed route with one or more commuter modes. However, it seems dose calculations are confined to this realm, with no known attempt at

quantifying dose for 24-hour personal exposure studies. One contributing factor may be due to insufficient data resolution for microenvironments and activities in the case of the many personal exposure studies that use gravimetric sampling. While the requirement to build a respiratory tract model, such as the ICRP model, to accurately measure dose uptake may be onerous for researchers. Thus, it seemed sensible to compare dose estimation obtained from the human respiratory tract model with the cruder method of Eqn. 5.13.

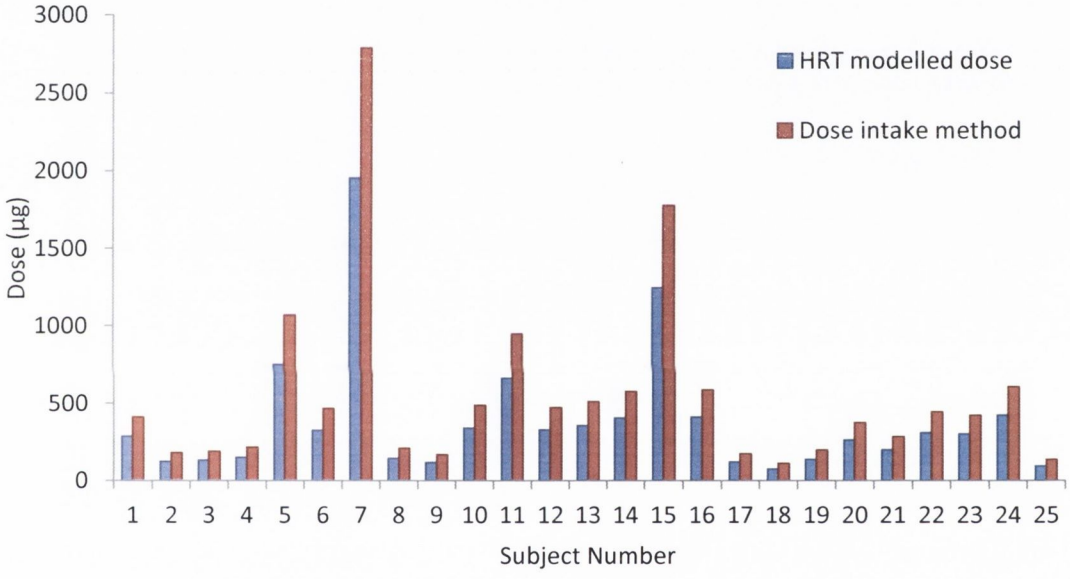


Figure 5.16: Comparison of total dose for 25 randomly selected 24-hour samples using two different estimation methods.

In order to compare the human respiratory tract method with the dose intake method that was commonly used in previous commuter studies, 25 volunteer samples were randomly selected from the overall dataset, which represented nearly 10% of all samples. The random selection of samples was done via Matlab, where specially tailored code was used in order to choose subjects from the overall dataset at random.

In total 12 male and 13 female sampling days were selected by the Matlab routine. For each of the selected samples, the 24-hour doses for each subject were calculated according to Eqn. 5.13. The inhalation rates for this calculation were the same as used in the human respiratory tract model (see Table 5.3), for both males and females. In this

case again, the reference subject respiratory parameters from the *ICRP Publication 66* were used. The calculated total dose for each 24-hour sample using this method was then compared with the human respiratory tract modelled dose (Figure 5.16).

The dose calculations using the intake method (Eqn. 5.13) were found to be greater than the human respiratory tract model on each occasion. This can be explained due to the respiratory tract model accounting for the expulsion of some of the inhaled particles during the exhalation of a breathing cycle. In contrast, the dose intake method assumes that all particles inspired are subsequently retained in the respiratory system, and therefore overstates the dose uptake.

## 5.8 Summary

In summary, the creation of the ICRP respiratory tract model enabled the personal exposures to $PM_{10}$ of the study population to be converted into dose uptake, which is relevant from a health viewpoint. This is due to the fact that not all PM inhaled from the ambient air is retained in the respiratory tract. Furthermore, the level of respiration and the physiological state of an individual, such as their lung capacity and so forth, will have a large bearing on the amount of particulates that enter their respiratory tract. As illustrated by the parameters of the lung model given, males will have higher ventilation rates and larger lung capacity than their female counterparts. Thus, the human respiratory tract model allowed for many of these factors to be accounted for when calculating dose.

The microenvironment found to contribute the largest amount of dose over 24 hours across the study population was while subjects were at work. This microenvironment had on average over twice the dose uptake associated with it than when the subject was active in their home. This can be attributed to a combination of higher personal $PM_{10}$ concentrations present, elevated breathing rates due to more time moving around, and finally, a longer duration on average spent at work than being in the home (excluding sleeping). The second highest dose was found to occur while individuals were exercising or playing sport. Even though the duration of these activities would last for

perhaps an hour, the high breathing due to the intensity of the activity would ultimately lead to a relatively high uptake of PM dose. In contrast, the activity of sleeping was often the activity that subjects spent the longest duration doing, however, this had a far lower dose uptake observed than those previously mentioned. This was due to the low breathing rate associated with this activity, and also the very low personal exposure concentrations found when people slept.

In other analysis, the male and female 24-hour dose uptakes were found to differ among the study population. This difference between the genders was statistically significant and was perhaps expected as the male inputs into the model for breathing characteristics, such as greater breathing capacity and frequency, meant that more particulates would migrate into the respiratory tract. Any deviation from this expected outcome may have been attributed to activity pattern differences, however, this was not the case as male and females followed more or less the same patterns.

The dose uptake that was calculated for the smoking population in the study highlighted the effect of the large concentrations that environmental tobacco smoke exerts on a microenvironment. As expected the in home dose uptake of smokers was far higher than that of non-smokers, and several times greater in magnitude in most cases. The dose of smokers compared to non-smokers was on average approximately 150% greater while the subjects were active in their homes. Perhaps more importantly from a health stand point, the dose uptake while sleeping was also twice as high in the homes of smokers than that of the non-smokers.

The analysis of the additional smoker data gathered by Smokers A and B was also consistent with the increased dosage values. These doses calculated in the model for the two smokers were for female subjects, although it is important to emphasis the dosages for males in these microenvironments would have been greater due to having a larger breathing capacity. The health of smokers is clearly going to be detrimentally impacted by virtue of the fact they are smokers in the first instance. However, the lingering effects of ETS seen in the analysis may exasperate the health effects further, with larger dose uptake even while sleeping than non-smokers experience. Garnering knowledge of

dose uptake of smokers may prove useful when quantifying the dose uptake for non-smokers who are subjected to ETS in certain microenvironments, whether it is a temporary sojourn in a location containing ETS or indeed in their own home. The impact on non-smokers living with smokers is particular pertinent (as was the case in the home of Smoker A). Individuals in residency with smokers will constantly be subjected to inflated particulate levels and other toxic gases, and this personal exposure and subsequent dose uptake will have an impact on the health of the individual.

The examination of the travel modes reported in the study by volunteers revealed that the activity of walking had the largest dose uptake of all modes. This activity, along with cycling, was assigned a higher exercise level in the model than the enclosed transit modes and therefore explains the elevated dose uptake. Travel by bus was not statistically significant from cycling, owing to relatively high personal concentrations found on buses throughout the sampling campaign. However, both bus and cycling were found to be statistically larger than the other enclosed transport modes such as car, train, and tram. The percentage of the total daily dose uptake amongst subjects was also found to be greater relative to the amount of time they spent in the transport microenvironment. Unlike previous studies, this time spent in the various transport environments was an accumulation of the different movements of the individuals throughout the day and were not exclusively rush hour commutes.

Finally, the last act of this chapter was to compare the dose obtained from using the human respiratory tract model with another common dose calculation method used in personal exposure studies. The dose estimation used in numerous commuter personal exposure studies relied upon calculating the dose intake, calculated by the measured breathing rate of the commuters multiplied by the pollutant concentration and duration. However, this assumed all particles were deposited once inhaled, which was not the case. The human respiratory tract model, however, did account for the exhalation of a portion of inhaled particles. The end result was the over estimation of dose when using the dose intake calculation, when compared to the respiratory tract model. In other studies the human respiratory tract model may be a useful tool where more detailed

knowledge is known, such as weight, age, height and specifically measured breathing rates for the particular activity of interest.

# Chapter 6

## Exposure Modelling

# 6 Exposure Modelling

In the previous sections, the results from the human personal exposure study provided important information for understanding the $PM_{10}$ exposures of the Dublin City study population. However, even though this information may be very useful, there are limitations when conducting personal exposure studies.

In general, personal exposure studies are expensive to conduct, particularly for population based studies that need a large number of participants. The costs incurred when conducting a large exposure study can be significant due to the amount of resources and manpower required, additionally, many studies offer financial incentives in order to recruit participants. Personal exposure studies are also burdensome on participants, which can cause problems with retaining participants and also with including at risk groups such as children, the elderly, and people with cardiac and lung diseases. The retention of participants was certainly an issue in this particular study as a number of participants discontinued monitoring after one or two sampling periods. In addition, result from a personal exposure study may only be applicable to the individual participants in the study and not representative of the general population. Therefore, personal exposure modelling is desirable as a potential solution to these problems.

## 6.1 Introduction to Exposure Modelling

Personal exposure modelling can prove to be a useful tool for the understanding of human exposures to environmental contaminants, provided the existence of a sufficient dataset in order to develop a model. The underlying concept of exposure models is to combine microenvironmental concentrations with human activity data to estimate the personal exposure of an individual, and to allow analysis of various exposure factors that influence personal exposures. The United States National Academy of Sciences suggests the following model as the fundamental expression for estimating inhalation exposure to an airborne agent (NAS, 1991):

$$E = \sum C_{ijk}\, t_{jk} \qquad \text{Eqn. 6.1}$$

Where $E$ is the inhalation exposure, the output of the modelling effort, $C_{ijk}$ is the concentration of air pollutant $i$ in microenvironment $j$ where subject $k$ spends time, and $t_{jk}$ is the time spent by subject $k$ in microenvironment $j$.

As an expansion on the model presented in Eqn. 6.1, Moschandreas et al. (2002) recommend a more detailed generic exposure model that should be considered in studying inhalation exposure to PM and its constituents. The following model (Eqn. 6.2) estimates total exposure as a sum of exposures at each of the microenvironments.

$$E_{ijk} = \sum_{ik}^{outdoors} C_{ik}t_{ik} + \sum_{ik}^{indoors} C_{ik}t_{ik} + \sum_{ik}^{occupational} C_{ik}t_{ik} + \sum_{ik}^{in\ transit} C_{ik}t_{ik} \qquad \text{Eqn. 6.2}$$

The symbols and subscripts of this of this equation denote variables indicated in Eqn. 6.1. The four microenvironments included in Eqn. 6.2 are the main ones to be addressed, although if other microenvironments are available they too can be included. If concentrations are not assumed to be constant over time, then the above equation involves integration over time.

Population exposure models use a statistical approach to randomly sample from distributions of available data for each exposure factor and predict the distribution of exposures of the population. The input distributions encompass the variability in the exposure factor data across many individuals and conditions, and the predicted distribution of exposures provides the range in exposures for the population of interest. Population exposure models also have limitations when there is insufficient data available to characterise variability in the exposure factors (Burke et al., 2001).

## 6.2 Exposure Model Development

In order to further assess the $PM_{10}$ personal exposure of the study population, models were developed to predict personal exposure based on the measured personal $PM_{10}$ concentration data in the various microenvironments, the time activity diaries, and GPS data. The initial models were based on the concepts of exposure modelling as presented previously.

The overall personal exposure study data set was divided into two separate and independent data sets which were used for the development and validation of the personal exposure models. In the development stage of the model, 90% of the collected 24-hour personal exposure samples (230 samples) were used to develop the model, while the remaining 10% of the samples (25 samples) were kept aside for validation purposes. The data for validating the model was chosen by a specially developed routine in Matlab for this task. The Matlab code randomly chose and removed 25 sampling days from the main dataset and stored them in separate file for use later during testing.

### *6.2.1 Integrated time-activity models*

There were two separate time activity weighted models used in order to predict personal exposure of the study subjects. The first model (Model 1) that was used was a time-activity weighted model based on the sum of the fraction of time in each microenvironment visited multiplied by the concentration in the microenvironment. For this model the microenvironment concentrations that were used were an average concentration based on the pooled population mean for the particular microenvironment. This time activity weighted model is shown as follows in Eqn. 6.3.

$$PE_{ij} = \frac{1}{T_{ij}} \sum C_k \times t_{ijk} \qquad \text{Eqn. 6.3}$$

Where $PE_{ij}$ is the personal exposure of person $i$ on day $j$, $t_{ijk}$ is the time spent in microenvironment $k$ by person $i$ on a day $j$, and $T_{ij}$ is the total time the subject $i$ spends

in all microenvironments on a day $j$. $C_k$ is the concentration representative of microenvironment $k$, and is a mean $PM_{10}$ concentration based on the overall data collected for each microenvironment in the study.

The second version (Model 2) of the time-activity weighted modelling technique used was similar to the previous model used in Eqn. 6.3. However, in this case the model used to predict personal exposure was a time-activity weighted model based on the microenvironmental concentration data from the specific individual. This model predicted personal exposure to $PM_{10}$ by integrating the time fraction spent in each individual microenvironment multiplied by the $PM_{10}$ concentration found in each of these visited microenvironments. The model is shown in Eqn. 6.4.

$$PE_{ij} = \frac{1}{T_{ij}} \sum C_{ik} \times t_{ijk} \qquad \text{Eqn. 6.4}$$

In this equation $PE_{ij}$ is again the personal exposure of person $i$ on a day $j$, $t_{ijk}$ is the time spent in microenvironment $k$ by person $i$ on a day $j$, $C_{ik}$ is the concentration representative of microenvironment $k$ for person $i$, and $T_{ij}$ is the total time the subject $i$ spends in all microenvironments on a day $j$. The $PM_{10}$ concentrations were unique to the subject as the concentrations used in this equation were based on the data directly collected by the volunteer over the course of their sampling. Thus, the mean concentrations for the subject's microenvironments such as home, work place, commutes and so on were used in this model.

### *6.2.2 Model evaluation*

In an article entitled '*Air Quality Model Evaluation and Uncertainty*', Hanna (1988) states that the fundamental model performance measures are the mean bias, the mean square error, and the correlation. Thus, model evaluation in this chapter will be carried out using some of these metrics.

The normalised mean bias (NMB) has been used to evaluate air pollution personal exposure models previously (Delgado-Saborit et al., 2009). The NMB is a measure of

the over or under estimation of a model, where positive values indicate over prediction and negative values indicate under prediction of a variable and is often expressed as a percentage. The mathematical expression for NMB is shown in Eqn. 6.5.

$$NMB = \frac{\sum_{i=1}^{N}(Y_{modelled} - Y_{observed})}{\sum_{i=1}^{N} Y_{observed}} \times 100 \qquad \text{Eqn. 6.5}$$

Where $Y_{modelled}$ is the predicted personal $PM_{10}$ concentration from the specific model, $Y_{observed}$ is the experimentally measured personal exposure concentration, and $N$ is the total number of samples in the testing dataset.

The other metric used in order to evaluate the models was the mean-squared error (MSE). MSE is a measure of the average of the square of the errors between the predicted and observed values. It is one of a number of ways to quantify the difference between values implied by an estimator and the true values of the quantity being estimated, and is arguably the most important criterion used to evaluate the performance. The MSE is a good overall measure of model performance and is easily interpreted as it has the same units as the modelled quantity. The formula for MSE can be seen below in Eqn. 6.6.

$$MSE = \frac{1}{N}\sum_{i=1}^{N}(Y_{modelled} - Y_{observed})^2 \qquad \text{Eqn. 6.6}$$

The reason for using a squared difference to measure the "loss" between $Y_{modelled}$ and $Y_{observed}$ is mostly convenience; properties of squared differences involving random variables are more easily examined than, say, absolute differences. The reason for taking an expectation is to remove the randomness of the squared difference by averaging over the distribution of the data. The MSE allows statistical models to be compared as a measure of how well they explain a given set of observations. A value of zero for the MSE of a model would mean the estimator predicted the observations with perfect accuracy, however, in reality this is practically never possible. For the purpose of communicating results in this chapter, the root mean square error (RMSE), rather

than the MSE, is used. This is because the RMSE is measured in the same units as the data, rather than in squared units, and is representative of a "typical" error. The equation for RMSE is displayed in Eqn. 6.7.

$$RMSE = \sqrt{\frac{1}{N}\sum_{i=1}^{N}(Y_{modelled} - Y_{observed})^2} \qquad \text{Eqn. 6.7}$$

The final gauge for the goodness-of-fit of a model was Pearson's correlation coefficient, denoted *R*. The Pearson correlation coefficient is a measure of the strength of a linear association between two variables, in this case between the modelled and observed personal exposure values. The correlation coefficient ranges from -1 to 1. A value of 1 implies that a linear equation describes the relationship between variables *x* and *y* perfectly, with all data points lying on a line for which *y* increases as *x* increases. A value of -1 implies that all data points lie on a line for which *y* decreases as *x* increases. Finally, a value of zero implies that there is no linear correlation between the variables.

## 6.3 Integrated Time-Activity Model Results

The data from the 25 randomly selected individual 24-hour samples were separated from the main dataset and used to validate the time-activity weighted models described in Section 6.2.1. Each of the 25 sampling days was inputted into the two models and the results of which have been graphically plotted. The individual 24-hour personal $PM_{10}$ exposure concentrations of the experimentally gathered data and the simulated data from both of the integrated time-activity models were plotted against each other and are shown in Figure 6.1.

The results of the first time-activity weighted model (Eqn. 6.4) were compared against the measured personal concentrations and are shown in Figure 6.2. For this model the concentrations used were based on the population means for each microenvironment. The result from this model indicated that the time-weighted model had a Pearson's

correlation coefficient of 0.24. The model also had a RMSE of 8.5 $\mu g/m^3$ and a NMB percentage of 12.7%.

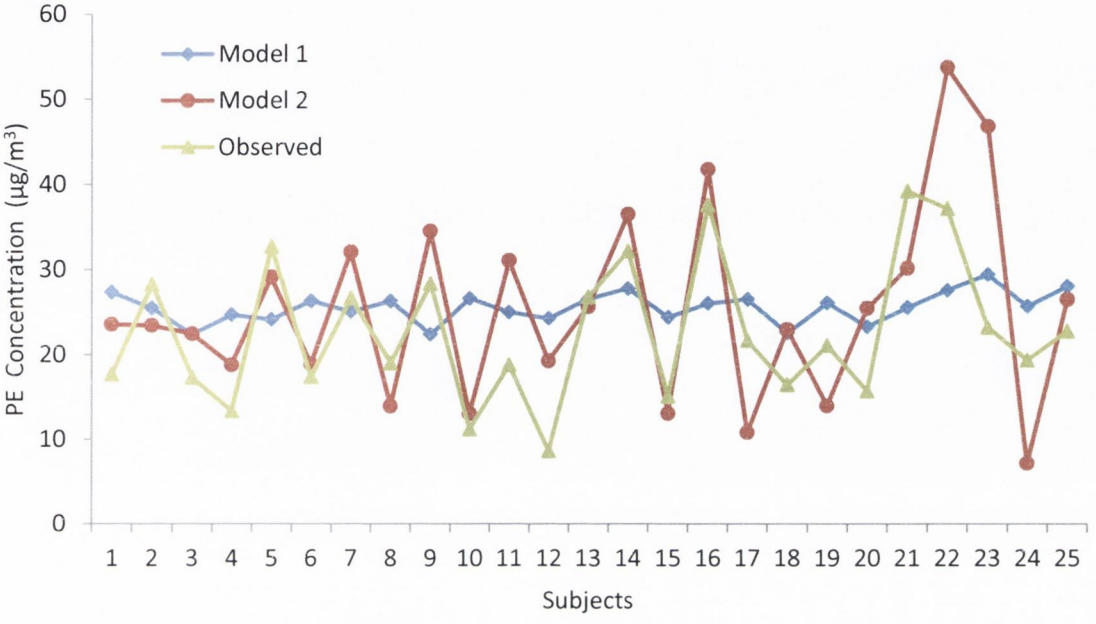


Figure 6.1: Plot of the 24-hour personal exposure concentrations of the observed data (green line), and the simulated 24-hour exposures of Model 1 (blue line) and 2 (red line) for each subject test case.

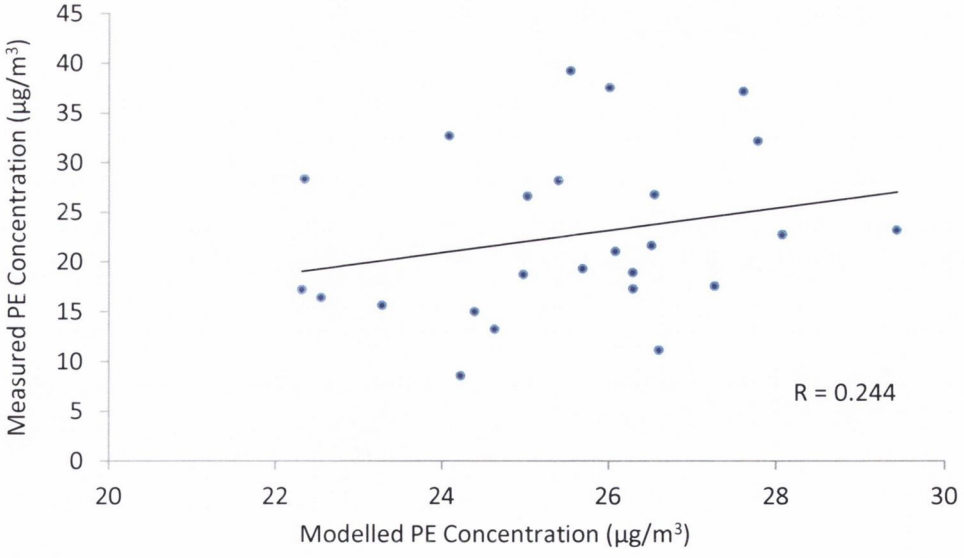


Figure 6.2: Correlation between the simulated 24-hour personal exposure $PM_{10}$ concentrations and the corresponding observed 24-hour concentrations for Model 1.

The second time-activity weighted model was based on the personal concentrations there were measured by the particular subject, rather than the population means as was the case with Model 1. Again, the results obtained from Model 2 were compared against the observed personal exposure concentrations for each subject. The results from this particular model showed that Model 2 correlated much better than Model 1, with a Pearson's correlation of approximately 0.67. The RMSE for the model was found to be 8.8 $\mu g/m^3$ and it had a NMB of 11.9%.

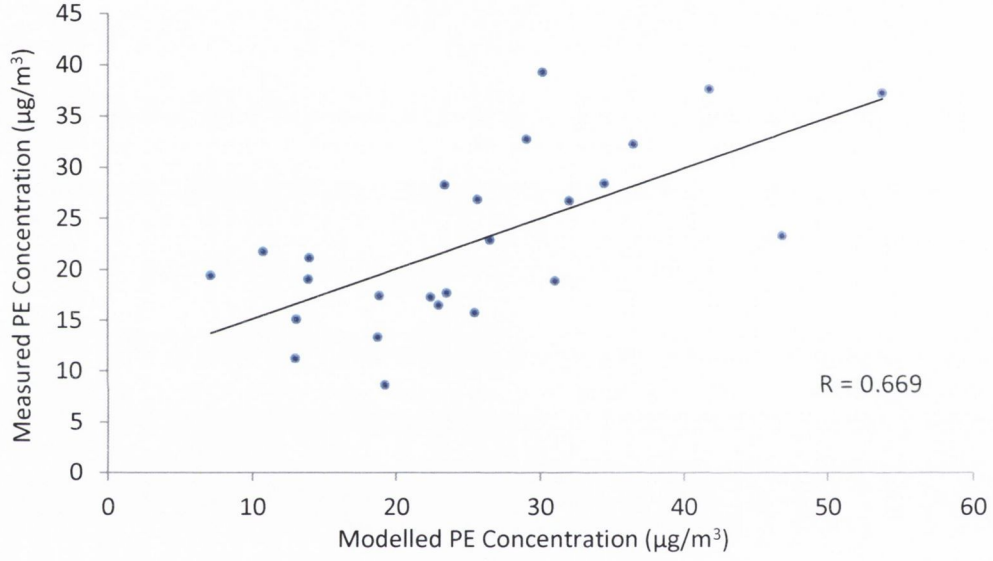


Figure 6.3: Correlation between the simulated 24-hour personal exposure $PM_{10}$ concentrations and the corresponding observed 24-hour concentrations for Model 2.

Whilst the RMSE and NMB of both Model 1 and 2 were very similar, the Pearson's correlation was much improved for Model 2. The impact of this larger correlation coefficient can be inspected visually in Figure 6.1, whereby the outputs of Model 2 are generally more responsive to the increases and decreases of the observed concentrations. The histograms of 25 of the observed personal exposure concentrations, the exposures obtained from Model 1, and the exposures from Model 2 are all shown in Figure 6.4. As seen from this figure, the results from Model 2 mirror the distribution of the observed values with greater accuracy. In contrast, the Model 1 personal exposure results are far more narrowly distributed around mean personal exposure concentration.

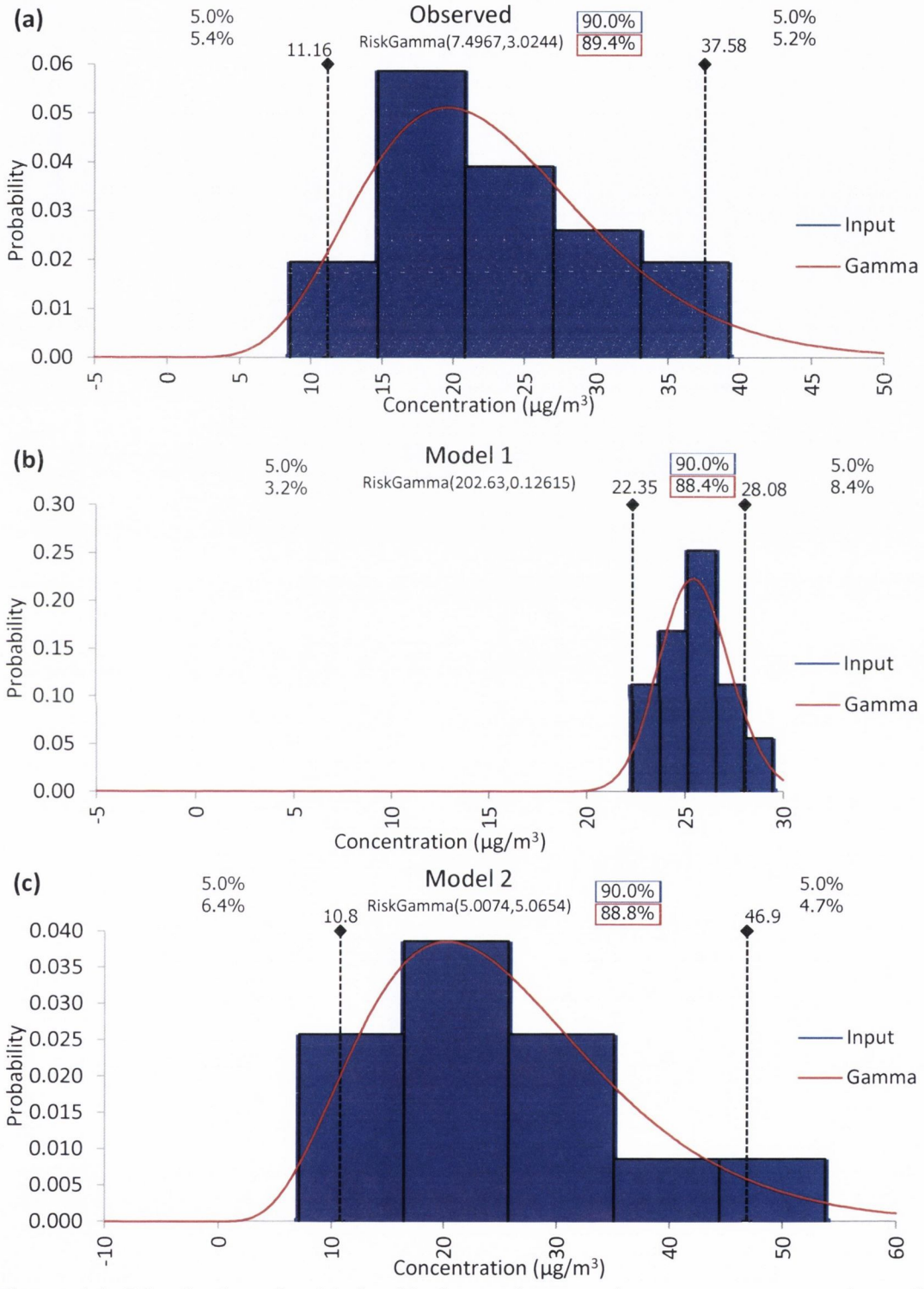


Figure 6.4: Distributions for (a) the 25 observed personal exposure concentrations, (b) the results obtained from Model 1, and (c) the results obtained from Model 2.

The population percentiles for the personal exposure distributions from Model 1 and 2 are presented and compared with the 25 experimentally sampled personal exposures in Figure 6.5. The figure demonstrates that Model 1 displayed little variability in forecasting the personal exposure concentrations, with all the predicted personal exposures of the volunteers lying between 22.3 $\mu g/m^3$ and 28.1 $\mu g/m^3$. However, the actual personal exposures (observed) values were seen to vary between 11.1 $\mu g/m^3$ and 37.6 $\mu g/m^3$. In contrast from Model 1, the results from Model 2 follow the trend of the 'Observed' line well in Figure 6.5. The predicted personal exposures from Model 2 vary between 10.8 $\mu g/m^3$ and 46.9 $\mu g/m^3$, although the model does slightly over estimate percentile exposures for the population.

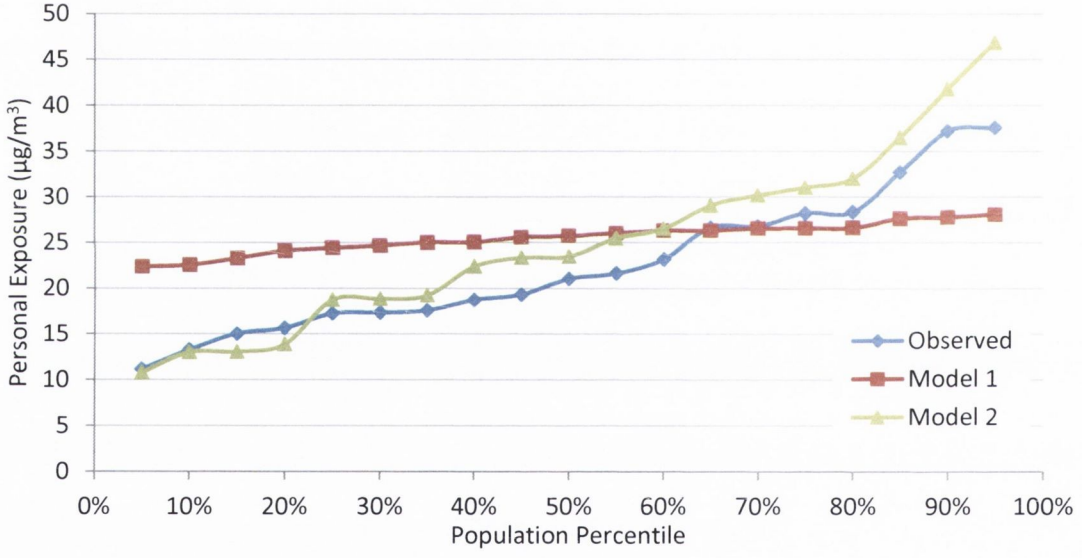


Figure 6.5: Comparison of the exposure distributions for the 25 observed concentrations, Model 1 results, and Model 2 results.

## 6.4 Exposure Simulation

This section describes the development of a Monte Carlo based simulation model system for the assessment of the integrated daily $PM_{10}$ personal exposures of the study population. The use of such models may prove useful in calculating public exposure for certain scenarios and assessing any health gains of environmental policies.

### *6.4.1 Population exposure simulation*

The first model developed using a Monte Carlo based technique was a simulation of the study population exposures. The term Monte Carlo is the name given to the technique of using random or pseudo-random numbers to sample from probability distributions. The input distributions can then be recreated with sufficient iterations of the Monte Carlo sampling.

This population model followed a similar format as that laid down in the *EXPOLIS* study (Jantunen and Kansanterveyslaitos, 1999). The sampling method used was also the method of Latin hypercube sampling (or LHS). This method offers improved sampling over traditional Monte Carlo sampling as the probability distributions are split into $n$ intervals of equal probability, where $n$ is also the number of iterations to be performed on the model. An example of stratification created for a normal distribution with 20 iterations is illustrated in Figure 6.6. The bands can be seen to get progressively wider towards the tails as the probability density drops away. In the first iteration one of these intervals is selected using a random number, and then a random number is selected from this interval. The process is repeated for all iterations, and after each iteration the chosen interval is marked as having already been used and therefore will not be selected again (Vose, 2008).

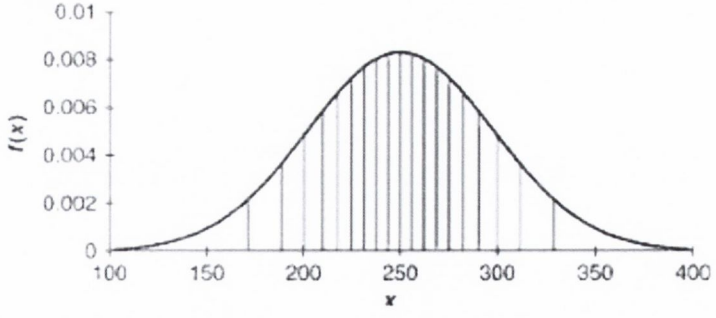


Figure 6.6: Example of the effect of stratification in Latin hypercube sampling (Vose, 2008).

In this microenvironmental model the personal exposure is the total of partial exposures determined by the combination of concentration of personal $PM_{10}$ in a

microenvironment and the time an individual spends in that microenvironment. The equation of which it is based on has been previously shown in Eqn. 6.1. In each microenvironment a homogeneous personal $PM_{10}$ exposure concentration was assumed also.

As already mentioned, a similar population exposure risk analysis was implemented as part of the *EXPOLIS* study. The model developed as part of that study was for personal $PM_{2.5}$ and was modelled on a general working population group between 25 to 55 years of age in Helsinki, Finland. However, the personal $PM_{2.5}$ exposure data was gathered using a gravimetric method, thus, the input concentration data was limited to generalised categories such as 'home indoors', 'home outdoor', 'work indoor', as well as small amounts of data for 'other indoor' and transport modes. Many of the relevant indoor microenvironments where there was no direct information on the concentration distributions had to be estimated indirectly using the outdoor concentration and penetration factors.

The study population consisting of purely office workers in this study enables more accurate simulation due to the relatively homogeneous nature of the population group, who follow more or less the same activity patterns. Also the main advantages of this study over the *EXPOLIS* study, for example, is that the distributions for each of the microenvironments visited by the subjects can be defined based on the real-time data collected, rather than relying heavily on estimation of personal exposures.

The model was implemented in the risk analysis software package @Risk (version 6.0, Palisade Corp.), which is an add-on programme to Microsoft Excel. The inputs to the model were the microenvironment concentrations ($C_i$) and the fraction of time ($f_i$) the population spent in each microenvironment. The input distributions of $C_i$ were defined first using the distribution fitting tool in @Risk, which fitted a specific distribution for microenvironments based on the sampled dataset of each. The distribution fitting had a lower bound limit of zero, but no upper limit, and the fitted distribution for each microenvironment was selected according to which was ranked the highest statistically. The statistical tests carried out for each type of distribution included the Akaike

information criterion (AIC), Bayesian information criterion (BIC), Chi-squared, Kolmogorov-Smirnov, and the Anderson-Darling statistics, all upon which the appropriate probability distribution was determined.

The application of the distribution fitting tool in @Risk on the main dataset enabled accurate probability distributions to be modelled for each microenvironment or activity. In the *EXPOLIS* study the air pollutant distributions for each microenvironment were assumed to follow a lognormal distribution. However, for this study specifically modelled distributions could be attained as a result of the real-time data gathered during monitoring campaign. The probability distributions for each microenvironment and activity are shown in Table 6.1.

Table 6.1: The types of distributions assigned to each of the main microenvironments and activities.

| **Microenvironment/ Activity** | **Type of Distribution** | **AIC** | **Distribution μ** ($\mu g/m^3$) | **Distribution σ** ($\mu g/m^3$) | **Input μ** ($\mu g/m^3$) | **Input σ** ($\mu g/m^3$) |
|---|---|---|---|---|---|---|
| Bus | Gamma | 932.1 | 43.1 | 30.1 | 43.1 | 31.6 |
| Café/Restaurant | Log-Logistic | 571.9 | 48.3 | 71.1 | 53.3 | 84.7 |
| Car | Gamma | 832.4 | 32.7 | 27.4 | 32.7 | 27.5 |
| Cycling | Log-Logistic | 551.9 | 25.8 | 63.5 | 24.5 | 24.7 |
| Home | Log-Logistic | 2049.5 | 27.1 | 23.0 | 26.4 | 20.7 |
| Other Indoor | Log-Logistic | 750.6 | 79.8 | N/A | 67.1 | 67.9 |
| Other Outdoor | Log-Normal | 267.7 | 21.6 | 25.8 | 20.9 | 20.7 |
| Pub | Log-Logistic | 141.5 | 43.8 | 42.7 | 43.7 | 35.1 |
| Recreation/Sport | Log-Normal | 313.6 | 60.0 | 60.8 | 58.2 | 46.3 |
| Shopping | Log-Logistic | 570.8 | 44.3 | 119.0 | 42.7 | 44.4 |
| Sleep | Pearson 6 | 1575.2 | 9.9 | 8.6 | 9.9 | 8.2 |
| Train | Gamma | 286.5 | 26.7 | 15.3 | 26.7 | 15.6 |
| Tram | Weibull | 75.0 | 14.4 | 8.2 | 14.5 | 8.4 |
| Walk | Log-Logistic | 1782.4 | 29.4 | 42.0 | 28.5 | 28.0 |
| Work | Pearson 6 | 2266.6 | 39.1 | 35.5 | 39.1 | 35.7 |

The time fraction inputs ($f_i$) of the model were defined using the population time activity data from Chapter 4. The population time activity means are shown in the Table

4.1, and along with the standard deviation of these times, were used to define beta distributions for the time fractions. A beta distribution is a continuous probability distribution defined on the interval [0, 1] and parameterised by two positive exponents, denoted by $\alpha$ and $\beta$, which control the shape of the distribution and hence are called shape parameters. The shape parameters were calculated according to Eqn. 6.8 and Eqn. 6.9.

$$\alpha = \left(\frac{1-\mu}{\sigma^2} - \frac{1}{\mu}\right) \times \mu^2 \qquad \text{Eqn. 6.8}$$

$$\beta = \alpha \times \left(\frac{1}{\mu} - 1\right) \qquad \text{Eqn. 6.9}$$

In the above equations, $\mu$ denotes the mean population time spent in a microenvironment or doing an activity, while $\sigma$ is the standard deviation for the time fractions. Once $\alpha$ and $\beta$ were calculated for each microenvironment, the beta distribution for the time fractions were created. An example of the beta distribution used for the time fraction ($f_i$) spent 'at work' for the population is illustrated in Figure 6.7.

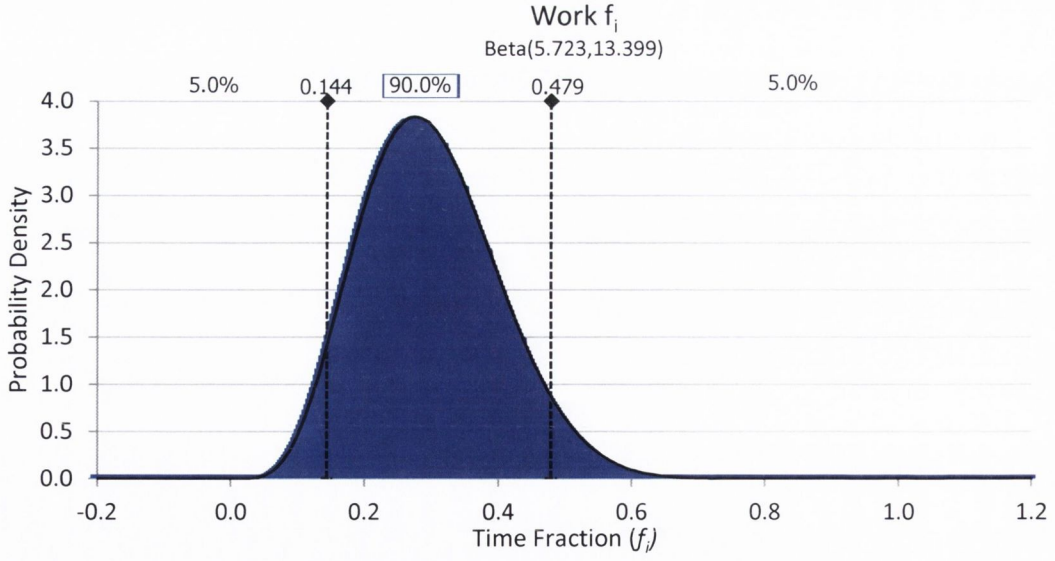


Figure 6.7: Beta distribution for the population time fraction of time spent at work.

The total of the various beta distributions for each microenvironment was required to equal unity (a 24-hour day) in order to correctly calculate the total daily exposure. This was achieved by dividing each individual time fraction, returned by the beta distributions, by the sum of all these time fractions. Once the microenvironment concentration distributions and their corresponding time fraction beta distributions were established, the model could be run.

The model was setup in the following manner. The simulation was run just once and the number of iterations was set to 10,000. As previously explained, the sampling type used was Latin hypercube, however in the intervening time span since the *EXPOLIS* researchers carried out their work, random number generation for this sampling technique has moved on. The random number generator is now carried out in @Risk using a Mersenne twister, which is a pseudorandom number generator developed in 1997 by Matsumoto and Nishimura that is based on a matrix linear recurrence over a finite binary field $F_2$. It was designed specifically to rectify many of the flaws found in older algorithms, and provides fast generation of high-quality pseudorandom numbers.

The simulated 24-hour personal exposures are compared graphically to the observed exposures in Figure 6.8. As can be seen in the figure, the simulated population exposure model closely mimics the experimentally observed 24 hour personal exposure of the population. Numerical comparisons of the modelled and the observed means, standard deviations, medians, and percentiles are also presented in Table 6.2.

Table 6.2: Observed and simulated population exposure distribution values ($\mu g/m^3$).

| | **Mean** | **SD** | **Median** | **Max** | **Percentiles** | | | | |
|---|---|---|---|---|---|---|---|---|---|
| | | | | | 25% | 50% | 75% | 90% | 95% |
| Observed | 25.5 | 15.3 | 21.6 | 105.7 | 14.9 | 21.6 | 32.3 | 46.9 | 52.3 |
| Model | 26.1 | 14.6 | 23.0 | 367.0 | 17.0 | 23.0 | 31.7 | 42.6 | 50.3 |

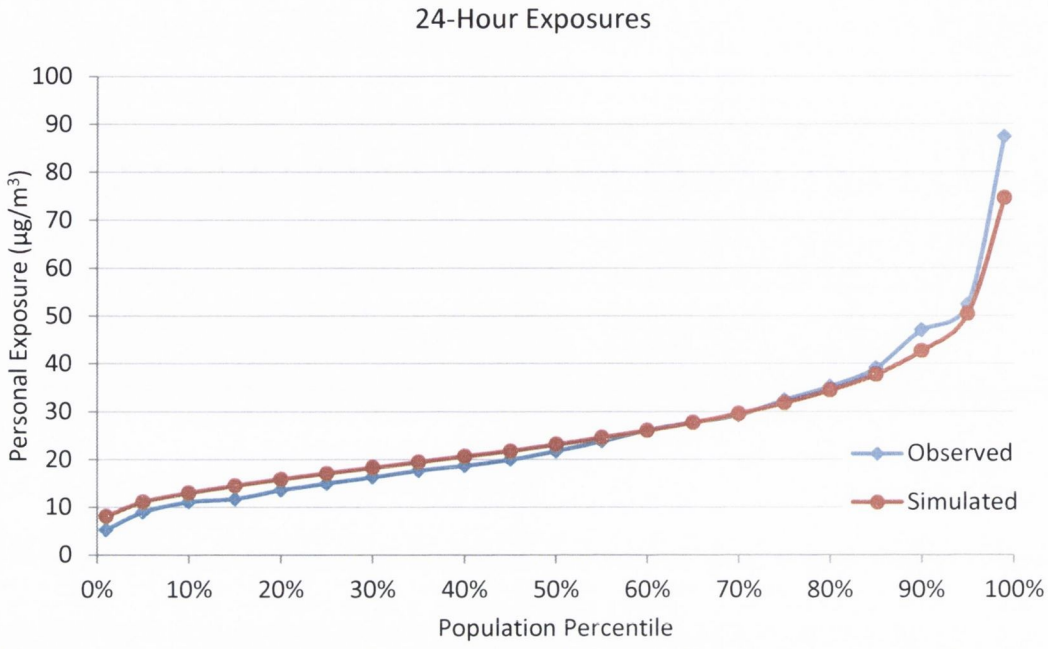


Figure 6.8: Comparison of observed and Latin Hypercube simulated exposure distributions.

The mean and standard deviations were quite similar for both, with the simulation model having a slightly larger mean (26.1 µg/m$^3$) and the observed exposures having the larger standard deviation (15.3 µg/m$^3$). The simulated exposure model also performed well with all percentiles being within 2% of the observed percentiles. However, where there was a large difference between the model and observed exposures was in the maximum exposures. The observed maximum 24-hour personal exposure was 105.7 µg/m$^3$, but the simulation model maximum was 367 µg/m$^3$. This was due extreme concentrations being generated by the Latin hypercube sampling.

The output results in @Risk also enable sensitivity analysis to be carried out on the exposure model. This type of analysis provides an overview of the relative influence of the input variables in determining the result of the output variable. The Spearman's rank correlation coefficients of the total personal exposure output versus each of the inputs are shown in Figure 6.9.

Figure 6.9 illustrates that the personal $PM_{10}$ exposure concentration in the workplace is the mostly highly correlated ($\rho$ = 0.75) with the total 24-hour personal exposure

concentration. This is followed by the $PM_{10}$ exposure concentration while active at home and the concentration while sleeping, which have moderate correlations of $\rho$ = 0.34 and $\rho$ = 0.26, respectively. All other input variables had relatively minor correlations with the total 24 hour personal exposure in the model.

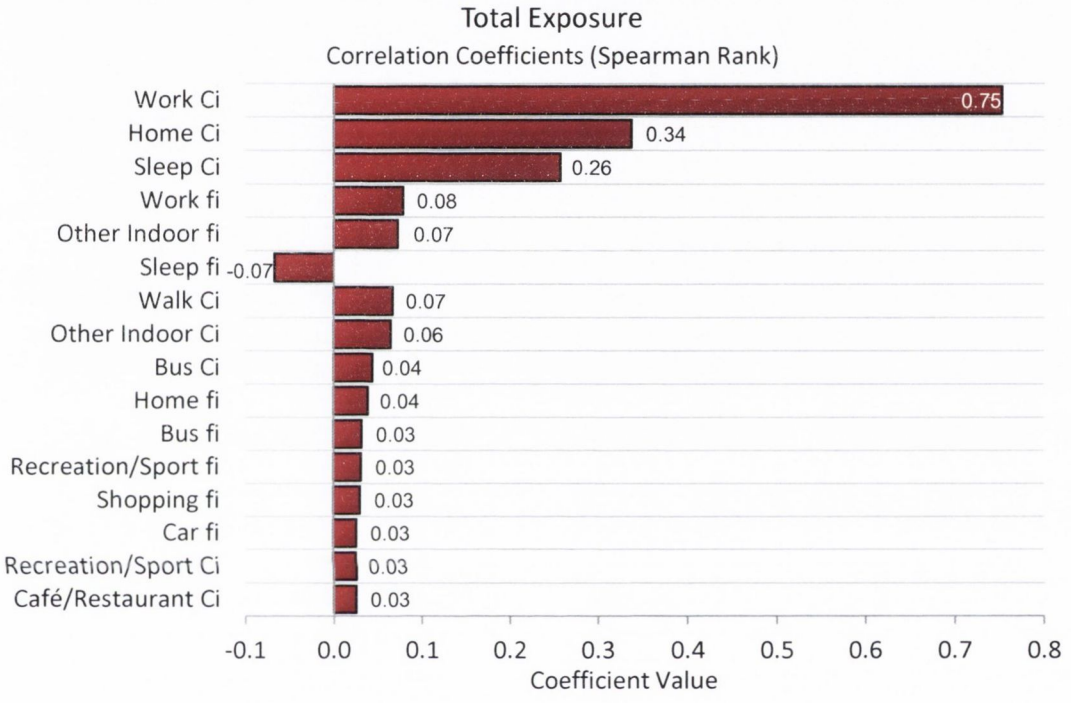


Figure 6.9: Correlation coefficients for simulated total exposure inputs of microenvironment concentrations ($C_i$) and the time fractions ($f_i$).

The extent of which each of the respective input variables could influence the total exposure output is illustrated in Figure 6.10. This figure shows the amount of change in total personal exposure due to a one standard deviation change in the input, while holding the other inputs constant. Thus, a one standard deviation increase in the 'at work' personal exposure concentration of the population would raise the total exposure by just over 10 $\mu g/m^3$.

Following 'at work', the input concentrations of 'at home', 'other indoor', and 'sleeping' had the potential to cause the next largest total exposure concentrations with a one standard deviation increase. Among the time fraction input variables the category

of 'other indoor' and time spent 'at work' could increase total exposure by 1.6 and 1.3 $\mu g/m^3$, respectively, if there was an increase of one standard deviation in either.

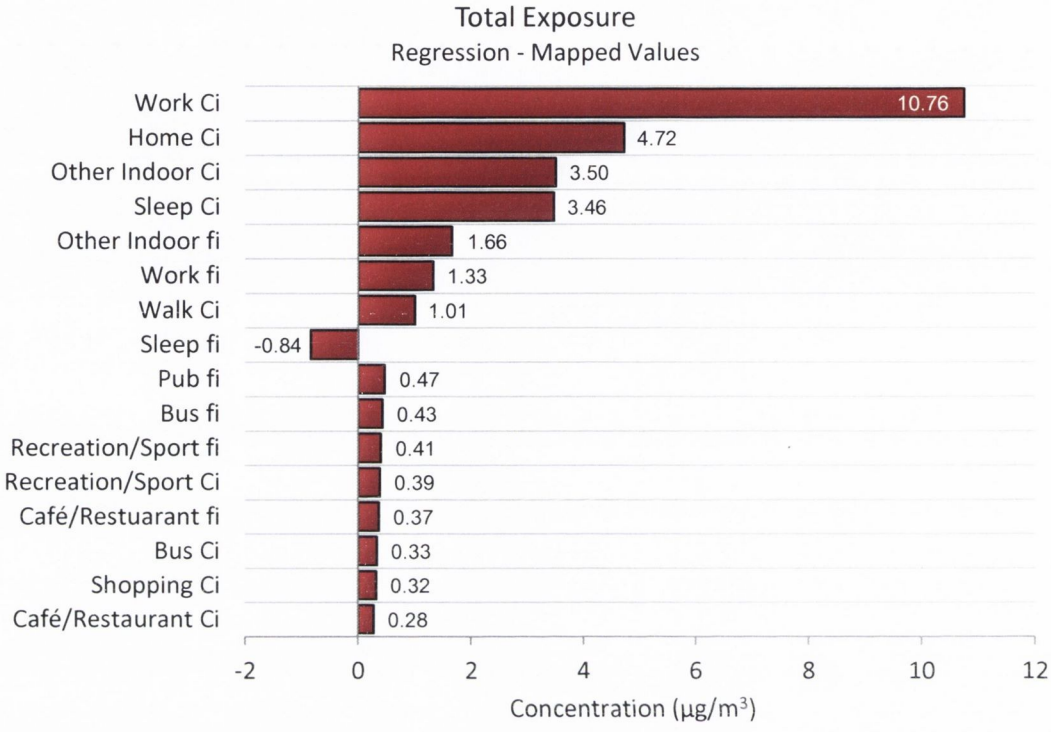


Figure 6.10: Tornado graph of the regression mapped values of the simulation model inputs. Each value represents the change in total exposure with a one standard deviation change in a particular input, with all others held constant.

The results from this population exposure simulation demonstrate that a handful of microenvironments are largely responsible for determining the $PM_{10}$ personal exposure concentration of individuals. The personal exposure concentrations in the home, while active and asleep, as well as the workplace were the most highly correlated to total exposure (Figure 6.9). The degree to which a one standard deviation change in the concentrations of these microenvironments influences total exposure was also highlighted by the regression mapped values in Figure 6.10. It is the impact of occupational exposure that is most consequential to the daily personal exposure of people, and thus, from an environmental health policy perspective, the concentration of air pollutants in workplaces deserves the greatest scrutiny.

### *6.4.2 Individual sample simulation*

In order to evaluate the personal exposure to $PM_{10}$ of individuals further, a probabilistic modelling approach was taken in an attempt to simulate the daily personal exposure of individuals more accurately. The already discussed time-weighted activity modelling approach may prove to be an overly simplistic method of estimating personal exposure, especially for the case of Eqn. 6.4 where the concentration ($C_k$) in microenvironments are set values determined by the population averages. This model ignores important factors such as demographics, as well as the stochastic nature of $C_k$ which can randomly vary over a time period due to random indoor sources. Thus, a model that randomly selects concentrations from probability distributions based on the experimentally gathered data, which accounts for factors such as smoking and gender differences etc., may prove to be more accurate for estimating the personal exposure.

A Monte Carlo approach was again adopted and based on Eqn. 6.4. However, where it differed was that the concentrations of each microenvironment were randomly selected from the population distribution for that specific microenvironment. These distributions were specially designed for each microenvironment again with the aid of the risk analysis software @Risk, and the model was implemented in Matlab (see Appendix F).

In order to simulate the 24-hour personal exposures for the each test subject, a probability density function was first defined for each microenvironment. The probability distributions were based on the personal exposure datasets of each microenvironment gathered by 90% of the study population, while the other 10% of personal exposure samples were used to test the model. The distributions used for each different microenvironment are shown in Figure 6.11, and vary slightly from those summarised in Table 6.1 which represented the entire study population.

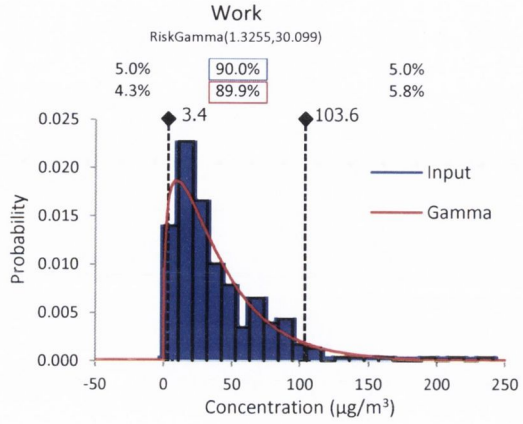
Work
RiskGamma(1.3255,30.099)
5.0%
4.3%
90.0%
89.9%
5.0%
5.8%
3.4
103.6
Input
Gamma
Probability
Concentration (µg/m³)

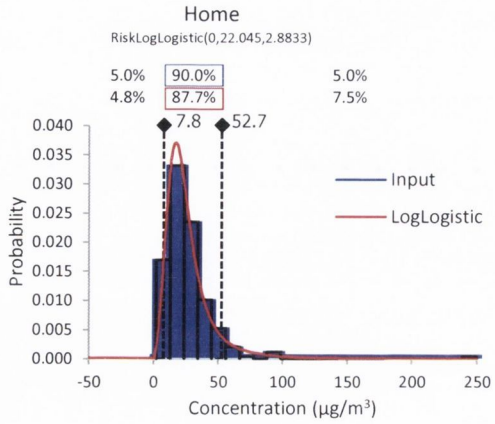
Home
RiskLogLogistic(0,22.045,2.8833)
5.0%
4.8%
90.0%
87.7%
5.0%
7.5%
7.8
52.7
Input
LogLogistic
Probability
Concentration (µg/m³)

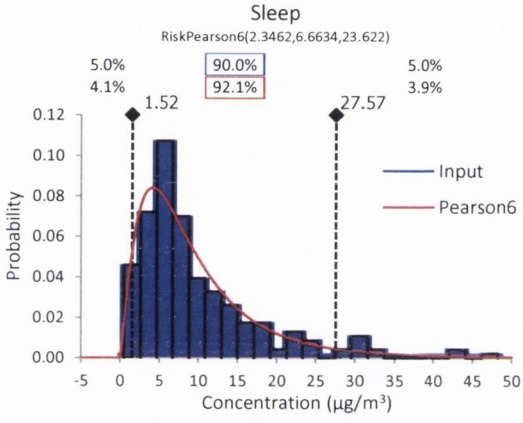
Sleep
RiskPearson6(2.3462,6.6634,23.622)
5.0%
4.1%
90.0%
92.1%
5.0%
3.9%
1.52
27.57
Input
Pearson6
Probability
Concentration (µg/m³)

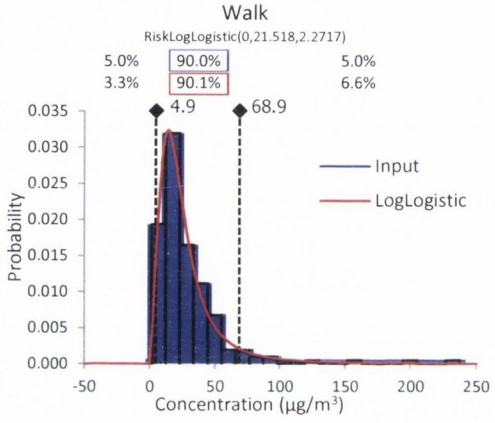
Walk
RiskLogLogistic(0,21.518,2.2717)
5.0%
3.3%
90.0%
90.1%
5.0%
6.6%
4.9
68.9
Input
LogLogistic
Probability
Concentration (µg/m³)

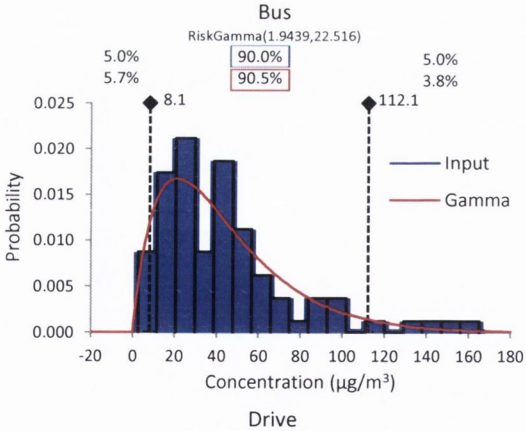
Bus
RiskGamma(1.9439,22.516)
5.0%
5.7%
90.0%
90.5%
5.0%
3.8%
8.1
112.1
Input
Gamma
Probability
Concentration (µg/m³)

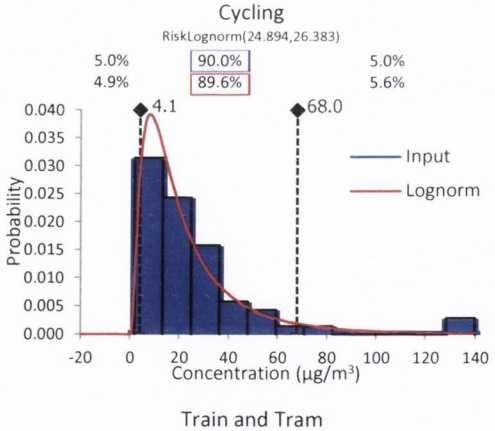
Cycling
RiskLognorm(24.894,26.383)
5.0%
4.9%
90.0%
89.6%
5.0%
5.6%
4.1
68.0
Input
Lognorm
Probability
Concentration (µg/m³)

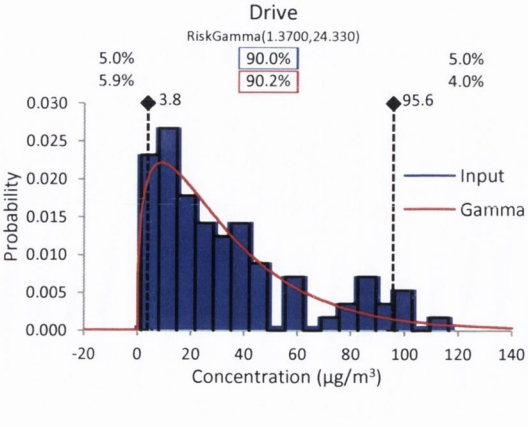
Drive
RiskGamma(1.3700,24.330)
5.0%
5.9%
90.0%
90.2%
5.0%
4.0%
3.8
95.6
Input
Gamma
Probability
Concentration (µg/m³)

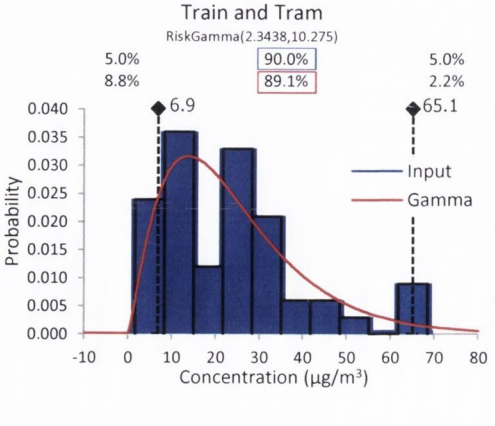
Train and Tram
RiskGamma(2.3438,10.275)
5.0%
8.8%
90.0%
89.1%
5.0%
2.2%
6.9
65.1
Input
Gamma
Probability
Concentration (µg/m³)

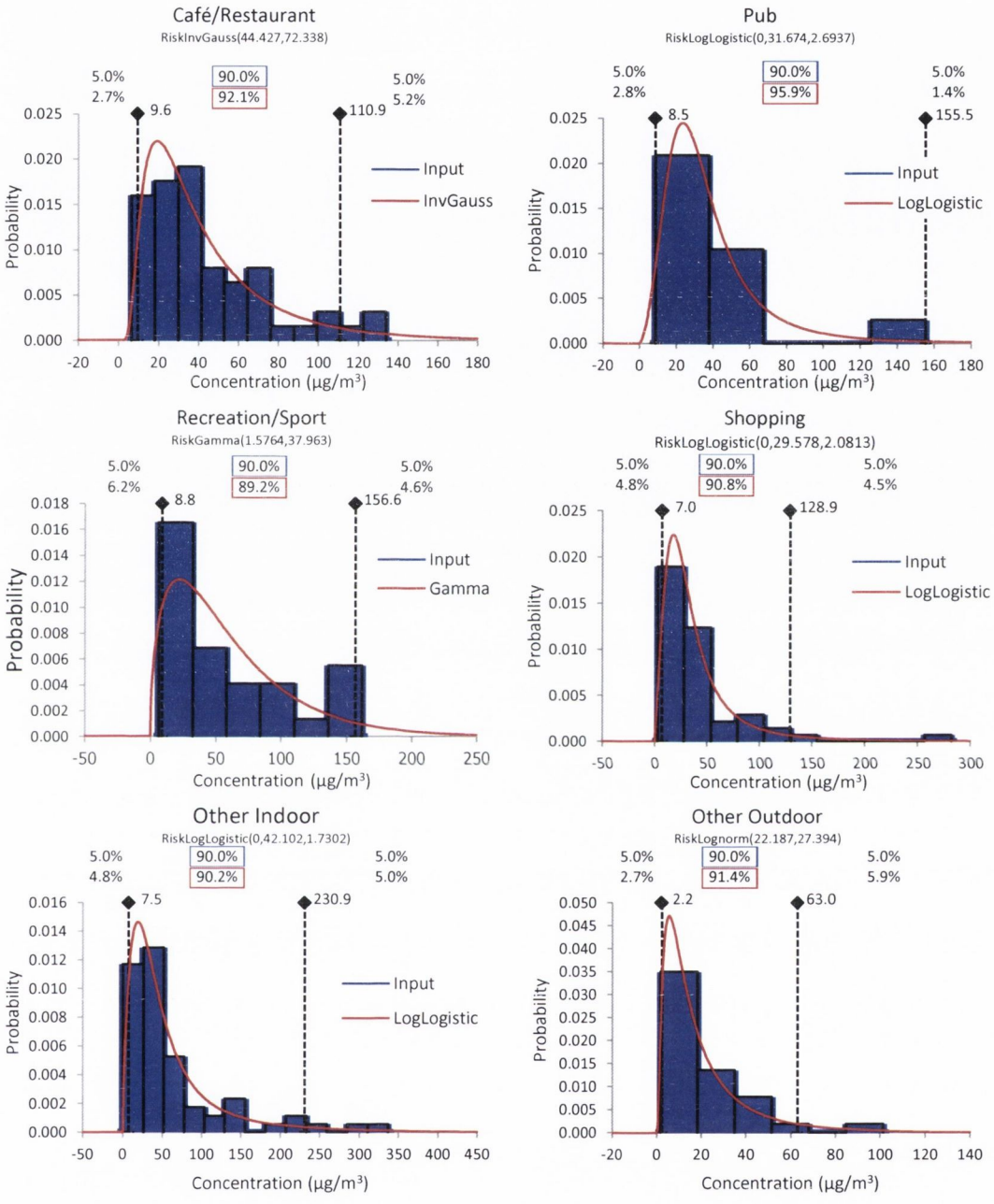


Figure 6.11: The probability distributions for all microenvironments.

Each of the time fractions of the 25 test subjects used in the previous time-weighted models were passed into Matlab and multiplied by the corresponding randomly sampled concentrations sampled from the distributions. The sum of these various exposures then gave the total 24-hour $PM_{10}$ personal exposure for each of the test subjects. The 25 subject samples were modelled four different times with the number of iterations of the

Monte Carlo sampling increasing on each occasion. The results of the tests are shown below in Table 6.3.

Table 6.3: Results of the different Monte Carlo simulations on the test sample days.

| **Number Of Iterations** | **N** | **R** | **RMSE** ($\mu g/m^3$) | **NMB** (%) |
|---|---|---|---|---|
| 10 | 25 | 0.056 | 10.3 | 22.0 |
| 100 | 25 | 0.359 | 8.2 | 14.2 |
| 1000 | 25 | 0.317 | 8.2 | 14.7 |
| 10000 | 25 | 0.256 | 8.3 | 14.6 |

The results of the Monte Carlo simulations for the test subjects when simulating total exposure with personal exposure concentrations sampled from the population distributions were found to be rather poor. The worst simulator of the total personal exposures of the subjects was unsurprisingly the model that iterated just 10 times when sampling from the various distributions. This model had a very low R of 0.056, along with the largest RMSE and NMB values of all the models. As the model only had 10 iterations in total, the dataset built for each microenvironment or activity was subject to far more variation from the population means.

The model with the best Pearson's correlation value returned, on the other hand, was the model that had 100 iterations specified which had an R of 0.359. This model had a similar RMSE value as the other two models of 1,000 and 10,000 iterations. All three models had a RMSE of approximately 8.2 $\mu g/m^3$. However, the 100 iteration model had a slightly smaller NMB percentage of 14.2% when compared to the 14.7% and 14.6% of the other two models. The results for the 100 iteration model are illustrated graphically in Figure 6.12 and Figure 6.13. All of these models offered a slight improvement on Model 1 in Section 6.3.1 which was based on the population mean concentrations for each microenvironment in order to calculate total 24-hour exposure. Model 1 had an R of 0.244, whereas the best Monte Carlo simulated model in comparison had an improved Pearson's correlation of R equal to 0.359. The RMSE for the Monte Carlo simulated exposures were marginally better too when compared with the RMSE of 8.5 $\mu g/m^3$ of Model 1.

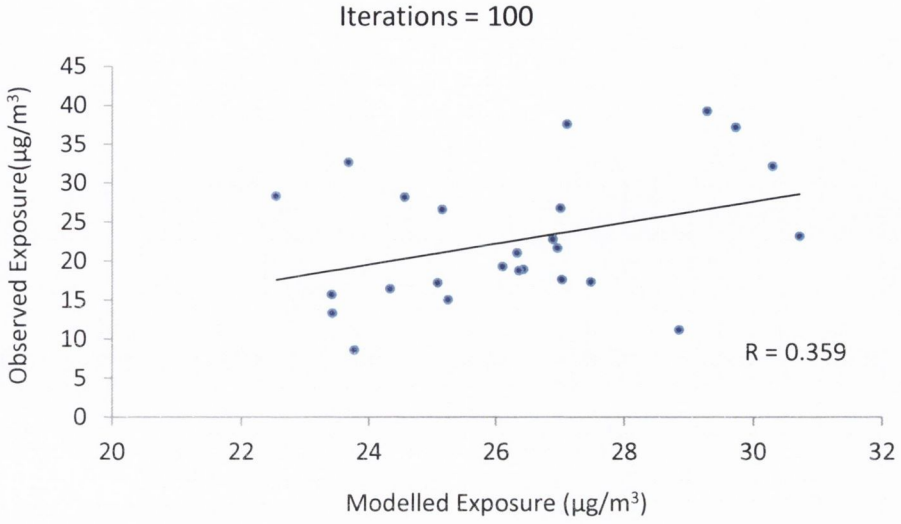


Figure 6.12: Linear regression of observed exposures versus modelled exposure for the 100 iterations simulation.

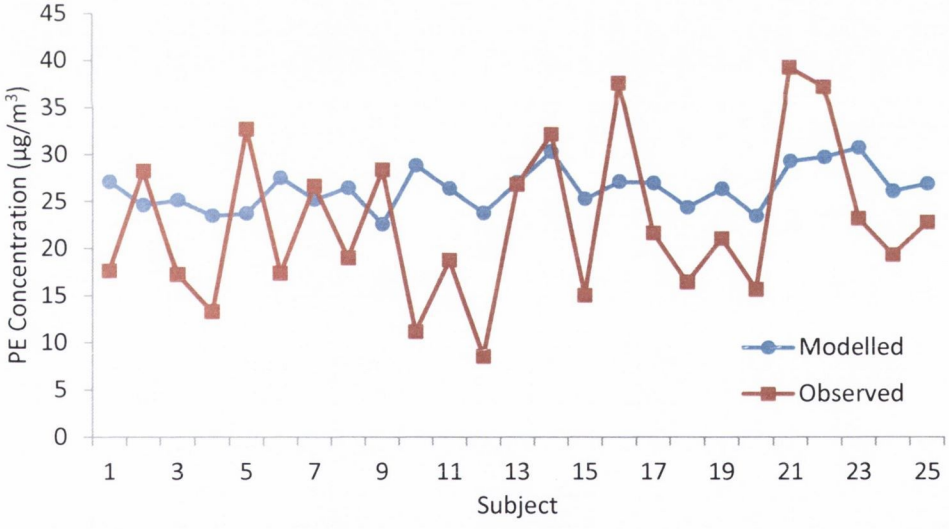


Figure 6.13: The 24-hour personal exposure concentrations of each of the 25 test subjects from the 100 iteration simulation.

In order to improve the capabilities of the Monte Carlo simulation for individuals further, two additional samples were added to the testing cases. These samples were from two smokers, which had not been represented in the randomly selected test cases. In order to model the smokers' 24-hour total exposure accurately, smoker specific distributions were defined for their place of residences. These distributions can be seen

in Figure 6.14 and Figure 6.15, and were defined using the smoker data in the main dataset along with the additional data collected by Smokers A and B during in home monitoring discussed in Chapter 4.

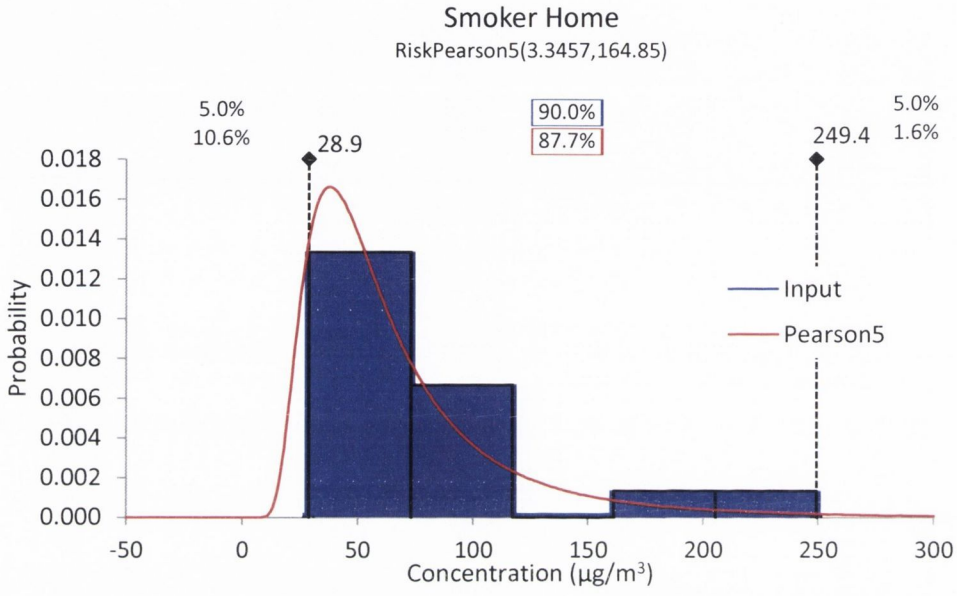


Figure 6.14: Probability distribution for the homes of smoking subjects.

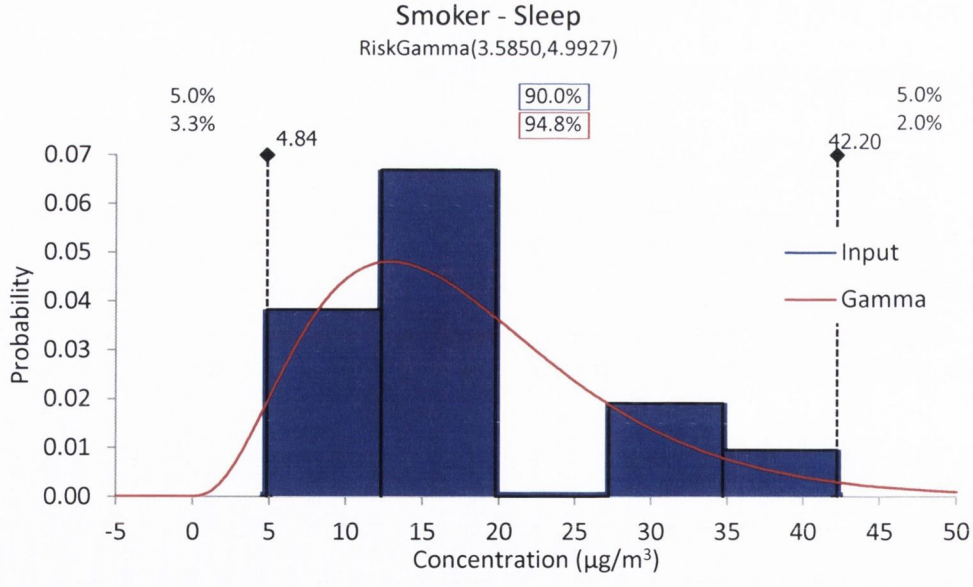


Figure 6.15: Probability distribution for the activity of sleeping for smokers.

The distribution with the best goodness-of-fit for the in-home personal exposure concentration of smokers was found to be a Pearson-5 distribution with a mean of 70.3 $\mu g/m^3$ and standard deviation of 60.6 $\mu g/m^3$. This was a significantly greater mean concentration than for non-smokers which had a mean of 24.6 $\mu g/m^3$ ($\sigma$ = 14.3 $\mu g/m^3$) once the smokers were separated. Similarly, at night when the subjects were sleeping the smoker Gamma distribution for this activity had a mean of 17.9 $\mu g/m^3$ with a standard deviation of 9.5 $\mu g/m^3$, compared to the remaining non-smoker mean of 9.5 $\mu g/m^3$ and standard deviation of 7.7 $\mu g/m^3$.

The results from the Monte Carlo simulation for the two smokers seemed to have greater accuracy than for the general population. The smoker exposures were simulated for four iteration specifications of 10, 100, 1,000, and 10,000, the same as the original 25 test cases. The mean concentration percentage difference between the observed and the modelled for the first smoker test case ranged between 13% and 17%, whilst for the other smoker it ranged between 4% and 7%. This contrasted with the 25 test cases from the non-smoking population which had a mean percentage difference of approximately 44% over the sample set.

In the case of the 100 iteration simulation, which happened to have the best Pearson's correlation amongst the modelled total exposures, the mean concentration percentage difference between the observed and the modelled for the two smoking cases was 7% and 17% of the observed exposures. The first smoker had a modelled exposure concentration of 44.4 $\mu g/m^3$, which was 6.9 $\mu g/m^3$ above the actual observed value. The second smoker's modelled personal exposure was 39.4 $\mu g/m^3$, which was only 2.6 $\mu g/m^3$ larger than the experimentally measured of 36.8 $\mu g/m^3$. The effect of these two cases on the R value of this simulation can be seen in Figure 6.16, whereby the R has increased from 0.359 previously to 0.536 in this case.

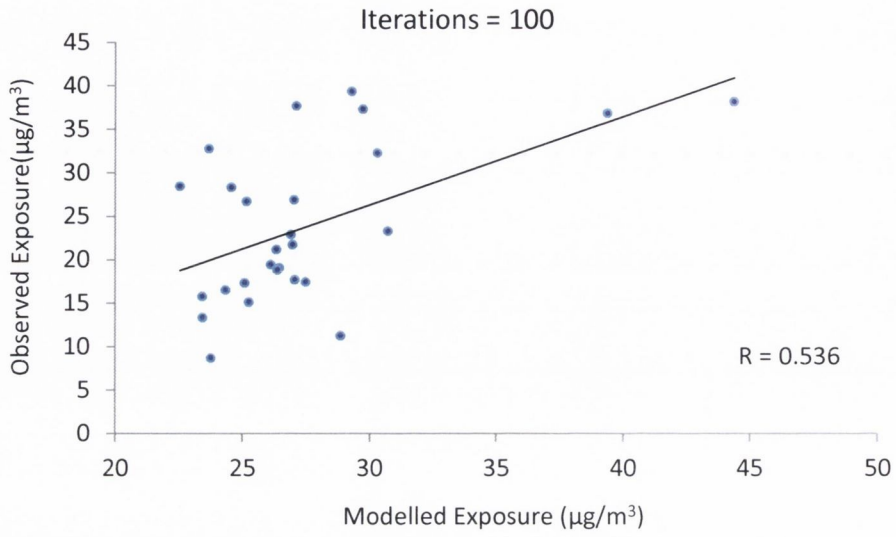


Figure 6.16: Monte Carlo simulated personal exposures with additional smoker test cases.

The example of the two smoker cases perfectly illustrates the advantages of how improved modelling accuracy can be achieved through knowledge of specific microenvironment particulate sources. The ability to define a distribution based on the experimentally sampled data collected from other smoking samples enabled a far closer total daily exposure for each subject to be modelled. The use of the general population distributions for many of the other activities was sufficient as most smokers reported mainly smoking at home. Therefore, attributing specific distributions for 'home' and 'sleeping' was of primary concern when modelling the smoker cases. The use of the general population distributions for calculation of exposures during time spent in their residence would have grossly underestimated the actual exposure concentrations.

## 6.5 Neural Network Modelling

An Artificial Neural Network (ANN) is an information processing paradigm that is inspired by the way biological nervous systems, such as the brain, process information. In their general form, ANNs refer to parallel model architecture able to perform numerical calculations based on distributed processing. An ANN consists of an input layer, one or more layers of neurons, and an output layer. The artificial neurons that compose an ANN operate according to a specified transfer function. The neurons

interact with each other through the use of neuron connections called weight factors. Each input is modified by a weight factor, which multiplies with the input value. The neuron will combine these weighted inputs and, with reference to a threshold value and activation function, use these to determine its output. Positive or negative weights correspond to connections that propagate or suspend, respectively, signals from other neurons. ANNs can be trained to perform a particular function by adjusting properly the values of these weights (Karakitsios et al., 2007).

Neural networks have the ability to derive meaning from complicated or imprecise data, and thus, can be used to extract patterns and detect trends that are too complex to be noticed by either humans or other computer techniques. The main characteristics of ANNs are as follows:

- Highly adaptive to non-parametric data distributions.
- No prior hypotheses about the relationships between the inputs.
- Very low sensitivity to error term assumptions.
- Higher tolerance to noise, chaotic components and heavy tails than most alternative computational methods.

An example of the fundamental building block for neural networks can be seen in Figure 6.17 which shows a single-input neuron.

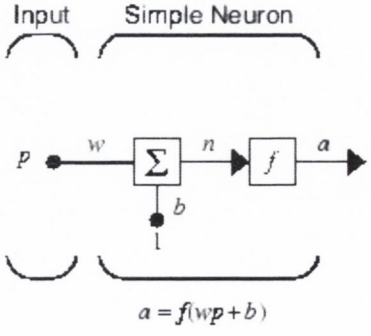


Figure 6.17: An example of a single input neuron.

There are three distinct functional operations that take place in this example neuron. First, the scalar input $p$ is multiplied by the scalar weight $w$ to form the product $wp$, again a scalar. Second, the weighted input $wp$ is added to the scalar bias $b$ to form the net input $n$. In this case, you can view the bias as shifting the function $f$ to the left by an amount $b$. The bias is much like a weight, except that it has a constant input of 1. Finally, the net input is passed through the transfer function $f$, which produces the scalar output $a$. The names given to these three processes are: the weight function, the net input function, and the transfer function.

The following subsections report on the application of ANNs to the personal exposure data gathered during this study. The applicability and capability of two types of ANN methods (FFNN and GRNN) for the prediction of 24-hour $PM_{10}$ personal exposure have been assessed.

### *6.5.1 Feed Forward Neural Networks*

A Feed Forward Neural Network (FFNN) consists of at least three layers - an input layer, a hidden layer, and an output layer. FFNNs can be used for any kind of input to output mapping and a schematic diagram is shown in Figure 6.18.

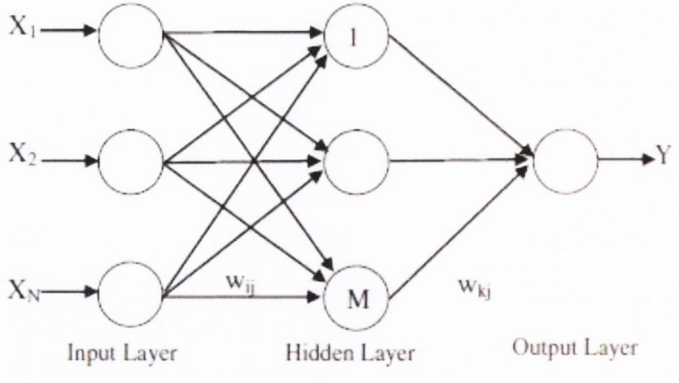


Figure 6.18: The general structure of a FFNN (Firat and Gungor, 2009).

The method in which a FFNN works is through each layer receiving a weighted input from a previous layer and then transmits its outputs to neurons in the next layer. The summation of weighted input signals are calculated with Eqn. 6.10, and this summation is transferred by a nonlinear activation function shown in Eqn. 6.11.

$$Y_{net} = \sum_{i=1}^{n} X_i \cdot w_i + w_o \qquad \text{Eqn. 6.10}$$

$$Y = f(Y_{net}) = \frac{1}{1 + e^{-Y_{net}}} \qquad \text{Eqn. 6.11}$$

In the above equations, $Y_i$ is the response of neuron $i$, $Y_{net}$ is the summation of weighted inputs, $X_i$ is the neuron input, $w_i$ is the weight coefficient of each neuron input, $w_o$ is bias, and $f(Y_{net})$ is the nonlinear activation function. The results of the FFNN are compared with the observed results and the network error is calculated with the MSE (Eqn. 6.6). The training process continues until this error reaches and acceptable value (Firat and Gungor, 2009).

For the model in this study, a back propagation learning algorithm, the supervised learning and sigmoid activation function are used for the training and testing phases. The FFNN model training was carried out using a back propagation algorithm known as the Levenberg-Marquardt algorithm which is described in further detail in the following subsection. Supervised learning is the most commonly used method for training a FFNN. In supervised learning the purpose of the neural network is to change its weights according to the inputs and outputs samples. The training task is complete once a network has established its input-output mapping with a defined minimum error (Zilouchian and Jamshidi, 2001). The procedure of a back propagation network is that the error at the output layer propagates backward to the input layer through the hidden layer in the network to obtain the final desired outputs.

#### *6.5.1.1 Levenberg-Marquardt Algorithm*

The problem of neural network learning can be viewed as a function optimisation problem, in which the best network parameters (weights and biases) are determined in

order to minimise network error (Priddy and Keller, 2005). In order to accomplish this, a number of function optimisation techniques from numerical linear algebra can be directly applied to network learning, one of the techniques being the Levenberg-Marquardt algorithm.

The Levenberg-Marquardt algorithm was independently developed by Kenneth Levenberg and Donald Marquardt (Levenberg, 1944; Marquardt, 1963), and provides a numerical solution to the problem of minimising a non-linear function. It has the advantages of being fast and having stable convergence, and in the field of ANNs it is suitable for small and medium-sized problems.

The Levenberg–Marquardt algorithm blends two other methods developed for neural network training - the steepest descent method and the Gauss–Newton algorithm. Fortunately, it inherits the speed advantage of the Gauss–Newton algorithm and the stability of the steepest descent method. It is more robust than the Gauss–Newton algorithm, because in many cases it can converge well even if the error surface is much more complex than the quadratic situation. Although the Levenberg–Marquardt algorithm tends to be slightly slower than Gauss–Newton algorithm (in convergent situations), it converges much faster than the steepest descent method.

The Levenberg-Marquardt algorithm is a very simple, but robust, method for approximating a function. It basically consists of solving the expression shown in Eqn. 6.12.

$$(J^T J + \lambda I)\delta = J^T E \qquad \text{Eqn. 6.12}$$

Where $J$ is the Jacobian matrix for the system, $\lambda$ is the Levenberg's damping factor, $\delta$ is the weight update vector that we want to find, and $E$ is the error vector containing the output errors for each input vector used on training the network. The $\delta$ term tells us by how much we should change our network weights to achieve a (possibly) better solution. The $J^T J$ matrix can also be known as the approximated Hessian. The $\lambda$ damping factor is adjusted at each iteration, and guides the optimisation process. If

reduction of $E$ is rapid, a smaller value can be used, bringing the algorithm closer to the Gauss–Newton algorithm, whereas if an iteration gives insufficient reduction in the residual, $\lambda$ can be increased, giving a step closer to the gradient descent direction.

### *6.5.2 Generalised Regression Neural Networks*

A General Regression Neural Network (GRNN) is a one-pass learning algorithm with a highly parallel structure (Specht, 1991). A GRNN does not require an iterative training procedure as back propagation networks do, and only needs a fraction of the training samples a back propagation network would need, which makes it particularly advantageous with sparse data in a real-time environment. It is a type of probabilistic neural network and a variation on radial basis neural networks. It approximates any arbitrary function between input and output vectors, drawing the function estimate directly from the training data. In addition, it is consistent that as the training set size becomes large, the estimation error approaches zero, with only mild restrictions on the function (Cigizoglu and Alp, 2006). A schematic diagram of a GRNN is shown in Figure 6.19.

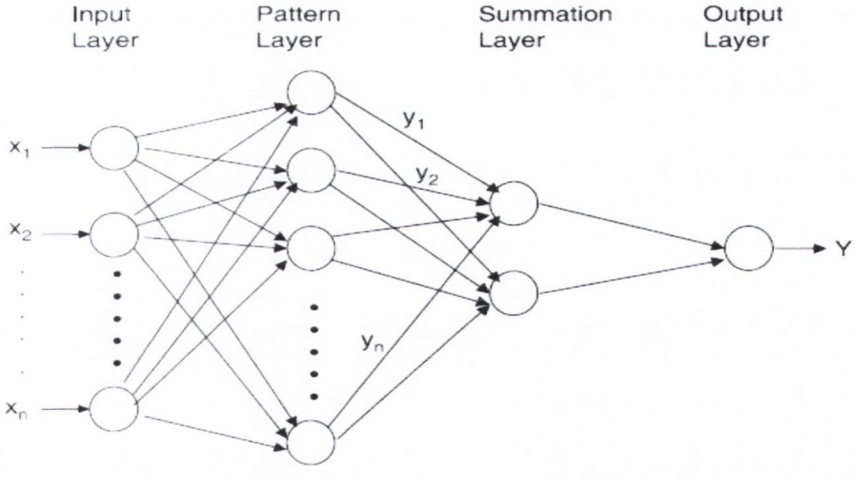


Figure 6.19: The general structure of a GRNN (Cigizoglu and Alp, 2006).

The first layer contains the input units, and the number of input units in each input layer depends on the total number of observations parameters. The first layer is connected to the second, and this second layer has the pattern units. The outputs of this second layer

are passed on to the summation units in the third layer. The summation layer has two different types of summation, which are a single division unit and summation units. The summation and output layer together perform a normalisation of output set (Cigizoglu and Alp, 2006). Radial basis and linear activation functions are used in hidden and output layers when training the network. Each pattern layer unit is connected to the two neurons in the summation layer, *S* and *D* summation neurons. The *S* summation neuron computes the sum of weighted responses of the pattern layer. Additionally, the *D* summation neuron is used to calculate un-weighted outputs of pattern neurons. The output layer divides the output of each *S* summation neuron by that of each *D* summation neuron, yielding the predicted value $Y_i'$ to an unknown input vector $x$ as:

$$Y_i' = \frac{\sum_{i=1}^{n} y_i \cdot exp[-D(x,x_i)]}{\sum_{i=1}^{n} exp[-D(x,x_i)]} \quad \text{Eqn. 6.13}$$

$$D(x,x_i) = \sum_{k=1}^{m} \left(\frac{x_i - x_{ik}}{\sigma}\right)^2 \quad \text{Eqn. 6.14}$$

Where $y_i$ is the weight connection between the $i$th neuron in the pattern layer and the *S* summation neuron, $n$ is the number of training patterns. In Eqn. 6.14, *D* is the Gaussian function, $m$ is the number of elements of an input vector, $x_k$ and $x_{ik}$ are the $j$th element of $x$ and $x_i$, respectively, and finally $\sigma$ is the spread parameter, the optimal value of which is determined experimentally (Firat and Gungor, 2009).

### *6.5.3 FFNN model development and results*

A two-layer feed-forward network with sigmoid hidden neurons and linear output neurons was designed and implemented in the software programme Matlab. The neural network fitting tool (*'nftool'*) GUI (graphical user interface) utilises the Matlab function *'fitnet'* to fit multi-dimensional mapping problems, given consistent data and enough neurons in its hidden layer. The ANN designed for the purposes of this study had 26 neurons in the hidden layer and was trained with the Levenberg-Marquardt algorithm. The architecture of the designed ANN is shown in Figure 6.20

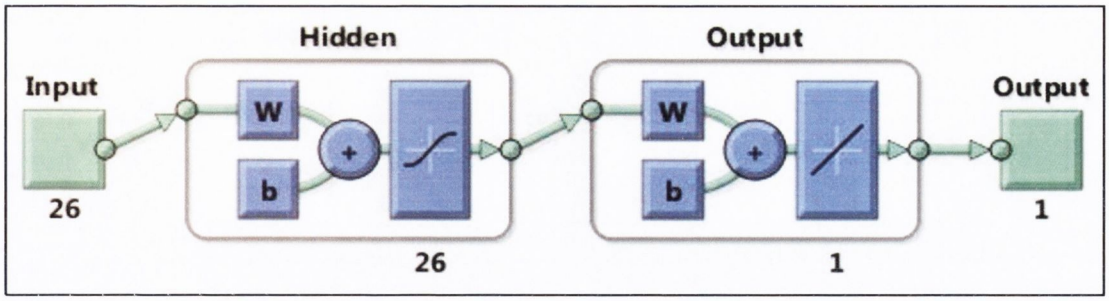


Figure 6.20: A schematic diagram of the FFNN used to predict the 24 hour exposures.

The starting point for developing the model was selecting the number of neurons in the hidden layer. There are many rule-of-thumb methods for determining the correct number of neurons to use in the hidden layers, such as the following:

- The number of hidden neurons should be between the size of the input layer and the size of the output layer.
- The number of hidden neurons should be two thirds the size of the input layer, plus the size of the output layer.
- The number of hidden neurons should be less than twice the size of the input layer.

Ultimately, the selection of architecture for the neural network will come down to trial and error. The default number of neurons set in Matlab was 10, but it was evident that this was causing underfitting in the network for the amount of inputs (26). Underfitting occurs when there are too few neurons in the hidden layers to adequately detect the signals in a complicated dataset. Thus, a larger amount of neurons were trialled, with the most satisfactory results being obtained between 20 and 28 neurons. Any more neurons in excess of this range resulted in overfitting. This occurs when the ANN has so much information processing capacity that the limited amount of information contained in the training set is not enough to train all of the neurons in the hidden layers. Finally however, a network architecture encompassing 26 neurons in the hidden layer was settled upon.

There were a total of 26 inputs parameters used for the ANN models and they are shown in Table 6.4. Initially modelling was conducted with a smaller amount of parameters, but better results were obtained when the selection was expanded to incorporate a greater number.

The inputs used consisted of three main types. The first main group was based on the time budgets of the study subjects. Each of these inputs was the time (in minutes) that each individual spent in the 15 major microenvironments or doing particular activities over each 24-hour sampling period. The 24-hour samples were also categorised, adding two further inputs, according to the subject's gender and whether or not they smoked during sampling. Additionally, various meteorological factors were included as inputs also. The majority of these variables were obtained from the Met Éireann meteorological station in the Phoenix Park. However, both wind speed and wind direction were gathered from the meteorological station at Dublin Airport. Finally, the targets for the FFNN were the 24-hour $PM_{10}$ mean personal exposures for each of the individual sampling days of the dataset.

Table 6.4: The input parameters for the FFNN and GRNN models.

| *Activity-Time Budget Inputs* | *Categorical Inputs* |
|---|---|
| Bus | Gender |
| Café/Restaurant | Smoker |
| Car | |
| Cycling | *Meteorological Inputs* |
| Home | Barometer Level Pressure (hPa) |
| Other Indoor | Global Radiation (j/cm$^2$) |
| Other Outdoor | Rainfall (mm) |
| Pub | Relative Humidity (%) |
| Recreation/Sport | Sea Level Pressure (hPa) |
| Shopping | Temperature (°C) |
| Sleeping | Wind Direction (Cosine) |
| Train | Wind Direction (Sine) |
| Tram | Wind Speed (m/s) |
| Walking | |
| Working | |

Once the inputs and the target were specified the model was ready to be trained. The model was trained with 70% of the data, while 15% of the data was set aside for both the validation and testing of the network. This equated to 179 of the 24 hour samples being used for training, with 38 samples each used for validation and testing. It should be noted the settings in Matlab allow for only certain percentages of a dataset to be specified for training, testing, and validation, therefore it was not possible to specify 25 test case samples as in previous models. The training samples were presented to the model and the network was adjusted according to the errors. The validation samples were used to measure network generalisation, and to halt training when generalisation stopped improving. The last set of samples, the testing samples, had no effect on training and so provided an independent measure of network performance during and after training.

The results of the network modelling are illustrated in Figure 6.21. The plots in Figure 6.21 show the correlations between the modelled and experimentally measured values for personal $PM_{10}$ exposure. As illustrated in the figure, the correlation for the training phase was very high ($R = 0.96$). However, the validation and testing phases were not as successful with Pearson's correlations of 0.43 and 0.49, respectively. The combined performance of the model was reasonably good with an overall Pearson's correlation found to be 0.79.

The output of the FFNN model was plotted alongside the original target data, which was the individual 24 hour personal exposure concentrations, and can be seen in Figure 6.22. This model output that is shown in the figure was the best fit according to the weights derived in the model. This output line is a combination of the training, validation, and testing data, and appears to recreate the target dataset quite well.

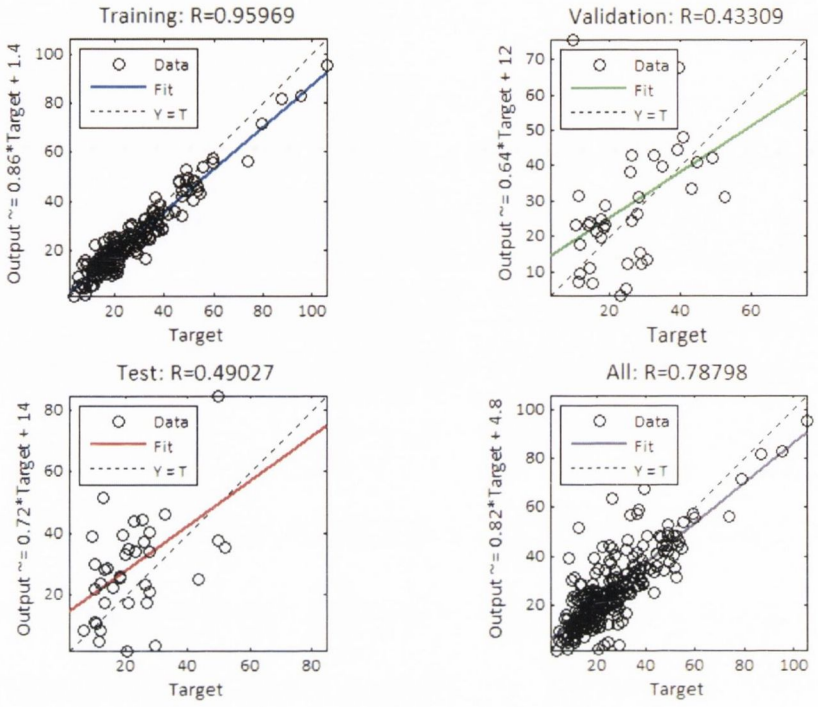


Figure 6.21: Correlations for the training, validation, testing and overall performance of the FFNN model (µg/m$^3$).

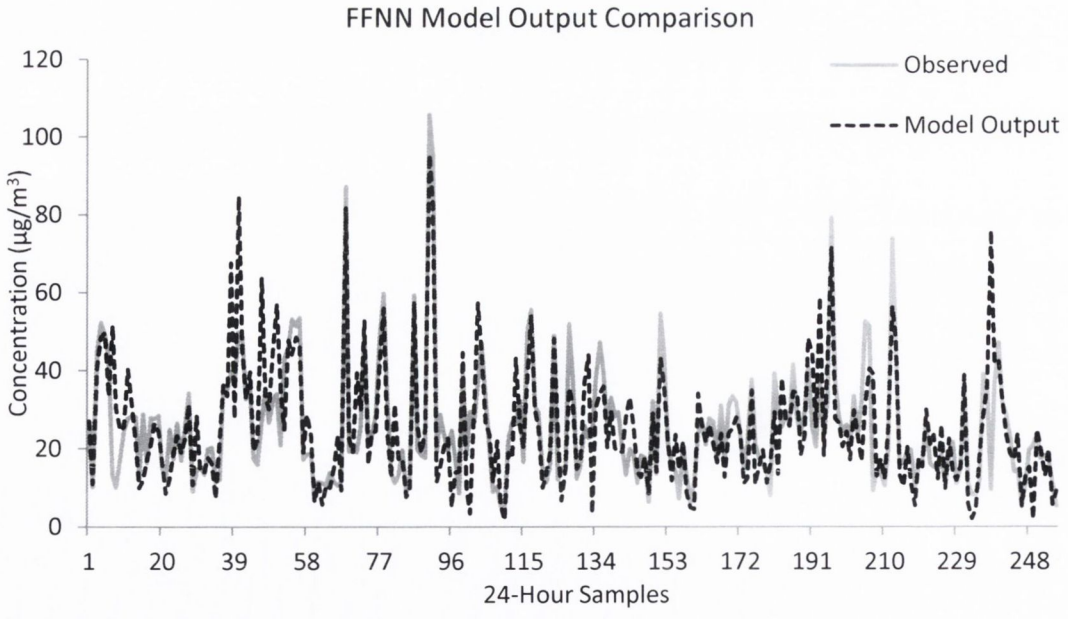


Figure 6.22: The model output (dotted line) compared with the observed 24-hour target data (grey line).

The performance of the model can be viewed in Figure 6.23. The best performance was found to occur during the third iteration (epoch 3), where the validation had a MSE of 269.7 (RMSE = 16.4 $\mu g/m^3$). The corresponding MSE for the training state at this point was just 27.1 (RMSE = 5.2 $\mu g/m^3$), while the testing performance had a MSE of 286.9 (RMSE = 16.9 $\mu g/m^3$). The MSEs illustrate that while the training of the model was very successful, the errors for the independently tested samples increased as the model was presented with the new inputs in order to simulate a corresponding 24-hour personal $PM_{10}$ exposure concentration.

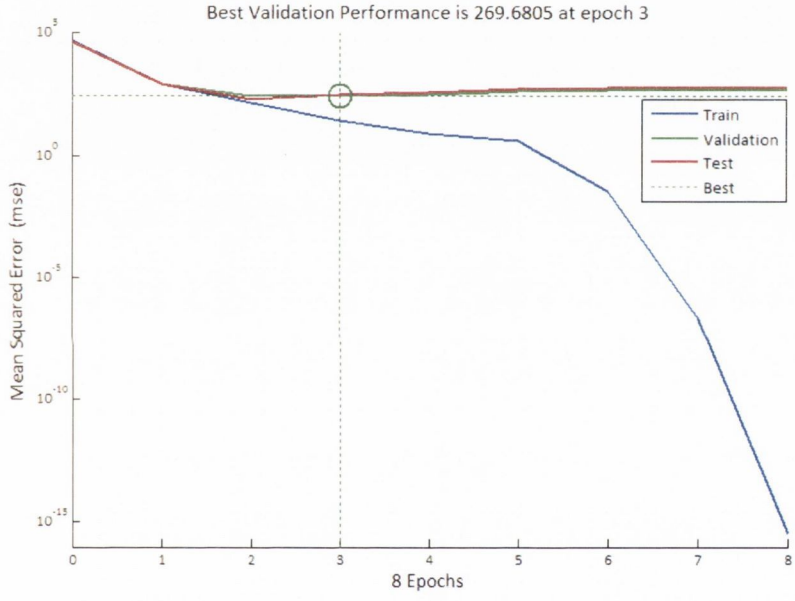


Figure 6.23: Plot of the training, validation, and test performances of the FFNN model.

The error histogram in Figure 6.24 shows nearly a Gaussian distribution of the errors in the model. The vast majority of errors in the model are close to zero, and particularly for the training phase of the model. As would be expected, the errors increase for the independently tested samples, while there is also one large outlier present in the validation sample set on the left-hand side of the graph. The model was found to be slightly biased towards overestimating personal exposure concentrations for the test cases, according to the NMB which was calculated as 32.6%. The residual errors for the predicted personal exposure concentrations are plotted in Figure 6.25, and they represent the observed minus the predicted personal concentrations. The residual errors

illustrate the tendency for overestimation in the model, with a greater quantity of the error values seen to be negative in the figure.

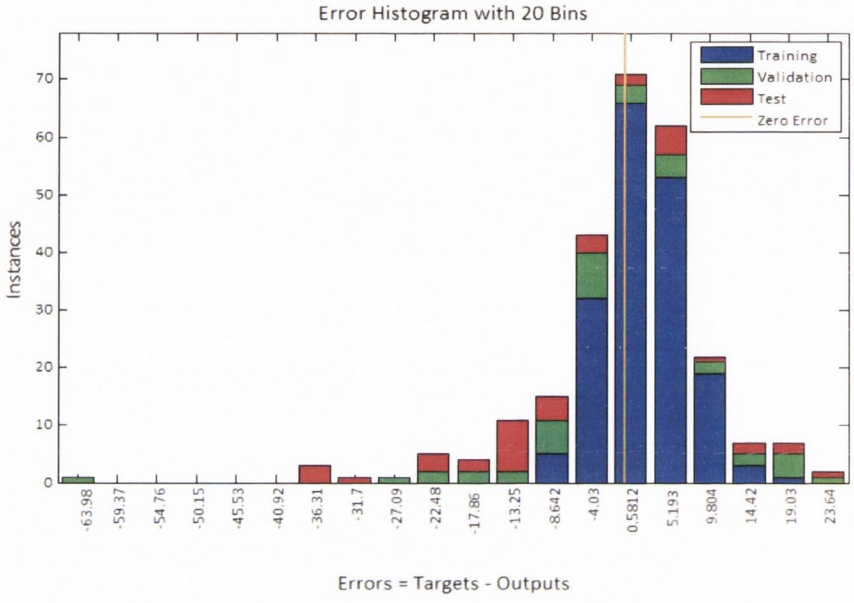


Figure 6.24: Error histogram for the FFNN model ($\mu g/m^3$).

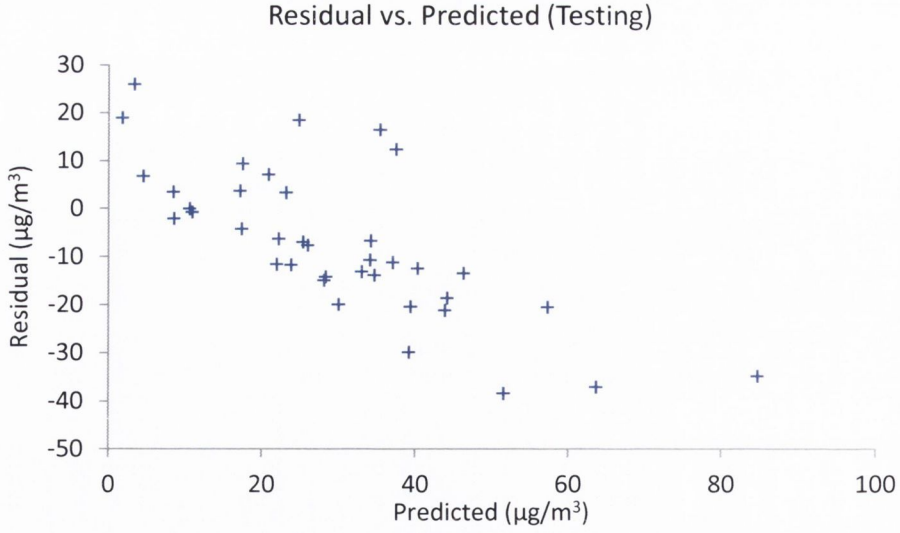


Figure 6.25: Residual errors of the FFNN predicted personal exposure data values.

### *6.5.4 GRNN model development and results*

The GRNN was designed and modelled in a Microsoft Excel add on software package called NeuralTools (version 6.0, Palisade Corp.). The inputs of the model were exactly the same as those used in the FFNN (see Table 6.4), as was the target data. There was no need to specify the number of neurons, as was the case with the FFNN, because GRNN networks have one neuron for each point in the training file. Thus, the only model parameter that required specification was the number of sample cases to test. This was set at 15% of the dataset to match the FFNN model, which left 217 samples available for training.

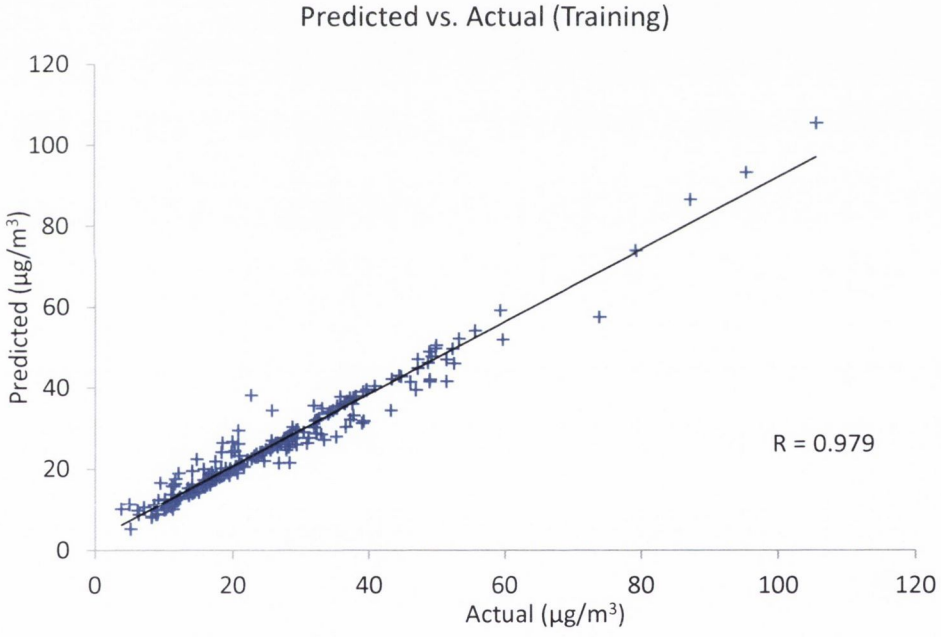


Figure 6.26: Regression of the GRNN model predicted personal exposures versus the observed data during model training.

The results of the training phase of the GRNN are illustrated in Figure 6.26. The training of the model was found to be excellent, with a Pearson's correlation of 0.98 and a MSE of 11.2 (RMSE = 3.4 µg/m$^3$). The errors that occurred during training are also shown in Figure 6.27. As can be seen from the figure, the error histogram was Gaussian in nature, centred around zero, with very few outside the range of ±5.0 µg/m$^3$.

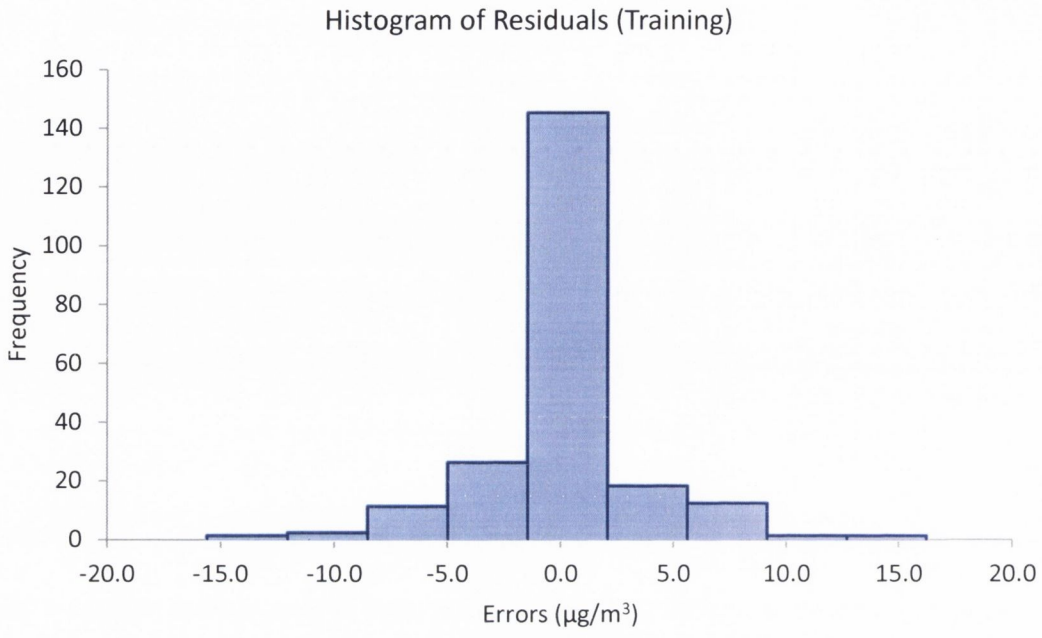


Figure 6.27: Histogram of the training errors between the targets and the outputs.

The results from the testing of the GRNN are shown in Figure 6.28. The predicted 24-hour personal exposures correlated moderately well with the corresponding experimentally observed personal exposures. The test cases were found to have a Pearson's correlation of 0.57, while the MSE was 119.5 (RMSE = 10.9 $\mu g/m^3$). The residual errors of the predicted 24-hour personal exposures are also shown in Figure 6.29. The errors between the observed and the predicted personal exposures primarily fall between $\pm 10$ $\mu g/m^3$. However, there were a number of outliers present, particularly at the bottom of the graph around the -20 to -25 $\mu g/m^3$ range. These are points in which the GRNN overestimated the personal exposures of the predicted values when compared to the actual observed concentrations.

Overall this GRNN network compared quite favourably to the FFNN. Both models had an excellent training performance, although the GRNN had a slightly better Pearson's correlation and MSE. The testing stage of the models did reveal a slightly larger disparity between the two, with the GRNN again performing better according to the correlation of the predicted values (0.57 versus 0.49) and the MSE (119.5 versus 286.9). The NMB of the GRNN (5.7%) was lower than the FFNN model (32.6%), meaning the

GRNN model was also less inclined to overestimate the personal exposure concentrations of the subjects.

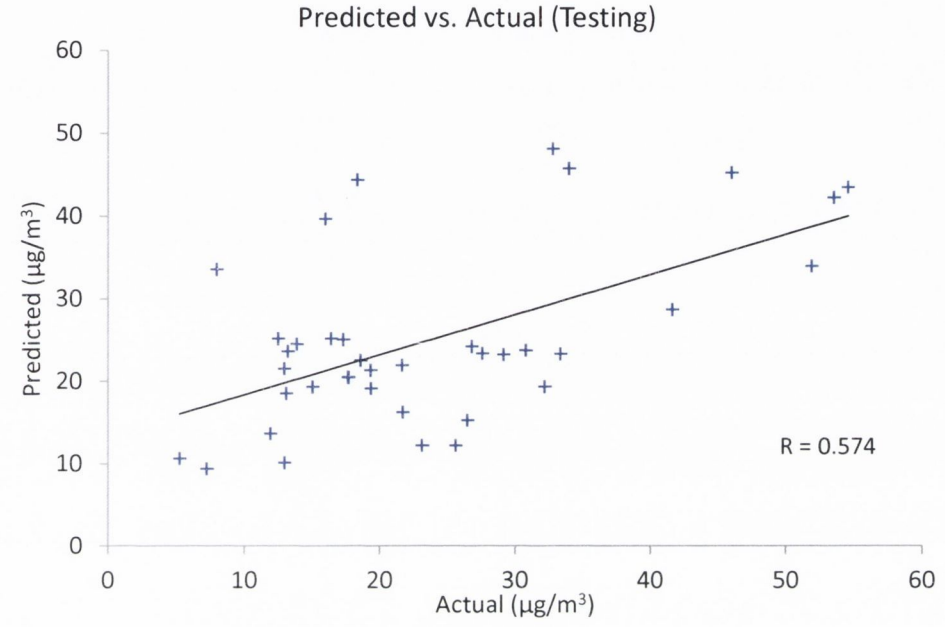


Figure 6.28: Correlation for the test cases between the predicted personal exposures and observed data.

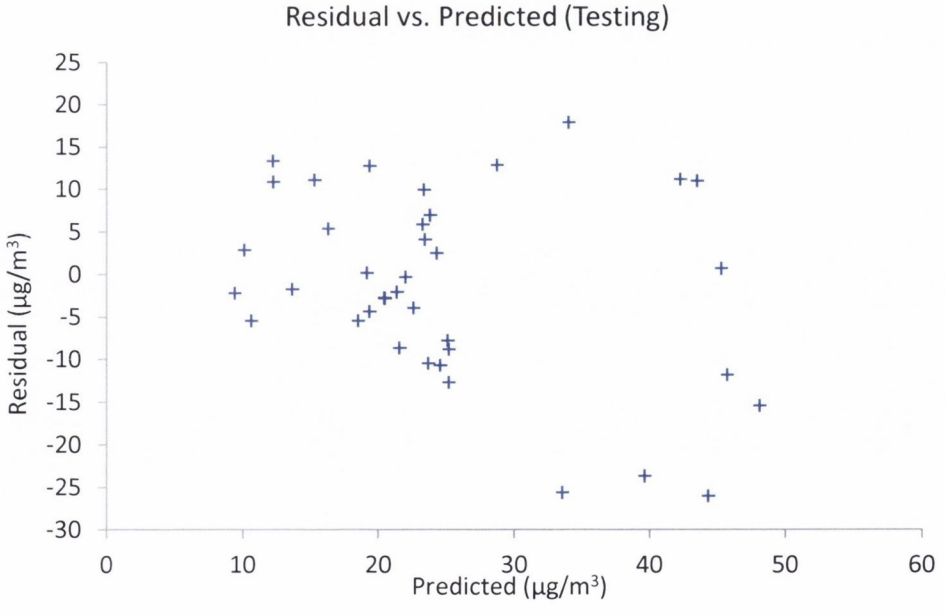


Figure 6.29: Residual errors of the GRNN predicted personal exposure data values.

## 6.6 Summary

This chapter has highlighted a number of different methods that can be utilised in order to predict the daily personal exposure of the study subjects. As mentioned at the beginning of the chapter, personal exposure modelling offers an alternative to the costly and burdensome monitoring technique that is personal sampling. The potential benefits of modelling the personal exposure of a given population are for aiding health impact investigations and subsequent policy decisions. A summary of the various personal exposure models used to predict individual exposures is provided in Table 6.5.

Table 6.5: Summary of each of the personal exposure models used for the prediction of individual 24 hour personal exposure concentrations ($\mu g/m^3$).

| **Model** | **N** | **R** | **RMSE** ($\mu g/m^3$) | **NMB** (%) |
|---|---|---|---|---|
| Time-Activity Model 1 | 25 | 0.24 | 8.5 | 12.7 |
| Time-Activity Model 2 | 25 | 0.67 | 8.8 | 11.9 |
| MC Model 100[a] | 25 | 0.36 | 8.2 | 14.2 |
| MC Model 1000[b] | 25 | 0.32 | 8.2 | 14.7 |
| MC Model with smokers[c] | 27 | 0.54 | 8.3 | 15.6 |
| FFNN | 38 | 0.49 | 16.9 | 32.6 |
| GRNN | 38 | 0.57 | 10.9 | 5.7 |

[a] Monte Carlo simulation model iterated 100 times
[b] Monte Carlo simulation model iterated 1000 times
[c] Monte Carlo simulation model inclusive of two smokers iterated 100 times

The first two models implemented were based on the traditional approach of integrated time-activity modelling. The concentrations used in time-activity Model 1 were based on the mean personal concentrations from the main microenvironments and activities encountered by the study subjects. On the other hand, time-cctivity Model 2 was based specifically on the sampling data gathered over the other sampling days in which the volunteer monitored. The resulting difference between these two approaches was particularly evident in Figure 6.1. The predicted values of Model 1 deviated little around the overall 24-hour mean concentration of the study population. In contrast, the predicted exposures of Model 2 followed the general trend of the actual personal

exposures with far greater accuracy. The improvement of Model 2 over Model 1 in this way was evident when the Pearson's correlations of each were compared. However, the RMSE and NMB of both models only marginally differed from each other (Table 6.5). This was perhaps due to many of the observed exposures samples that were modelled being close to the population mean, and by inference Model 1. Model 2 would inevitably perform more admirably in circumstances whereby the observed personal exposures of individuals to be modelled were more extreme and digressed with greater severity from the population mean.

The risk analysis modelling using a Latin Hypercube sampling based approach (Section 6.4.1) demonstrated that a population exposure model that closely mimics the actual population exposures could be created. The model designed in this study built on previous work by Jantunen and Kansanterveyslaitos (1999), whereby a greater knowledge of activities and microenvironments allowed more distributions to be realistically simulated. This probabilistic risk analysis approach also highlighted which activities or microenvironments had the greatest influence on the overall population personal exposure. The sensitivity analysis revealed the $PM_{10}$ concentrations at work and at home to have the greatest impact on personal exposure. The outcome of analysis such as this may influence the direction of future policy efforts for environmental exposure mitigation.

The second part of the personal exposure simulation subsection was an attempt to simulate individual 24-hour exposures rather than just a general population exposure model. This Monte Carlo based modelling approach was analogous to the integrated time-activity weighted Model 1. However, rather than just use the population average for a microenvironment as an input, specifically defined distributions were used based on the experimentally sampled exposures. This approach resulted in only a moderate improvement over that of Model 1 and was best for the mid-range iterative models, with iterations of 100 and 1000. This was primarily due to the low iterative model having too much variation when sampling from distributions, while a high number of iterations were more likely to regress to the mean and produce similar results to Model 1. Greater modelling accuracy was found when distributions were defined for individuals where a

known particle emitting source was present. This was the case for smokers when improved in home personal exposure estimation was achieved by using smoker specific distributions in the model. The results from both of the two best performing Monte Carlo models, as well as the model including smokers, are summarised in Table 6.5.

The last two modelling methods of this chapter consisted of utilising two different types of ANNs in order to predict the 24-hour personal exposure of randomly selected subjects. The two model types selected were the FFNN and the GRNN on account of their ability to extract patterns and detect trends that are too complex for other computational techniques. Their high tolerance to noise in datasets combined with being highly adaptive to non-parametric distributions made them ideal for modelling personal exposure data.

The results from the ANN modelling saw both the FFNN and GRNN perform reasonably well. The two methods performed extremely well during training, with very high Person's correlations and low RMSEs from each. The numbers of errors did however increase during the respective testing phases of each network. This was to be expected as the testing samples were independent of the data used to train each model. Overall though the GRNN performed slightly better than the FFNN during the testing phase. This may be due to the fact that there were less training samples available to the FFNN as 15% of samples are used for validation.

The ANNs did have greater Pearson's correlation coefficients than both the integrated time-weighted Model 1 and the Monte Carlo simulated individual daily exposures. However, the correlation coefficients were not as high as the integrated time-weighted Model 2, which modelled personal exposure based on each individual subject's previous samples. The RMSEs for the ANNs for the testing phase were also larger than the other models, but it should be cautioned that a larger amount of samples were simulated (38 samples) when compared to the other models (25 samples). Thus, this introduced the possibility of a greater number of outlying data points. The GRNN model also had a lower NMB percentage of 5.7% compared with the 32.6% of the

FFNN model, illustrating that the FFNN model is more likely to overestimate personal exposure concentrations.

# Chapter 7

## Background and Regression Modelling

# 7 Background and Regression Modelling

The purpose of this chapter is to assess determinants that may have had an impact on the $PM_{10}$ personal exposure concentrations of the individuals in the study. The variables that are assessed include various meteorological parameters as well as the influence that background concentrations have on personal exposure.

As already mention in Chapter 2, meteorological factors such as wind and rain can have a significant effect on outdoor PM concentrations. The outdoor concentrations in turn have the ability to migrate indoors and influence personal exposure. Therefore it is important to assess the degree to which weather parameters affect personal exposures also.

In a previous review, Wallace (2000) found personal exposure studies to generally have poor correlations between personal exposure concentrations and ambient outdoor concentrations, moreover, the correlations often approached zero. Numerous studies have found low associations between these two PM variables (Oglesby et al., 2000; Adgate et al., 2002; Brown et al., 2008; Crist et al., 2008), although personal monitoring studies by Branis and Kolomazníková (2010), Borgini et al. (2011), and Sarnat et al. (2006) have found good correlations in contrast. Clearly in the context of this study the relationship between FSMs and personal exposure warrants further investigation.

## 7.1 Regression Analysis

The term 'regression analysis' refers to the fitting of equations to statistical data, and includes many techniques for modelling and analysing several variables, when the focus is on the relationship between a dependent variable and one or more independent variables. Regression analysis can aid the understanding of how a typical value of a dependent variable changes when any one of the independent variables is varied, while the other independent variables are held fixed.

### *7.1.1 Simple linear regression*

Much of the analysis in this chapter will rely upon the simple linear regression model. This model consists of a single regressor $x$ that has a relationship with a response $y$ that is a straight line, and can be viewed in Eqn. 7.1.

$$y = \beta_o + \beta_1 x + \varepsilon \qquad \text{Eqn. 7.1}$$

In the model, the intercept $\beta_o$ and the slope $\beta_1$ are unknown constants and ε is a random error component. The errors are assumed to have a mean zero and unknown variance $\sigma^2$. Additionally, errors are assumed to be uncorrelated meaning that the value of one error does not depend on the value of any other error.

### *7.1.2 Multiple linear regression*

An expansion of the simple linear regression model is one that involves more than one regressor variable and is called a multiple linear regression model. This model (Eqn. 7.2) was used to assess effect of multiple predictor variables on personal exposure. In general, the response $y$ maybe be related to $k$ regressor or predictor variables.

$$y = \beta_o + \beta_1 x_1 + \beta_2 x_2 + \ldots + \beta_k x_k + \varepsilon \qquad \text{Eqn. 7.2}$$

The parameters $\beta_j$, $j = 0, 1, \ldots, k$, are called the regression coefficients. The parameter $\beta_j$ represents the expected change in response $y$ per unit change in $x_j$ when all of the remaining variables $x_i$ ($i \neq j$) are held constant. For this reason the parameters $\beta_j$, $j = 1, 2, \ldots, k$, are often called the partial regression coefficients. Multiple linear regression models are often used as empirical models for approximating functions. That is, the true functional relationship between $y$ and $x_1, x_2, \ldots, x_k$ is unknown, but over certain ranges of the regressor variables the linear regression model is an adequate approximation to the true unknown function (Montgomery et al., 2012).

## 7.2 Fixed Site Monitor Comparison

The following section describes the use of linear regression in order to assess the influence of suburban and urban fixed site monitor (FSM) $PM_{10}$ concentration data on the personal exposures of the volunteers in this study.

### *7.2.1 FSM locations in Dublin*

The EPA and the various county councils in Dublin operate a network of PM FSMs around the Greater Dublin Area. $PM_{10}$ is the size fraction that is primarily monitored, although there are a number of monitoring stations that also record $PM_{2.5}$ concentrations. The data that is available from these monitoring sites is daily average concentration data only.

The locations of the FSMs in the Dublin region are shown in Figure 7.1. The locations marked with the red pins are the sites that monitor $PM_{10}$ concentrations exclusively, while the dual $PM_{10}$ and $PM_{2.5}$ monitoring locations of Coleraine Street and Rathmines are marked with a green pin. Finally, the Marino FSM (blue pin) was the only site that monitored $PM_{2.5}$ concentrations exclusively.

The monitoring stations are also classified into different categories based on their positioning. There are four main category types of 'Urban traffic', 'Urban background', 'Suburban traffic', and 'Suburban background'. For example, Phoenix Park and Winetavern Street are two of the main FSM locations where data is taken for use in this study, and they are classified as suburban background and urban traffic, respectively. The main difference between these two is that the Phoenix Park site is relatively isolated and not located near any heavily trafficked roads, whereas the monitoring station at Winetavern Street is adjacent to a roadway and will have vehicles constantly passing nearby.

It should also be noted that there was a shortage of $PM_{10}$ monitoring locations that were operated on the north side of the city. To compensate for this lack of relevant data near the homes of volunteers residing in this area, the $PM_{2.5}$ concentrations from the Marino

FSM were used when available by assuming that the recorded $PM_{2.5}$ concentrations were 70% of what the $PM_{10}$ concentrations would be. This was the conversion factor proposed by Martuzzi et al. (2006) and is also the conversion factor used in the EU funded *APHEIS* programme (Medina et al., 2009). This conversion factor was compared with data from the collocated $PM_{2.5}$ and $PM_{10}$ monitoring site in Rathmines. It was found that over a three year period at the Rathmines FSM from 2009 to 2011, the $PM_{2.5}$ concentrations were on average 67% of the recorded $PM_{10}$ concentrations. Thus, the conversion factor of 0.7 was deemed acceptable for use in converting $PM_{2.5}$ concentrations to $PM_{10}$ when required to do so in this study.

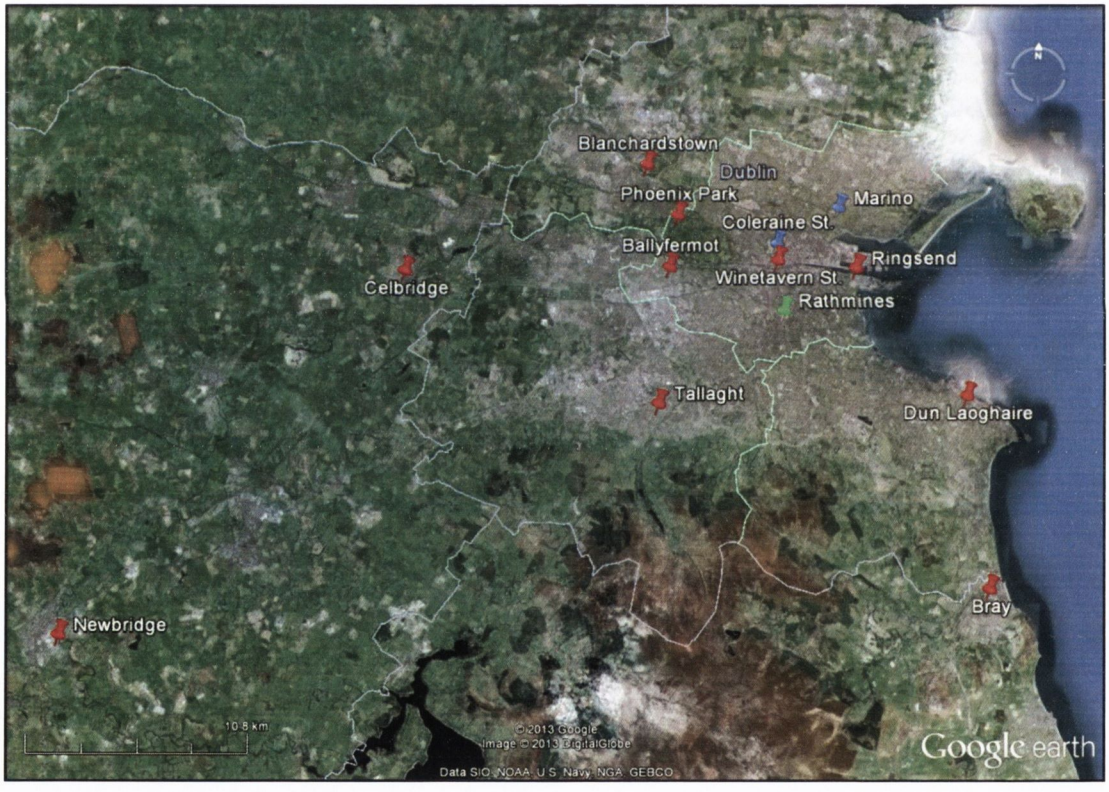


Figure 7.1: Locations of the FSMs showing $PM_{10}$ (red), $PM_{2.5}$ (blue), and collocated $PM_{10}$ and $PM_{2.5}$ (green) monitoring sites.

### *7.2.2 Phoenix Park FSM analysis*

The first analysis of the outdoor concentration for the study population was to compare the personal exposure concentrations with a background monitor in Dublin City. The EPA background monitoring site in the Phoenix Park was identified as perhaps the best

representation of the ambient background concentration for the city. Thus, the correlation between this background $PM_{10}$ monitoring station and the personal $PM_{10}$ exposures was assessed by means of regression analysis, with the following model:

$$Log_{10}(PE_i) = \beta_o + \beta_1 Log_{10}(X_i) \qquad \text{Eqn. 7.3}$$

Where $PE_i$ is the personal exposure of an individual on a particular day $i$, $\beta_o$ and $\beta_1$ are constants and $X_i$ is the background concentration ($\mu g/m^3$) as measured by the FSM. The personal exposure and the Phoenix Park FSM data were both log-transformed also because both datasets were log normally distributed. The log normal distribution of the 24-hour personal exposure concentrations has been mentioned in previous chapters, however the data obtained from the Phoenix Park was also tested for normality using the Anderson-Darling normality test. The results of this test confirmed the non-normally distributed nature of the Phoenix Park data (AD test statistic = 18.056; $p < 0.005$)

An issue that arose in comparing the FSM concentrations with the personal exposures was due to the discrepancy in the time frames for each dataset. This problem manifested because each individual 24-hour monitoring period taken by the study volunteers usually commenced in the morning time and overlapped into the following day. In contrast, the data obtained from the FSM was for a daily period of midnight to midnight. However, this issue was resolved by calculating time-weighted averages of the fixed site concentrations to correspond to the personal 24-hour measuring period. The time-weighted averages for the FSM data were calculated according to Eqn. 7.4.

$$\frac{t_{day\,1}C_{day\,1} + t_{day\,2}C_{day\,2}}{t_{total}} \qquad \text{Eqn. 7.4}$$

Where $t_{day\ 1,2}$ was the amount of measuring time in minutes on Days 1 and 2, respectively; $C_{day\ 1,2}$ was the concentration of the FSM on Days 1 and 2, respectively; and $t_{total}$ was the total amount of time (minutes) spent monitoring.

The data obtained from the Phoenix Park monitoring station is illustrated in a comparison with the 24-hour personal $PM_{10}$ exposure data in Figure 7.2. As seen from the chart, the 24-hour personal exposure data tended to be far greater than the corresponding background concentrations measured by the FSM in the Phoenix Park. However, there are a number of occasions that the background data exceeded the personal data. In general, many of the peaks and troughs found in the exposure dataset seem to be mirrored, albeit on a smaller scale, by the background concentrations.

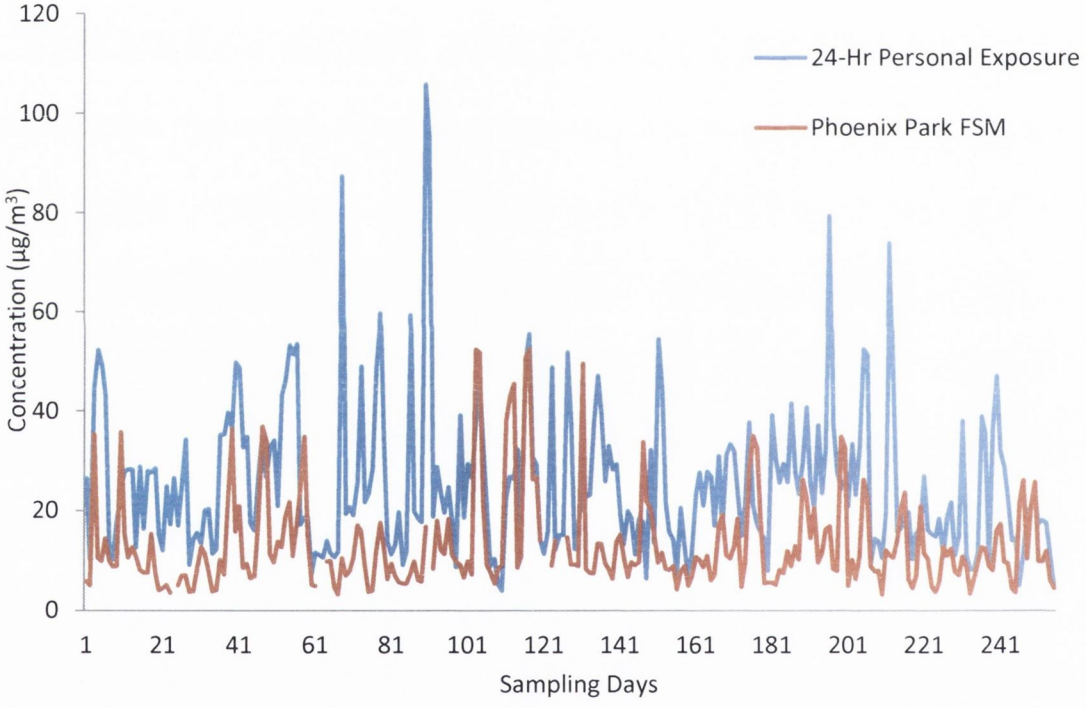


Figure 7.2: A graph of all subject sampling days showing the background concentration measured at the Phoenix Park (red line) and the 24-hr personal exposures (blue line).

The results from the linear regression analysis of the relationship between the log transformed personal exposure concentrations and the similarly log transformed $PM_{10}$ background concentrations, as measured in the Phoenix Park, are illustrated in Figure 7.3.

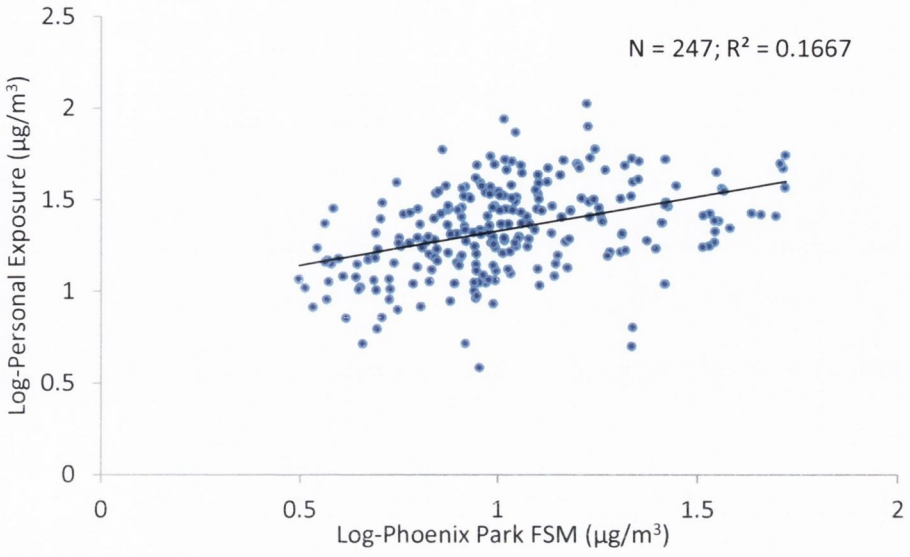


Figure 7.3: Linear regression plot of the log-transformed 24-hr $PM_{10}$ personal exposure concentrations versus the background concentration measured at the Phoenix Park.

The results show that there was a moderate correlation (R = 0.41) between the 24-hour personal exposure concentrations and the Phoenix Park background monitoring station. The fitted linear regression model is shown in Eqn. 7.5

$$Log_{10}(PE_i) = 0.953 + 0.377Log_{10}(X_b) \qquad \text{Eqn. 7.5}$$

In the equation $PE_i$ is the personal exposure of person $i$, and $X_b$ is the concentration recorded at the background site in the Phoenix Park. This fitted line model had a low coefficient of determination ($R^2$ = 0.167) and therefore would be a relatively poor predictor of 24-hour $PM_{10}$ personal exposure. It should be noted that the number of samples (N = 247) in this analysis was less than the total in the personal exposure dataset (N = 255), and this was as a result of missing data from the FSM dataset.

As a further analysis of the background $PM_{10}$ concentration data from the Phoenix Park FSM, the data was compared against the mean personal exposure concentrations of the study subjects while they were located in the city centre. The personal exposure concentrations used to represent this were taken as the mean occupational personal

exposures, as this was the activity that dominated the amount of time spent in the city centre. The results from this comparison are displayed in Figure 7.4

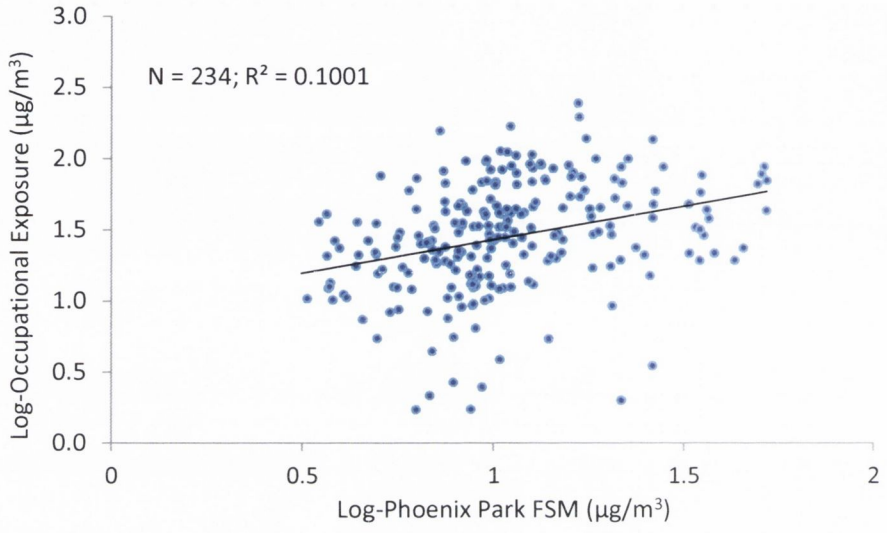


Figure 7.4: Linear regression plot of the log-transformed occupational $PM_{10}$ personal exposure concentrations versus the background concentration measured at the Phoenix Park.

The results again show there is a relatively poor correlation (R = 0.32) between the occupational personal exposure (representing the mean personal exposure concentration of time spent in the city centre) and the background concentrations as recorded by the Phoenix Park FSM. The simple linear regression model for this comparison can be seen in Eqn. 7.6.

$$Log_{10}(PE_w) = 0.959 + 0.47Log_{10}(X_b) \qquad \text{Eqn. 7.6}$$

$PE_w$ is the occupational personal exposure of each subject, while the background concentration from the Phoenix Park FSM is denoted by $X_b$. The coefficient of determination was low ($R^2$ = 0.10) for fitted line in the figure, again indicating this model is a poor predictor for the occupational personal exposure of subjects.

### *7.2.3 FSM near to workplace analysis*

A second analysis was undertaken in order to assess the relationship between the personal exposure concentrations and the FSMs that were closest to the places of work of all subjects. The main FSM in the heart of Dublin City was the monitoring station located at Winetavern Street in Dublin 2. This was the main FSM used as it was often the most centrally located and nearest to the work locations of the individuals. However, the FSM data from Coleraine Street, along with Ringsend and Rathmines, were also used in cases where there were gaps in the Winetavern Street data or the workplace in question was located closer to those other stations. The data for the FSMs close to the workplaces of the subjects was, like the Phoenix Park data, log normally distributed and non-normality of the data was confirmed by the Anderson-Darling test (AD test statistic = 15.705; $p < 0.005$).

The results of the linear regression analysis can be seen in Figure 7.5. Again, as in the case of the Phoenix Park comparison, the correlation between the 24 hour personal exposures and the monitoring stations closest to the workplaces only moderate (R = 0.394).

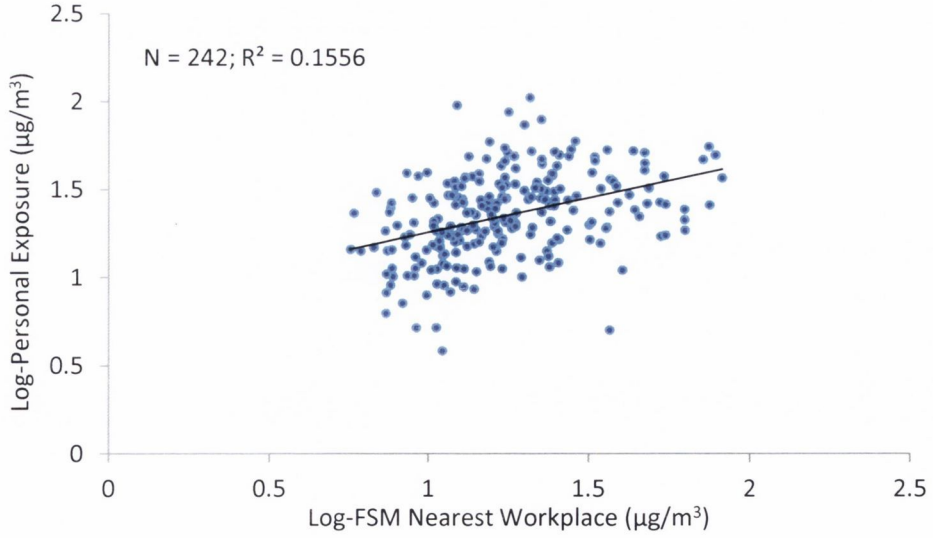


Figure 7.5: Linear regression plot of the log-transformed 24-hr $PM_{10}$ personal exposure concentrations versus the corresponding FSMs nearest to the workplace of each individual.

The fitted linear regression model for scatter plot is given in Eqn. 7.7. This equation explains only 15.6% of the variability in the 24-hour personal exposure concentration data ($R^2 = 0.156$).

$$Log_{10}(PE_i) = 0.867 + 0.295Log_{10}(X_w) \quad \text{Eqn. 7.7}$$

In this equation $PE_i$ is the 24-hour personal $PM_{10}$ exposure concentration and $X_w$ is the outdoor $PM_{10}$ concentration as recorded be the nearest FSM to the subject's workplace.

### *7.2.4 FSM near to home analysis*

The final background monitoring data that was considered was that of FSMs which were located closest to the home locations of the volunteers. Due to the amount of time that the subjects spent in their residences, 59% on average per day, background stations in the vicinity of their home location may have been expected to be most correlated with the 24-hour personal exposure concentration. In this instance, many of the more suburban FSMs such as Ballyfermot, Blanchardstown, Bray, Celbridge, Dun Laoghaire, Marino, Newbridge, Rathmines, and Ringsend, were used in order to obtain the $PM_{10}$ concentrations for the general area of a subject's residence.

On this occasion again, the distribution of concentrations from these background sites were found to be non-normal from the results of the Anderson-Darling test (AD test statistic = 13.634; $p < 0.005$). Figure 7.6 illustrates the relationship between the 24-hour personal $PM_{10}$ exposure concentrations and the FSM which was located nearest to each individual home location.

The results from the linear regression analysis yet again reveal the FSMs close to the homes of the volunteers as an unreliable predictor for the 24-hour personal exposures. The Pearson's correlation between the FSMs and personal exposure in this case was similar to the previous two examples ($R = 0.377$). The linear model for this analysis is presented in Eqn. 7.8.

$$Log_{10}(PE_i) = 0.6097 + 0.3733Log_{10}(X_h) \quad \text{Eqn. 7.8}$$

In this case again the $PE_i$ is the 24-hour personal $PM_{10}$ exposure concentration, while the predictor term $X_h$ represents the $PM_{10}$ concentration recorded by a nearby FSM to an individual's home. The coefficient of determination for this equations is low also ($R^2$ = 0.142), meaning the near home FSMs are equally as poor a predictor of 24-hour personal exposure as the near work and background FSMs.

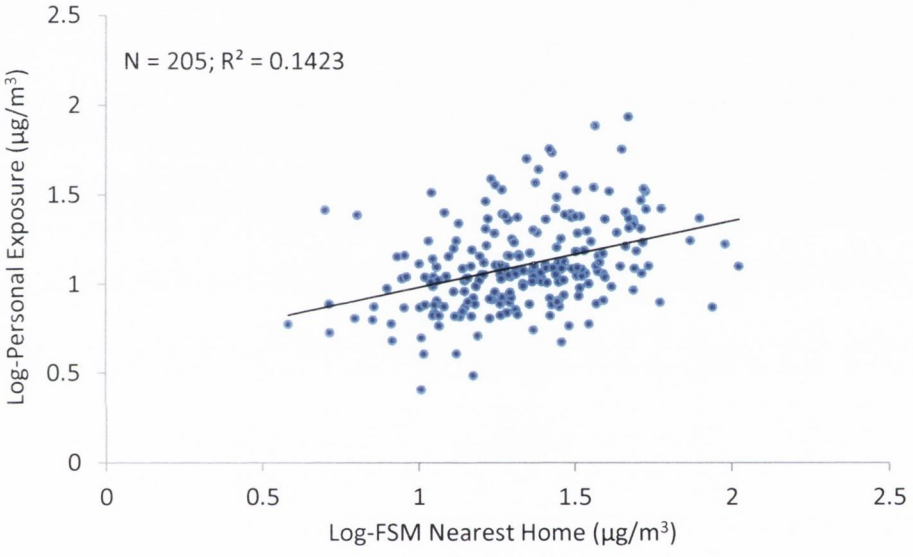


Figure 7.6: Linear regression plot of the 24-hr $PM_{10}$ personal exposure concentrations versus the corresponding FSMs nearest to the workplace of each individual.

### *7.2.5 MLR of combined FSMs*

As a further analysis of the various FSMs and their relationships with personal exposure to $PM_{10}$, a multiple linear regression (MLR) analysis of all three FSM categories was carried out. The result of this analysis are shown in Table 7.1. The MLR analysis found none of the log transformed FSM predictors to be statistically significant ($p < 0.05$) when predicting the transformed personal exposure. However, the FSM in the Phoenix Park had a relatively low p-value of 0.155 compared with the other two FSM predictors. The overall coefficient of determination for this model (Eqn. 7.9) was relatively low with $R^2$ adjusted equal to 0.171.

Table 7.1: Multiple linear regression analysis of log transformed 24-hour personal exposure concentrations versus the FSM data.

| **Predictors** | **Coef** | **SE Coef** | **T** | **P** |
|---|---|---|---|---|
| Constant | 0.836 | 0.088 | 9.50 | 0.000 |
| $Log_{10}$ Phoenix Park | 0.220 | 0.154 | 1.43 | 0.155 |
| $Log_{10}$ FSM Near Work | 0.174 | 0.157 | 1.11 | 0.268 |
| $Log_{10}$ FSM Near Home | 0.070 | 0.132 | 0.53 | 0.598 |
| *Summary of Model* | | | | |
| S = 0.2266 R-Sq = 18.3% R-Sq(adj) = 17.1% | | | | |

The MLR model is shown in the following equation:

$$Log(PE_i) = 18.7 + 0.28Log(X_b) + 0.31Log(X_w) - 0.12Log(X_h) \qquad \text{Eqn. 7.9}$$

Where $PE_i$ is again the 24-hour personal exposure ($\mu g/m^3$) for person $i$, and $X_{b,\ w,\ h}$ are the outdoor concentrations of measured at the Phoenix Park, nearest FSM to the workplace of the subject, and nearest FSM to the subject's residence, respectively.

### *7.2.6 Relationship between FSMs and occupational exposure*

The relationship between the FSMs located close to the work places of the study subjects and the personal exposure concentrations of the subjects while they were at work was investigated in an additional analysis. The previous regression was carried out to assess the influence of (log transformed) city centre FSMs data on the total 24-hour personal exposure concentrations and was found to have a Pearson's correlation of 0.394. Figure 7.7 shows the resulting scatter from plotting the transformed work time personal exposures versus the FSMs. The Pearson's correlation between predictor and response for this analysis was weaker (R = 0.319) than the previous comparison with the 24 hour exposure data.

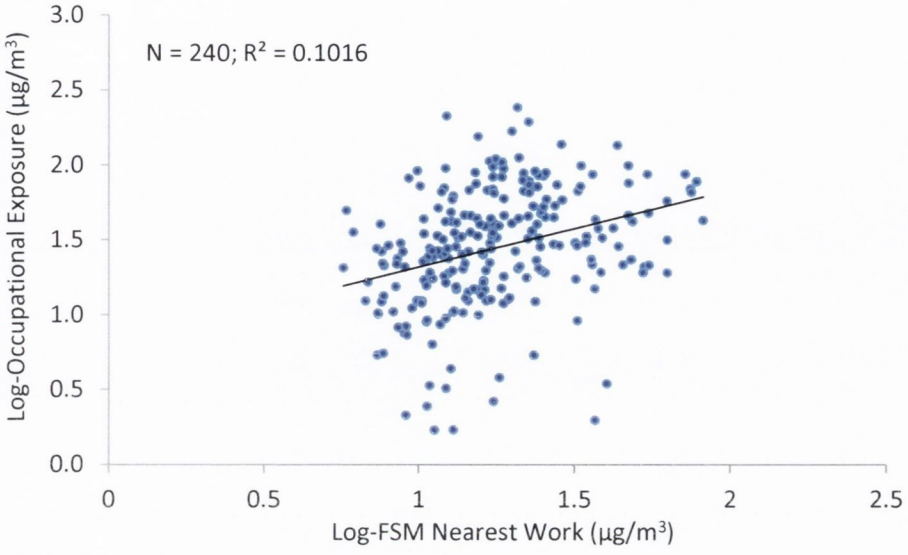


Figure 7.7: Plot of the $PM_{10}$ personal exposure concentration while at work versus the corresponding FSM concentration nearest to the workplace of each individual.

The overall performance of the model can be viewed in Table 7.2. The model was found to have an $R^2$ of only 10.2% which was in fact lower than the equivalent value ($R^2$ = 0.156) when the total 'Log-24hr personal exposure' was regressed against the near 'Log-workplace FSM' data. It should be noted that the FSM data were daily values, and may not have fully reflected the higher concentrations that would no doubt have been present in the city during the working day. However, the poor performance of the model is most likely attributable to unknown (or unstated) PM sources within the workplaces of the volunteers.

Table 7.2: Model summary with the dependent variable as the Log-occupational exposure ($\mu g/m^3$) and the predictor of Log-FSM concentration ($\mu g/m^3$) nearest to each working location.

| **Predictor** | **Coef** | **SE Coef** | **T** | **P** |
|---|---|---|---|---|
| Constant | 0.805 | 0.1256 | 6.41 | 0.000 |
| $Log_{10}$ FSM Concentration Near Work | 0.513 | 0.0991 | 5.18 | 0.000 |

S = 0.3754 R-Sq = 10.2% R-Sq(adj) = 9.8%

### *7.2.7 Spatial variability*

In order to further analyse the influence of FSMs close to the working locations of all volunteers on the personal exposure concentrations while at work, a spatial variable was added to the regression analysis. This new variable was the distance (in kilometres) that each particular FSM was from the workplace of a volunteer. This variable was included to assess whether or not FSMs located nearer to volunteer workplaces had a greater influence on occupational personal exposure. The main FSM located in Dublin City centre was positioned at Winetavern Street in Dublin 2, and this was the FSM that was primarily used, provided data was available, as the FSM closest to subject workplaces. The data collected by the GPS enabled the distance between the FSM and a workplace to be accurately measured. The average distance a FSM was from the work location of subjects was 1.4 km, with a standard deviation of 0.4 km. This was far less than, for example, the mean distance between each home location and the nearest FSM which was observed to be 3.4 km with a similar standard deviation ($\sigma$ = 3.4 km). The regression model obtained on inclusion of the distance variable is shown in Eqn. 7.10.

$$Log_{10}(PE_w) = 0.636 + 0.519Log_{10}(X_w) + 0.119X_d \qquad \text{Eqn. 7.10}$$

Where $PE_w$ is the $PM_{10}$ personal exposure concentration ($\mu g/m^3$) for person $i$ while at work on a sampling day, $X_w$ is the concentration ($\mu g/m^3$) as recorded by the nearest FSM to the individual's workplace, and $X_d$ is the distance from that FSM to the work location of person $i$. The distance variable $X_d$ was not however log transformed as the FSM and personal exposure concentrations were.

The model results are summarised in Table 7.3. The addition of the distance predictor variable did not however have the desired effect of improving the model. The coefficient of determination barely increased to 0.113 in this model compared to the model seen in the previous Section 7.2.6, which had an $R^2$ of 10.2. On examination of the significance of the predictors also, the distance variable was found not to be statistically significant in determining occupational personal exposure with a p-value of 0.081.

Table 7.3: Model summary for Log-occupational personal exposure with predictor variables of Log-$PM_{10}$ concentration ($\mu g/m^3$) from the FSM nearest to each workplace and the distance (km) to that FSM.

| Predictor | Coef | SE Coef | T | P |
|---|---|---|---|---|
| Constant | 0.636 | 0.1518 | 4.02 | 0.000 |
| $Log_{10}$ FSM Concentration Near Work | 0.519 | 0.0987 | 5.26 | 0.000 |
| Distance from Workplace to FSM | 0.119 | 0.0678 | 1.75 | 0.081 |

S = 0.3737 R-Sq = 11.3% R-Sq(adj) = 10.6%

## 7.3 Meteorological Determinants

In order to assess the influence of meteorological variables on determining daily personal exposure to $PM_{10}$ a stepwise MLR was undertaken. The term 'stepwise' refers to a step-by-step iterative construction of the regression model that involves automatic selection of independent variables. The procedure of this regression model involved the selection of a statistically significant independent variable after each step in the MLR. The regression steps ceased when no more statistically significant variables could be found in order to add to the model.

The meteorological variables that were used in the model were those obtained at the Dublin Airport and Phoenix Park meteorological stations, as discussed in Chapter 3. The majority of the meteorological data were available at the Phoenix Park station apart from wind speed and direction which was obtained from the Met Éireann weather station at Dublin Airport. In total, 9 meteorological variables were utilised for the model, with the results of the stepwise MLR model shown in the following tables.

It should be noted the meteorological variables also included the wind direction transformed into both sine and cosine components as it was a circular covariate. Additionally, when determining the wind direction for a particular 24-hour sampling period, standard methods like taking the arithmetic mean were avoided due to wind direction being circular data. Thus the predominant wind direction on any given day was used, such as the example in Figure 7.8

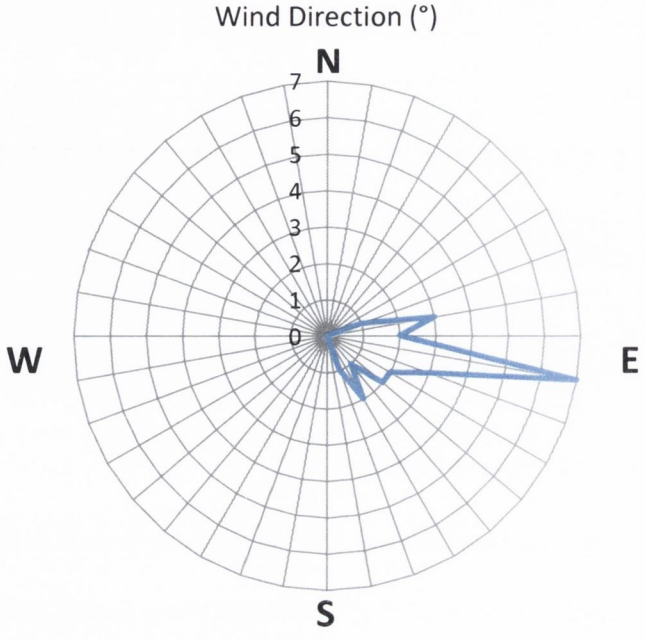


Figure 7.8: Example of a wind rose created from Dublin Airport meteorological data for a randomly selected day, illustrating the predominant wind direction on that day.

The summary of the model is shown in Table 7.4. The dependent variable in this analysis was the log transformed daily personal exposure data. The table indicates that the stepwise MLR iterated twice before no further improvements could be made to the model, with no more statistically significant predictors available. The included independent variables were found to be temperature and sea level pressure. The Pearson's correlation for the model after this first step was found to be moderate ($R = 0.208$). The coefficient of determination ($R^2$) of this model explained just 4.4% of the variability in 24-hour personal exposure. On the second iteration, the addition of sea level pressure as a predictor only marginally increased the $R^2$ and $R^2$-adjusted to 0.058 and 0.051, respectively.

Table 7.4: Model summary for the stepwise MLR of influence of weather variables on log transformed 24-hr exposure.

| Model[c] | R | R-Squared | Adjusted R-Squared | Std. Error of the Estimate | Durbin-Watson |
|---|---|---|---|---|---|
| 1 | .208[a] | .044 | .040 | .2412 | |
| 2 | .241 | .058 | .051 | .2399 | 1.223 |

a. Predictors: (Constant), Temperature

b. Predictors (Constant). Temperature, Sea Level Pressure

c. Dependent Variable: $Log_{10}$ 24-hr Personal Exposure

The ANOVA in Table 7.5 tested the statistical significance of the model at each step. As can be seen from the table, the model after both iterations was statistically significant ($p = 0.001$).

Table 7.5: ANOVA of the stepwise MLR model.

| Model | | Sum of Squares | df | Mean Square | F | Sig. |
|---|---|---|---|---|---|---|
| 1 | Regression | .669 | 1 | .669 | 11.496 | .001 |
| | Residual | 14.726 | 253 | .058 | | |
| | Total | 15.395 | 254 | | | |
| 2 | Regression | 0.894 | 2 | .447 | 7.765 | .001 |
| | Residual | 14.501 | 252 | .058 | | |
| | Total | 15.395 | 254 | | | |

The coefficients for the MLR model can be found in Table 7.6. The coefficient for temperature in model is negative, indicating warmer temperatures will decrease the dependent variable, the 24-hour personal exposure. Temperature is also the more significant of the two predictor variables with $p = 0.001$ The difference between the terms 'unstandardised' and 'standardised' coefficients is that the standardised coefficients in the table are the estimates resulting from an analysis carried out on the independent variables that have been standardised so that their variances are 1.

Table 7.6: Coefficients of the predictors in the MLR model for steps 1 and 2.

| Model | | Unstandardised Coefficients | | Standardised Coefficients | | |
|---|---|---|---|---|---|---|
| | | **B** | **Std. Error** | **Beta** | **t** | **Sig.** |
| 1 | (Constant) | 1.431 | .031 | | 45.558 | .000 |
| | Temperature | -.010 | .003 | -.208 | -3.391 | .001 |
| 2 | (Constant) | -.888 | 1.175 | | -.756 | .450 |
| | Temperature | -.010 | .003 | -.202 | -3.297 | .001 |
| | Sea Level Pressure | .002 | .001 | .121 | 1.975 | .049 |

The final table (Table 7.7) shows the variables that were used in the MLR analysis and which were chosen for the model. In this case the first predictor chosen for the model was temperature as this was the most statistically significant variable, and the second predictor was sea level pressure. However, after the second iteration it was found that there were no more statistically significant meteorological variables present that could be added to improve the model further. The variable that was the sine of wind direction was the next nearest variable to significance ($p = 0.172$), while barometer pressure at the metrological station and cosine of wind direction also had relatively low p-values ($p = 0.201$ and $p = 0.203$, respectively). This indicates that wind direction, although not significant in this analysis, may be found to play an important role in influencing daily personal exposure given further investigation. The end result of the second step, in the absence of further significant variables, was the discontinuation of the stepwise regression procedure, and the final model consisting of just the single predictor of temperature.

Table 7.7: Excluded variables from the MLR model after the second iteration.

| Model | | Beta In | t | Sig. | Partial Correlation | Collinearity Statistics |
|---|---|---|---|---|---|---|
| | | | | | | Tolerance |
| 2 | Rainfall | -.040 | -.540 | .590 | -.034 | .694 |
| | Barometer Pressure | -19.336 | -1.282 | .201 | -.081 | .000 |
| | Relative Humidity | .043 | .674 | .501 | .043 | .907 |
| | Global Radiation | -.070 | -.971 | .333 | -.061 | .724 |
| | Wind Speed | -.044 | -.613 | .541 | -.039 | .719 |
| | Sin of Wind Direction | -.084 | -1.369 | .172 | -.086 | .995 |
| | Cos of Wind Direction | -.080 | -1.276 | .203 | -.080 | .942 |

## 7.4 Analysis of Multiple Determinants

In order to improve on the MLR models seen thus far, a MLR was carried out using a combination of a large number of variables. Many of the variables were similar to that used in the ANNs from Chapter 6. The variables used included all the meteorological variables from the previous section (Section 7.2.7), the log transformed background concentrations from the Phoenix Park FSM, the time fractions that each volunteer spent in a microenvironment, and finally, two categorical variables of gender and whether or not the subject was a smoker.

The results of the analysis are summarised in Table 7.8. The stepwise MLR applied during this analysis was found to have taken four steps before the procedure ceased operation. The first step in the MLR analysis found the predictor variable of the background concentration at the Phoenix Park to be most significant, and thus was selected first. Following this initial step, three more predictor variables were added to the model which included the categorical variables of 'gender' and 'smoker', as well as the time fraction of a 24-hour period spent at home. The net result of adding the additional predictor variables was the increasing of the coefficient of determination ($R^2$)

from an initial 0.084 to 0.175 by the end of the fourth step. The adjusted $R^2$ also increased to 0.161 from a starting value of 0.08 following the first iteration.

Table 7.8: Model summary for the MLR analysis.

| Model[e] | R | R-Square | Adjusted R-Square | Std. Error of the Estimate | Durbin-Watson |
|---|---|---|---|---|---|
| 1 | .408[a] | .167 | .163 | .22312 | |
| 2 | .456[b] | .208 | .202 | .21797 | |
| 3 | .476[c] | .226 | .217 | .21589 | |
| 4 | .493[d] | .243 | .230 | .21404 | 1.217 |

a. Predictors: (Constant), $Log_{10}$ Phoenix Park FSM

b. Predictors: (Constant), $Log_{10}$ Phoenix Park FSM, Gender

c. Predictors: (Constant), $Log_{10}$ Phoenix Park FSM, Gender, Home

d. Predictors: (Constant), $Log_{10}$ Phoenix Park FSM, Gender, Home, Smoker

e. Dependent Variable: $Log_{10}$ Daily Exposure

The ANOVA in Table 7.9 tested the statistical significance of the model at each step. As can be seen from the table, the model was statistically significant after each of the four iterations ($p < 0.000$).

Table 7.9: ANOVA of the stepwise MLR model.

| Model | | Sum of Squares | df | Mean Square | F | Sig. |
|---|---|---|---|---|---|---|
| 1 | Regression | 2.440 | 1 | 2.440 | 49.021 | .000 |
| | Residual | 12.197 | 245 | .050 | | |
| | Total | 14.637 | 246 | | | |
| 2 | Regression | 3.045 | 2 | 1.523 | 32.048 | .000 |
| | Residual | 11.592 | 244 | .048 | | |
| | Total | 14.637 | 246 | | | |
| 3 | Regression | 3.312 | 3 | 1.104 | 23.683 | .000 |
| | Residual | 11.326 | 243 | .047 | | |
| | Total | 14.637 | 246 | | | |
| 4 | Regression | 3.551 | 4 | .888 | 19.376 | .000 |
| | Residual | 11.087 | 242 | .046 | | |
| | Total | 14.637 | 246 | | | |

The coefficients for the model predictors are given in Table 7.10. As can be seen from the model coefficients, the most significant variables were the background

concentration and the gender of the subjects. The gender coefficient being negative reveals that female personal exposure concentrations will be slightly lower than their male counterparts. The addition of the smoker categorical variable also had the effect of raising the constant coefficient between steps three and four by a greater amount than seen in the previous steps. The majority of subjects will be non-smokers so the relatively large negative coefficient for the 'smoker' predictor in the model will reduce their predicted personal exposure, and negate the effects of the larger constant coefficient.

Table 7.10: Coefficients of the predictors in the MLR model for steps 1 to 4.

| | | Unstandardised Coefficients | | Standardised Coefficients | | |
|---|---|---|---|---|---|---|
| **Model** | | **B** | **Std. Error** | **Beta** | **t** | **Sig.** |
| 1 | (Constant) | .953 | .057 | | 16.695 | .000 |
| | Phoenix Park | .377 | .054 | .408 | 7.002 | .000 |
| 2 | (Constant) | 1.108 | .071 | | 15.667 | .000 |
| | Phoenix Park | .363 | .053 | .393 | 6.885 | .000 |
| | Gender | -.102 | .029 | -.204 | -3.568 | .000 |
| 3 | (Constant) | 1.158 | .073 | | 15.840 | .000 |
| | Phoenix Park | .361 | .052 | .392 | 6.925 | .000 |
| | Gender | -.089 | .029 | -.178 | -3.084 | .002 |
| | Home | .000 | .000 | -.137 | -2.391 | .018 |
| 4 | (Constant) | 1.483 | .159 | | 9.300 | .000 |
| | Phoenix Park | .352 | .052 | .382 | 6.783 | .000 |
| | Gender | -.089 | .029 | -.178 | -3.117 | .002 |
| | Home | .000 | .000 | -.145 | -2.541 | .012 |
| | Smoker | -.159 | .069 | -.128 | -2.285 | .023 |

The final table from the model analysis shown is Table 7.11 which includes the excluded variables from the MLR model after the final step taken by the model. In total 23 of potential predictor variables were not chosen by the stepwise MLR due to lacking statistical significance. Interestingly, the predictor variable of 'Temperature' only had a significance of 0.565 after the fourth step of the model, while the significance of 'Sea level pressure' was similar at 0.572. This contrasts with the results of the meteorological

MLR model, where both variables were found to be the only significant variables amongst all the meteorological parameters.

Table 7.11: Excluded variables from the MLR model after the last step.

| Model | | Beta In | t | Sig. | Partial Correlation |
|---|---|---|---|---|---|
| 4 | Rainfall | -.033 | -.572 | .568 | -.037 |
| | Barometer Pressure | -.036 | -.564 | .574 | -.036 |
| | Sea Level Pressure | -.036 | -.566 | .572 | -.036 |
| | Temperature | .039 | .576 | .565 | .037 |
| | Relative Humidity | .050 | .873 | .384 | .056 |
| | Global Radiation | -.080 | -1.409 | .160 | -.090 |
| | Wind Speed | .039 | .637 | .525 | .041 |
| | Sin of Wind Direction | -.038 | -.675 | .500 | -.043 |
| | Cos of Wind Direction | -.082 | -1.461 | .145 | -.094 |
| | Work | .011 | .124 | .901 | .008 |
| | Sleep | -.068 | -1.154 | .250 | -.074 |
| | Pub | .040 | .704 | .482 | .045 |
| | Walk | .018 | .309 | .758 | .020 |
| | Car | -.045 | -.790 | .431 | -.051 |
| | Train | .033 | .584 | .559 | .038 |
| | Bus | .092 | 1.618 | .107 | .104 |
| | Tram | -.070 | -1.246 | .214 | -.080 |
| | Cycle | .014 | .255 | .799 | .016 |
| | Shopping | -.014 | -.247 | .805 | -.016 |
| | Sport | .043 | .740 | .460 | .048 |
| | Café | -.059 | -1.020 | .309 | -.066 |
| | Other Indoor | .060 | 1.041 | .299 | .067 |
| | Other Outdoor | .017 | .294 | .769 | .019 |

In general this MLR analysis had limited success as the final model only accounted for 23% in the variability of daily personal exposure to $PM_{10}$ according to the adjusted $R^2$ value. This particular model did however have the largest coefficient of determination amongst the regression models seen thus far.

## 7.5 Baseflow Separation Methods

A number of base-flow separation techniques were adapted to the $PM_{10}$ personal exposure time series data as a potential way to derive predictions of background concentrations. Initial work was carried out using a number of these methods previously

(McNabola et al., 2011), however this was done with a limited number of samples (n = 10). In this analysis, a larger number of samples were used and the $PM_{10}$ concentrations from the FSM near the home of each subject sample were also considered. The code for each of the baseflow separation methods was also written using Matlab (see Appendix E).

### *7.5.1 Conceptual design*

The concept behind the adaption of hydrological methods to personal exposure data in this section derives from the fact that the contribution of background concentration from a 24-hour time series of personal exposure has similarities in nature to that of baseflow separation in the field of stream-flow hydrology. The contribution of groundwater is required to be separated from a time series of overall stream discharge to assess the contribution of surface run-off to a storm flow (Eckhardt, 2008). In hydrology the flow of water in a stream is often assumed to comprise a component of flow associated with baseflow, or in other words, flow from groundwater (Aksoy et al., 2009). Surface run-off can be viewed as 'quick-response flow' which results in rapidly occurring spikes in the time series flow record while the baseflow produces a more steady response due to the slow nature of flow through the aquifers and may therefore be described as 'slow-response flow'. Similar to background PM concentrations, baseflow varies both temporally and spatially and is influenced by 'local emissions' of precipitation. Baseflow is likely to increase in response to a local rainfall event or decrease in response to dry periods.

In light of the nature of this relationship between surface run-off and baseflow, similarities therefore seem to exist with the relationship between personal exposure and background concentration. Personal exposure is susceptible to the effects of various air pollution sources and as a result presents a series of rapid response spikes in its time series history. Personal exposure could therefore be described as 'quick-response exposure'. In contrast, background concentration is slow to respond to instantaneous increases in local air pollution concentration and instead provides a steady response to the overall air quality of the locality which can be viewed as 'slow-response exposure'.

Although differences may exist in the underlying mechanics of the two relationships, the two are analogous to an extent. Thus it was assumed that adapting baseflow separation techniques to personal exposure time series data could provide useful predictions of background PM concentrations. The application to air pollution of two of these baseflow separation techniques commonly used in stream-flow hydrology are explored in the following subsections.

### *7.5.2 Boughton method*

The Boughton method is an analytical technique to predict baseflow in hydrology. This separation method works by increasing the base flow at each time step, either at a constant rate or varied by a fraction of the run-off (Boughton, 1988). A logic function was used in order to predict background concentrations from the time series data of subjects in this study. This function operated by either decreasing or increasing the background concentration at each time step according to a recession constant multiplied by the previous personal exposure. The increase or decrease at a particular time step of the background concentration was based upon whether or not the overall personal exposure was increasing or decreasing at that point. The background concentration increased or decreased in line with the personal exposure but the rate at which this occurred was different.

The recession coefficients $a$ and $b$ for the increase and decrease of the background concentration were also different. The magnitude of both constants was optimised by trial and error to obtain the best fit relationship between the measured reference and predicted background concentrations. Additionally the predicted concentration at each time step was never allowed to be less than zero or greater than the measured personal exposure at that time.

### *7.5.3 Sliding-interval method*

The sliding-interval method is another technique from the area of hydrology that is used for hydrographic separation. It assigns a baseflow to each daily record in the hydrograph based on the lowest discharge found within a fixed time period before and after that

particular day (Pettyjohn and Henning, 1979). In this study the method was employed to obtain background concentration predictions by using a sliding time period which chose the minimum concentration from a number of different time step periods.

The first period that was tested was a five time step period, corresponding to a 10 minute period, and this was extended to both 15 and 30 time step periods, representing a half hour and an hour periods. After each selection the interval would slide one time step ahead and thus would select a minimum value again from this new, but over lapping period. The results were optimised by trial and error to obtain the best degree of damping of the personal exposure time series by modifying the length of the sliding interval.

### *7.5.4 Baseflow separation results: Boughton method*

The recession constants $a$ and $b$ used in for the Boughton method during the initial trialling of the baseflow separation methods (McNabola et al., 2011) were set as $a = 0.1$ and $b = 0.45$. These values were chosen at the time as the values that gave the best fit results and were obtained through trial and error. Thus, these values were also selected for the recession constants for use in the expanded analysis seen here.

There was 30 personal exposure samples used for the baseflow separation in the expanded analysis, and this included 13 female and 17 male 24-hour samples. The performance of the Boughton method can be seen in Figure 7.9, in which the predicted background concentrations from the subject samples are compared with the actual monitoring station values for each particular day.

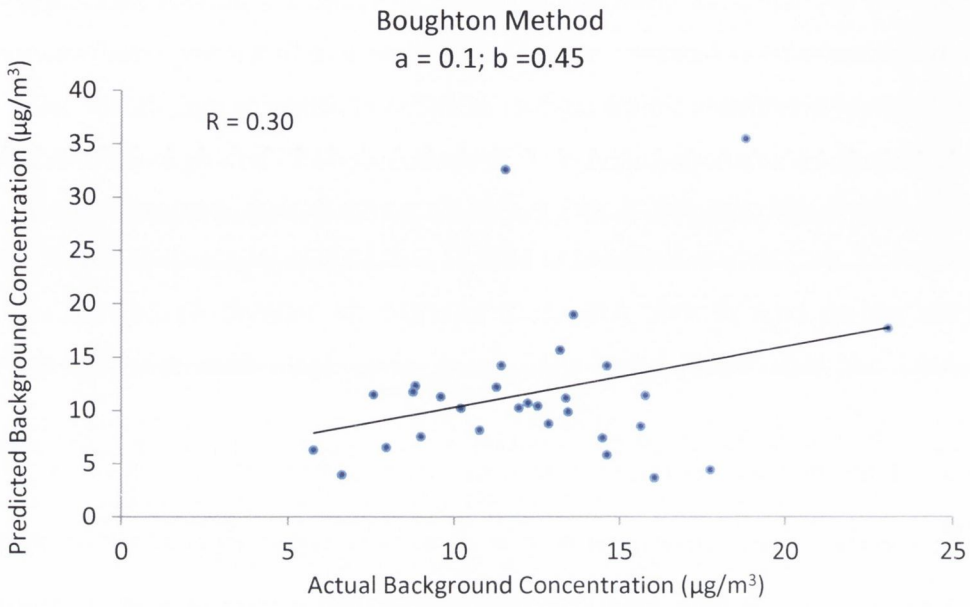


Figure 7.9: Comparison of the Boughton method predicted background concentrations versus the observed background concentrations ($\mu g/m^3$).

The Boughton separated background prediction was found to give only a moderate Pearson's correlation between the predicted and observed background concentrations, with R = 0.30. Figure 7.10 shows a typical output of a Boughton separated background concentration from a personal exposure time series plot.

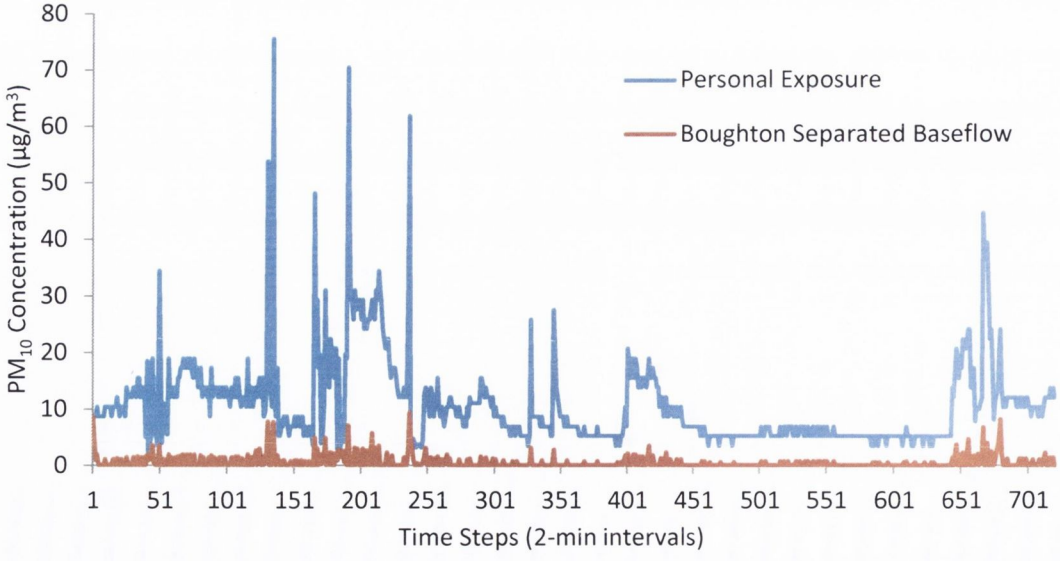


Figure 7.10: Time series plots of a 24-hour personal exposure sample and Boughton separated baseflow for the sample.

The performance of the Boughton method using the particular recession constants seen in the previous example ($a$ = 0.1 and $b$ = 0.45) was disappointing. Therefore in an attempt to improve the performance of the baseflow separation a number of other constant values for $a$ and $b$ were trialled. Better fitting results were subsequently obtained with $a$ = 0.2 and $b$ = 1.0. The higher value of recession constants produced a series of more rapidly increasing and decreasing spikes in response to events in the personal exposure time series. The results from using the new recession constants are illustrated in Figure 7.11.

The results from this altered Boughton method analysis show a slightly improved Pearson's correlation between the observed background concentrations and the predicted concentrations (R = 0.34).

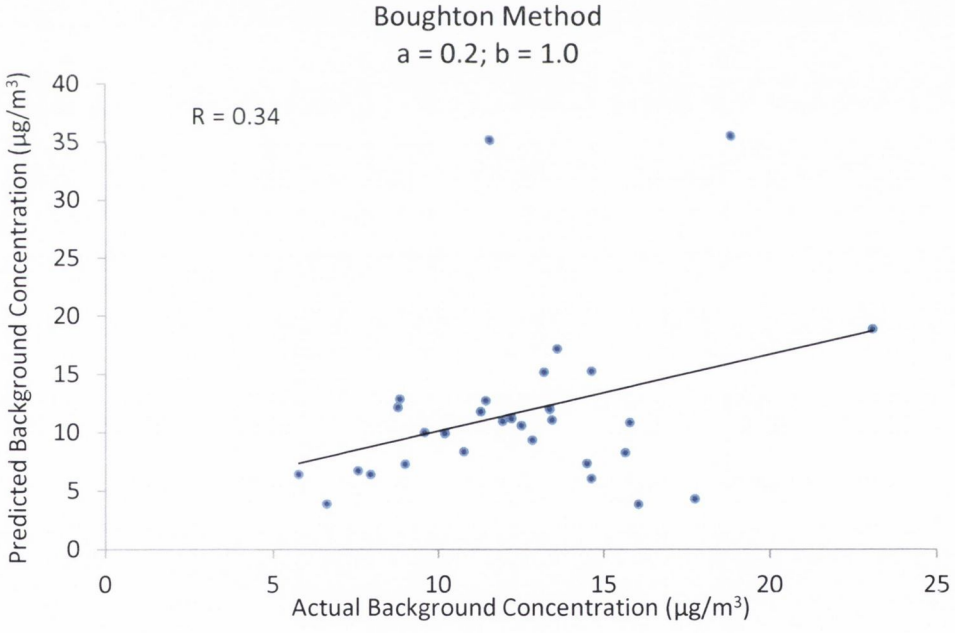


Figure 7.11: Comparison of the second Boughton method predicted background concentrations versus the observed background concentrations ($\mu g/m^3$).

### *7.5.5 Baseflow separation results: Sliding interval method*

The personal exposure concentrations of 30 samples were also subjected to a sliding interval filter separation technique. Each of the randomly select samples was smoothed

over three specified time periods, as previously described. An example of a personal exposure 24-hour sample and the three sliding intervals (10 minutes, 30 minutes, and 1 hour) used to separate the background concentration are shown in Figure 7.12. The sliding interval method was found to produce a lower frequency response than that of the Boughton method. This is evident on visual inspection of Figure 7.12, whereby the baseflow separations of each sliding interval time series do not have the same type of peaks as seen in the Boughton method of Figure 7.10.

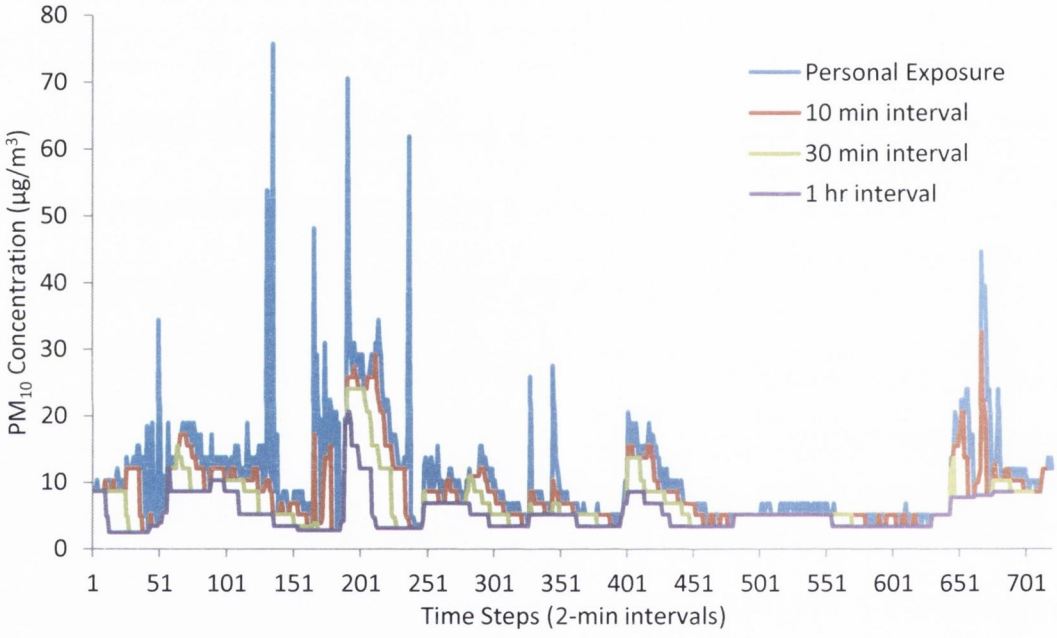


Figure 7.12: Time series plots of a 24-hour personal exposure sample and three sliding interval separated baseflows for the sample.

The results of the sliding interval baseflow separated background concentrations are illustrated in the following graphs. The first sliding interval trialled was for a 5 time step, or 10 minute period. Figure 7.13 shows the comparison between this 10 minute sliding interval predicted background concentrations and the actual background concentrations for each sampling day. A moderate Pearson's correlation was found between the predicted and observed background concentrations ($R = 0.42$) for this 10 minute interval.

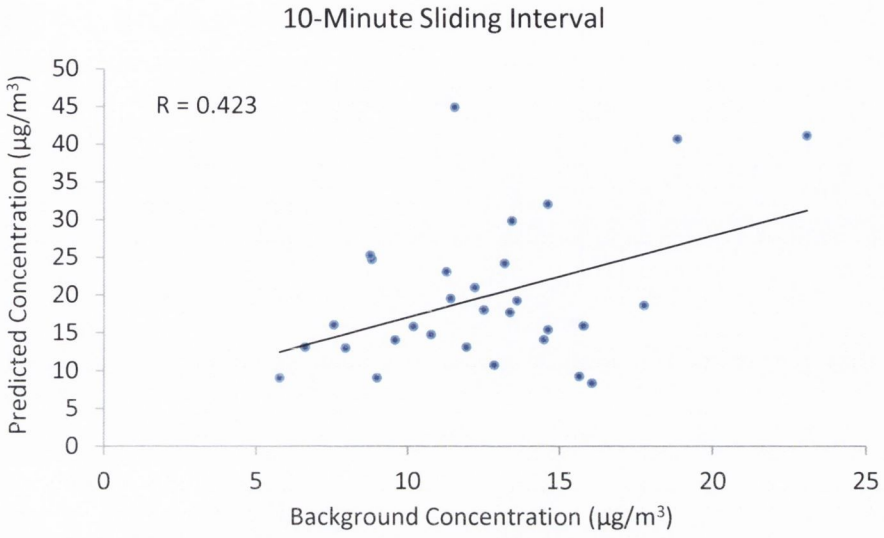


Figure 7.13: Comparison of sliding interval separated (10 mins) predicted background concentrations versus the observed background concentrations (µg/m$^3$).

Following this initial analysis, two further sliding intervals with more time steps were also tested to gauge the improvements that could be made with alternative time intervals. The first analysis trialled was with the sliding interval time period increased to 30 minutes. Figure 7.14 illustrates the comparison between this 30-minute sliding interval predicted background concentrations and the actual background concentrations for each sampling day. As can be seen, the Pearson's correlation slightly improved with this time interval (R = 0.44) over the previous 10-minute sliding interval.

The next sliding interval time step period used was for a 1-hour sliding interval. The results of using this longer time interval are shown in Figure 7.15. Similarly to the previous example where the time interval was increased from 10 to 30 minutes, the Pearson's correlation for this 1 hour interval improved marginally yet again (R = 0.451). The net result of the increasing intervals was the absolute difference between the predicted and actual background concentrations falling from an average of 8.4 µg/m$^3$ for the 10-minute interval, to 4.7 µg/m$^3$ for the 1-hour sliding interval.

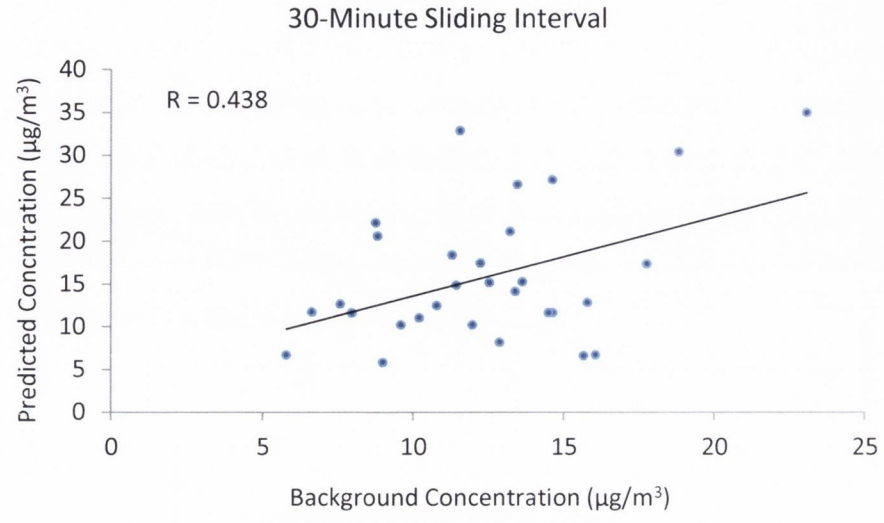


Figure 7.14: Comparison of sliding interval separated (30 mins) predicted background concentrations versus the observed background concentrations ($\mu g/m^3$).

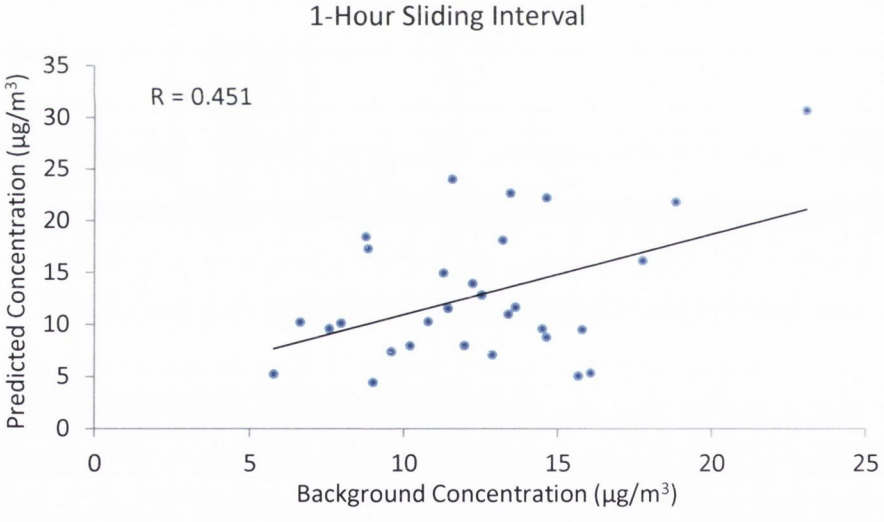


Figure 7.15: Comparison of sliding interval separated (1 hour) predicted background concentrations versus the observed background concentrations ($\mu g/m^3$).

## 7.6 Summary

This chapter explored a number of different possible determinants for the personal exposure of the study population. The variables considered were primarily the background $PM_{10}$ concentrations and also the meteorological conditions present over

the course of the personal sampling campaign. While the primary method of analysis used consisted of simple and multiple linear regressions, the personal exposures of volunteers were also examined further with the use hydrological baseflow separation methods.

The influence of background concentrations was assessed using three different FSM locations. The first was the Phoenix Park was taken as a general background monitoring site for the Dublin region due to its relatively withdrawn location from major city traffic. The two other FSM categories that were examined were the FSM monitors located nearest to the place of work of each volunteer, as well as the FSMs closest to each subject's home. Typically the FSM closest to each city centre workplace was the monitor located on Winetavern Street. However, the FSMs near individual homes varied far more depending on where a subject lived, and in a number of cases there was no nearby FSM present or else data was unavailable.

In order to carry out the regression analysis, the personal exposure data along with the data obtained from the FSMs were log transformed due to the log normal nature of the data distributions of each. The simple linear regression analysis of the three different FSM categories, the Phoenix Park, FSM nearest to home, and FSM nearest to work, showed that the background concentrations were relatively poorly correlated with the 24 hour personal exposure results. Of the individual linear regressions, it was found that the transformed Phoenix Park background data was slightly more correlated with personal exposure than the other two FSM categories, although the correlation was only moderate ($R = 0.41$). Again, when all three FSM categories were included in a multiple linear regression model the log transformed Phoenix Park FSM variable displayed the most significance ($p = 0.155$). The overall model was a weak predictor of personal exposure with 17.1% of variability accounted for in the model according to the adjusted $R^2$ value.

Further analysis was conducted into the relationship between the 'FSM nearest work' data, and its relationship with the occupational exposures of the subjects. The results from this analysis found a low correlation ($R = 0.319$) between the log transformed

occupational exposures and city centre FSM concentrations. Moreover, the addition of the distance to FSM variable did not offer much improvement to the regression model with the adjusted $R^2$ barely changing, and was not found to be a statistically significant variable ($p = 0.081$).

A multiple linear regression was carried out on a number of meteorological parameters obtained from Met Éireann. These measurements had primarily been taken at a meteorological site in the Phoenix Park, however both wind direction and speed were unavailable from this site so the Dublin Airport metrological measurements were used in their absence. The results of the analysis again revealed that many of the outdoor variables, in this case the weather data, were not significant in determining daily personal exposure. In fact, the only significant meteorological parameters found in this stepwise regression were temperature and sea level pressure. This indicated that colder weather will increase personal exposure, while sea level pressure was only just significant but the positive coefficient for predictor means that personal exposure will increase with increasing pressure at sea level. However, this model was found to be a poor predictor of the log transformed daily personal exposure concentrations ($R^2$-adj = 0.051).

The final MLR analysis conducted involved combining both the background concentration data with the metrological data, as well as other potential determinants such as time spent in each microenvironment, along with categories such as 'gender' and 'smoker'. This model had the best coefficient of determination of all regression models ($R^2$-adj = 0.23). In total the four iterations of the stepwise model selected the variables Log-Phoenix Park FSM concentration, time spent at home, gender, and smoker as the only significant predictors.

The use of hydrological baseflow separation techniques as a means of obtaining the ambient background concentrations on a sampling day was moderately successful. The initial approach taken was using the Boughton method which was a logic function which assessed whether the personal exposure time series was increasing or decreasing at a particular time step. The resulting output for the background was found to have a

high frequency response. The output of the initial Boughton analysis was moderately correlated to the actual background concentrations, however this was marginally improved upon with further adjustment of the recession constants *a* and *b*.

The second hydrological approach taken to separating the background concentrations from the personal exposure data was using a sliding interval filter method. In total three different interval time periods were employed. The response of the resulting outputs was found to be of a lower frequency than the corresponding outputs from the Boughton method. The sliding interval method results were also better correlated to the observed background concentrations than those found with the Boughton method. The Pearson's correlation for each of the sliding time intervals was found to increase as the interval time steps grew ever larger. Overall, the hydrological baseflow separation techniques, such as those seen here, have potential as a useful tool for predicting personal exposure data from background concentrations.

In summary, this analysis has highlighted the relationship between background air quality measurements and personal exposure measurements. However, the correlation is weak in general and therefore, taken in isolation, background air quality data is a poor indicator of the personal exposure of a given population.

# Chapter 8

Discussion

# 8 Discussion

## 8.1 Overview of Topics Raised

A number of topics for discussion have been raised throughout the preceding chapters of this study. The results reported in Chapter 4 highlighted the large amount of time that individuals spent indoors, along with the main microenvironments and activities that dominated their daily time-activity budgets. The activity patterns of each of the study subjects subsequently dictated their 24-hour personal exposure to $PM_{10}$. Each of the personal exposures from the major activities and microenvironments are discussed in detail in the following sub-sections. The effects of additional factors that may inflate personal exposure are also examined. While the differences between the personal exposures of the main office worker study population and an alternative occupation was also reported.

The results of various modelling techniques were reported in several of the chapters. The human respiratory tract model was used to estimate the uptake of $PM_{10}$ into the lungs for each microenvironment. A number of different modelling methods were employed in order to simulate personal exposures which included statistical and probabilistic approaches, as well as the adaptation of machine learning techniques for prediction of personal exposure. The determinants of personal exposure to $PM_{10}$ such as background concentration and meteorological conditions were investigated and their influence on personal exposure was reported. Additionally, hydrological methods were applied to the personal exposure time series data in order to obtain background concentrations. Many of these modelling approaches raised interesting topical discussion points that will be discussed hereafter.

## 8.2 Time-Activity Patterns

The time-activity budgets of the population recruited for this study were found to be very similar to that of other studies. The most interesting result from the analysis of the time-activity budgets of the study population was that 92% of time was spent in indoor microenvironments by the volunteers. The rest of the time budgets consisted of a further

3% of time spent in enclosed transit and just 5% of each day spent in an outdoor microenvironment. Interestingly, this was comparable to the results found in both the large American (NHAPS) and Canadian (CHAPS) time-activity pattern surveys (Leech et al., 1996; Klepeis et al., 2001). The respondents in both of these surveys reported spending slightly larger amounts of time outdoors, 6.92% amongst NHAPS respondents and 6.05% for the CHAPS. While more time was spent in a vehicle also (5.74% and 5.33%, respectively). However, as these surveys sampled across a wide spectrum of the population and at weekends also, a larger proportion of time spent outside would be expected. The greater amount of time spent in vehicles too is perhaps a reflection of the car culture pervasive in North America compared with Ireland.

In the NHAPS survey, an average of 20% of respondents reported spending time in an office or factory and for an average duration of 388 minutes. The amount of time spent in the office for the volunteers in this study was notably higher at 448 minutes on average. This difference may well be explained due to the NHAPS figure including a variety of occupations. However, in a personal exposure study by Brauer et al. (2000), the 18 office workers recruited were found to spend a mean time of 385 minutes in work, while industrial workers were at work for 457 minutes on average.

The proportion of time spent at home by the subjects of this study at 59%, was also perhaps a result of the additional time spent in the workplace. Both the NHAPS and CHAPS studies reported a higher proportion of time spent at home (68.7% and 65.9% respectively), while the more directly comparable office workers in the study by Brauer et al. (2000) were found to be at home for 69.8% of the time.

Although both Leech et al. (1996) and Klepeis et al. (2001) reported the proportion of time spent within enclosed transit modes during both activity surveys, the specific modes were not stated. While Brauer et al. (2000) merely stated the travel time for workers, which with a mean value of 14 minutes would be far less than the travel times for the various modes in this study which had a range of 20 to 58 minutes, depending on the mode type.

As a comparison of the social habits across different populations, the proportion of time spent in cafés, public houses and restaurants by respondents in the NHAPS and CHAPS surveys was approximately 1.8% on average (Leech et al., 1996; Klepeis et al., 2001). The subjects of this study were in these locations for an average of 1.4% of their time, although this figure was based on midweek days only.

The large amount of time spent indoors by the subjects in this study highlights the importance for policy makers to ensure the air quality in workplaces and other indoor public places meet sufficient air quality standards. However, most of this time is spent indoors in the home, so it is ultimately difficult to control for much of the indoor PM personal exposure.

## 8.3 Personal Exposure Concentrations

A number of interesting results were found from the personal exposure sampling campaign. Perhaps the most important result from an environmental health perspective of the general study population was that the mean 24-hour personal exposure for the study population was found to be 25.5 $\mu g/m^3$. This concentration value is lower than both the current annual (40 $\mu g/m^3$) and daily (50 $\mu g/m^3$) EPA mean limit concentrations for $PM_{10}$. However, it should be cautioned that with a standard deviation for the 24-hour personal exposure of 15.3 $\mu g/m^3$, and a maximum observed 24-hour concentration of 105.7 $\mu g/m^3$, a number of volunteer were close to, or else exceeded, the daily limit value.

The overall mean personal exposure concentration for the study population also served to highlight an important discrepancy between the outdoor fixed site monitors, and the actual $PM_{10}$ concentrations the study population were exposed to. The mean background $PM_{10}$ concentration at the Phoenix Park fixed site monitor for the sampling days of the study was just 13 $\mu g/m^3$. This illustrates how the 24-hour personal exposures of the study population were subject to many indoor particulate sources, which in this case increased their personal exposure on average by 50% above background levels. This observation may be a useful consideration for future epidemiological investigators

when using background PM concentration data to assess the health impact on a study cohort.

The ambient concentrations for this study were far lower than those found in many other personal sampling studies. This was also true of the average personal concentration found, which were lower than many other personal exposure studies in literature. For instance, in Slovakia Brauer et al. (2000) found that outdoor $PM_{10}$ concentrations were 35 $\mu g/m^3$ in summer and slightly higher at 45 $\mu g/m^3$ in winter. The gravimetrically sampled mean office worker personal concentration of that particular study was 3.1 times the outdoor concentration in summer and 2.1 times the wintertime concentration. These figures were also lower than for the other two groups of industrial workers and students included in the study.

There was found to be a dearth of personal sampling studies on office workers to directly compare results with, whilst there is also little in the way of real-time sampling using nephelometer devices either. However, there are examples of other studies completed for alternative subject demographics. In the Netherlands, Janssen et al. (1997) collected 24-hour personal $PM_{10}$ exposure samples gravimetrically from 45 school children and observed an average exposure concentration of 105.2 (± 28.7) $\mu g/m^3$. The recorded ambient $PM_{10}$ concentrations during the monitoring campaign were similar to that found in Slovakia, at 38.5 (± 5.6) $\mu g/m^3$.

A number of other personal exposure studies have been carried out for $PM_{2.5}$ concerning different occupations. Although not directly comparable to the $PM_{10}$ personal exposure results of this study, they may be compared roughly as $PM_{2.5}$ may compose 70% of $PM_{10}$ (Martuzzi et al., 2006). Branis and Kolomazníková (2010) found a mean $PM_{2.5}$ concentration for a student who carried out year-long monitoring in the Czech Republic was 55.7 $\mu g/m^3$. Borgini et al. (2011) measured personal daily $PM_{2.5}$ exposures of a number of high school students in Milan and found personal exposures of 75.9 (± 58.1) $\mu g/m^3$ on average.

As part of the EXPOLIS study, Kruize et al. (2003) reported the mean 48-hour gravimetrically sampled $PM_{2.5}$ personal exposures for the general population from four study cities. Personal exposures were highest for Athens with a mean of 37 $\mu g/m^3$, and this was followed by Prague and Basel (35 and 31 $\mu g/m^3$, respectively). However Helsinki's average $PM_{2.5}$ personal concentration for the general population was 19 $\mu g/m^3$. This level of exposure would put it in line with the personal $PM_{10}$ concentrations found in this study for the Dublin population, assuming the 0.7 ratio of $PM_{2.5}$ to $PM_{10}$ suggested by Martuzzi et al. (2006). This ratio was also found to be the approximate ratio (0.67) at the Rathmines FSM in Dublin when the 2009 to 2011 $PM_{2.5}$ and $PM_{10}$ measurements were compared.

Many of the studies referenced are from far more polluted areas than Dublin and may explain why many of the personal exposures discussed are far higher. Perhaps only Helsinki is comparable to Dublin as Finland benefits from cleaner northern air masses much like Ireland does from Atlantic air masses. Also, these studies were sampling from a wide spectrum of volunteer types rather than exclusively office workers which may explain the variation in personal exposures.

### *8.3.1 Occupational exposure*

One of the exposure results obtained during the sampling campaign that exerts great influence on the overall 24-hour personal exposure of an individual was the occupational exposure concentration. The mean occupational personal exposure (39 $\mu g/m^3$) for the office workers in this study was found to be 65% higher than the overall 24-hour mean personal exposure, and three times greater than the background concentration in the Phoenix Park. This was a key finding as this microenvironment plays an important role in the day to day personal exposure concentrations of individuals, with an individual spending an average of 30% of every weekday in work. The population standard deviation for the 'at work' personal exposure concentration was also found to be 36 $\mu g/m^3$. The significance of the occupational exposure mean and standard deviation should not be understated as it suggests the study population was exposed to high $PM_{10}$ concentrations for prolonged periods of time. Indeed, the large

standard deviation reveals that a number of volunteers would have workplace concentrations that exceed the EPA's mean daily limit concentration. For policy makers, this is an important are to address in insuring that workplace PM concentrations are lowered, which will result in health benefits for workers.

There was found to be a lack of directly comparable studies in the literature in which to compare the occupational exposure of office workers. For example, perhaps due to the limitations of the temporal resolution of the gravimetric sampling used, Brauer et al. (2000) did not report specific occupational exposures of the office workers in their study. However, the overall personal exposure of office workers was found to be less than that of industrial workers and students.

There are some studies that have measured personal exposure to $PM_{2.5}$ of office workers rather than $PM_{10}$. Again, the results from these studies are not directly comparable but can give a good indication of what sort of personal exposure concentrations have been found to exist in an office environment. In Mexico, Tovalin-Ahumada et al. (2007) used gravimetric sampling on various occupations in Mexico City and Puebla and found mean occupational personal $PM_{2.5}$ concentrations for office workers in each city to be 140.4 (± 50.7) $\mu g/m^3$ and 74.3 (± 24.3) $\mu g/m^3$, respectively. A study by Mosqueron et al. (2002), in which a gravimetric method was also employed, found in-office personal concentrations of 34.5 (± 38.6) $\mu g/m^3$ amongst 55 primarily female Parisian office employees. The Mexican average personal concentrations are clearly far higher than those work place concentrations encountered in this study. However, the Parisian study concentrations would be far more similar to the equivalent concentrations in this study. One potential reason for the discrepancy between the personal exposure of subjects in the Mexican and French studies becomes apparent on inspection of the sampling population. In the Paris study, the researchers excluded 60 of the 200 subjects because they were smokers, whereas in contrast, the Mexican study population included 21 smokers among the total study population of 53 individuals.

A comparison with another occupation was also undertaken in this study. A small number of taxi drivers were recruited to monitor their occupational exposures over a

number of work shifts. The mean occupational exposures for the four drivers ranged from as little as 6 $\mu g/m^3$ to 21 $\mu g/m^3$. What was most interesting about the monitoring of the taxi driver personal exposures was that the drivers that worked mostly during the early hours of the morning and outside the city centre had noticeably lower occupational exposures. The single driver that sampled on an approximately 9 am to 5 pm schedule was found to have the highest occupational $PM_{10}$ exposure of 21 (± 36) $\mu g/m^3$. Moreover, this driver also spent most of his time within the city centre. Perhaps a surprise finding of this study was that the taxi drivers, albeit a small cohort, had a lower occupational exposure to $PM_{10}$ than the office workers.

Mohammadyan et al. (2010a) carried out gravimetric sampling of taxi driver $PM_{10}$ personal exposure in Iran. The results of that study showed a massive mean occupational exposure of 184.7 $\mu g/m^3$. In other studies on taxi drivers, Tovalin-Ahumada et al. (2007) found drivers to have an average occupational personal $PM_{2.5}$ exposure of 178 (± 160.2) $\mu g/m^3$ in Mexico City. However the authors of that particular study noted that the mean annual $PM_{10}$ concentrations ranged between 61 and 114 $\mu g/m^3$ for the Mexico City region, far in excess of the concentrations that are found in Dublin. Zagury et al. (2000) measured personal exposure to black smoke of day-time working taxi drivers in Paris and found mean concentrations of 168 (± 53) $\mu g/m^3$.

In many cases in the literature there has been a large disparity between the occupational personal exposures sampled elsewhere and those found in Dublin. However, this may be explained due to the fact that many of these locations are far more heavily polluted than Dublin, while in some cases ETS may also inflate concentrations due to a lack of occupational smoking legislation. In the case of taxi drivers, the samples taken in other locations would be subject to increased emissions from older vehicle fleets as well as possibly far more congestion on the roads. The quality of the taxi vehicles most likely would have been of a lower standard in a number of the study locations, such as Iran and Mexico. Moreover, these studies also tended to collect their samples during daylight and peak hours, while some of the drivers of this current study chose to work night shifts. The resulting occupational exposures would therefore be lowered due to the decreased amount of traffic and other PM emissions at night time around the city.

### *8.3.2 Commuter exposure*

The travel personal exposures encountered by the study population in this study were observed to be quite variable. The primary results from the commuter exposures were that the highest $PM_{10}$ personal exposure concentrations were found while travelling by bus (43 $\mu g/m^3$), while travel by tram had the lowest personal exposure associated with it (14 $\mu g/m^3$).

In literature, much of the personal exposure sampling studies have focused on commuter personal exposure over short periods exclusively, rather than daily exposure. Many of the sampling campaigns in literature have also focused on personal exposure to $PM_{2.5}$ (Adams et al., 2001c; Kaur et al., 2005a; McNabola et al., 2008b), along with primarily focusing on the commute modes of bus, cycling, driving, and walking. When sampling commuter personal exposure to $PM_{10}$, Strak et al. (2010) gravimetrically measured the morning time rush hour $PM_{10}$ exposure of 14 cyclists in Utrecht and found a mean exposure of 45 $\mu g/m^3$. In another study in Arnhem, Zuurbier et al. (2010) reported median $PM_{10}$ exposures for a small sample set of subjects commuting during the morning rush hour by bike, bus, and car of 46.7, 49.8 and 39.3 $\mu g/m^3$, respectively. This study also utilised gravimetric sampling equipment to collect their commuter $PM_{10}$ samples.

Evidently from the examples given, the commuter $PM_{10}$ personal exposures of many studies from literature will have higher commuting exposure concentrations than found in this study. This is because the personal exposures reported in this study were not limited to sampling during set time periods in order to coincide with peak traffic conditions, and therefore potentially the peak outdoor concentrations also. However, the commutes during peak time traffic hours could conceivably be analysed separately with a review of the activity logs and GPS data, Another factor observed in the travel patterns of the subjects in this study was a propensity for travelling to work either early or late in the morning, in order to avoid rush hour traffic. Consequently this meant that they were also avoiding the peak commuting time air pollutant concentrations. Interestingly though, the highest mean personal $PM_{2.5}$ concentrations in a previous

study in Dublin were also found to occur when commuting by bus (McNabola et al., 2008b).

The lower personal exposure concentrations for the train and tram in this study, compared with other travel modes, were most likely due to the ventilation systems on board, as well as relative isolation from traffic. It should also be noted that there was little within the literature regarding $PM_{10}$ personal exposures while on trains and trams. Although, Adams et al. (2001c) reported above ground London tube line $PM_{2.5}$ personal concentrations of 29.3 $\mu g/m^3$, which was over eight times less than the corresponding concentration for an underground line.

### *8.3.3 Cooking*

The activity of cooking posed one of the more challenging questions over the course of the experimental sampling campaign. The difficulty arose due to the nature of particles released during a cooking event and this begged the question of how could the Aerocet-531 monitors be calibrated for such a difficult to control source. The particulates released for some cooking events may be due to smoke from burning, however much of the time cooking will release large quantities of water vapour in the form of steam.

Previous researchers have recognised the heterogeneous nature of cooking emissions when more the than one type is on-going, as well as the need to calibrate for each individual event (Jenkins et al., 2004; Fischer and Koshland, 2007). In the case of such a study as this one, it was not feasible to calibrate the personal samplers for each individual event and this issue was compounded due to the difficulty in replicating cooking location conditions also. Each kitchen would have had its own unique set of unknown air exchange rates and air volumes. Many of the subjects also failed to reliably report all the cooking events on-going and ventilation conditions present, such as use of a cooker fan. Therefore, the cooking events were removed from the dataset to prevent artificial inflation of personal exposure concentrations while in the home from the monitor accidently detecting water vapour.

The impact of removing cooking from those volunteer samples was a dramatic lowering of in home personal concentrations from 71.4 to 25.9 $\mu g/m^3$. It was also observed that the highest personal concentrations from a variety of cooking occurred due to frying (312.6 $\mu g/m^3$) and this was followed by grilling (200.1 $\mu g/m^3$) and boiling (105.6 $\mu g/m^3$). While the lowest concentration amongst cooking sources tended to occur when the subject was toasting (51.2 $\mu g/m^3$). The large amounts of particles emitted when frying by volunteers is similar to what has been observed previously in studies (Abt et al., 2000a; Wallace et al., 2004), while grilling was also found to be a large emitter of particulates (He et al., 2004).

### *8.3.4 ETS exposure*

This study found that the impact of tobacco smoke on personal exposure of individuals was to greatly raise their 24-hour personal exposure concentration. However, it should be noted that during smoking events the Aerocet-531 monitor was merely recording the ETS suspended in the ambient air of the microenvironment. The personal measurements were not measuring the particulates actually inhaled by a smoker.

The average increase in the 24-hour personal exposure for people who reported ETS exposure, compared with non-ETS exposed individuals, was approximately 10 $\mu g/m^3$. The majority of smokers in the study mainly reported that they smoked in their homes, and as a result the mean concentration while they were active at home was 64 $\mu g/m^3$ and 19 $\mu g/m^3$ at night while sleeping. Both figures are far above the equivalent study population averages, where night time personal exposures were 10 $\mu g/m^3$ and exposure concentrations while active in the home of 26.4 $\mu g/m^3$. This finding has grave consequences for non-smokers who are in residence with a smoker in particular, as not only will second hand smoke during a smoking event damage their health, but they will continue to be subjected to higher particulate concentrations long after the event.

One difficulty of the study sampling campaign was in the recruitment of smokers. Many of the smokers recruited in the main study were in fact found to be irregular smokers or else only smoked on a social basis. Also, strict smoking legislation in Ireland meant that

the opportunity to smoke during working hours or public places was quite limited, thus most smoking occurred at home in the evening time. A combination of these factors was the reason why personal sampling was carried out additionally for a number of days in the homes of individuals who smoked with greater regularity. The data collected in these two homes provided a supplementary dataset which quantified the peak personal exposure concentrations and lingering aftermath due to smoking in an indoor setting.

The mean personal exposures found in the homes of smokers were far in excess of that of non-smokers. Examples of some of the peak personal $PM_{10}$ concentrations found was 853 $\mu g/m^3$ in the home of Smoker A, while the largest peak concentration in Smoker B's home was 603 $\mu g/m^3$. Other studies have also observed similar large short term peaks (Chao et al., 1998). In general, studies have concluded that smoking is the most important source of indoor PM concentrations (Dockery and Spengler, 1981; Quackenboss et al., 1991; Neas et al., 1994). For non-smokers who live with or are in the presence of smokers, their personal exposure will be greatly affected by the ETS emissions. However, from a health perspective Piccardo et al. (2010) concluded that secondary smoke, such as that found to linger in the homes of smokers in this study, should be considered in studies about health of active smokers also.

## 8.4 Uptake of $PM_{10}$

The ICRP human respiratory tract model implemented as part of this study enabled the dose uptake for the study population to be accurately estimated. Previously, studies have relied on measuring ventilation rates, primarily for transport microenvironment personal exposure, and multiplying this by the sampled personal exposure concentrations in order to estimate dose uptake of a pollutant (O'Donoghue et al., 2007a; Zuurbier et al., 2010).

Possibly the most important factor in determining the dose uptake of an individual was the exertion level of an individual while in a microenvironment or partaking in a particular activity. The larger volumes of air passing through the respiratory tract when breathing rates are elevated will inevitably lead to greater deposition of inhaled

particles. This was evident when examining the activities and locations where the highest doses were recorded. The second highest mean dose was found when individuals were involved in sport. This activity was assigned to the heavy exertion category and as result the mean dose uptake amongst volunteers was 127.6 μg. The contribution of greater breathing rates to dose also manifests itself with the different travel modes. A key finding from the dose calculation of the commuting modes was that even though the activities of cycling and walking were not found to have the largest personal exposure concentrations, they did in fact have the largest mean dose uptake associated with them (18.8 μg, respectively) due to elevated respiration. Finally, the statistically significant differences found between male and female PM dose uptakes also serve to illustrate this point.

The most important result from the human respiratory tract modelling was the identification of the microenvironments in which the study subjects experienced the largest dose uptakes. The highest dose uptakes were found to occur in the two microenvironments where the volunteers tended to spend most of their day, which were while they were at work and active at home (216 μg and 81.8 μg, respectively). However, dose uptake while the subjects slept was much lower in comparison (22.9 μg) despite spending almost a third of the day sleeping. This was due to a combination of the low breathing rate and low personal exposure concentrations found during this activity. In fact, several of the locations and activities that made up a small fraction of a person's day in comparison had, on average, higher dose uptake associated. These included the previously mentioned activity of sport, as well as public houses (28.9 μg) and the category 'other indoor' (28.2 μg).

The effect of smoking was also apparent when the doses for subjects were calculated. The average 24-hour dose for smokers, excluding the directly inhaled quantities of cigarette smoke, was approximately 27% greater than that of non-smokers. The majority of this difference occurred due to the raised concentrations in the homes of smokers as a result of ETS. The in-home uptake was 150% greater for smokers than non-smokers. The strict smoking laws regarding smoking in public places in Ireland reduces the

opportunity for smoking in indoor locations, which also reduces the potential dose for the majority of people from ETS.

## 8.5 Modelling of Personal Exposure

The challenge in modelling the personal exposure of individuals was evident from the results reported in Chapter 6. Part of the reason why exposure modelling is undertaken is because of the difficulty and expense in conducting large scale population exposure studies. Often epidemiological studies that seek to assess the impact of air pollutants on the health of a study cohort have to rely upon background concentrations. However, background concentrations can be a poor surrogate for the actual exposure concentrations of the individuals. Thus, the ability to estimate personal exposures based on the activities of a person may be a more useful tool for epidemiological studies.

The modelling conducted in this study consisted of three different approaches, which were the time-activity weighted models, the Monte Carlo based modelling, and the machine learning models. The time-activity modelling was the simplest and easiest approach to implement, and is commonly employed in personal exposure studies. The time-activity model designated 'Model 2' was found to have the best correlation ($R = 0.67$) between the predicted values and the actual measured personal exposure concentrations. This was perhaps no surprise, as this model had the input parameters for each sample based on the actual individual's data from other samples that he or she collected. In contrast, the time-activity weighted Model 1 which was based on the population average concentrations had a significantly lower correlation ($R = 0.24$), with the predicted personal exposures also displaying very little variation.

The type of approach seen in Model 1, in which the input concentrations for each activity and microenvironment are based on the population averages, was subsequently altered. The methodology for this new approach was based on random sampling from specifically designated probability distributions, rather than just using a mean concentration value for each activity or microenvironment. This Monte Carlo sampling approach resulted in an improvement over Model 1, with correlations between the

measured and predicted personal exposures found to be best using 100 iterations (R = 0.36). The addition of smoker specific 'at home' and 'sleeping' distributions also improved results, which serves to illustrate the benefits of accurate knowledge of indoor PM sources when attempting to make a prediction for a subject.

An overall population risk assessment model was also developed which utilised Latin hypercube sampling with a Mersenne twister random number generator. This model accurately mimicked the actual daily personal exposure dataset. The sensitivity analysis generated from the model output illustrated the importance of occupational exposure, with the 'at work' concentrations exerting the biggest influence on the overall 24-hour personal exposure of the study subjects. In contrast, similar analysis on $PM_{2.5}$ by Jantunen and Kansanterveyslaitos (1999) found the largest influence on personal exposure in Helsinki was the personal exposure concentration in the home. The 'at home' and 'sleeping' concentrations in this study were the next two greatest influencing factors on 24-hour personal exposures after 'work'.

The machine learning techniques used in this study also displayed good potential as a means of predicting PM personal exposure. The use of ANNs in personal exposure studies as a predictive technique is limited to just one example in which a FFNN was used as a means of modelling exposure to a number of VOCs (Aquilina et al., 2010). However, ANNs have been employed in numerous other fields for predictive purposes such as civil and traffic engineering (Firat and Gungor, 2009; Dunne and Ghosh, 2011). Although the testing performance of the FFNN and GRNN models used did not quite match that of the time-activity weighted Model 2, they were not reliant upon previous personal exposure samples from subject whose exposure was being modelled. Once a dataset for personal exposure has been established and the networks, they can then be used then for prediction of previously unseen exposure samples. Also, with additional pertinent inputs the model performance may improve further.

## 8.6 Determinants of Personal Exposure

In Chapter 7, a number of potential determinants were examined on whether or not they influenced personal exposure concentrations, and if so to what extent. The determinants examined were FSM sites around Dublin City, as well as the meteorological conditions that existed on the sampling days for each subject. The assessment of all variables was carried out by using simple and multiple linear regression.

The data obtained from the FSMs were divided into three categories which were included a general background site for the city (the Phoenix Park FSM), the nearest FSM to each individual's workplace, and finally, the FSM that was located closest to the home of each subject. The $PM_{10}$ concentration data of each category was found to be log normally distributed, therefore a log transformation was carried out on each FSM dataset, as well as the personal exposure data. This was because one of the assumptions of linear regression is that errors are normally distributed. Violations of normality compromise the estimation of coefficients and the calculation of confidence intervals.

The primary results from the regression analysis on the relationship between the transformed FSMs and personal exposure data revealed the $PM_{10}$ concentration data from the Phoenix Park FSM was the most highly correlated with the personal exposure data out of all the FSM categories. However, the correlation between the two was at best moderate, and the simple linear regression model obtained accounted for only a small proportion of the variability in the personal exposure data ($R^2$ = 0.167). The Phoenix Park FSM model was only marginally improved upon with inclusion of all three FSM categories in a MLR model ($R^2$ = 0.183 and $R^2$-adj = 0.171). The regression model of the log transformed occupational personal exposures and FSMs nearest to the workplaces also displayed a low coefficient of determination ($R^2$ = 0.102).

The multiple linear regression with the weather parameters solely included was an even poorer model than the FSM models. The only significant weather variables were found to be temperature and sea level pressure, while the stepwise model returned an $R^2$-adj of just 0.051 after two iterations. Clearly, the large amount of time that each subject spent

indoors meant that meteorological parameters were a poor determinant for the 24-hour personal exposures.

The best performing MLR model was the analysis carried out in which the meteorological and log transformed Phoenix Park FSM data variables were combined with the fractions of time spent in each microenvironment and two further categorical variables. The resulting predictor variables from this model included the categorical variables of gender and smoking status, as well as time spent at home and the Phoenix Park FSM data. This model had an adjusted $R^2$ of 0.023, meaning a huge amount of variability in the exposure data was not explained by the model. The coefficients for the selected predictor variables suggested that females will have lower exposure concentrations than males, while perhaps more obviously smokers will have larger personal exposures. The transformed Phoenix Park FSM data was also the most statistically significant of the variables ($p < 0.000$), hence why it was chosen first.

## 8.7 Baseflow Separation

The use of the baseflow separation methods was an attempt at converting common hydrological techniques for use in the field of air quality. It was envisaged that this would result in the creation a useful means at deriving background concentrations data from personal exposure time series data. The two methods tested in Chapter 7 were the Boughton method and the sliding interval method. These two techniques were chosen as they were the methods that displayed the most promise in early test cases (McNabola et al., 2011). However, in this analysis the application of the two methods proved less successful than previously seen.

The best method in this analysis was found to be the sliding interval with a time interval of 1 hour. The results from that case found a Pearson's correlation of 0.451 when the modelled background data was compared to the actual concentrations. The highest correlation found using the Boughton method was 0.34. In the earlier assessment seen in McNabola et al. (2011), in which only 10 samples were modelled using a variety of these methods, the Boughton method had been found to perform the best ($R = 0.77$),

while the sliding interval also had a high correlation associated (R = 0.72). The degradation of the correlations seen here are most likely just to the increased variability in the larger dataset. The moderate correlation between the background concentrations and the personal exposure data found during the linear regression analysis maybe affecting the results of the baseflow separations.

## 8.8 Limitations of the Study

In this study there were limitations associated with various aspects of the work conducted. Some of these limitations were touched upon in brief previously in earlier chapters, while others have not been previously mentioned.

There were a number of limitations related to the equipment and methodology used during the study. One of the limitations of the Aerocet-531 monitor was the battery life of the instrument, which meant the instrument could only remain unplugged for a limited amount of time (approximately six hours). This meant that the volunteers had to be stationary in order to keep it plugged in for large portions of the day. Thus, this was a major consideration in selecting office workers to partake in the study. Another minor limitation of using the Aerocet-531 monitor was that the inlet nozzle could not be attached to the lapel of the volunteer, so that it was directly in the breathing zone of the volunteer at all times. This issue was mostly negated by the volunteers locating the instrument as close to themselves as possible when stationary at home or in work, and again this was an advantage of having a study population of office workers who could locate the instrument beside them at their desk. However, due to the noise of the monitor while operating, it was often not positioned as close to the volunteer as desirable while sleeping.

The constraints on calibrating the Aerocet-531 for cooking events have been alluded to previously in Chapter 5. The need for the filter based Haz-Dust EPAM-5000 instrument to sample for approximately eight hours in order to collect a sufficient amount of particle mass meant that calibrating for cooking was not feasible, as it was not realistic to cook for this duration. This difficulty, combined with the mix of various cooking

events often reported meant that the simplest solution was to exclude the data values from cooking. However, further research into the concentrations from different cooking events and the effect they have on the Aerocet-531 would be useful in adding to the knowledge base in this area for future studies.

There were also various limitations accompanying the modelling techniques that were employed in previous chapters. As stated in Chapter 6, the human respiratory tract model was developed for a Caucasian male and female lung. Ideally, there would be alternative parameters included for other races and to account for variability in height and weight of the subjects. However, as the vast majority of volunteers were Caucasian, and the exact heights and weights were not available, the model parameters were therefore limited to the profile of an average Caucasian person. Another aspect of the HRT model that may have influenced the dose uptake calculations was the assignment of the breathing characteristics during each activity. For example, the exertion level of each individual while at work was divided into 40% 'at rest' and 60% 'light exercise'. This ratio, as explained in Chapter 6, was dictated from the available literature, however, it was not possible to confirm for each individual sample if this was in fact the actual amount of time spent at these exertion levels. Similarly, other activities such as 'at home' may have included periods of greater exertion which were not documented by the volunteer. These discrepancies would have been very difficult to take account of in the absence of extremely accurate activity reporting. However, overall the assigned exertion levels provided a reasonable estimate for the purpose of dose uptake calculation of the study population.

The problems arising from inaccurate or incomplete activity diary reports were not limited to the dose uptake calculations. Many of the volunteers reported only the microenvironment they were situated in without giving specific details on any potential particle emitting sources present. For example, as seen in Chapter 4, a significant percentage (46%) of those who reported cooking never specified the exact nature and type of the cooking event. This problem of unknown or unnoticed particle sources may manifest itself in other areas of the dataset also. One of the major areas where this may be the case is while the subjects are in their workplaces. Unlike the 'at home'

microenvironment, which in general had relatively few unexplained peaks in each volunteer dataset, the workplace data was often found to contain peaks. These unexplained peaks in personal exposure concentrations could have come from any number of potential sources, for example, activities of colleagues, photocopy machines, printers, etc.

One advantage of this study, compared with personal exposure studies conducted elsewhere, was the utilisation of the GPS to track the movement of each volunteer in conjunction with an activity diary. Instead of having to solely rely on information contained in the activity diaries about commutes and other movements, the GPS provided information on the precise moment a volunteer left their home or workplace. This also meant that a transition between being on a bus and walking, for instance, was easily observable and compensated for activity diaries which were deficient in information.

Unexplained variability in the data, or unreported events, can also have an effect on some of the modelling techniques used. For instance, the neural network models relied upon recognising patterns among the training data inputs in order to establish relationships. Ideally, high personal exposure concentrations would be explained by an activity taking place that could be added as an input. This in turn would further minimise the errors and lead to more accurate personal exposure predictions. However, this is difficult to achieve unless the subject has been particularly observant of their surroundings and possible particulate sources.

Another limitation of the neural network modelling was the large amount of data required to train the model. The models could have been trained with less data, although that would more than likely increased the errors of the model. In contrast, the time-activity models can be carried out with less data, for example, Model 2 was based on only a few previous days' data from each particular subject. However, the benefit of the neural networks is that they can be used to predict any random individual's personal exposure. The time-activity Model 2 needs previous samples from that same person, while predictions from time-activity Model 1 display very little variability because each

microenvironment input is assigned an average value based on the sample population dataset.

The quality of data that is input into the personal exposure models is important in order to obtain accurate results. This is certainly the case with the Monte Carlo simulations conducted in Chapter 6. Although Monte Carlo simulation is an extremely powerful tool, it is reliant on good data being fed into it. The main limitation of the Monte Carlo simulations used in this study is that the occupational distributions are only defined for one type of individual (office worker), so for the model to be used for the wider population more data would be required for other workplaces. There were also just a dozen distributions defined for specific microenvironments, which means more data would have to be gathered to include additional activities and locations. While the Monte Carlo sampling was useful for simulating individual exposures, the Latin hypercube simulation was useful for evaluating the population exposures. The model was also limited by the available data and would need additional data to model new scenarios, locations, and population groups.

The obvious disadvantage of using the baseflow separation techniques to derive background concentration from personal exposure time series data is the fact that they are designed for hydrology. In both cases of this analysis the performance of the different techniques was influenced by the spatial and temporal resolution of the background concentration measurements to which they were being compared. It was assumed in the analysis that, in theory, the personal exposure of subjects can never fall below the background concentration of the environment in which they are exposed. However, only outdoor background monitoring stations were available, and for example, the FSM nearest to the subject office locations was often located in an exterior roadside environment. Clearly the background concentration of indoor office–type environments, in which subjects spent a significant portion of their time, could differ from the urban roadside concentration. In addition the background PM concentrations change with time and the 24-hour average measurements provided may have given insufficient resolution for the optimum performance of the separation techniques presented. Both of these limitations in the resolution of the available background data

may explain the relatively low accuracy and/or precision of the techniques, but there may be scope for improvement of these analysis methods with the inclusion of higher resolution data.

# Chapter 9

## Conclusions and Recommendations

# 9 Conclusions and Recommendations

## 9.1 Conclusions

The primary objective of this study was to quantify the $PM_{10}$ personal exposure concentrations of office workers in Dublin City on a real-time basis. This was the first study of its kind carried out in Ireland, in which real-time 24-hour personal exposure monitoring was employed. The study was also unique from an international perspective, as previously, real time personal exposure monitoring had not been conducted over a daily period for such a large cohort. The main findings and conclusions arising from this study are listed in the following paragraphs.

The daily personal exposure of Dublin office workers to particulate air pollution was quantified. The average $PM_{10}$ personal exposure concentration of the study population was found to be well below the EPA 24-hour limit of 50 $\mu g/m^3$ for $PM_{10}$. However, the average occupational exposure for the study populous was found to be closer to the daily limit value.

A statistical analysis of the dataset was completed, which highlighted the microenvironments where high personal exposure concentrations were recorded. By far the most important locations dictating personal exposure to $PM_{10}$ were the home and workplace of an individual. This was a result of the vast majority of a person's day being spent within these two microenvironments.

The highest mean personal $PM_{10}$ concentration was found in the category 'Other indoor', while the lowest exposure concentration was found while sleeping. The 'Other indoor' category was used to define places that were visited once-off during sampling, and examples include factories, laboratories, libraries, meetings, etc. Some of these locations may have been homes of other individuals or venues where smoking and other combustion processes were on-going.

Much work has previously been conducted into studying commuter personal exposure to air pollutants. However, the study subjects were found to spend only a small

proportion of their time in this microenvironment, and therefore the contribution of commuting to the overall daily exposure was limited.

Of the various travel modes used by volunteers in this study, the highest mean $PM_{10}$ personal exposure concentration was sampled by those using the bus. The bus mode was followed by car travel, which had the second highest mean personal exposure concentration, while the lowest personal exposures were observed on the rail travel modes of the train and tram.

Exposure to ETS was found to be a large factor in raising personal exposure concentrations among subjects.

The taxi drivers were found to have a lower mean occupational personal exposure concentration than the office worker subjects of the main 24-hour personal exposure study.

The personal dose for each of the volunteers was examined using the human respiratory tract model to calculate the uptake of $PM_{10}$. The model accounted for exertion levels, exposure duration, and so forth, and showed dose uptake of $PM_{10}$ to be greatest while at work.

The result from the respiratory tract model alters the hierarchy of the activities and microenvironments from the perception given by the mean personal exposure concentrations. The categories such as 'Other indoor', 'Recreation/Sport', 'Cafés/Restaurants' and 'Pubs' had the highest mean personal exposure concentrations. However, many of these locations and activities were found to contribute relatively small amounts to overall dose as a result of the short durations and low exertion levels associated with each. Only the activity 'Recreation/Sport' was found to contribute a large amount to the dose of an individual due to the elevated breathing rates associated.

The respiratory tract model results showed that male uptake of $PM_{10}$ was significantly higher than the uptake of female subjects.

A number of novel predictive models were developed using numerical, statistical, and machine learning techniques. The task of accurately modelling personal exposure was found to be difficult due to the large amount of unknown variability within the personal exposure sampling data. The best modelling results were obtained when input concentrations were based on the data previously gathered by that subject, rather than the population averages.

The exposure risk analysis model that was created using the software package @Risk demonstrated that the concentration present in the workplace was the greatest influencing factor on the 24-hour personal exposure of the study population.

The adaption of neural network mathematical techniques to the task of predicting $PM_{10}$ personal exposure was found to be relatively successful. The training of both the GRNN and FFNN was found to be extremely well correlated with few errors, although during testing of each model the errors did increase.

The relationship between personal exposures of the subjects and the ambient $PM_{10}$ background concentrations near homes, workplaces, and the city centre, was also investigated. Outdoor determinants such as background $PM_{10}$ concentrations and meteorological conditions were found to have relatively poor correlations with the personal exposure data. Among the meteorological parameters, it was temperature that was found to be correlated most.

The use of hydrological baseflow separation techniques was moderately successful in relating personal exposure to the background concentrations on sampling days. Of the two methodologies used in this study, the sliding interval method, coupled with a larger period, was found to perform best.

## 9.2 Recommendations for Future Research

The following topics were raised during the project which should be addressed in research on the subject:

- A specifically designed study to calibrate the Aerocet-531 instrument for different cooking events may prove useful for future personal sampling campaigns.

- The study has provided a glimpse of general activity patterns of a Monday to Friday working study population. However, information has not been gathered on the activity patterns of individuals at weekends. Further personal sampling or surveying of activities may provide valuable information to enable a full seven day exposure risk analysis to be conducted.

- The expansion of personal monitoring to other occupations in Dublin, as well as non-workers and sedentary individuals, would contribute further to a database on different personal exposures.

- Personal exposure sampling could be extended to other locations around Ireland where background concentrations may be less, or in some cases even greater, than Dublin, although personal exposures may not necessarily follow this trend.

- Steps should be taken to examine the composition and toxicity of the particles found in the homes and work places of subjects in Dublin, as well as the ambient air in the city.

- During the taxi driver sampling campaign, it was found that there was a difference between personal exposures of the drivers who worked during daylight hours and those who chose to work in the early hours of the morning. Future research may investigate the diurnal difference in occupational exposure involving a much expanded sample number.

- Further refinement of the machine learning techniques used in this study, for example with the addition of extra inputs or other determining factors, may improve model performance and the ability to predict exposure in the future.

- Land-use regression models have been applied for air pollution mapping in a number of cities. The use of the personal exposure measurements could be used in a development of a similar LUR model for Dublin City.

- The gathered personal exposure data may prove useful in the future development of a mobile application, in which information on personal exposure as a result of certain movements and activities may be disseminated to the public.

- Indoor $PM_{10}$ concentrations were found to be the largest contributor to daily personal exposure, while some indoor microenvironments had far greater concentrations than the outdoor ambient air. Therefore, future research could be conducted in order to identify some of the particle sources in the various locations, as well as develop models which account for these sources.

- The microenvironments that displayed the highest personal exposure concentrations should be investigated further to assess the contribution of $PM_{2.5}$ in these locations.

# References

# References


Abbey, D. E., Colome, S. D., Mills, P. K., Burchette, R., Beeson, W. L. & Tian, Y. 1993. Chronic disease associated with long-term concentrations of nitrogen dioxide. *Journal Name: Journal of Esposure Analysis and Environmental Epidemiology; (United States); Journal Volume: 3:2*, Medium: X; Size: Pages: 181-202.

Abbey, D. E., Nishino, N., McDonnell, W. F., Burchette, R. J., Knutsen, S. F., Beeson, W. L. & Yang, J. X. 1999. Long-term inhalable particles and other air pollutants related to mortality in nonsmokers. *American Journal of Respiratory and Critical Care Medicine,* 159, 373-382.

Abdullahi, K. L., Delgado-Saborit, J. M. & Harrison, R. M. 2013. Emissions and indoor concentrations of particulate matter and its specific chemical components from cooking: A review. *Atmospheric Environment,* 71, 260-294.

Abt, E., Suh, H. H., Allen, G. & Koutrakis, P. 2000a. Characterization of Indoor Particle Sources: A Study Conducted in the Metropolitan Boston Area. *Environmental Health Perspectives,* 108, 35-44.

Abt, E., Suh, H. H., Catalano, P. & Koutrakis, P. 2000b. Relative Contribution of Outdoor and Indoor Particle Sources to Indoor Concentrations. *Environmental Science & Technology,* 34, 3579-3587.

Adams, H. S., Kenny, L. C., Nieuwenhuijsen, M. J., Colvile, R. N. & Gussman, R. A. 2001a. Design and validation of a high-flow personal sampler for PM2.5. 11, 5-11.

Adams, H. S., Nieuwenhuijsen, M. J. & Colvile, R. N. 2001b. Determinants of fine particle (PM2.5) personal exposure levels in transport microenvironments, London, UK. *Atmospheric Environment,* 35, 4557-4566.

Adams, H. S., Nieuwenhuijsen, M. J., Colvile, R. N., McMullen, M. A. S. & Khandelwal, P. 2001c. Fine particle (PM2.5) personal exposure levels in transport microenvironments, London, UK. *Science of The Total Environment,* 279, 29-44.

Adgate, J. L., Ramachandran, G., Pratt, G. C., Waller, L. A. & Sexton, K. 2002. Spatial and temporal variability in outdoor, indoor, and personal PM2.5 exposure. *Atmospheric Environment,* 36, 3255-3265.

Aksoy, H., Kurt, I. & Eris, E. 2009. Filtered smoothed minima baseflow separation method. *Journal of Hydrology,* 372, 94-101.

Alm, S., Jantunen, M. J. & Vartiainen, M. 1999. Urban commuter exposure to particle matter and carbon monoxide inside an automobile. 9, 237-244.

Altshuler, B. 1959. Calculation of regional deposition of aerosol in the respiratory tract. *Bulletin of Mathematical Biology,* 21, 257-270.

Anderson, H. R. 2009. Air pollution and mortality: A history. *Atmospheric Environment,* 43, 142-152.

Anderson, H. R., Institute, H. E. & Committee, H. E. I. I. S. O. 2010. *Outdoor air pollution and health in the developing countries of Asia: a comprehensive review*, Health Effects Institute.

Aquilina, N. J., Delgado-Saborit, J. M., Gauci, A. P., Baker, S., Meddings, C. & Harrison, R. M. 2010. Comparative modeling approaches for personal exposure to particle-associated PAH. *Environ Sci Technol,* 44, 9370-6.

Ayers, G. P., Keywood, M. D. & Gras, J. L. 1999. TEOM vs. manual gravimetric methods for determination of PM2.5 aerosol mass concentrations. *Atmospheric Environment,* 33, 3717-3721.

Begum, B. A., Paul, S. K., Dildar Hossain, M., Biswas, S. K. & Hopke, P. K. 2009. Indoor air pollution from particulate matter emissions in different households in rural areas of Bangladesh. *Building and Environment,* 44, 898-903.

Bell, M. L., Davis, D. L. & Fletcher, T. 2003. A Retrospective Assessment of Mortality from the London Smog Episode of 1952: The Role of Influenza and Pollution. *Environ Health Perspect,* 112.

Bernmark, E., Wiktorin, C., Svartengren, M., Lewne, M. & Aberg, S. 2006. Bicycle messengers: energy expenditure and exposure to air pollution. *Ergonomics,* 49, 1486-95.

Borgini, A., Tittarelli, A., Ricci, C., Bertoldi, M., De Saeger, E. & Crosignani, P. 2011. Personal exposure to PM2.5 among high-school students in Milan and background measurements: The EuroLifeNet study. *Atmospheric Environment,* 45, 4147-4151.

Boughton, W. C. 1988. Patitioning streamflow by computer. *The Institute of Engineers: Civil Engineering Transactions,* 30, 285-291.

Boulter, P. G. & Latham, S. 2009. Emission factors 2009: Report 4 - a review of methodologies for modellin cold-start emssions. Department of Transport (UK).

Bowman, C. T. 1992. Control of combustion-generated nitrogen oxide emissions: Technology driven by regulation. *Symposium (International) on Combustion,* 24, 859-878.

Branis, M. & Kolomazníková, J. 2010. Year-long continuous personal exposure to PM2.5 recorded by a fast responding portable nephelometer. *Atmospheric Environment,* 44, 2865-2872.

Brauer, M., Hirtle, R. D., Hall, A. C. & Yip, T. R. 1999. Monitoring personal fine particle exposure with a particle counter. *Journal of Exposure Science and Environmental Epidemiology,* 9.

Brauer, M., Hruba, F., Mihalikova, E. V. A., Fabianova, E., Miskovic, P., Plzikova, A., Lendacka, M., Vandenberg, J. & Cullen, A. 2000. Personal exposure to particles in Banska Bystrica, Slovakia. 10, 478-487.

Brimblecombe, P. 1987. *Big Smoke: History of Air Pollution in London Since Medieval Times*, Routledge.

Brown, K. W., Sarnat, J. A., Suh, H. H., Coull, B. A., Spengler, J. D. & Koutrakis, P. 2008. Ambient site, home outdoor and home indoor particulate concentrations as proxies of personal exposures. *J Environ Monit,* 10, 1041-51.

Brunekreef, B., Smit, H. A., Biersteker, K., Boleij, J. S. M. & Lebret, E. 1982. Indoor carbon monoxide pollution in The Netherlands. *Environment International,* 8, 193-196.

Buckland, A. T. & Middleton, D. R. 1999. Nomograms for calculating pollution within street canyons. *Atmospheric Environment,* 33, 1017-1036.

Buonanno, G., Morawska, L. & Stabile, L. 2009. Particle emission factors during cooking activities. *Atmospheric Environment,* 43, 3235-3242.

Burke, J. M., Zufall, M. J. & Ozkaynak, H. 2001. A population exposure model for particulate matter: case study results for PM2.5 in Philadelphia, PA. *J Expo Anal Environ Epidemiol,* 11, 470-489.

Burnett, R. T., Brook, J., Dann, T., Delocla, C., Philips, O., Cakmak, S., Vincent, R., Goldberg, M. S. & Krewski, D. 2000. Association between particulate- and gas-phase components of urban air pollution and daily mortality in eight Canadian cities. *Inhalation Toxicology,* 12, 15-39.

Bylin, G., Lindvall, T., Rehn, T. & Sundin, B. 1985. Effects of short-term exposure to ambient nitrogen dioxide concentrations on human bronchial reactivity and lung function. *European journal of respiratory diseases,* 66, 205-17.

CAHN 2006. *Instruction Manual for Model C-33 Microbalance*, Thermo Scientific.

Ceburnis, D., Yin, J., Allen, A. G., Jennings, S. G., Harrison, R. M., Wright, E., Fitzpatrick, M., Healy, T. & Barry, E. 2006. Local and regional air pollution in Ireland during an intensive aerosol measurement campaign. *J Environ Monit,* 8, 479-87.

Chakrabarti, B., Fine, P. M., Delfino, R. & Sioutas, C. 2004. Performance evaluation of the active-flow personal DataRAM PM2.5 mass monitor (Thermo Anderson pDR-1200) designed for continuous personal exposure measurements. *Atmospheric Environment,* 38, 3329-3340.

Chan, L. Y., Lau, W. L., Zou, S. C., Cao, Z. X. & Lai, S. C. 2002a. Exposure level of carbon monoxide and respirable suspended particulate in public transportation modes while commuting in urban area of Guangzhou, China. *Atmospheric Environment,* 36, 5831-5840.

Chan, T. L., Dong, G., Leung, C. W., Cheung, C. S. & Hung, W. T. 2002b. Validation of a two-dimensional pollutant dispersion model in an isolated street canyon. *Atmospheric Environment,* 36, 861-872.

Chang, L. T., Koutrakis, P., Catalano, P. J. & Suh, H. H. 2003. Assessing the importance of different exposure metrics and time-activity data to predict 24-H personal PM2.5 exposures. *J Toxicol Environ Health A,* 66, 1825-46.

Chantal, D. 2001. A realistic two-dimensional model of aerosol transport and deposition in the alveolar zone of the human lung. *Journal of Aerosol Science,* 32, 1161-1174.

Chao, C. Y. & Cheng, E. C. 2002. Source Apportionment of Indoor PM2.5 and PM10 in Homes. *Indoor and Built Environment,* 11, 27-37.

Chao, C. Y. & Wong, K. K. 2002. Residential indoor PM10 and PM2.5 in Hong Kong and the elemental composition. *Atmospheric Environment,* 36, 265-277.

Chao, C. Y. H., Tung, T. C. W. & Burnett, J. 1998. Influence of Different Indoor Activities on the Indoor Particulate Levels in Residential Buildings. *Indoor and Built Environment,* 7, 110-121.

Chate, D. M. & Pranesha, T. S. 2004. Field studies of scavenging of aerosols by rain events. *Journal of Aerosol Science,* 35, 695-706.

Chitano, P., Hosselet, J. J., Mapp, C. E. & Fabbri, L. M. 1995. Respiratory effects of air pollution - effect of oxidant air pollutants on the respiratory system - insights from experimental animal research. *European Respiratory Journal,* 8, 1357-1371.

Cigizoglu, H. K. & Alp, M. 2006. Generalized regression neural network in modelling river sediment yield. *Advances in Engineering Software,* 37, 63-68.

Clancy, L., Goodman, P., Sinclair, H. & Dockery, D. W. 2002. Effect of air-pollution control on death rates in Dublin, Ireland: an intervention study. *The Lancet,* 360, 1210-1214.

Clayton, C. A., Perritt, R. L., Pellizzari, E. D., Thomas, K. W., Whitmore, R. W., Wallace, L. A., Ozkaynak, H. & Spengler, J. D. 1993. Particle Total Exposure Assessment Methodology (PTEAM) study: distributions of aerosol and elemental concentrations in personal, indoor, and outdoor air samples in a southern California community. *Journal of exposure analysis and environmental epidemiology,* 3, 227-50.

Cohen, M. A., Adar, S. D., Allen, R. W., Avol, E., Curl, C. L., Gould, T., Hardie, D., Ho, A., Kinney, P., Larson, T. V., Sampson, P., Sheppard, L., Stukovsky, K. D., Swan, S. S., Liu, L. J. S. & Kaufman, J. D. 2009. Approach to Estimating Participant Pollutant Exposures in the Multi-Ethnic Study of Atherosclerosis and Air Pollution (MESA Air). *Environmental Science & Technology,* 43, 4687-4693.

Colome, S. D., Kado, N. Y., Jaques, P. & Kleinman, M. 1992. Indoor-outdoor air pollution relations: particulate matter less than 10 [mu]m in aerodynamic diameter (PM10) in homes of asthmatics. *Atmospheric Environment. Part A. General Topics,* 26, 2173-2178.

Cozzi, E., Wingard, C. J., Cascio, W. E., Devlin, R. B., Miles, J. J., Bofferding, A. R., Lust, R. M., Van Scott, M. R. & Henriksen, R. A. 2007. Effect of ambient particulate matter exposure on hemostasis. *Translational Research,* 149, 324-332.

Crist, K. C., Liu, B., Kim, M., Deshpande, S. R. & John, K. 2008. Characterization of fine particulate matter in Ohio: Indoor, outdoor, and personal exposures. *Environmental Research,* 106, 62-71.

Cullis, C. F. & Hirschler, M. M. 1989. Man's emissions of carbon monoxide and hydrocarbons into the atmosphere. *Atmospheric Environment (1967),* 23, 1195-1203.

Cyrys, J., Pitz, M., Bischof, W., Wichmann, H. E. & Heinrich, J. 2004. Relationship between indoor and outdoor levels of fine particle mass, particle number concentrations and black smoke under different ventilation conditions. *J Expo Anal Environ Epidemiol,* 14, 275-283.

Dabberdt, W. F., Ludwig, F. L. & Johnson jr, W. B. 1973. Validation and applications of an urban diffusion model for vehicular pollutants. *Atmospheric Environment (1967),* 7, 603-618.

Day, D. E. & Malm, W. C. 2001. Aerosol light scattering measurements as a function of relative humidity: a comparison between measurements made at three different sites. *Atmospheric Environment,* 35, 5169-5176.

de Nazelle, A., Fruin, S., Westerdahl, D., Martinez, D., Ripoll, A., Kubesch, N. & Nieuwenhuijsen, M. 2012. A travel mode comparison of commuters' exposures to air pollutants in Barcelona. *Atmospheric Environment,* 59, 151-159.

deCastro, B. R., Sax, S. N., Chillrud, S. N., Kinney, P. L. & Spengler, J. D. 2006. Modeling time-location patterns of inner-city high school students in New York and Los Angeles using a longitudinal approach with generalized estimating equations. *J Expos Sci Environ Epidemiol,* 17, 233-247.

Delgado-Saborit, J. M., Aquilina, N. J., Meddings, C., Baker, S. & Harrison, R. M. 2009. Model Development and Validation of Personal Exposure to Volatile Organic Compound Concentrations. *Environ Health Perspect,* 117.

Dennekamp, M., Howarth, S., Dick, C. A., Cherrie, J. W., Donaldson, K. & Seaton, A. 2001. Ultrafine particles and nitrogen oxides generated by gas and electric cooking. *Occup Environ Med,* 58, 511-6.

Derwent, R. G., Davies, T. J., Delaney, M., Dollard, G. J., Field, R. A., Dumitrean, P., Nason, P. D., Jones, B. M. R. & Pepler, S. A. 2000. Analysis and interpretation of the continuous hourly monitoring data for 26 C2–C8 hydrocarbons at 12 United Kingdom sites during 1996. *Atmospheric Environment,* 34, 297-312.

Derwent, R. G., Middleton, D. R., Field, R. A., Goldstone, M. E., Lester, J. N. & Perry, R. 1995. Analysis and interpretation of air quality data from an urban roadside location in Central London over the period from July 1991 to July 1992. *Atmospheric Environment,* 29, 923-946.

Dimitroulopoulou, C., Ashmore, M. R. & Byrne, M. A. 2001a. Modelling the Contribution of Passive Smoking to Exposure to $PM_{10}$ in UK Homes. *Indoor and Built Environment,* 10, 209-213.

Dimitroulopoulou, C., Ashmore, M. R., Byrne, M. A. & Kinnersley, R. P. 2001b. Modelling of indoor exposure to nitrogen dioxide in the UK. *Atmospheric Environment,* 35, 269-279.

Dockery, D. W., Pope, C. A., Xu, X., Spengler, J. D., Ware, J. H., Fay, M. E., Ferris, B. G. & Speizer, F. E. 1993. An Association between Air Pollution and Mortality in Six U.S. Cities. *New England Journal of Medicine,* 329, 1753-1759.

Dockery, D. W., Schwartz, J. & Spengler, J. D. 1992. Air pollution and daily mortality: Associations with particulates and acid aerosols. *Environmental Research,* 59, 362-373.

Dockery, D. W. & Spengler, J. D. 1979. Personal exposure to respirable particulates and sulfates: Measurement and prediction. U.S. Environmental Protection Agency, Research Triangle Park, N.C US EPA.

Dockery, D. W. & Spengler, J. D. 1981. Indoor-outdoor relationships of respirable sulfates and particles. *Atmospheric Environment (1967),* 15, 335-343.

Dor, F., Lemoullec, Y. & Festy, B. 1995. Exposure of city residents to carbon-monoxide and monocyclic aromatic-hydrocarbons during commuting trips in the Paris metropolitan-area. *Journal of the Air & Waste Management Association,* 45, 103-110.

Duan, N. 1982. Models for human exposure to air pollution. *Environment International,* 8, 305-309.

Dublin City Council, Council, S. D. C., Council, F. C. & Council, D. L.-R. C. 2009. Dublin Regional Air Quality Management Plan 2009-2012.

Dunne, S. & Ghosh, B. 2011. Regime-Based Short-Term Multivariate Traffic Condition Forecasting Algorithm. *Journal of Transportation Engineering,* 138, 455-466.

Eckhardt, K. 2008. A comparison of baseflow indices, which were calculated with seven different baseflow separation methods. *Journal of Hydrology,* 352, 168-173.

EDGAR. 2005. *EDGAR 32FT2000 dataset* [Online]. Available: **http://themasites.pbl.nl/en/themasites/edgar/index.html** [Accessed 18/1/12 2012].

EEA 2007. *Air pollution in Europe 1990-2004,* Luxembourg, Office for Official Publications of the European Communities.

Elgethun, K., Fenske, R. A., Yost, M. G. & Palcisko, G. J. 2002. Time-Location Analysis for Exposure Assessment Studies of Children Using a Novel Global Positioning System Instrument. *Environ Health Perspect,* 111.

Elminir, H. K. 2005. Dependence of urban air pollutants on meteorology. *Science of The Total Environment,* 350, 225-237.

EPA 2010. Trends in SO2 emissions 1990-2008. Johnstown Castle, Co. Wexford: EPA.

European Commission 2011. *Energy, transport and environment indicators,* Publication office of the European Union, Luxembourg, European Union.

European Environment Agency 2012. Air Quality in Europe 2012. Copenhagen, Denmark.

Fajardo, O. A. & Rojas, N. Y. 2012. Particulate matter exposure of bicycle path users in a high-altitude city. *Atmospheric Environment,* 46, 675-679.

Fang, S. C., Cassidy, A. & Christiani, D. C. 2010. A Systematic Review of Occupational Exposure to Particulate Matter and Cardiovascular Disease. *International Journal of Environmental Research and Public Health,* 7, 1773-1806.

Fernandez-Bremauntz, A. A. & Ashmore, M. R. 1995. Exposure of commuters to carbon monoxide in Mexico city—I. Measurement of in-vehicle concentrations. *Atmospheric Environment,* 29, 525-532.

Ferro, A. R., Kopperud, R. J., McBride, S. J., Ott, W. R. & Switzer, P. Year. Human exposure to particles due to indoor cleaning activities. *In:* Air Pollution VII, 1999. Southampton, UK: WIT Press, 487-496.

Filleul, L., Rondeau, V., Vandentorren, S., Le Moual, N., Cantagrel, A., Annesi-Maesano, I., Charpin, D., Declercq, C., Neukirch, F., Paris, C., Vervloet, D., Brochard, P., Tessier, J. F., Kauffmann, F. & Baldi, I. 2006. Twenty-five-year mortality and air pollution: Results from the French PAARC survey. *Epidemiology,* 17, S70-S70.

Findeisen, W. 1935. Über das Absetzen kleiner, in der Luft suspendierter Teilchen in der menschlichen Lunge bei der Atmung. *Pflügers Archiv European Journal of Physiology,* 236, 367-379.

Firat, M. & Gungor, M. 2009. Generalized Regression Neural Networks and Feed Forward Neural Networks for prediction of scour depth around bridge piers. *Advances in Engineering Software,* 40, 731-737.

Fischer, S. L. & Koshland, C. P. 2007. Field performance of a nephelometer in rural kitchens: effects of high humidity excursions and correlations to gravimetric analyses. *J Expo Sci Environ Epidemiol,* 17, 141-50.

Folinsbee, L. J., Horstman, D. H., Kehrl, H. R., Harder, S., Abdulsalaam, S. & Ives, P. J. 1994. Respiratory response to repeated prolonged exposure to 0.12-ppm ozone. *American Journal of Respiratory and Critical Care Medicine,* 149, 98-105.

Fuentes, J. D., Lerdau, M., Atkinson, R., Baldocchi, D., Bottenheim, J. W., Ciccioli, P., Lamb, B., Geron, C., Gu, L., Guenther, A., Sharkey, T. D. & Stockwell, W. 2000. Biogenic hydrocarbons in the atmospheric boundary layer: A review. *Bulletin of the American Meteorological Society,* 81, 1537-1575.

Gemci, T., Shortall, B., Allen, G. M., Corcoran, T. E. & Chigier, N. 2003. A CFD study of the throat during aerosol drug delivery using heliox and air. *Journal of Aerosol Science,* 34, 1175-1192.

Glytsos, T., Ondráček, J., Džumbová, L., Kopanakis, I. & Lazaridis, M. 2010. Characterization of particulate matter concentrations during controlled indoor activities. *Atmospheric Environment,* 44, 1539-1549.

Gómez-Perales, J. E., Colvile, R. N., Nieuwenhuijsen, M. J., Fernández-Bremauntz, A., Gutiérrez-Avedoy, V. J., Páramo-Figueroa, V. H., Blanco-Jiménez, S., Bueno-López, E., Mandujano, F., Bernabé-Cabanillas, R. & Ortiz-Segovia, E. 2004. Commuters' exposure to PM2.5, CO, and benzene in public transport in the metropolitan area of Mexico City. *Atmospheric Environment,* 38, 1219-1229.

Goodman, P., Agnew, M., McCaffrey, M., Paul, G. & Clancy, L. 2007. Effects of the Irish Smoking Ban on Respiratory Health of Bar Workers and Air Quality in Dublin Pubs. *Am. J. Respir. Crit. Care Med.,* 175, 840-845.

Götschi, T., Oglesby, L., Mathys, P., Monn, C., Manalis, N., Koistinen, K., Jantunen, M., Hänninen, O., Polanska, L. & Künzli, N. 2002. Comparison of Black Smoke and PM2.5 Levels in Indoor and Outdoor Environments of Four European Cities. *Environmental Science & Technology,* 36, 1191-1197.

Guenther, A. 2002. The contribution of reactive carbon emissions from vegetation to the carbon balance of terrestrial ecosystems. *Chemosphere,* 49, 837-844.

Guenther, A., Hewitt, C. N., Erickson, D., Fall, R., Geron, C., Graedel, T., Harley, P., Klinger, L., Lerdau, M., McKay, W. A., Pierce, T., Scholes, B., Steinbrecher, R., Tallamraju, R., Taylor, J. & Zimmerman, P. 1995. A global model of natural volatile organic compound emissions. *Journal of Geophysical Research,* 100, 8873-8892.

Gulliver, J. & Briggs, D. J. 2004. Personal exposure to particulate air pollution in transport microenvironments. *Atmospheric Environment,* 38, 1-8.

Haefelibleuer, B. & Weibel, E. R. 1988. Morphometry of the human pulmonary acinus. *Anatomical Record,* 220, 401-414.

Haller, L., Claiborn, C., Larson, T., Koenig, J., Norris, G. & Edgar, R. 1999. Airborne Particulate Matter Size Distributions in an Arid Urban Area. *Journal of the Air & Waste Management Association,* 49, 161-168.

Hanna, S. R. 1988. Air quality model evaluation and uncertainty. *JAPCA,* 38, 406-12.

Hänninen, O., Kruize, H., Lebret, E. & Jantunen, M. 2003. EXPOLIS simulation model: PM2.5 application and comparison with measurements in Helsinki. *J Expo Anal Environ Epidemiol,* 13, 74-85.

Harrison, R. M. 2001. *Pollution: Causes, Effects and Control*, Royal Society of Chemistry.

Harrison, R. M., Delgado-Saborit, J. M., Baker, S. J., Aquilina, N. J., Meddings, C., Harrad, S., Matthews, I., Vardoulakis, S. & Anderson, H. R. 2009. Measurement and Modeling of Exposure to Seleced Air Toxics for Health Effects Studies and Verification by Biomarkers. Boston, Massachusetts: Health Effects Institute.

He, C., Morawska, L., Hitchins, J. & Gilbert, D. 2004. Contribution from indoor sources to particle number and mass concentrations in residential houses. *Atmospheric Environment,* 38, 3405-3415.

Hester, R. E. & Harrison, R. M. 1995. *Volatile organic compounds in the atmosphere*, Royal Society of Chemistry.

Heyder, J. & Rudolf, G. 1984. Mathematical models of particle deposition in the human respiratory tract. *Journal of Aerosol Science,* 15, 697-707.

Higgins, I. T. T., Darcy, J. B., Gibbons, D. I., Avol, E. L. & Gross, K. B. 1990. Effect of exposures to ambient ozone on ventilatory lung-function in children. *American Review of Respiratory Disease,* 141, 1136-1146.

Hill, M. K. 2010. *Understanding Environmental Pollution*, Cambridge University Press.

Hoek, G., Brunekreef, B., Goldbohm, S., Fischer, P. & van den Brandt, P. A. 2002. Association between mortality and indicators of traffic-related air pollution in the Netherlands: a cohort study. *The Lancet,* 360, 1203-1209.

Holgate, S. T. 1992. *Sulphur dioxide, acid aerosols and particulates,* London, HM Stationary Office.

Holmes, N. S., Morawska, L., Mengersen, K. & Jayaratne, E. R. 2005. Spatial distribution of submicrometre particles and CO in an urban microscale environment. *Atmospheric Environment,* 39, 3977-3988.

Horstman, D. H., Folinsbee, L. J., Ives, P. J., Abdulsalaam, S. & McDonnell, W. F. 1990. Ozone concentration and pulmonary response relationships for 6.6-hour exposures with 5 hours of moderate exercise to 0.08, 0.10, and 0.12 ppm. *American Review of Respiratory Disease,* 142, 1158-1163.

Hussein, T., Glytsos, T., Ondráček, J., Dohányosová, P., Ždímal, V., Hämeri, K., Lazaridis, M., Smolík, J. & Kulmala, M. 2006. Particle size characterization and emission rates during indoor activities in a house. *Atmospheric Environment,* 40, 4285-4307.

ICRP 1994. *Human respiratory tract model for radiological protection: a report of a Task Group of the International Commission on Radiological Protection*, Pergamon.

Int Panis, L., de Geus, B., Vandenbulcke, G., Willems, H., Degraeuwe, B., Bleux, N., Mishra, V., Thomas, I. & Meeusen, R. 2010. Exposure to particulate matter in traffic: A comparison of cyclists and car passengers. *Atmospheric Environment,* 44, 2263-2270.

IPCC 2001. Intergovernmental Panel on Climate Change, Climate Change 2001: The Scientific Basis. New York: Cambridge University Press.

Jans, M. P., Proper, K. I. & Hildebrandt, V. H. 2007. Sedentary Behavior in Dutch Workers: Differences Between Occupations and Business Sectors. *American Journal of Preventive Medicine,* 33, 450-454.

Janssen, N. A., de Hartog, J. J., Hoek, G., Brunekreef, B., Lanki, T., Timonen, K. L. & Pekkanen, J. 2000. Personal exposure to fine particulate matter in elderly subjects: relation between personal, indoor, and outdoor concentrations. *J Air Waste Manag Assoc,* 50, 1133-43.

Janssen, N. A., Hoek, G., Brunekreef, B., Harssema, H., Mensink, I. & Zuidhof, A. 1998a. Personal sampling of particles in adults: relation among personal, indoor, and outdoor air concentrations. *Am J Epidemiol,* 147, 537-47.

Janssen, N. A., Hoek, G., Harssema, H. & Brunekreef, B. 1997. Childhood exposure to PM10: relation between personal, classroom, and outdoor concentrations. *Occup Environ Med,* 54, 888-894.

Janssen, N. A. H., Hoek, G., Harssema, H. & Brunekreef, B. 1998b. Personal sampling of airborne particles: Method performance and data quality. *Journal of exposure analysis and environmental epidemiology,* 8, 37-49.

Jantunen, M. & Kansanterveyslaitos 1999. *Air pollution exposure in European cities, the EXPOLIS study*, KTL, National Public Health Institute.

Jenkins, P. L., Phillips, T. J., Mulberg, E. J. & Hui, S. P. 1992. Activity patterns of Californians: Use of and proximity to indoor pollutant sources. *Atmospheric Environment. Part A. General Topics,* 26, 2141-2148.

Jenkins, R. A., Ilgner, R. H., Tomkins, B. A. & Peters, D. W. 2004. Development and application of protocols for the determination of response of real-time particle monitors to common indoor aerosols. *J Air Waste Manag Assoc,* 54, 229-41.

Jensen, P., Rouquier, J.-B., Ovtracht, N. & Robardet, C. 2010. Characterizing the speed and paths of shared bicycle use in Lyon. *Transportation Research Part D: Transport and Environment,* 15, 522-524.

Jerrett, M., Burnett, R. T., Pope, C. A., Ito, K., Thurston, G., Krewski, D., Shi, Y., Calle, E. & Thun, M. 2009. Long-Term Ozone Exposure and Mortality. *New England Journal of Medicine,* 360, 1085-1095.

Johnson, T., Long, T. & Ollison, W. 2000. Prediction of hourly microenvironmental concentrations of fine particles based on measurements obtained from the Baltimore scripted activity study. *Journal of exposure analysis and environmental epidemiology,* 10, 403-11.

Jones, N. C., Thornton, C. A., Mark, D. & Harrison, R. M. 2000. Indoor/outdoor relationships of particulate matter in domestic homes with roadside, urban and rural locations. *Atmospheric Environment,* 34, 2603-2612.

Karakitsios, S. P., Papaloukas, C. L., Kassomenos, P. A. & Pilidis, G. A. 2007. Assessment and prediction of exposure to benzene of filling station employees. *Atmospheric Environment,* 41, 9555-9569.

Kaur, S., Clark, R. D. R., Walsh, P. T., Arnold, S. J., Colvile, R. N. & Nieuwenhuijsen, M. J. 2006. Exposure visualisation of ultrafine particle counts in a transport microenvironment. *Atmospheric Environment,* 40, 386-398.

Kaur, S., Nieuwenhuijsen, M. & Colvile, R. 2005a. Personal exposure of street canyon intersection users to PM2.5, ultrafine particle counts and carbon monoxide in Central London, UK. *Atmospheric Environment,* 39, 3629-3641.

Kaur, S., Nieuwenhuijsen, M. J. & Colvile, R. N. 2005b. Pedestrian exposure to air pollution along a major road in Central London, UK. *Atmospheric Environment,* 39, 7307-7320.

Kaur, S., Nieuwenhuijsen, M. J. & Colvile, R. N. 2007. Fine particulate matter and carbon monoxide exposure concentrations in urban street transport microenvironments. *Atmospheric Environment,* 41, 4781-4810.

Kelly, I. & Clancy, L. 1984. Mortality in a general hospital and urban air pollution. *Ir Med J,* 77, 322-4.

Kesselmeier, J., Ciccioli, P., Kuhn, U., Stefani, P., Biesenthal, T., Rottenberger, S., Wolf, A., Vitullo, M., Valentini, R., Nobre, A., Kabat, P. & Andreae, M. O. 2002. Volatile organic compound emissions in relation to plant carbon fixation and the terrestrial carbon budget. *Global Biogeochemical Cycles,* 16.

Khalade, A., Jaakkola, M. S., Pukkala, E. & Jaakkola, J. J. K. 2010. Exposure to benzene at work and the risk of leukemia: a systematic review and meta-analysis. *Environmental Health,* 9.

Kimbell, J. S., Overton, J. H., Subramaniam, R. P., Schlosser, P. M., Morgan, K. T., Conolly, R. B. & Miller, F. J. 2001. Dosimetry Modeling of Inhaled Formaldehyde: Binning Nasal Flux Predictions for Quantitative Risk Assessment. *Toxicological Sciences,* 64, 111-121.

King, A. M., Pless-Mulloli, T., Merefield, J. & Stone, I. 2000. New Directions: TEOMs and the volatility of UK non-urban PM10: a regulatory dilemma. *Atmospheric Environment,* 34, 3211-3212.

Kingham, S., Meaton, J., Sheard, A. & Lawrenson, O. 1998. Assessment of exposure to traffic-related fumes during the journey to work. *Transportation Research Part D: Transport and Environment,* 3, 271-274.

Klepeis, N. E., Nelson, W. C., Ott, W. R., Robinson, J. P., Tsang, A. M., Switzer, P., Behar, J. V., Hern, S. C. & Engelmann, W. H. 2001. The National Human

Activity Pattern Survey (NHAPS): a resource for assessing exposure to environmental pollutants. *J Expo Anal Environ Epidemiol,* 11, 231-252.

Koblinger, L. & Hofmann, W. 1990. Monte Carlo modeling of aerosol deposition in human lungs. Part I: Simulation of particle transport in a stochastic lung structure. *Journal of Aerosol Science,* 21, 661-674.

Koistinen, K. J., Hänninen, O., Rotko, T., Edwards, R. D., Moschandreas, D. & Jantunen, M. J. 2001. Behavioral and environmental determinants of personal exposures to PM2.5 in EXPOLIS - Helsinki, Finland. *Atmospheric Environment,* 35, 2473-2481.

Koistinen, K. J., Kosua, A., Tenhol, V., Hänninen, O., Jantunten, M. J., Oglesby, L., Kuenzli, N. & Georgoulis, L. 1999. Fine particle ($PM_{2.5}$) measurement methodology, quality assurance procedure and pilot results of the EXPOLIS study. *Journal of the Air and Waste Management Association,* 49, 1212-1220.

Koolpiruck, D., Prakoonwit, S. & Balachandran, W. 2004. Numerical modeling of inhaled charged aerosol deposition in human airways. *Industry Applications, IEEE Transactions on,* 40, 1239-1248.

Koppmann, R. 2007. *Volatile organic compounds in the atmosphere*, Blackwell Pub.

Koutrakis, P., Briggs, S. L. K. & Leaderer, B. P. 1992. Source apportionment of indoor aerosols in Suffolk and Onondaga counties, New York. *Environmental Science & Technology,* 26, 521-527.

Kraft, M., Eikmann, T., Kappos, A., Künzli, N., Rapp, R., Schneider, K., Seitz, H., Voss, J.-U. & Wichmann, H. E. 2005. The German view: Effects of nitrogen dioxide on human health – derivation of health-related short-term and long-term values. *International Journal of Hygiene and Environmental Health,* 208, 305-318.

Kruize, H., Hänninen, O., Breugelmans, O., Lebret, E. & Jantunen, M. 2003. Description and demonstration of the EXPOLIS simulation model: Two examples of modeling population exposure to particulate matter. *J Expo Anal Environ Epidemiol,* 13, 87-99.

Kumar, N., Chu, A. & Foster, A. 2007. An empirical relationship between PM2.5 and aerosol optical depth in Delhi Metropolitan. *Atmospheric Environment,* 41, 4492-4503.

Lai, H. K., Kendall, M., Ferrier, H., Lindup, I., Alm, S., Hänninen, O., Jantunen, M., Mathys, P., Colvile, R., Ashmore, M. R., Cullinan, P. & Nieuwenhuijsen, M. J.

2004. Personal exposures and microenvironment concentrations of PM2.5, VOC, NO2 and CO in Oxford, UK. *Atmospheric Environment,* 38, 6399-6410.

Lanki, T., Alm, S., Ruuskanen, J., Janssen, N. A. H., Jantunen, M. & Pekkanen, J. 2002. Photometrically measured continuous personal PM2.5 exposure: Levels and correlation to a gravimetric method. *J Expo Anal Environ Epidemiol,* 12, 172-178.

Laulainen, N. S., Laboratory, P. N. & Energy, U. S. D. o. 1993. *Summary of conclusions and recommendations from a visibility science workshop: technical basis and issues for a national assessment of visibility impairment, National Center for Atmospheric Research, Boulder, Colorado, September 19-20, 1991*, Pacific Northwest Laboratory.

Lee, S. C., Chiu, M. Y., Ho, K. F., Zou, S. C. & Wang, X. 2002. Volatile organic compounds (VOCs) in urban atmosphere of Hong Kong. *Chemosphere,* 48, 375-382.

Lee, S. C., Li, W.-M. & Yin Chan, L. 2001. Indoor air quality at restaurants with different styles of cooking in metropolitan Hong Kong. *Science of The Total Environment,* 279, 181-193.

Leech, J. A., Wilby, K., McMullen, E. & Laporte, K. 1996. Canadian human time-activity pattern survey report of methods and population surveyed. *Chron Dis Can,* 17, 118-123.

Letz, R., Ryan, P. B. & Spengler, J. D. 1984. Estimated distributions of personal exposure to respirable particles. *Environmental Monitoring and Assessment,* 4, 351-359.

Levenberg, K. 1944. A method for the solution of certain problems in least squares. *Quart. Applied Math.,* 2, 164-168.

Lewné, M., Nise, G., Lind, M.-L. & Gustavsson, P. 2006. Exposure to particles and nitrogen dioxide among taxi, bus and lorry drivers. *International Archives of Occupational and Environmental Health,* 79, 220-226.

Li, W.-M., Lee, S. C. & Chan, L. Y. 2001. Indoor air quality at nine shopping malls in Hong Kong. *Science of The Total Environment,* 273, 27-40.

Liao, C.-M., Chen, S.-C., Chen, J.-W. & Liang, H.-M. 2006. Contributions of Chinese-style cooking and incense burning to personal exposure and residential PM concentrations in Taiwan region. *Science of The Total Environment,* 358, 72-84.

Linn, W. S., Avol, E. L., Peng, R. C., Shamoo, D. A. & Hackney, J. D. 1987. Replicated dose-response study of sulfur-dioxide effects in normal, atopic, and asthmatic volunteers. *American Review of Respiratory Disease,* 136, 1127-1134.

Linn, W. S., Szlachcic, Y., Gong, H., Jr., Kinney, P. L. & Berhane, K. T. 2000. Air Pollution and Daily Hospital Admissions in Metropolitan Los Angeles. *Environ Health Perspect,* 108.

Lipfert, F. W., Perry, H. M., Jr., Miller, J. P., Baty, J. D., Wyzga, R. E. & Carmody, S. E. 2000. The Washington University-EPRI Veterans' Cohort Mortality Study: preliminary results. *Inhal Toxicol,* 12 Suppl 4, 41-73.

Liu, L. J., Slaughter, J. C. & Larson, T. V. 2002. Comparison of light scattering devices and impactors for particulate measurements in indoor, outdoor, and personal environments. *Environ Sci Technol,* 36, 2977-86.

Long, C. M., Suh, H. H. & Koutrakis, P. 2000. Characterization of indoor particle sources using continuous mass and size monitors. *J Air Waste Manag Assoc,* 50, 1236-50.

Lowenthal, D. H., Rogers, C. F., Saxena, P., Watson, J. G. & Chow, J. C. 1995. Sensitivity of estimated light extinction coefficients to model assumptions and measurement errors. *Atmospheric Environment,* 29, 751-766.

Magari, S. R., Hauser, R., Schwartz, J., Williams, P. L., Smith, T. J. & Christiani, D. C. 2001. Association of heart rate variability with occupational and environmental exposure to particulate air pollution. *Circulation,* 104, 986-91.

Marquardt, D. 1963. An Algorithm for Least-Squares Estimation of Nonlinear Parameters. *Journal of the Society for Industrial and Applied Mathematics,* 11, 431-441.

Martonen, T. B., Zhang, Z. & Lessmann, R. C. 1993. Fluid Dynamics of the Human Larynx and Upper Tracheobronchial Airways. *Aerosol Science and Technology,* 19, 133-156.

Martuzzi, M., Mitis, F., Iavarone, I. & Serinelli, M. 2006. *Health impact of PM10 and Ozone in 13 Italian cities,* Copenhagen, World Health Organization Regional Office for Europe.

McDonnell, W. F., Abbey, D. E., Nishino, N. & Lebowitz, M. D. 1999. Long-Term Ambient Ozone Concentration and the Incidence of Asthma in Nonsmoking Adults: The Ahsmog Study. *Environmental Research,* 80, 110-121.

McDonnell, W. F., Nishino-Ishikawa, N., Petersen, F. F., Chen, L. H. & Abbey, D. E. 2000. Relationships of mortality with the fine and coarse fractions of long-term ambient PM10 concentrations in nonsmokers. 10, 427-436.

McGettigan, M., Duffy, P., Hyde, B., Hanley, E., O'Brien, P., Ponzi, J. & Black, K. 2010. National Inventory Report 2010. Johnstown Castle Estate, Co. Wexford: EPA.

McMurry, P. H., Zhang, X. & Lee, C.-T. 1996. Issues in aerosol measurement for optics assessments. *J. Geophys. Res.,* 101, 19189-19197.

McNabola, A., Broderick, B., Johnston, P. & Gill, L. 2006. Effects of the Smoking Ban on Benzene and 1,3-Butadiene Levels in Pubs in Dublin. *Journal of Environmental Science and Health, Part A: Toxic/Hazardous Substances and Environmental Engineering,* 41, 799 - 810.

McNabola, A., Broderick, B. M. & Gill, L. W. 2007. Optimal cycling and walking speed for minimum absorption of traffic emissions in the lungs. *J Environ Sci Health A Tox Hazard Subst Environ Eng,* 42, 1999-2007.

McNabola, A., Broderick, B. M. & Gill, L. W. 2008a. Reduced exposure to air pollution on the boardwalk in Dublin, Ireland. Measurement and prediction. *Environment International,* 34, 86-93.

McNabola, A., Broderick, B. M. & Gill, L. W. 2008b. Relative exposure to fine particulate matter and VOCs between transport microenvironments in Dublin: Personal exposure and uptake. *Atmospheric Environment,* 42, 6496-6512.

McNabola, A., McCreddin, A., Gill, L. W. & Broderick, B. M. 2011. Analysis of the relationship between urban background air pollution concentrations and the personal exposure of office workers in Dublin, Ireland, using baseline separation techniques. *Atmospheric Pollution Research,* 2, pp 80-88.

Medina, S., Tertre, A. & Saklad, M. 2009. The Apheis project: Air Pollution and Health—A European Information System. *Air Quality, Atmosphere & Health,* 2, 185-198.

Mendell, M. J., Lei-Gomez, Q., Mirer, A. G., Seppanen, O. & Brunner, G. 2008. Risk factors in heating, ventilating, and air-conditioning systems for occupant symptoms in US office buildings: the US EPA BASE study. *Indoor Air,* 18, 301-16.

Met Éireann. 2012. *Climate of Ireland* [Online]. Met Eireann. Available: **http://www.met.ie/climate/climate-of-ireland.asp** [Accessed 2/2/12 2012].

Met One Instruments 2003. *Aerocet 531 Operation Manual,* Grants Pass, Oregon, Met One Instruments Inc.

Michaels, R. A. 1998. Permissible daily airborne particle mass levels encompass brief excursions to the "London Fog" range, which may contribute to daily mortality and morbidity in communities. *Applied Occupational and Environmental Hygiene,* 13, 385-394.

Michaels, R. A. & Kleinman, M. T. 2000. Incidence and Apparent Health Significance of Brief Airborne Particle Excursions. *Aerosol Science and Technology,* 32, 93 - 105.

Miller, G. T. & Spoolman, S. 2009. *Environmental Science*, Cengage Learning.

Mohammadyan, M. 2011. Determinants of Personal Exposure to PM2.5 in Office Workers. *Indoor and Built Environment.*

Mohammadyan, M., Alizadeh, A. & Etemadinejad, S. 2010a. Personal Exposure to PM10 among Taxi Drivers in Iran. *Indoor and Built Environment,* 19, 538-545.

Mohammadyan, M., Ashmore, M. R. & Shabankhani, B. 2010b. Indoor PM2.5 Concentrations in the Office, Café, and Home. *International Journal of Occupational Hygiene,* 2, 57-62.

Mohammadyana, M., Alizadeha, A. & Mohammadpourb, R. A. 2009. Personal Exposure to PM10 Among Bus Drivers in Sari, Iran. *Indoor and Built Environment,* 18, 83-89.

Molnár, P., Janhäll, S. & Hallquist, M. 2002. Roadside measurements of fine and ultrafine particles at a major road north of Gothenburg. *Atmospheric Environment,* 36, 4115-4123.

Monn, C., Fuchs, A., Högger, D., Junker, M., Kogelschatz, D., Roth, N. & Wanner, H. U. 1997. Particulate matter less than 10 μm (PM10) and fine particles less than 2.5 μm (PM2.5): relationships between indoor, outdoor and personal concentrations. *Science of The Total Environment,* 208, 15-21.

Montgomery, D. C., Peck, E. A. & Vining, G. G. 2012. *Introduction to Linear Regression Analysis*, John Wiley & Sons.

Moschandreas, D. J., Watson, J., D'Abreton, P., Scire, J., Zhu, T., Klein, W. & Saksena, S. 2002. Chapter three: methodology of exposure modeling. *Chemosphere,* 49, 923-946.

Mosqueron, L., Momas, I. & Le Moullec, Y. 2002. Personal exposure of Paris office workers to nitrogen dioxide and fine particles. *Occup Environ Med,* 59, 550-555.

Muir, D. & Laxen, D. P. H. 1995. Black smoke as a surrogate for PM10 in health studies? *Atmospheric Environment,* 29, 959-962.

Mukherjee, P. & Viswanathan, S. 2001. Carbon monoxide modeling from transportation sources. *Chemosphere,* 45, 1071-1083.

Nafstad, P., Haheim, L. L., Oftedal, B., Gram, F., Holme, I., Hjermann, I. & Leren, P. 2003. Lung cancer and air pollution: a 27 year follow up of 16 209 Norwegian men. *Thorax,* 58, 1071-1076.

Nafstad, P., Haheim, L. L., Wisloff, T., Gram, F., Oftedal, B., Holme, I., Hjermann, I. & Leren, P. 2004. Urban air pollution and mortality in a cohort of Norwegian men. *Environmental Health Perspectives,* 112, 610-615.

Nardini, S., Cagnin, R., Invernizzi, G., Ruprecht, A., Boffi, R. & Formentini, S. 2004. Indoor particulate matter measurement as a tool in the process of the implementation of smoke-free hospitals. *Monaldi Arch Chest Dis,* 61, 183-92.

NAS 1991. *Human Exposure Assessment for Airborne Pollutants*, Taylor & Francis.

Neas, L. M., Dockery, D. W., Ware, J. H., Spengler, J. D., Ferris, B. G. & Speizer, F. E. 1994. Concentration of Indoor Particulate Matter as a Determinant of Respiratory Health in Children. *American Journal of Epidemiology,* 139, 1088-1099.

Nevers, N. D. 2000. *Air pollution control engineering*, McGraw-Hill.

NOAA. 2012. *Temperature inversions* [Online]. Salt Lake City. Available: **http://www.wrh.noaa.gov/slc/climate/TemperatureInversions.php** [Accessed 2012].

O'Donoghue, R. T., Broderick, B. M. & Delaney, K. 2007b. Assessing the impacts of infrastructural road changes on air quality: A case study. *Transportation Research Part D: Transport and Environment,* 12, 529-536.

O'Donoghue, R. T., Gill, L. W., McKevitt, R. J. & Broderick, B. 2007a. Exposure to hydrocarbon concentrations while commuting or exercising in Dublin. *Environment International,* 33, 1-8.

O'Mahony, M., Gill, L. W., Broderick, B., English, L. & Ahern, A. 2000. Scope of Transport Impacts on the Environment. *Environmental Research Technological Development and Innovation (ERTDI) Programme 2000 – 2006.* Dublin.

Oberdörster, G. 2000. Pulmonary effects of inhaled ultrafine particles. *International Archives of Occupational and Environmental Health,* 74, 1-8.

Oglesby, L., Kunzli, N., Roosli, M., Braun-Fahrlander, C., Mathys, P., Stern, W., Jantunen, M. & Kousa, A. 2000. Validity of ambient levels of fine particles as surrogate for personal exposure to outdoor air pollution--results of the European EXPOLIS-EAS Study (Swiss Center Basel). *J Air Waste Manag Assoc,* 50, 1251-61.

Olson, D. A. & Burke, J. M. 2005. Distributions of PM2.5 Source Strengths for Cooking from the Research Triangle Park Particulate Matter Panel Study. *Environmental Science & Technology,* 40, 163-169.

Ott, W. R. & Siegmann, H. C. 2006. Using multiple continuous fine particle monitors to characterize tobacco, incense, candle, cooking, wood burning, and vehicular sources in indoor, outdoor, and in-transit settings. *Atmospheric Environment,* 40, 821-843.

Özkaynak, H. & Spengler, J. D. 1996. The role of outdoor particulate matter in assessing total human exposure. *In:* WILSON, R. & SPENGLER, J. D. (eds.) *Particles in our air: Concentrations and health effects.* Boston: Harvard University Press.

Özkaynak, H., Xue, J., Weker, R., Butler, D., Koutrakis, P. & Spengler, J. D. 1996. The Particle Team (PTEAM) study: analysis of the data. Final Report, Vol III. Boston: Harvard School of Public Health: EPA.

Park, S.-K., Kim, S.-D. & Lee, H. 2004. Dispersion characteristics of vehicle emission in an urban street canyon. *Science of The Total Environment,* 323, 263-271.

Park, S. K., O'Neill, M. S., Vokonas, P. S., Sparrow, D. & Schwartz, J. 2005. Effects of air pollution on heart rate variability: The VA Normative Aging Study. *Environmental Health Perspectives,* 113, 304-309.

Pérez Ballesta, P., Field, R. A., Fernández-Patier, R., Galán Madruga, D., Connolly, R., Baeza Caracena, A. & De Saeger, E. 2008. An approach for the evaluation of exposure patterns of urban populations to air pollution. *Atmospheric Environment,* 42, 5350-5364.

Pettyjohn, W. A. & Henning, R. 1979. Preliminary estimate of groundwater recharge rates, related streamflow and water quality in Ohio. Ohio State University, Water Resources Centre.

Pfafflin, J. R. & Ziegler, E. N. 2006. *Encyclopedia of environmental science and engineering: A-L*, CRC Press.

Piccardo, M. T., Stella, A. & Valerio, F. 2010. Is the smokers exposure to environmental tobacco smoke negligible? *Environ Health,* 9, 5.

Pope, C. A., 3rd, Burnett, R. T., Thun, M. J., Calle, E. E., Krewski, D., Ito, K. & Thurston, G. D. 2002. Lung cancer, cardiopulmonary mortality, and long-term exposure to fine particulate air pollution. *JAMA,* 287, 1132-41.

Pope, C. A., 3rd & Dockery, D. W. 2006. Health effects of fine particulate air pollution: lines that connect. *J Air Waste Manag Assoc,* 56, 709-42.

Pope, C. A., 3rd, Ezzati, M. & Dockery, D. W. 2009. Fine-particulate air pollution and life expectancy in the United States. *N Engl J Med,* 360, 376-86.

Pope, C. A., Thun, M. J., Namboodiri, M. M., Dockery, D. W., Evans, J. S., Speizer, F. E. & Heath, C. W. 1995. Particulate air pollution as a predictor of mortality in a prospective study of U.S. adults. *American Journal of Respiratory and Critical Care Medicine,* 151, 669-674.

Pope III, C. A., Verrier, R. L., Lovett, E. G., Larson, A. C., Raizenne, M. E., Kanner, R. E., Schwartz, J., Villegas, G. M., Gold, D. R. & Dockery, D. W. 1999. Heart rate variability associated with particulate air pollution. *American Heart Journal,* 138, 890-899.

Priddy, K. L. & Keller, P. E. 2005. *Artificial Neural Networks: An Introduction*, SPIE Press.

Quackenboss, J. J., Krzyzanowski, M. & Lebowitz, M. D. 1991. Exposure assessment approaches to evaluate respiratory health effects of particulate matter and nitrogen dioxide. *J Expo Anal Environ Epidemiol,* 1, 83-107.

Quanjer, P. H. 1983. *Standardized Lung Function Testing: Report Working Party "Standardization of Lung Function Tests"*, Pergamon.

QUARG 1996. Airborne Particulate Matter in the United Kingdom. *Third Report of the Quality of Urban Air Review Group.* Department of the Environment.

Querol, X., Alastuey, A., Moreno, T., Viana, M. M., Castillo, S., Pey, J., Rodríguez, S., Artiñano, B., Salvador, P., Sánchez, M., Garcia Dos Santos, S., Herce Garraleta, M. D., Fernandez-Patier, R., Moreno-Grau, S., Negral, L., Minguillón, M. C., Monfort, E., Sanz, M. J., Palomo-Marín, R., Pinilla-Gil, E., Cuevas, E., de la Rosa, J. & Sánchez de la Campa, A. 2008. Spatial and temporal variations in airborne particulate matter (PM10 and PM2.5) across Spain 1999–2005. *Atmospheric Environment,* 42, 3964-3979.

Querol, X., Alastuey, A., Rodríguez, S., Viana, M. M., Artíñano, B., Salvador, P., Mantilla, E., do Santos, S. G., Patier, R. F., de La Rosa, J., de la Campa, A. S., Menéndez, M. & Gil, J. J. 2004a. Levels of particulate matter in rural, urban and industrial sites in Spain. *Science of The Total Environment,* 334-335, 359-376.

Querol, X., Alastuey, A., Ruiz, C. R., Artiñano, B., Hansson, H. C., Harrison, R. M., Buringh, E., ten Brink, H. M., Lutz, M., Bruckmann, P., Straehl, P. & Schneider, J. 2004b. Speciation and origin of PM10 and PM2.5 in selected European cities. *Atmospheric Environment,* 38, 6547-6555.

Quintana, P. J., Samimi, B. S., Kleinman, M. T., Liu, L. J., Soto, K., Warner, G. Y., Bufalino, C., Valencia, J., Francis, D., Hovell, M. H. & Delfino, R. J. 2000. Evaluation of a real-time passive personal particle monitor in fixed site residential indoor and ambient measurements. *J Expo Anal Environ Epidemiol,* 10, 437-45.

Quintana, P. J. E., Valenzia, J. R., Delfino, R. J. & Liu, L. J. S. 2001. Monitoring of 1-Min Personal Particulate Matter Exposures in Relation to Voice-Recorded Time–Activity Data. *Environmental Research,* 87, 199-213.

Ramachandran, G., Adgate, J. L., Pratt, G. C. & Sexton, K. 2003. Characterizing Indoor and Outdoor 15 Minute Average PM 2.5 Concentrations in Urban Neighborhoods. *Aerosol Science and Technology,* 37, 33-45.

Rank, J., Folke, J. & Homann Jespersen, P. 2001. Differences in cyclists and car drivers exposure to air pollution from traffic in the city of Copenhagen. *Science of The Total Environment,* 279, 131-136.

Raub, J. 1999. Carbon Monoxide (2nd Edition). *In:* WHO (ed.) *International Program on Chemical Safety, Environmental Health Criteria.* WHO.

Retronaut. 2012. *London Smog, December 1952* [Online]. Available: **http://www.retronaut.co/2011/04/london-smog-december-1952/** [Accessed 09/01/12].

Rich, D. Q., Mittleman, M. A., Link, M. S., Schwartz, J., Luttmann-Gibson, H., Catalano, P. J., Speizer, F. E., Gold, D. R. & Dockery, D. W. 2006. Increased risk of paroxysmal atrial fibrillation episodes associated with acute increases in ambient air pollution. *Environmental Health Perspectives,* 114, 120-123.

Roger, L. J., Horstman, D. H., McDonnell, W., Kehrl, H., Ives, P. J., Seal, E., Chapman, R. & Massaro, E. 1990. Pulmonary function, airway responsiveness, and respiratory symtoms in asthmatics following exercise in NO2. *Toxicology and Industrial Health,* 6, 155-171.

Rojas-Bracho, L., Suh, H. H. & Koutrakis, P. 2000. Relationships among personal, indoor, and outdoor fine and coarse particle concentrations for individuals with COPD. *J Expo Anal Environ Epidemiol,* 10, 294-306.

Rudolf, W. 1994. Concentration of air-pollutants inside cars driving on higways and in downtown areas. *Science of The Total Environment,* 147, 433-444.

Ruprecht, A. A., Invernizzi, G., Dautzenberg, B., Clancy, L., Precioso, J., De Marco, C., Boffi, R., Mazza, R., Lopez, M. J. & Moshammer, H. 2011. Mass Calibration and Relative Humidity Compensation Requirements for Optical Portable Particulate Matter Monitors: The IMPASHS (Impact of Smoke-free Policies in Eu Member States) Wp2 Preliminary Results. *Epidemiology,* 22, S206 10.1097/01.ede.0000392314.24613.c6.

Russell, W. T. 1926. The relative influence of fog and low temperature on the mortality from respiratory disease. *The Lancet,* 208, 1128-1130.

Ryan, B. P., Spengler, J. D. & Letz, R. 1986. Estimating personal exposures to NO2. *Environment International,* 12, 395-400.

Salome, C. M., Brown, N. J., Marks, G. B., Woolcock, A. J., Johnson, G. M., Nancarrow, P. C., Quigley, S. & Tiong, J. 1996. Effect of nitrogen dioxide and other combustion products on asthmatic subjects in a home-like environment. *European Respiratory Journal,* 9, 910-918.

Sarnat, J. A., Koutrakis, P. & Suh, H. H. 2000. Assessing the relationship between personal particulate and gaseous exposures of senior citizens living in Baltimore, MD. *J Air Waste Manag Assoc,* 50, 1184-98.

Sarnat, S. E., Coull, B. A., Schwartz, J., Gold, D. R. & Suh, H. H. 2006. Factors affecting the association between ambient concentrations and personal exposures to particles and gases. *Environmental Health Perspectives,* 114, 649-654.

Scapellato, M. L., Canova, C., de Simone, A., Carrieri, M., Maestrelli, P., Simonato, L. & Bartolucci, G. B. 2009. Personal PM10 exposure in asthmatic adults in Padova, Italy: seasonal variability and factors affecting individual concentrations of particulate matter. *International Journal of Hygiene and Environmental Health,* 212, 626-636.

Schwartz, J. & Morris, R. 1995. Air pollution and hospital admissions for cardiovascular disease in Detroit, Michigan. *American Journal of Epidemiology,* 142, 23-35.

Seaton, A., Soutar, A., Crawford, V., Elton, R., McNerlan, S., Cherrie, J., Watt, M., Agius, R. & Stout, R. 1999. Particulate air pollution and the blood. *Thorax,* 54, 1027-32.

See, S. W. & Balasubramanian, R. 2006. Risk assessment of exposure to indoor aerosols associated with Chinese cooking. *Environmental Research,* 102, 197-204.

Šega, K. & Fugaš, M. 1982. Personal exposure versus monitoring station data for respirable particles. *Environment International,* 8, 259-263.

Sloane, C. S. 1984. Optical properties of aerosols of mixed composition. *Atmospheric Environment (1967),* 18, 871-878.

Smith, M. T. 2010. Advances in Understanding Benzene Health Effects and Susceptibility. *In:* FIELDING, J. E., BROWNSON, R. C. & GREEN, L. W. (eds.) *Annual Review of Public Health, Vol 31.* Palo Alto: Annual Reviews.

Smith, M. T., Zhang, L., McHale, C. M., Skibola, C. F. & Rappaport, S. M. 2011. Benzene, the exposome and future investigations of leukemia etiology. *Chemico-Biological Interactions,* 192, 155-159.

Smith, S. M., Stuhmiller, J. H. & Januszkiewicz, A. J. 1996. Evaluation of lethality estimates for combustion gases in military scenarios. *Toxicology,* 115, 157-165.

Specht, D. F. 1991. A general regression neural network. *IEEE Trans Neural Netw,* 2, 568-76.

Spengler, J. D., Dockery, D. W., Turner, W. A., Wolfson, J. M. & Ferris Jr, B. G. 1981. Long-term measurements of respirable sulfates and particles inside and outside homes. *Atmospheric Environment (1967),* 15, 23-30.

Spengler, J. D., Treitman, R. D., Tosteson, T. D., Mage, D. T. & Soczek, M. L. 1985. Personal exposures to respirable particulates and implications for air pollution epidemiology. *Environmental Science & Technology,* 19, 700-707.

Stieb, D. M., Beveridge, R. C., Brook, J. R., Smith-Doiron, M. A. R. C., Burnett, R. T., Dales, R. E., Beaulieu, S., Judek, S. & Mamedov, A. 2000. Air pollution, aeroallergens and cardiorespiratory emergency department visits in Saint John, Canada. 10, 461-477.

Strak, M., Boogaard, H., Meliefste, K., Oldenwening, M., Zuurbier, M., Brunekreef, B. & Hoek, G. 2010. Respiratory health effects of ultrafine and fine particle exposure in cyclists. *Occup Environ Med,* 67, 118-24.

Subramaniam, R. P., Richardson, R. B., Morgan, K. T., Kimbell, J. S. & Guilmette, R. A. 1998. Computational fluid dynamics simulations of inspiratory airflow in the human nose and nasopharynx. *Inhalation Toxicology,* 10, 91-120.

Tager, I. B., Balmes, J., Lurmann, F., Ngo, L., Alcorn, S. & Künzli, N. 2005. Chronic Exposure to Ambient Ozone and Lung Function in Young Adults. *Epidemiology,* 16, 751-759 10.1097/01.ede.0000183166.68809.b0.

Taulbee, D. B. & Yu, C. P. 1975. Theory of aerosol deposition in human respiratory tract. *Journal of Applied Physiology,* 38, 77-85.

Thatcher, T. L. & Layton, D. W. 1995. Deposition, resuspension, and penetration of particles within a residence. *Atmospheric Environment,* 29, 1487-1497.

Toren, K., Bergdahl, I. A., Nilsson, T. & Jarvholm, B. 2007. Occupational exposure to particulate air pollution and mortality due to ischaemic heart disease and cerebrovascular disease. *Occup Environ Med,* 64, 515-9.

Tovalin-Ahumada, H., Whitehead, L. & Blanco, S. 2007. Personal exposure to PM2.5 and element composition—A comparison between outdoor and indoor workers from two Mexican cities. *Atmospheric Environment,* 41, 7401-7413.

Tunnicliffe, W. S., Hilton, M. F., Harrison, R. M. & Ayres, J. G. 2001. The effect of sulphur dioxide exposure on indices of heart rate variability in normal and asthmatic adults. *European Respiratory Journal,* 17, 604-608.

Turner, M. C., Krewski, D., Pope, C. A., Chen, Y., Gapstur, S. M. & Thun, M. J. 2011. Long-term Ambient Fine Particulate Matter Air Pollution and Lung Cancer in a Large Cohort of Never-Smokers. *American Journal of Respiratory and Critical Care Medicine,* 184, 1374-1381.

UK Department of the Environment 2004. *Airborne Particles: What is the appropriate measurement on which to base a standard? A Discussion Document,* London, HM Stationary Office.

US EPA 2000. Air Quality Criteria for Carbon Monoxide. Washington DC.

US EPA 2004. Air Quality Criteria for Particulate Matter (Final Report). Washington DC.

US EPA 2009. Integrated Science Assessment for Particulate Matter. US EPA Research Triangle Park, NC.

US EPA. 2012. *Relative size of particulate matter* [Online]. Available: **http://www.epa.gov/pm/basic.html** [Accessed 04/01/12 2012].

Vallejo, M., Lerma, C., Infante, O., Hermosillo, A. G., Riojas-Rodriguez, H. & Manuel, C. 2004. Personal exposure to particulate matter less than 2.5[thinsp][mu]m in Mexico City: a pilot study. *J Expo Anal Environ Epidemiol,* 14, 323-329.

Vallero, D. A. 2008. *Fundamentals of air pollution*, Elsevier.

Van Roosbroeck, S., Jacobs, J., Janssen, N. A. H., Oldenwening, M., Hoek, G. & Brunekreef, B. 2007. Long-term personal exposure to PM2.5, soot and NOx in children attending schools located near busy roads, a validation study. *Atmospheric Environment,* 41, 3381-3394.

van Wijnen, J. H., Verhoeff, A. P., Jans, H. W. & van Bruggen, M. 1995. The exposure of cyclists, car drivers and pedestrians to traffic-related air pollutants. *Int Arch Occup Environ Health,* 67, 187-93.

Vardoulakis, S., Gonzalez-Flesca, N. & Fisher, B. E. A. 2002. Assessment of traffic-related air pollution in two street canyons in Paris: implications for exposure studies. *Atmospheric Environment,* 36, 1025-1039.

Violante, F. S., Barbieri, A., Curti, S., Sanguinetti, G., Graziosi, F. & Mattioli, S. 2006. Urban atmospheric pollution: Personal exposure versus fixed monitoring station measurements. *Chemosphere,* 64, 1722-1729.

Vose, D. 2008. *Risk Analysis: A Quantitative Guide*, John Wiley & Sons.

Vrijkotte, T. 1990. *Ventilation and Heart Rate in the Urban Traffic: Pilotstudy to Predict Ventilation from Heart Rate and Power Output, During Bicycling and*

*Driving, Using Data from a Submaximal Test on a Bicycle Ergometer*, Vrije Universiteit.

Walker, A. P. 2004. Controlling particulate emissions from diesel vehicles. *Topics in Catalysis,* 28, 165-170.

Wallace, L. 1996. Indoor particles: a review. *J Air Waste Manag Assoc,* 46, 98-126.

Wallace, L. 2000. Correlations of Personal Exposure to Particles with Outdoor Air Measurements: A Review of Recent Studies. *Aerosol Science and Technology,* 32, 15-25.

Wallace, L. & Ott, W. 2011. Personal exposure to ultrafine particles. *J Expos Sci Environ Epidemiol,* 21, 20-30.

Wallace, L., Williams, R., Rea, A. & Croghan, C. 2006a. Continuous weeklong measurements of personal exposures and indoor concentrations of fine particles for 37 health-impaired North Carolina residents for up to four seasons. *Atmospheric Environment,* 40, 399-414.

Wallace, L., Williams, R., Suggs, J. & Jones, P. 2006b. Estimating contributions of outdoor fine particles to indoor concentrations and personal exposures: effects of household characteristics and personal activities. *In:* EPA, U. (ed.). National Exposure Research Laboratory. Research Triangle Park, NC: US EPA.

Wallace, L. A., Emmerich, S. J. & Howard-Reed, C. 2004. Source Strengths of Ultrafine and Fine Particles Due to Cooking with a Gas Stove. *Environmental Science & Technology,* 38, 2304-2311.

Wallace, L. A., Mitchell, H., O'Connor, G. T., Neas, L., Lippmann, M., Kattan, M., Koenig, J., Stout, J. W., Vaughn, B. J., Wallace, D., Walter, M., Adams, K. & Liu, L. J. 2003. Particle concentrations in inner-city homes of children with asthma: the effect of smoking, cooking, and outdoor pollution. *Environ Health Perspect,* 111, 1265-72.

Watt, M., Godden, D., Cherrie, J. & Seaton, A. 1995. Individual exposure to particulate air pollution and its relevance to thresholds for health effects: A study of traffic wardens. *Occup Environ Med,* 52, 790-792.

Weijers, E. P., Khlystov, A. Y., Kos, G. P. A. & Erisman, J. W. 2004. Variability of particulate matter concentrations along roads and motorways determined by a moving measurement unit. *Atmospheric Environment,* 38, 2993-3002.

Whitby, K. T. 1978. The physical characteristics of sulfur aerosols. *Atmospheric Environment (1967),* 12, 135-159.

WHO 2000. *Air quality guidelines for Europe*, World Health Organization, Regional Office for Europe.

WHO 2006. *Air Quality Guidelines : Global Update 2005 : Particulate Matter, Ozone, Nitrogen Dioxide, and Sulfur Dioxide,* Copenhagen, Denmark, World Health Organization.

Wilson, W. E. & Brauer, M. 2006. Estimation of ambient and non-ambient components of particulate matter exposure from a personal monitoring panel study. *J Expos Sci Environ Epidemiol,* 16, 264-274.

Wong, C.-M., Ma, S., Anthony Johnson, H. & Lam, T.-H. 2001. Effect of Air Pollution on Daily Mortality in Hong Kong. *Environmental Health Perspectives,* 109, 335-340.

Wu, C.-F., Delfino, R. J., Floro, J. N., Quintana, P. J. E., Samimi, B. S., Kleinman, M. T., Allen, R. W. & Sally Liu, L. J. 2005. Exposure assessment and modeling of particulate matter for asthmatic children using personal nephelometers. *Atmospheric Environment,* 39, 3457-3469.

Yeh, H. C., Schum, G. M., Raabe, O. G. & Phalen, R. F. 1976. Models of tracheobronchial geometry in man and experimental animals. *Health Physics,* 31, 533-533.

Yin, J., Allen, A. G., Harrison, R. M., Jennings, S. G., Wright, E., Fitzpatrick, M., Healy, T., Barry, E., Ceburnis, D. & McCusker, D. 2005. Major component composition of urban PM10 and PM2.5 in Ireland. *Atmospheric Research,* 78, 149-165.

Zagury, E., Le Moullec, Y. & Momas, I. 2000. Exposure of Paris taxi drivers to automobile air pollutants within their vehicles. *Occup Environ Med,* 57, 406-10.

Zhang, J., Liu, Y., Sun, X., Yu, S. & Yu, C. 2008. Computational fluid dynamics simulations of respiratory airflow in human nasal cavity and its characteristic dimension study. *Acta Mechanica Sinica,* 24, 223-228.

Zilouchian, A. & Jamshidi, M. 2001. *Intelligent Control Systems Using Soft Computing Methodologies*, Taylor & Francis.

Zmirou, D., Gauvin, S., Pin, I., Momas, I., Just, J., Sahraoui, F., Le Moullec, Y., Bremont, F., Cassadou, S., Albertini, M., Lauvergne, N., Chiron, M., Labbe, A.

& Investigators, V. 2002. Five epidemiological studies on transport and asthma: objectives, design and descriptive results. *Journal of exposure analysis and environmental epidemiology,* 12, 186-96.

Zubair, M., Abdullah, M. Z., Ismail, R., Shuaib, I. L., Hamid, S. A. & Ahmad, K. A. 2011. A critical overview of limitations of CFD modelling in nasal airflow and its corrective approach. *Journal of Medical and Biological Engineering.*

Zuk, M., Rojas, L., Blanco, S., Serrano, P., Cruz, J., Angeles, F., Tzintzun, G., Armendariz, C., Edwards, R. D., Johnson, M., Riojas-Rodriguez, H. & Masera, O. 2007. The impact of improved wood-burning stoves on fine particulate matter concentrations in rural Mexican homes. *J Expo Sci Environ Epidemiol,* 17, 224-32.

Zuurbier, M., Hoek, G., Oldenwening, M., Lenters, V., Meliefste, K., van den Hazel, P. & Brunekreef, B. 2010. Commuters' Exposure to Particulate Matter Air Pollution Is Affected by Mode of Transport, Fuel Type, and Route. *Environ Health Perspect,* 118.

Zuurbier, M., Hoek, G., van den Hazel, P. & Brunekreef, B. 2009. Minute ventilation of cyclists, car and bus passengers: an experimental study. *Environ Health,* 8, 48.

# Appendix A

Office Worker and Taxi Driver Activity Diaries

## Example of the office worker activity diary:

| Time | Activities | | | | | | | | | |
|---|---|---|---|---|---|---|---|---|---|---|
| | At Work | At Home | Sleeping | Commuting | Cooking | Shopping | Sports/ Recreation | Socialising | Smoking | Comments/Other Activities |
| 0000-0100 | | | | | | | | | | |
| 0100-0200 | | | | | | | | | | |
| 0200-0300 | | | | | | | | | | |
| 0300-0600 | | | | | | | | | | |
| 0600-0700 | | | | | | | | | | |
| 0700-0800 | | | | | | | | | | |
| 0800-0900 | | | | | | | | | | |
| 0900-1000 | | | | | | | | | | |
| 1000-1100 | | | | | | | | | | |
| 1100-1200 | | | | | | | | | | |
| 1200-1300 | | | | | | | | | | |
| 1300-1400 | | | | | | | | | | |
| 1400-1500 | | | | | | | | | | |
| 1500-1600 | | | | | | | | | | |
| 1600-1700 | | | | | | | | | | |
| 1700-1800 | | | | | | | | | | |
| 1800-1900 | | | | | | | | | | |
| 1900-2000 | | | | | | | | | | |
| 2000-2100 | | | | | | | | | | |
| 2100-2200 | | | | | | | | | | |
| 2200-2300 | | | | | | | | | | |
| 2300-2400 | | | | | | | | | | |

## Example of the taxi driver activity diary:

| Time | Activities | | | | | |
|---|---|---|---|---|---|---|
| | At Work | Windows Open | Fan On | Air Conditioning On | Smoking | Comments/Other Activities |
| 0000-0100 | | | | | | |
| 0100-0200 | | | | | | |
| 0200-0300 | | | | | | |
| 0300-0600 | | | | | | |
| 0600-0700 | | | | | | |
| 0700-0800 | | | | | | |
| 0800-0900 | | | | | | |
| 0900-1000 | | | | | | |
| 1000-1100 | | | | | | |
| 1100-1200 | | | | | | |
| 1200-1300 | | | | | | |
| 1300-1400 | | | | | | |
| 1400-1500 | | | | | | |
| 1500-1600 | | | | | | |
| 1600-1700 | | | | | | |
| 1700-1800 | | | | | | |
| 1800-1900 | | | | | | |
| 1900-2000 | | | | | | |
| 2000-2100 | | | | | | |
| 2100-2200 | | | | | | |
| 2200-2300 | | | | | | |
| 2300-2400 | | | | | | |

# Appendix B

MS Visual Basic Code for Personal Sample Summary

**Microsoft Visual Basic code for summarising means and standard deviations of samples:**

```
Option Explicit
Dim i As Double
Dim Total(23, 3) As Double
Dim num(23, 3) As Double
Dim average(23, 3) As Double
Dim sum(23, 3) As Double
Dim SquareSum(23, 3) As Double
Dim SDeviation(23, 3) As Double
Dim a As Double
Dim z As Double
Dim total_v As Double
Dim average_v As Double
Dim counter_v As Double

Private Sub CommandButton3_Click()
z = 0

Do

For i = 0 To 16
    For a = 0 To 2
    Total(i, a) = 0
    num(i, a) = 0
    average(i, a) = 0
    SquareSum(i, a) = 0
    SDeviation(i, a) = 0
    Next
Next

i = 12

Do

'Filling arrays with PM data. The num array gives the number of values
for 'activity.The total array gets the total of PM values for each
activity.Column '13 is activities, Column 12 is days


If Cells(i, 4 + z) <> "" Then
    num(Cells(i, 13) - 1, Cells(i, 14) - 1) = num(Cells(i, 13) - 1,
Cells(i, 14) - 1) + 1
    Total(Cells(i, 13) - 1, Cells(i, 14) - 1) = Total(Cells(i, 13) -
1, Cells(i, 14) - 1) + Cells(i, 4 + z)
   SquareSum(Cells(i, 13) - 1, Cells(i, 14) - 1) = SquareSum(Cells(i,
13) - 1, Cells(i, 14) - 1) + (Cells(i, 4 + z)) ^ 2
    End If

    i = i + 1
Loop Until Cells(i, 14) = ""


'This gets the average values for each activity on each day. It
divides each element of the total array by each element of the num
array


For i = 0 To 16
    For a = 0 To 2
        If num(i, a) <> 0 Then
            average(i, a) = Total(i, a) / num(i, a)
```

```
        End If
    Next
Next

For i = 0 To 16
    For a = 0 To 2
        If num(i, a) > 1 Then
            If (SquareSum(i, a) / num(i, a)) - average(i, a) ^ 2 >= 0
Then
            SDeviation(i, a) = Sqr((SquareSum(i, a) / num(i, a)) -
average(i, a) ^ 2)
            Else
            SDeviation(i, a) = 0
            End If
        End If
    Next
Next

'This prints out the average values for each activity on the worksheet
"Averages"

    For i = 0 To 16
        For a = 0 To 2
            If num(i, a) = 0 Then
                Worksheets("24-hr Averages").Cells(i + 2 + a * 17, 4 +
z) = " "
                Worksheets("24-hr St Deviation").Cells(i + 2 + a * 17,
4 + z) = " "
                Worksheets("24-hr Averages").Cells(i + 2 + a * 17, 9)
= " "
            Else
                Worksheets("24-hr Averages").Cells(i + 2 + a * 17, 4 +
z) = 1000 * average(i, a)
                Worksheets("24-hr St Deviation").Cells(i + 2 + a * 17,
4 + z) = 1000 * SDeviation(i, a)
                Worksheets("24-hr Averages").Cells(i + 2 + a * 17, 9)
= num(i, a)
            End If
        Next
    Next


z = z + 1
Loop Until z = 5


'Daily average

Dim k As Double
Dim Totald(2) As Double
Dim numd(2) As Double
Dim averaged(2) As Double
Dim SquareSumd(2) As Double
Dim SDeviationd(2) As Double
Dim y As Double

y = 0

Do

For k = 0 To 2

    Totald(k) = 0
    numd(k) = 0
    averaged(k) = 0
```

```
    SquareSumd(k) = 0
    SDeviationd(k) = 0

Next

k = 12

Do

If Cells(k, 4 + y) <> "" Then
    numd(Cells(k, 14) - 1) = numd(Cells(k, 14) - 1) + 1
    Totald(Cells(k, 14) - 1) = Totald(Cells(k, 14) - 1) + Cells(k, 4 +
y)
    SquareSumd(Cells(k, 14) - 1) = SquareSumd(Cells(k, 14) - 1) +
(Cells(k, 4 + y)) ^ 2
End If

    k = k + 1
Loop Until Cells(k, 14) = ""


'This gets the average values for each day. It divides each element of
the total array by each element of the num array


For k = 0 To 2
    If numd(k) <> 0 Then
            averaged(k) = Totald(k) / numd(k)
    End If
Next

For k = 0 To 2
        If numd(k) > 1 Then
            If (SquareSumd(k) / numd(k)) - averaged(k) ^ 2 >= 0 Then
            SDeviationd(k) = Sqr((SquareSumd(k) / numd(k)) -
averaged(k) ^ 2)
            Else
            SDeviationd(k) = 0
            End If
        End If
    Next


For k = 0 To 2
    If numd(k) = 0 Then
        Worksheets("24-hr Averages").Cells(2 + k, 12 + y) = " "
        Worksheets("24-hr St Deviation").Cells(2 + k, 10 + y) = " "
    Else
       Worksheets("24-hr Averages").Cells(2 + k, 12 + y) = 1000 *
averaged(k)
       Worksheets("24-hr St Deviation").Cells(2 + k, 10 + y) = 1000 *
SDeviationd(k)
    End If
Next


y = y + 1
Loop Until y = 5

End Sub
```

# Appendix C

Examples of 24 Hour Personal Exposure Data

**Example of the 24-hour personal exposure concentrations (μg/m$^3$) obtained from the first four volunteers.**

| Volunteer Number | 24-hr Average | Work | Home | Sleep | Pub | Walk | Car | Train | Bus | Tram | Cycle | Shop | Sport | Café | Other Indoor I | Other Indoor II | Other Outdoor |
|---|---|---|---|---|---|---|---|---|---|---|---|---|---|---|---|---|---|
| 1 | 18.7 | 46.3 | 10.8 | 3.0 | | 14.5 | 11.3 | | | | | | | | | | |
| 1 | 39.7 | 91.0 | 18.3 | 4.3 | | 91.1 | 33.5 | | 39.8 | 28.1 | | | | | 30.9 | | |
| 1 | 25.8 | 41.9 | 16.7 | 21.9 | | 161.8 | | | 53.3 | | | | | | | | |
| 1 | 33.0 | 48.2 | 7.2 | 22.4 | | | | | 32.5 | | | | | | | | |
| 1 | 28.2 | 71.8 | 16.5 | 3.4 | | 17.7 | | | | | | | | | | | |
| 1 | 29.3 | 69.8 | 15.6 | 3.5 | | 19.0 | 38.8 | | | | | 77.6 | | 108.8 | 22.8 | | |
| 2 | 19.4 | 21.6 | 18.8 | 15.1 | | | | | | | 31.1 | | | | | | 36.1 |
| 2 | 13.2 | 12.2 | 20.8 | 8.4 | | | | | | | 29.2 | | | | | | |
| 2 | 19.9 | 25.2 | 26.3 | 10.0 | | 20.3 | | | 60.2 | | 16.5 | | | | | | |
| 2 | 18.4 | 19.8 | 39.2 | 8.1 | | | | | | | 13.5 | | | | | | |
| 2 | 11.2 | 12.6 | 11.6 | 4.8 | | 84.8 | | | | | 17.2 | | | 35.0 | 56.6 | | |
| 2 | 18.3 | 14.9 | 18.7 | 10.8 | | 201.7 | | | | | 48.6 | | | 46.4 | 99.8 | | |
| 3 | 26.4 | 17.1 | 17.7 | 23.9 | 29.9 | 16.6 | 38.2 | | | | 12.7 | | 75.0 | | | | |
| 3 | 10.1 | 21.2 | 8.7 | 3.7 | | 17.2 | 45.6 | | 21.2 | | | | | | | | |
| 3 | 17.7 | | 17.6 | 7.6 | | | | | | | | 37.8 | | | | | |
| 3 | 6.4 | | 7.8 | 2.1 | | | | | | | 25.1 | | | | 10.5 | | |
| 3 | 32.1 | 33.2 | 25.8 | 11.5 | | 11.6 | 78.8 | | 58.4 | | 5.6 | 35.5 | 156.6 | 23.4 | | | |
| 3 | 13.5 | | 16.6 | 6.6 | | 9.0 | | | 46.2 | | | | | | | | |
| 4 | 21.7 | 33.5 | 19.5 | 8.0 | | 17.8 | | | | 18.3 | | | | | | | |
| 4 | 15.7 | 22.1 | 14.4 | 9.2 | | 15.3 | | | | | | | | | | | 13.1 |
| 4 | 14.1 | 14.6 | 14.9 | 13.0 | | | | | | | 14.7 | | | | | | |
| 4 | 7.1 | 10.4 | 5.6 | 1.1 | | 11.2 | | | | | | | | 70.5 | 7.6 | | 28.4 |
| 4 | 20.5 | 7.5 | 3.4 | 0.8 | | 5.7 | 3.8 | | | 17.9 | | | 161.8 | | 55.6 | | |
| 4 | 13.0 | 12.9 | 12.7 | 12.4 | | 17.7 | | | | 25.9 | | | | | | | |

# Appendix D

Summary of Volunteer Profiles

**Summary profiles for the experimental sampling campaign study population.**

| Subject | Gender | Sampling Days | Ethnicity | Self-identified Smoker | Home Location | Area Code | Home Type |
|---|---|---|---|---|---|---|---|
| 1 | F | 6 | White | No | Portland Place | Dublin 1 | Apartment |
| 2 | M | 6 | White | No | Rathmines | Dublin 6 | Apartment |
| 3 | F | 6 | White | No | Nottingham Street | Dublin 1 | Terrace |
| 4 | M | 6 | White | No | Smithfield | Dublin 7 | Apartment |
| 5 | F | 3 | White | No | Termonfeckin | Co. Louth | Detached |
| 6 | M | 6 | White | No | Whitehall | Dublin 9 | Semi-detached |
| 7 | M | 5 | White | No | Sandyford | Dublin 18 | Apartment |
| 8 | M | 2 | White | No | Blackrock | Co.Dublin | Semi-detached |
| 9 | M | 2 | White | No | Porterstown | Dublin 15 | Apartment |
| 10 | F | 6 | White | No | Dartry | Dublin 6 | Apartment |
| 11 | F | 4 | White | No | Malahide Road | Dublin 3 | Semi-detached |
| 12 | F | 4 | White | No | Dollymount | Dublin 3 | Apartment |
| 13 | F | 3 | Asian | Yes | Dun Laoghaire | Co.Dublin | Apartment |
| 14 | M | 6 | White | No | Kilkea | Co. Kildare | Detached |
| 15 | M | 1 | White | No | Rathfarnham | Dublin 14 | Semi-detached |
| 16 | M | 6 | White | No | Dartry | Dublin 6 | Apartment |
| 17 | F | 6 | White | No | Rathfarnham | Dublin 14 | Semi-detached |
| 18 | M | 3 | White | No | Ballsbridge | Dublin 4 | Apartment |
| 19 | M | 6 | White | No | Drimnagh | Dublin 12 | End of terrace |
| 20 | F | 6 | White | Yes | Walkinstown | Dublin 12 | End of terrace |
| 21 | M | 6 | White | No | Stoneybatter | Dublin 7 | Apartment |
| 22 | M | 5 | White | No | Bray | Co. Wicklow | Semi-detached |
| 23 | M | 3 | White | No | Sutton | Dublin 13 | Detached |
| 24 | M | 4 | White | No | Baldoyle | Dublin 13 | Apartment |
| 25 | F | 2 | White | No | Phibsborough | Dublin 11 | Apartment |
| 26 | F | 3 | White | No | Cabra | Dublin 7 | Terraced |
| 27 | F | 3 | White | No | Drumcondra | Dublin 9 | Terraced |
| 28 | M | 2 | White | No | Ballyboden | Dublin 16 | Semi-detached |
| 29 | M | 6 | White | No | Newbridge | Co. Kildare | Terraced |

| Subject | Gender | Sampling Days | Ethnicity | Self-identified Smoker | Home Location | Area Code | Home Type |
|---|---|---|---|---|---|---|---|
| 30 | M | 6 | White | No | Castleknock | Dublin 15 | Apartment |
| 31 | F | 1 | White | No | Smithfield | Dublin 7 | Apartment |
| 32 | M | 5 | White | No | Celbridge | Co. Kildare | Detached |
| 33 | M | 7 | White | No | Maynooth | Co. Kildare | Semi-detached |
| 34 | M | 3 | Hispanic | Yes | Donnycarney | Dublin 9 | Terraced |
| 35 | M | 6 | White | No | Ballinteer | Dublin 16 | Apartment |
| 36 | M | 3 | White | No | Phibsboro | Dublin 7 | Terraced |
| 37 | M | 7 | White | Yes | East Wall | Dublin 3 | Terraced House |
| 38 | F | 5 | White | No | Portmarnock | Co. Dublin | Semi-detached |
| 39 | F | 3 | White | No | Harold's Cross | Dublin 6w | Terraced |
| 40 | M | 6 | White | No | Dorset Street | Dublin 1 | Apartment |
| 41 | F | 5 | White | No | Smithfield | Dublin 7 | Apartment |
| 42 | F | 6 | White | No | Kilnamanagh | Dublin 24 | Semi-detached |
| 43 | F | 1 | White | No | Ringsend | Dublin 4 | Apartment |
| 44 | F | 3 | White | No | IFSC | Dublin 1 | Apartment |
| 45 | F | 3 | White | No | Celbridge | Co. Kildare | Semi-detached |
| 46 | F | 4 | White | No | Phibsborough | Dublin 7 | Terraced House |
| 47 | M | 3 | White | Yes | Phibsborough | Dublin 7 | Terraced |
| 48 | F | 8 | White | Yes | Finglas | Dublin 11 | Semi-detached |
| 49 | M | 1 | White | No | Tallaght | Dublin 24 | Semi-detached |
| 50 | F | 3 | White | No | Drumcondra | Dublin 9 | End of terrace |
| 51 | M | 6 | White | No | Ballsbridge | Dublin 4 | Apartment |
| 52 | M | 2 | White | No | Sandymount | Dublin 4 | Detached |
| 53 | M | 2 | White | No | Lurgan Street | Dublin 7 | Terraced |
| 54 | M | 6 | White | No | Clane | Co.Kildare | Detached |
| 55 | F | 6 | White | No | Whitehall | Dublin 9 | Semi-detached |
| 56 | M | 6 | White | No | Stillorgan | Co.Dublin | Terraced |
| 57 | M | 2 | White | No | Walkinstown | Dublin 12 | End of terrace |
| 58 | M | 3 | White | Yes | Clondalkin | Dublin 22 | End of terrace |
| 59 | M | 6 | White | No | Clonsilla | Dublin 15 | Semi-detached |

# Appendix E

The Human Respiratory Tract Model

**Matlab code for the Human Respiratory Tract Model:**

```
i = 1;
Rtotal = zeros(1,1);
RegionDep = zeros(1,10);

for i = 1

dae = 10; % aerodynamic particle diameter
dth = 10; %thermodynamic particle diameter (micrometers)
de = 10; % equivalent particle volume diameter
D = 0.2; % particle diffusion coefficent cm^2/sec
U = 1; %Wind speed m/s
%Fn = 1; % Oro-nasal factor
ShapeFactor = 1.5;
P = 76; %Pressure in cm Hg
UnitDensity = 1;
Density = 3;

ActivityLevel = activity(i);
ExposureTime = time(i);
Ca = concentration(i);
gender = 1;


if gender == 1;
    FRC = 3301;
    VdET = 50;
    VdBB = 49;
    Vdbb = 47;
    VdTotal = 146;
    Height = 176;
    do = 1.65;
    d9 = 0.165;
    d16 = 0.051;
    SFt = 1;
    SFb = 1;
    SFa = 1;

end

if gender==1&&ActivityLevel==1;
    B=0.0075; % 0.45m^3/hr converted to m^3/min as time input in mins
    fr=12;  %Respiration frequency (per minute)
    Vt=625; %Tidal Volume (in mL) of exposed subject
    V=250;  %V(dot) Volumetric flow rate (in mL^s) of inspired air
    Vn=250; % Vn(dot) Component of volumetric flow rate that is
inspired through the nose
    Fn =1;
end

if gender==1&&ActivityLevel==2;
    B=0.009;  % 0.54m^3/hr
    fr=12;
    Vt=750;
    V=300;
    Vn=300;
```

```
    Fn =1;
end

if gender==1&&ActivityLevel==3;
    B=0.025;  % 1.5m^3/hr
    fr=20;
    Vt=1250;
    V=833;
    Vn=833;
    Fn = 1;
end

if gender==1&&ActivityLevel==4;
    B=0.05;  % 3 m^3/hr
    fr=26;
    Vt=1920;
    V=1670;
    Vn=1670;
    Fn =0.5;
end

if gender==1&&ActivityLevel==5;
    B=0.03;  % 3 m^3/hr
    fr=21;
    Vt=1430;
    V=1000;
    Vn=1000;
    Fn=1;
end

if gender == 2;
    FRC = 2681;
    VdET = 40;
    VdBB = 40;
    Vdbb = 44;
    VdTotal = 124;
    Height = 163;
    do = 1.53;
    d9 = 0.159;
    d16 = 0.048;
    SFt = 1.08;
    SFb = 1.04;
    SFa = 1.07;
end

    if gender==2&&ActivityLevel==1;
    B=0.0053;  % 0.32m^3/hr
    fr=12;
    Vt=444;
    V=178;
    Vn=178;
    Fn=1;
    end

if gender==2&&ActivityLevel==2;
    B=0.0065;  % 0.39m^3/hr
    fr=14;
```

```
    Vt=464;
    V=217;
    Vn=217;
    Fn=1;
end

if gender==2&&ActivityLevel==3;
    B=0.02083;  % 1.25m^3/hr
    fr=21;
    Vt=992;
    V=694;
    Vn=694;
    Fn=1;
end

if gender==2&&ActivityLevel==4;
    B=0.045;  % 2.7m^3/hr
    fr=33;
    Vt=1364;
    V=1500;
    Vn=1500;
    Fn=0.5;
end

if gender==2&&ActivityLevel==5;
    B=0.025;
    fr=25;
    Vt=1000;
    V= 833;
    Vn=833;
    Fn=1;
end

% Scaling


I0 = Ca * ExposureTime* B;


% Aerodynamic deposition for inhalation and exhalation through the
nose
% Region ET1
a1 = 3.0*10^-4;
R1 = (dae^2)*Vn*(SFt^3);
p1 = 1;

ETAae1 = 0.5*(1-(1/(a1*(R1^p1)+1)));

a1t= 18;
R1t = D*((Vn*SFt)^-0.25);
p1t = 0.5;

ETAt1 = 0.5*(1-exp(-a1t*(R1t^p1t)));

phi1n = 1;

% ET2
```

```
a2 = 5.5*10^-5;
R2 = (dae^2)*Vn*(SFt^3);
p2 = 1.17;

ETAae2 = 1-(1/(a2*(R2^p2)+1));

a2t = 15.1;
R2t = D*((Vn*SFt)^-0.25);
p2t = 0.538;

ETAt2 = 1-exp(-a2t*(R2t^p2t));

phi2n = 1;

%BB

a3 = 4.08*10^-6;
R3 = (dae^2)*V*(SFt^2.3);
p3 = 1.152;

ETAae3 = 1-exp(-a3*(R3^p3));

Psi = 1 + 100*exp(-(log10(100 + (10/(dth^0.9))))^2);
a3t = 22.02*(SFt^1.24)*Psi;
    tB = (VdBB/V) * (1 + (( 0.5*Vt)/FRC));
R3t = D*tB;
p3t = 0.6391;

ETAt3 = 1 - exp(-a3t*(R3t^p3t));

phi3n = 1 - ((VdET)/Vt);
phi7n = phi3n;

%bb

a4 = 0.1147;
tb = (Vdbb/V) * (1 + (( 0.5*Vt)/FRC));
R4 = (0.056 + tb^1.5)*(dae^(tb^-0.25));
p4 = 1.173;

ETAae4 = 1-exp(-a4*R4^p4);

a4t = (-76.8)+ 167*(SFb^0.65);
R4t = D*tb;
p4t = 0.5676;

ETAt4 = 1 - exp(-a4t*(R4t^p4t));

VdashDBB = VdBB*(1+Vt/FRC);
phi4n = 1 - ((VdET + VdashDBB)/Vt);

phi6n = phi4n;


%AI
```

```
a5=0.146*(SFa^0.98);
tA = (Vt - VdET - (VdBB + Vdbb)*(1+(Vt/FRC)))/V;
R5= (dae^2)*tA;
p5= 0.6495;

ETAae5 = 1-exp(-a5*R5^p5);

a5t = 170 + 103*(SFa^2.13);

R5t = D*tA;
p5t = 0.6101;

ETAt5 = 1 - exp(-a5t*(R5t^p5t));

VdashDBB = VdBB*(1+(Vt/FRC));
VdashDbb = Vdbb*(1+(Vt/FRC));

phi5n = 1 - ((VdET + VdashDBB + VdashDbb)/Vt);


%bb

a6=0.1147;
tb = (Vdbb/V)*(1 + ((0.5*Vt/FRC)));
R6=(0.056 + tb^1.5)*(dae^(tb^-0.25));
p6 = 1.173;

ETAae6 = 1-exp(-a6*R6^p6);

a6t = (-76.8)+ 167*(SFb^0.65);
R6t = D*tb;
p6t = 0.5676;

ETAt6 = 1 - exp(-a6t*(R6t^p6t));

%BB

a7= 2.04*10^-6;
R7= (dae^2)*V*(SFt^2.3);
p7=1.152;

ETAae7 = 1-exp(-a7*R7^p7);

Psi = 1 + 100*exp(-(log10(100 + (10/(dth^0.9))))^2);
a7t = 22.02*(SFt^1.24)*Psi;
R7t = D*tB;
p7t = 0.6391;

ETAt7 = 1 - exp(-a7t*(R7t^p7t));

% ET2

a8= 5.5*10^-5;
R8= (dae^2)*Vn*(SFt^3);
p8=1.17;

ETAae8 = 1-(1/(a2*(R8^p8)+1));
```

```
a8t = 15.1;
R8t = D*((Vn*SFt)^-0.25);
p8t = 0.538;

ETAt8 = 1-exp(-a8t*(R8t^p8t));

phi8n = 1;

% Region ET1
a9= 3.0*10^-4;
R9=(dae^2)*Vn*(SFt^3);
p9=1;

ETAae9 = 0.5*(1-(1/(a1*(R9^p9)+1)));

a9t= 18;
R9t = D*((Vn*SFt)^-0.25);
p9t = 0.5;

ETAt9 = 0.5*(1-exp(-a9t*(R9t^p9t)));

phi9n = 1;

% Combined deposition efficiencies

ETA1 = (ETAae1^2 + ETAt1^2)^0.5;
ETA2 = (ETAae2^2 + ETAt2^2)^0.5;
ETA3 = (ETAae3^2 + ETAt3^2)^0.5;
ETA4 = (ETAae4^2 + ETAt4^2)^0.5;
ETA5 = (ETAae5^2 + ETAt5^2)^0.5;
ETA6 = (ETAae6^2 + ETAt6^2)^0.5;
ETA7 = (ETAae7^2 + ETAt7^2)^0.5;
ETA8 = (ETAae8^2 + ETAt8^2)^0.5;
ETA9 = (ETAae9^2 + ETAt9^2)^0.5;

ETA = ETA1 + ETA2 + ETA3 + ETA4 + ETA5 + ETA6 + ETA7 + ETA8 + ETA9;

%Regional deposition for the fraction of intake inhaled and exhaled
through
%the mouth

% Filter 1, Region ET2

a1m = 1.1*10^-4;
R1m = (dae^2)*((V*SFt^3)^0.6)*((Vt*SFt^2)^-0.2);
p1m = 1.4;

ETAae1m = 1-(1/(a1m*(R1m^p1m) + 1));

a1mt = 9;
R1mt = D*((Vn*SFt)^-0.25);
p1mt = 0.5;

ETAth1m = 1 - exp(-a1mt*(R1mt^p1mt));

phi1m = 1;
```

```
% Filter 2, Region BB

a2m = 4.08*10^-.6;
R2m = (dae^2)*V*(SFt^2.3);
p2m = 1.152;

ETAae2m = 1-exp(-a2m*(R2m^p2m));

PSImt = 1 + 100*exp(-(log10(100 + 10/(dth^0.9)))^2);
a2mt = 22.02*(SFt^1.24)*PSImt;
R2mt = D*tB;
p2mt = 0.6391;

ETAth2m = 1 - exp(-a2mt*(R2mt^p2mt));

phi2m = 1 - ((VdET)/Vt);
phi6m = phi2m;

% Filter 3, Region bb

a3m = 0.1147;
R3m = (0.056 + tb^1.5)*(dae^(tb^-0.25));
p3m = 1.173;

ETAae3m = 1-exp(-a3m*(R3m^p3m));

a3mt = -76.8 + 167*(SFb^0.65);
R3mt = D*tb;
p3mt = 0.5676;

ETAth3m = 1 - exp(-a3mt*(R3mt^p3mt));

 VdashDBB = VdBB*(1+Vt/FRC);
    phi3m = 1 - ((VdET + VdashDBB)/Vt);
    phi5m = phi3m;

%Filter 4, Region AI

a4m = 0.146*(SFa^0.98);
R4m = (dae^2)*tA;
p4m = 0.6495;

ETAae4m = 1-exp(-a4m*(R4m^p4m));

a4mt = 170 + 103*(SFa^2.13);
R4mt = D*tA;
p4mt = 0.6101;

ETAth4m = 1 - exp(-a4mt*(R4mt^p4mt));

 VdashDBB = VdBB*(1+(Vt/FRC));
 VdashDbb = Vdbb*(1+(Vt/FRC));

 phi4m = 1 - ((VdET + VdashDBB + VdashDbb)/Vt);
```

```
%Filter 5, Region bb

a5m = 0.1147;
R5m = (0.056 + tb^1.5)*(dae^(tb^-0.25));
p5m = 1.173;

ETAae5m = 1-exp(-a5m*(R5m^p5m));

a5mt = -76.8 + 167*(SFb^0.65);
R5mt = D*tb;
p5mt = 0.5676;

ETAth5m = 1 - exp(-a5mt*(R5mt^p5mt));

% Filter 6, Region BB

a6m = 2.04*10^-6;
R6m = (dae^2)*V*(SFt^2.3);
p6m = 1.152;

ETAae6m = 1-exp(-a6m*(R6m^p6m));

PSImt = 1 + 100*exp(-(log10(100 + 10/(dth^0.9)))^2);
a6mt = 22.02*(SFt^1.24)*PSImt;
R6mt = D*tB;
p6mt = 0.6391;

ETAth6m = 1 - exp(-a6mt*(R6mt^p6mt));

%Filter 7, Region ET2

a7m = 1.1*10^-4;
R7m = (dae^2)*((V*SFt^3)^0.6)*((Vt*SFt^2)^-0.2);
p7m = 1.4;

ETAae7m = 1-(1/(a7m*(R7m^p7m) + 1));

a7mt = 9;
R7mt = D*((Vn*SFt)^-0.25);
p7mt = 0.5;

ETAth7m = 1 - exp(-a7mt*(R7mt^p7mt));

phi7m = 1;

% Combined deposition efficiencies

ETA1m = (ETAae1m^2 + ETAth1m^2)^0.5;
ETA2m = (ETAae2m^2 + ETAth2m^2)^0.5;
ETA3m = (ETAae3m^2 + ETAth3m^2)^0.5;
ETA4m = (ETAae4m^2 + ETAth4m^2)^0.5;
ETA5m = (ETAae5m^2 + ETAth5m^2)^0.5;
ETA6m = (ETAae6m^2 + ETAth6m^2)^0.5;
ETA7m = (ETAae7m^2 + ETAth7m^2)^0.5;

ETAm = ETA1m + ETA2m + ETA3m + ETA4m + ETA5m + ETA6m + ETA7m;
```

```
nI = 1 - (0.5*(1-((7.6*10^(-4)*(dae^2.8)+1)^-1))+((1*10^(-
5))*(U^2.75)*exp(0.055*dae)));
n0 = (1-nI);


% NOSE
% nEpsilon jj = Phijj/Phi(jj-1)
nEpsilon1 = 1 ;
nEpsilon2 = phi2n/phi1n ;
nEpsilon3 = phi3n/phi2n ;
nEpsilon4 = phi4n/phi3n ;
nEpsilon5 = phi5n/phi4n ;
nEpsilon6 = phi6n/phi5n ;
nEpsilon7 = phi7n/phi6n ;
nEpsilon8 = phi8n/phi7n ;
nEpsilon9 = phi9n/phi8n ;


% nDej = nDe(j-1) *Nj *nEpsilonj * ((1/N(j-1)) - 1)        for j = 1,N
nDe1 = ETA1 * (1-n0);
nDe2 = nDe1 * ETA2 * nEpsilon2 * ((1/ETA1)-1);
nDe3 = nDe2 * ETA3 * nEpsilon3 * ((1/ETA2)-1);
nDe4 = nDe3 * ETA4 * nEpsilon4 * ((1/ETA3)-1);
nDe5 = nDe4 * ETA5 * nEpsilon5 * ((1/ETA4)-1);
nDe6 = nDe5 * ETA6 * nEpsilon6 * ((1/ETA5)-1);
nDe7 = nDe6 * ETA7 * nEpsilon7 * ((1/ETA6)-1);
nDe8 = nDe7 * ETA8 * nEpsilon8 * ((1/ETA7)-1);
nDe9 = nDe8 * ETA9 * nEpsilon9 * ((1/ETA8)-1);

% I0 already calculated!
nI1 = I0 * (1-nDe1) ;
nI2 = nI1 * (1-nDe2) ;
nI3 = nI2 * (1-nDe3) ;
nI4 = nI3 * (1-nDe4) ;
nI5 = nI4 * (1-nDe5) ;
nI6 = nI5 * (1-nDe6) ;
nI7 = nI6 * (1-nDe7) ;
nI8 = nI7 * (1-nDe8) ;
nI9 = nI8 * (1-nDe9) ;


%MOUTH
% mEpsilon jj = Phijj/Phi(jj-1)
mEpsilon1 = 1 ;
mEpsilon2 = phi2m/phi1m ;
mEpsilon3 = phi3m/phi2m ;
mEpsilon4 = phi4m/phi3m ;
mEpsilon5 = phi5m/phi4m ;
mEpsilon6 = phi6m/phi5m ;
mEpsilon7 = phi7m/phi6m ;


% mDej = mDe(j-1) *Nj *mEpsilonj * ((1/N(j-1)) - 1)        for j = 1,N
mDe1 = ETA1m * (1-n0);
mDe2 = mDe1 * ETA2m * mEpsilon2 * ((1/ETA1m)-1);
mDe3 = mDe2 * ETA3m * mEpsilon3 * ((1/ETA2m)-1);
mDe4 = mDe3 * ETA4m * mEpsilon4 * ((1/ETA3m)-1);
```

```
mDe5 = mDe4 * ETA5m * mEpsilon5 * ((1/ETA4m)-1);
mDe6 = mDe5 * ETA6m * mEpsilon6 * ((1/ETA5m)-1);
mDe7 = mDe6 * ETA7m * mEpsilon7 * ((1/ETA6m)-1);

% I0 already calculated!
mI1 = I0 * (1-mDe1) ;
mI2 = mI1 * (1-mDe2) ;
mI3 = mI2 * (1-mDe3) ;
mI4 = mI3 * (1-mDe4) ;
mI5 = mI4 * (1-mDe5) ;
mI6 = mI5 * (1-mDe6) ;
mI7 = mI6 * (1-mDe7) ;


% Total Deposition I (ug)
% I0 = already calculated
I1 = nI1*Fn + (1-Fn)*mI1 ;
I2 = nI2*Fn + (1-Fn)*mI2 ;
I3 = nI3*Fn + (1-Fn)*mI3 ;
I4 = nI4*Fn + (1-Fn)*mI4 ;
I5 = nI5*Fn + (1-Fn)*mI5 ;
I6 = nI6*Fn + (1-Fn)*mI6 ;
I7 = nI7*Fn + (1-Fn)*mI7 ;
I8 = nI8*Fn  ;
I9 = nI9*Fn  ;

% Regional Lung Deposition (ug)
RI0 = 0 ;
RI1 = I0 - I1 ;
RI2 = I1 - I2 ;
RI3 = I2 - I3 ;
RI4 = I3 - I4 ;
RI5 = I4 - I5 ;
RI6 = I5 - I6 ;
RI7 = I6 - I7 ;
RI8 = I7 - I8 ;
RI9 = I8 - I9 ;

Rtotal(i) = RI0 + RI1 + RI2 + RI3 + RI4 + RI5 + RI6 + RI7 + RI8 + RI9;


RegionDep(1) = I0;
RegionDep(2) =I1;
RegionDep(3) =I2;
RegionDep(4) =I3;
RegionDep(5) =I4;
RegionDep(6) =I5;
RegionDep(7) =I6;
RegionDep(8) =I7;
RegionDep(9) =I8;
RegionDep(10) =I9;

end
```

# Appendix F

Matlab Code for Monte Carlo Simulation of Exposures

**Matlab code for Monte Carlo simulation of personal exposures:**

```
load('MonteCarloTest3.mat');
A = untitled;

load('MaleWork_LogN.mat');
load('FemaleWork_Weibull.mat');
load('Home_LogLogistic.mat');
load('Pub_LogLogistic.mat');
load('Walk_LogLogistic.mat');
load('Cycle_LogNormal.mat');
load('TrainTram_Gamma.mat');
load('Shop_LogLogistic.mat');
load('Cafe_InvGauss.mat');
load('OtherIndoor_LogLogistic.mat');
load ('OtherOutdoor_LogN.mat');
load('SmokerHome_InvGauss');

m=100;

Workft = zeros(27,1);
Homeft = zeros(27,1);
Sleepft = zeros(27,1);
Pubft = zeros(27,1);
Walkft = zeros(27,1);
Driveft = zeros(27,1);
Trainft = zeros(27,1);
Busft = zeros(27,1);
Luasft= zeros(27,1);
Cycleft = zeros(27,1);
Shopft = zeros(27,1);
Recreationft = zeros(27,1);
Cafeft = zeros(27,1);
OtherIndoorft = zeros(27,1);
OtherOutdoorft = zeros(27,1);

TotalExposure = zeros(27,1);
TestMatrix = zeros(27,15);


for i = 1:27

    Workft(i) = A(i,1);
    Homeft(i) = A(i,2);
    Sleepft(i) = A(i,3);
    Pubft(i) = A(i,4);
    Walkft(i) = A(i,5);
    Driveft(i) = A(i,6);
    Trainft(i) = A(i,7);
    Busft(i) = A(i,8);
    Luasft(i) = A(i,9);
    Cycleft(i) = A(i,10);
    Shopft(i) = A(i,11);
    Recreationft(i) = A(i,12);
    Cafeft(i) = A(i,13);
    OtherIndoorft(i) = A(i,14);
```

```
    OtherOutdoorft(i) = A(i,15);
    SmokerCheck = A(i,16);
    SexCheck = A(i,17);

    if SexCheck == 1

        WorkSample(:,1) = random(MaleWork_LogN, m, 1);

    else

        WorkSample(:,1) = random(FemaleWork_Weibull, m, 1);

    end

    if SmokerCheck == 1

       HomeSample(:,1) = random(SmokerHome_InvGauss, m, 1);

       SSleepAlpha = 3.585;
       SSleepBeta = 4.9927;
       SleepSample(:,1) = gamrnd(SSleepAlpha, SSleepBeta, m, 1);


    else

        HomeSample(:,1) = random(Home_LogLogistic, m, 1);

        SleepMu = 9.786;
        SleepSigma = 8.373;
        SleepSkew = 2.8164;
        SleepKurt = 21.6181;
        SleepSample(:,1) =
pearsrnd(SleepMu,SleepSigma,SleepSkew,SleepKurt,m,1);
%returns an m-by-n matrix of random numbers drawn from the
%distribution
%in the Pearson system with mean mu, standard deviation sigma,
%skewness skew, and kurtosis kurt

    end

PubSample(:,1) = random(Pub_LogLogistic, m, 1);

WalkSample(:,1) = random(Walk_LogLogistic, m, 1);

DriveAlpha = 1.37;
DriveBeta = 24.33;
DriveSample(:,1) = gamrnd(DriveAlpha, DriveBeta, m, 1);

BusAlpha = 1.9439;
BusBeta = 22.516;
BusSample(:,1) = gamrnd(BusAlpha, BusBeta, m, 1);

CycleSample(:,1) = random(Cycle_LogNormal, m, 1);

TrainTramSample(:,1) = random(TrainTram_Gamma, m, 1);

ShopSample(:,1) = random(Shop_LogLogistic, m, 1);
```

```
CafeSample = random(Cafe_InvGauss, m, 1);

RecreationAlpha = 1.5764;
RecreationBeta = 37.963;
RecreationSample(:,1) = gamrnd(RecreationAlpha, RecreationBeta, m, 1);
% R = gamrnd(A,B,m,n) generates an m-by-n array containing random
numbers from the gamma distribution

% with parameters A and B. A and B can each be scalars or arrays of
the same size as R.

OtherIndoorSample(:,1) = random(OtherIndoor_LogLogistic, m, 1);

OtherOutdoorSample(:,1) = random(OtherOutdoor_LogN, m, 1);

WorkExpose = zeros(m,1);
HomeExpose = zeros(m,1);
SleepExpose = zeros(m,1);
PubExpose = zeros(m,1);
WalkExpose = zeros(m,1);
DriveExpose = zeros(m,1);
BusExpose = zeros(m,1);
CycleExpose = zeros(m,1);
TrainTramExpose = zeros(m,1);
ShopExpose = zeros(m,1);
CafeExpose = zeros(m,1);
RecreationExpose = zeros(m,1);
OtherIndoorExpose = zeros(m,1);
OtherOutdoorExpose = zeros(m,1);

    for j=1:m

   WorkExpose(j,1) = WorkSample(j);
   HomeExpose(j,1) = HomeSample(j);
   SleepExpose(j,1) = SleepSample(j);
   PubExpose(j,1) = PubSample(j);
   WalkExpose(j,1) = WalkSample(j);
   DriveExpose(j,1) = DriveSample(j);
   BusExpose(j,1) = BusSample(j);
   CycleExpose(j,1) = CycleSample(j);
   TrainTramExpose(j,1) = TrainTramSample(j);
   ShopExpose(j,1) = ShopSample(j);
   CafeExpose(j,1) = CafeSample(j);
   RecreationExpose(j,1) = RecreationSample(j);
   OtherIndoorExpose(j,1) = OtherIndoorSample(j);
   OtherOutdoorExpose(j,1) = OtherOutdoorSample(j);

    end

Mwx = mean(WorkExpose);
Mhx = mean(HomeExpose);
Msx = mean(SleepExpose);
Mpx = mean(PubExpose);
Mwalkx = mean(WalkExpose);
Mdx = mean(DriveExpose);
Mbx = mean(BusExpose);
```

```
Mcx = mean(CycleExpose);
Mtx = mean(TrainTramExpose);
Ms2x = mean(ShopExpose);
Mcrx = mean(CafeExpose);
Mrx = mean(RecreationExpose);
Moix = mean(OtherIndoorExpose);
Moox = mean(OtherOutdoorExpose);


a = Mwx*Workft(i);
TestMatrix(i,1) = a;

b = Mhx*Homeft(i);
TestMatrix(i,2) = b;

c = Msx*Sleepft(i);
TestMatrix(i,3) = c;

d = Mpx*Pubft(i);
TestMatrix(i,4) = d;

e = Mwalkx*Walkft(i);
TestMatrix(i,5) = e;

f = Mdx*Driveft(i);
TestMatrix(i,6) = f;

g = Mbx*Busft(i);
TestMatrix(i,7) = g;

h = Mcx*Cycleft(i);
TestMatrix(i,8) = h;

q =  Mtx*Trainft(i);
TestMatrix(i,9) = q;

k = Ms2x*Shopft(i);
TestMatrix(i,10) = k;

l = Mcrx*Cafeft(i);
TestMatrix(i,11) = l;

n = Mrx*Recreationft(i);
TestMatrix(i,12) = n;

o = Moix*OtherIndoorft(i);
TestMatrix(i,13) = o;

p = Moox*OtherOutdoorft(i);
TestMatrix(i,14) = p;

TotalExposure(i) = a + b + c + d + e + f + g + h + q + k + l + n + o +
p;

end
```

# Appendix G

Matlab Code for Baseflow Separation Methods

**Matlab Code for the Boughton Method:**

```
Boughton_input = untitled;

a = 0.1;
b = 1;
A = zeros(720, 30);

for z = 1:30

A(1,z) = Boughton_input(1,z);

for i = 1:719

    j = i+1;

    if (Boughton_input(i,z) < Boughton_input(j,z))
        K = A(i,z) + a*Boughton_input(j,z);
    else
        K = A(i,z) - b*Boughton_input(j,z);
    end

    if(K<0)
        output = 0;
    else

      if(Boughton_input(i,z) < Boughton_input(j,z))
          K1 = A(i,z) + a*Boughton_input(j,z);
      else
          K1= A(i,z) - b*Boughton_input(j,z);
      end

      if(K1>Boughton_input(j,z))
          output2 = Boughton_input(j,z);
      else
            if(Boughton_input(i,z) < Boughton_input(j,z))
                K2 = A(i,z)+ a*Boughton_input(j,z);
            else
                 K2 = A(i,z)- b*Boughton_input(j,z);
            end
            output2 = K2;
      end

      output = output2;
    end

    A(j, z) = output;

end
end


%Sliding interval with 1 hour period
```

**Matlab code for the Sliding Interval Method:**

```
Sliding_input = untitled;

result = 0;
Sliding_ouput = zeros(690,30);
Min_check = zeros(30,1);


for k = 1:30

for o = 1:690
    j =1;

   for i = o:o+29
       Min_check(j,1) = Sliding_input(i, k);
       j = j+1;
   end

   result= min(Min_check);
   Sliding_output(o, k) = result;

   o = o+1;
end

end
```